Gastrointestinal and urinary Dysfunction in animal models of Parkinson's disease

Abdul-Azim Hassan

Department of Clinical, pharmaceutical and biological sciences

Submitted to the University of Hertfordshire in partial fulfilment of the requirement of the degree of PhD

October 2024

DECLARATION

This dissertation is the result of my own work and includes nothing, which is the

outcome of work done in collaboration except where specifically indicated in the text.

It has not been previously submitted, in part or whole, to any university of institution for

any degree, diploma, or other qualification.

In accordance with the Schedule Ai (PhD) guidelines, this thesis is does not exceed

80,000 words (excluding any footnotes, appendices or bibliography.).

Signed: Abdul-Azim Hassan

Date: 12/10/2024

i

ABSTRACT

Parkinson's disease (PD) is a common neurodegenerative disease resulting from the loss of dopaminergic neurons in the nigrostriatal tract. Classical motoric symptoms of tremor, instability, hunched posture, and slowness of movement are most commonly associated with the disease. Non-motor symptoms (NMS) of PD have historically been under-recognised, despite mentions of many NMS such as sleep disturbances, autonomic dysfunction, and pain in James Parkinson's original description of the disease. NMS are also largely treated currently by symptomatic therapies. Holistic treatments are not possible due to our lack of understanding of the link between pathophysiology of motor and non-motor symptoms.

Gastrointestinal and urinary symptoms greatly affect the quality of life of patients with PD and present important challenges to the management of the disease as it progresses. The most frequently reported issues with these systems are bladder dysfunction in the form of nocturia, increased frequency, increased urgency and gastrointestinal dysfunction presenting as constipation, excess salivation and dysphagia. Research into NMS is necessary not only to aid therapeutic intervention to the debilitating symptoms, but to understand at risk populations and identify biomarkers for progression of disease.

We have chosen to use different models of Parkinson's disease in different animals to unearth common changes in their pathology which may lead to GI dysfunction. We have looked at models with differing extents of pathology, as NMSs are present at various stages of the disease. Our work has focussed on evaluation of overt local adaptive changes that may occur because of central dopaminergic loss, using various ex vivo assays.

To characterise the functional effects of Kv7 modulation in the gastrointestinal tract we used a mouse ex vivo motility assay. We determined that pharmacological inhibition of Kv7 channels increased peristaltic like motor activity and Kv7 activation diminished peristaltic like motor activity in the ileum and colon. Kv7.4 expression was visualised to be present on smooth muscle cells and myenteric neurons of the gastrointestinal tract via. In the same ex vivo assay set up we found that the ileum of MPTP treated animals were more active in our motility assay compared to the ileum tissue from sham treated controls.

Animals treated with 6-OHDA intrastriatally, to induce a partial lesion, showed significant changes in the dorsal motor nucleus of vagus (DMV) and alterations in nitrergic transmission in the bladder and ileum. We also observed functional consequences of increased Kv7 channel expression in the bladder.

Finally, rare tissues obtained from MPTP treated marmoset revealed a potential vulnerability to neurodegenerative insults in dopaminergic neurons of the substantia nigra that contain the Kv7.4 channel. The Kv7.4 channel was also affected in peripheral tissues in this model with reduced expression in various cell types of the ileum and increased expression in the bladder detrusor muscle.

The results suggest that central nigrostriatal dopaminergic denervation is associated with overactivity in both the bladder and ileum in these models. This can result in dysregulated smooth muscle motor activity, leading to gastrointestinal and urinary dysfunction such as constipation and urinary urgency. The mechanisms that we have uncovered here require further validation, to assess their role in the human condition, and understand whether they can be targeted to alleviate the autonomic symptoms of PD. Our findings will hopefully enable future assessments to be performed in human samples and lead to a translational path from pre-clinical to clinical therapeutic interventions.

ACKNOWLEDGEMENTS

In the name of God, the most Beneficent the most Merciful.

Without Him nothing is possible and with Him nothing is impossible.

Thanks must start with God who has sustained me and forgiven me. He has guided me with His Book, His Messenger and The Holy Household (pbut). He has given me strength through him and through those around me to continue through this journey.

Thanks goes to my parents who have prayed for me, looked after me, and supported me to succeed. My wife who has given me the time and space to succeed, often at her own cost. My grandparents, siblings and children who have encouraged me to succeed.

My supervisors, Professor Iravani and Dr Keating, have guided me through this journey complimenting each other's style, each in their own way helping me through my experiments and my write up. Special thanks to Professor Iravani who picked me to be his first PhD student at UH and gave me a chance where others had not. Thanks to the staff at UH and KCL that helped make my experiments possible with their various contributions.

To all those who have shown me kindness along this journey be it extended family, friends or university staff, thank you so much.

My aim has been and always will be, to use the skills gained in my life to help people and make the world a better place. Success is in the journey and the effort; the outcome is in God's hands.

Abdul-Azim Hassan

CONTENTS

1 INTRODUCTION	23
1.1 The history of Parkinson's disease	23
1.2 Current knowledge	24
1.3 Symptoms of PD	25
1.3.1 Motor symptoms 26	
1.3.2 Non-motor symptoms 27	
1.4 Gastrointestinal and urinary dysfunction in PD	30
1.4.1 Gastrointestinal symptoms in PD 30	
1.4.2 Urinary symptoms and Parkinson's disease 33	
1.5 PATHOPHYSIOLOGY OF PD	35
1.5.1 Neurodegeneration and Motor circuit pathophysiology 35	
1.5.2 The basal ganglia and PD 36	
1.5.3 Extranigral pathology 36	
1.5.4 Lewy pathology 36	
1.6 PARKINSON'S DISEASE THERAPY	39
1.6.1 Treatment of motor symptoms 39	
1.6.2 Treatment of non-motor symptoms 40	
1.7 Gastroenterology and the Urinary Bladder	42
1.7.1 The gastrointestinal tract 42	
1.7.2 The urinary bladder 46	
1.8 PATHOLOGY OF GI DYSFUNCTION IN PD	48
1.9 Pathology of urinary dysfunction in PD	52
1.10 Animal models of PD	53
1.10.2 Gastrointestinal and urinary dysfunction in animal models of PD	60
1.11 The K _v 7 Channel	67
1.12 AIMS OF THE INVESTIGATION	69
2 METHODS	72
2.1 Animal Models	72
2.1.1 MPTP mouse model (Sub-acute MPTP dosing regimen) 72	
2.1.2 6OHDA rat model 73	
2.1.3 MPTP marmoset model 73	

2.2 In vitro colonic and ileal motility bioassay
2.2.1 Experimental Procedure 76
2.2.2 Data analysis 77
2.3 Organ bath contractility
2.3.1 Experimental Procedure 78
2.3.2 Data analysis 78
2.4 Immunohistochemistry
2.4.1 Gut and Bladder Tissue 79
2.4.2 Brain tissue 80
2.4.3 Image analysis 82
2.5 QPCR82
2.5.1 Comparison of the use of FFPE and frozen tissue for qPCR studies 83
2.6 Western blot
3 K _v 7 CHANNEL REGULATION OF GASTROINTESTINAL MOTOR
ACTIVITY IN A MURINE MODEL OF PERISTALSIS97
3.1 Introduction
3.2 Methods
3.2.1 Animals 100
3.2.2 In vitro colonic and ileal motility bioassay 100
3.2.3 Drugs 100
3.2.4 Immunohistochemistry 101
3.3 RESULTS
3.3.1 Peristaltic motor complexes of the ileum and colon show different motility
pattern profiles in our system. 102
3.3.2 Kv7 Channel activators reduce CPMC and IPMC activity. 107
3.3.3 XE-991, A Kv7 Channel blocker, increases CPMC and IPMC activity. 114
3.3.4 The Retigabine induced decrease in CPMC activity is inhibited by $K_{\nu}7$
channel blocker XE-991 118
3.3.5 Immunohistochemistry confirms the presence of Kv7.4 positive structures in
the smooth muscle layers and the myenteric plexus. 120
3.4 Discussion
4 Kv7 CHANNEL REGULATION OF GASTROINTESTINAL MOTOR
ACTIVITY IN AN MPTP MOUSE MODEL131
4.1 Introduction
4.2 Methods 124

4.2.1 Animals 134
4.2.2 In vitro colonic and ileal motility bioassay 135
4.2.3 Experimental Procedure 135
4.2.4 Drugs 135
4.2.5 Immunohistochemistry 135
4.3 RESULTS
4.3.1 MPTP administration to mice led to a bilateral lesion due to a significant
loss of dopaminergic neurons in the SNpc. 136
4.3.2 The ileum of MPTP treated mice displays an altered motility profile to that of
sham treated mice. 138
4.3.3 Kv7 channel modulators effect IPMC activity similarly in the isolated ileum
of MPTP treated and sham mice. 142
4.3.4 Colon motility in MPTP treated mice is similar to that of sham treated mice.
147
4.3.5 Kv7 channel modulators effect CPMC activity similarly in the isolated colon
of MPTP treated and sham mice. 151
4.4 DISCUSSION
5 CONTRACTILITY IN THE GASTROINTESTINAL AND URINARY
SMOOTH MUSCLE IN A PARTIAL LESION MODEL OF PARKINSON'S
DISEASE
5.1 Introduction
5.2 Methods
5.2.1 Animals 168
5.2.2 Organ bath contractility 169
5.2.3 Drugs 170
5.2.4 Immunohistochemistry 170
5.2.5 Western blot 171
5.3 RESULTS
5.3.1 Unilateral injection of 6-OHDA into the striatum led to a loss of TH+ cells in
the Substantia Nigra 172
5.3.2 The ipsilateral DMV of 6-OHDA treated rats show loss of ChAT+ve neurons
and TH-ir fibres. 175
5.3.3 The extent of TH+ve cell loss in the SN did not correlate with response to
EFS in the gastrointestinal tract and the bladder in this model of PD. 178

5.3.4 Electrical field stimulation (EFS) and carbachol (CCh) stimulation of
isolated gastrointestinal and urinary bladder strips revealed no differences in
treatment groups. 181
5.3.5 The effect of K_v 7 activator Retigabine on isolated segments and K_v 7.4
expression was not significantly different between treatment groups in
gastrointestinal tissue. 184
5.3.6 The isolated segments of bladder from 6-OHDA treated rats show increased
response to the Kv7 activator Retigabine and increased Kv7.4 expression. 189
5.3.7 Impairment of relaxation mechanisms in the gastrointestinal tract of the
partial unilateral lesion 6-OHDA model 191
5.3.8 Striatal 6-OHDA administration leads to impairment of the nitrergic system
in the bladder. 196
5.3.9 A reduction in the non-cholinergic, non-purinergic EFS evoked contraction is
seen in bladder tissues from 6-OHDA rats. 199
5.4 DISCUSSION
6 CHANGES IN KCNQ4 ENCODED Kv7.4 CHANNEL IN THE MPTP
TREATED PRIMATE MODEL OF PARKINSON'S DISEASE213
6.1 Introduction
6.2 Methods
6.2.1 Animals 217
6.2.2 Immunohistochemistry 218
6.2.3 qPCR 218
6.2.4 Image analysis 219
6.2.5 Data analysis 219
6.3 RESULTS
6.3.1 A reduction in KCNQ4-ir, TH positive neurons is observed in the SNpc of
MPTP treated marmosets. 219
6.3.2 The expression of KCNQ4 positive structures is reduced within the layers of
the gastrointestinal wall of the MPTP primate model. 222
6.3.3 KCNQ4 positive structures are present on smooth muscle cells of the
gastrointestinal tract 226
6.3.4 The expression of KCNQ4 positive structures is increased in the muscular
layer of the bladder in the MPTP primate model. 228
6.3.5 A significant reduction in KCNQ4 mRNA expression in the ileum of MPTP
treated marmosets. 230

6.4 Discussion	231	
7 GENERAL DISCUSSION	238	
8 APPENDICES	24	
9 REFERENCES	255	
LIST OF TABLES		
TABLE 1 NON MOTOR SYMPTOMS OF PD 29		
TABLE 2 FEATURES OF ANIMAL MODELS OF PD. 54		
TABLE 3 ANTIBODIES USED IN PROTEIN DETECTION FROM RAT TISSUES.	171	
TABLE 4 LOG EC50 CONTRACTILE RESPONSE TO CCH IN DIFFERENT TISSU SHAM AND 6-OHDA TREATED RATS. 182	ES FROM NAIVE,	

LIST OF FIGURES

FIGURE 1 CLINICAL SYMPTOMS AND TIME COURSE OF PD PROGRESSION 26
FIGURE 2 PATHOLOGICAL FINDINGS IN CONNECTIONS BETWEEN THE CNS AND THE
GASTROINTESTINAL TRACT (GIT) IN PD PATIENTS. 50
FIGURE 3 LUMINAL DISTENSION OF INTESTINAL SEGMENTS IN A MOTILITY ORGAN BATH
LEADS TO PERISTALTIC LIKE MOTOR COMPLEXES. 76
FIGURE 4 REPRESENTATIVE IMAGES OF SECTIONS USED IN BRAIN
IMMUNOHISTOCHEMISTRY. 81
FIGURE 5 NANODROP RESULTS FROM FFPE VS FROZEN TISSUE MRNA EXTRACTION.87
FIGURE 6 SUMMARY BOX PLOTS OF COMPARISON OF FFPE VS FROZEN TISSUE AND QPCR
DATA OF FFPE TISSUE. 89
FIGURE 7 BIOANALYSER TRACES SHOWING RNA DEGRADATION IN FFPE TISSUE. 91
FIGURE 8 PERISTALTIC MOTOR COMPLEXES OF THE ILEUM AND THE COLON. 102
FIGURE 9 A COMPARISON OF COLONIC AND ILEUM MOTOR COMPLEXES 104
FIGURE 10 INDIVIDUAL PERISTALTIC MOTOR COMPLEXES OF THE ILEUM AND THE COLON.
106
FIGURE 11 ASSESSMENT OF CONTRACTILITY IN THE ILEUM AND THE COLON. 107
FIGURE 11 ASSESSMENT OF CONTRACTILITY IN THE ILEUM AND THE COLON. 107
FIGURE 12 THE EFFECT OF THE KV7 OPENER RETIGABINE ON CPMC ACTIVITY 109
FIGURE 13 THE EFFECT OF THE KV7 OPENER ML213 ON CPMC ACTIVITY 111
FIGURE 14 THE EFFECT OF THE KV7 OPENER RETIGABINE ON IPMC ACTIVITY 113
FIGURE 15 THE EFFECT OF THE KV7 BLOCKER XE-991 ON CPMC ACTIVITY 115
FIGURE 16 THE EFFECT OF THE KV7 BLOCKER XE-991 ON IPMC ACTIVITY 117
FIGURE 17 Kv7 BLOCKADE HAS AN INHIBITORY EFFECT ON RETIGABINE INDUCED
DECREASE OF CPMC ACTIVITY. 119

- FIGURE 18 EXPRESSION OF KCNQ4-IR IN THE SMOOTH MUSCLE LAYERS AND MYENTERIC PLEXUS OF THE MURINE COLON 121
- FIGURE 19 THE EFFECT OF MPTP ADMINISTRATION ON THE SNPC AND MOUSE BODY WEIGHT. 137
- FIGURE 20 A COMPARISON OF IPMC ACTIVITY IN SHAM AND MPTP TREATED MICE. 139
- FIGURE 21 TRACES OF A SINGLE IPMC OF A SHAM AND MPTP TREATED ANIMAL. 141
- FIGURE 22 ASSESSMENT OF CONTRACTILITY IN THE ILEUM OF SHAM AND MPTP TREATED MICE. 142
- FIGURE 23 KV7 ACTIVATION DECREASES IPMC ACTIVITY SIMILARLY IN TISSUES FROM SHAM AND MPTP TREATED MICE. 144
- FIGURE 24 KV7 BLOCKADE INCREASE IPMC ACTIVITY SIMILARLY IN TISSUES FROM SHAM AND MPTP TREATED MICE. 146
- FIGURE 25 A COMPARISON OF CPMC ACTIVITY IN SHAM AND MPTP TREATED MICE.

 148
- FIGURE 26 TRACES OF A SINGLE CPMC OF A SHAM AND MPTP TREATED ANIMAL. 150
- FIGURE 27 ASSESSMENT OF CONTRACTILITY IN THE COLON OF SHAM AND MPTP TREATED MICE. 151
- FIGURE 28 Kv7 ACTIVATION DECREASES CPMC ACTIVITY SIMILARLY IN TISSUES FROM SHAM AND MPTP TREATED MICE. 153
- FIGURE 29 Kv7 BLOCKADE INCREASE CPMC ACTIVITY SIMILARLY IN TISSUES FROM SHAM AND MPTP TREATED MICE. 155
- FIGURE 30 SERIES OF TYROSINE HYDROXYLASE IMMUNOSTAINED SECTIONS SHOWING LOSS IN THE SUBSTANTIA NIGRA OF 6-OHDA TREATED RATS. 173
- FIGURE 31 QUANTIFICATION OF THE LOSS OF TH-IR NEURONES IN THE SN OF 6-OHDA TREATED RATS. 174

- FIGURE 32 CORRESPONDING SECTIONS OF THE DMV SHOW LOSS OF CHAT+VE NEURONS AND TH-IR FIBRES IN 6-OHDA TREATED RATS. 176
- FIGURE 33 QUANTIFICATION OF THE LOSS OF TH-IR FIBRES AND CHAT+VE NEURONS IN THE DMV OF 6-OHDA TREATED RATS. 178
- FIGURE 34 COMPARISON OF 6-OHDA TREATMENT AND EFFECTS WITH RESPONSE TO EFS 180
- FIGURE 35 DOSE RESPONSE CURVES TO CARBACHOL AND EFS FREQUENCY RESPONSE

 CURVES IN VARIOUS TISSUES FROM CONTROL AND 6-OHDA TREATED RATS. 183
- FIGURE 36 RESPONSES OF GASTROINTESTINAL TISSUES FROM TREATED AND UNTREATED RATS TO 10HZ EFS, IN THE PRESENCE OF KV7 CHANNEL ACTIVATOR RETIGABINE.

 185
- FIGURE 37 KCNQ4-IMMUNOREACTIVITY IN THE COLON OF 6-OHDA TREATED AND UNTREATED RATS. 187
- FIGURE 38 KCNQ4-IMMUNOREACTIVITY IN THE ILEUM OF 6-OHDA TREATED AND UNTREATED RATS. 188
- FIGURE 39 RETIGABINE HAS A LARGER EFFECT ON BLADDER TISSUE FROM 6-OHDA TREATED ANIMALS DUE TO INCREASED KCNQ4 EXPRESSION. 190
- FIGURE 40 RESPONSES OF GASTROINTESTINAL TISSUES FROM TREATED AND UNTREATED RATS TO 10HZ EFS, IN THE PRESENCE OF SILDENAFIL. 192
- FIGURE 41 EXPRESSION OF PROTEINS RELEVANT TO THE NITRERGIC AND CHOLINERGIC SYSTEM IN THE COLON OF 6-OHDA TREATED AND UNTREATED RATS. 194
- FIGURE 42 EXPRESSION OF PROTEINS RELEVANT TO THE NITRERGIC AND CHOLINERGIC SYSTEM IN THE ILEUM OF 6-OHDA TREATED AND UNTREATED RATS. 196
- FIGURE 43 CONTRACTILE RESPONSES IN BLADDER TISSUE FROM 6-OHDA TREATED

 ANIMALS ARE LARGER DUE TO ALTERED EXPRESSION OF PROTEINS INVOLVED IN THE

 NITRERGIC SYSTEM. 198
- FIGURE 44 RESPONSES OF BLADDER TISSUES TO EFS, IN THE PRESENCE OF ATROPINE AND ATP DESENSITISATION. 200

- Figure 45 Immunofluorescent staining for KCNQ4 in TH+ve neurons of the $$\operatorname{NPc}$$ 220
- FIGURE 46 QUANTITATIVE ANALYSIS OF KCNQ4 AND TH IN THE SNPC OF NORMAL AND MPTP COMMON MARMOSETS 221
- FIGURE 47 KCNQ4-IMMUNOREACTIVITY IN THE GASTROINTESTINAL TRACT OF NAÏVE AND MPTP TREATED MARMOSETS. 223
- FIGURE 48 QUANTITATIVE ANALYSIS OF KCNQ4-IR IN THE ILEUM AND COLON OF NORMAL AND MPTP COMMON MARMOSETS. 225
- FIGURE 49 IMMUNOFLUORESCENT STAINING FOR KCNQ4 IN SMOOTH MUSCLE LAYERS OF GASTROINTESTINAL TRACT IN NAIVE MARMOSETS. 227
- FIGURE 50 KCNQ4-IMMUNOREACTIVITY IN THE BLADDER MUSCLE OF NAÏVE AND MPTP TREATED MARMOSETS. 229
- FIGURE 51 MRNA EXPRESSION OF KCNQ4 IN DIFFERENT TISSUES FROM NAIVE AND MPTP TREATED MARMOSETS. 231
- FIGURE 52 SUMMARY OF THESIS FINDINGS 240

LIST OF ABBREVIATIONS AND ACRONYMS

6-OHDA	6-hydroxydopamine
ACh	Acetylcholine
ANOVA	Analysis of variance
АТР	Adenosine triphosphate
AUC	Area under the curve
B00	Bladder outflow obstruction
BSA	Bovine serum albumin
cAMP	Cyclic adenosine monophosphate
cGMP	Cyclic guanosine monophosphate
ChAT	Choline acetyltransferase
CNS	Central nervous system
COMT	Catechol-O-methyl transferase
СРМС	Colonic peristalsis-like motor complex
CSF	Cerebrospinal fluid
DA	Dopamine
DAG	Diacylglycerol
DAT	Dopamine transporter
DBS	Deep brain stimulation
DMSO	Dimethyl sulfoxide
DMV	Dorsal motor nucleus of vagus

DNA	Deoxyribonucleic acid
DO	Detrusor overactivity
DR	Dopamine receptor
DSM	Detrusor smooth muscle
EC	Effective concentration
EFS	Electric field stimulation
eNOS	Endothelial nitric oxide synthase
ENS	Enteric nervous system
EPAC	Exchange protein directly activated by cAMP
FDA	Food and drug administration
FFPE	Formalin fixed paraffin embedded
FITC	Fluorescein isothiocyanate
GABA	γ-Aminobutyric acid
GBA	Glucocerebrosidase
GC	Guanylyl cyclase
GFAP	Glial fibrillary acidic protein
GI	Gastrointestinal
GID	Gastrointestinal dysfunction
GIDS	Gastrointestinal dysfunction survey
GIT	Gastrointestinal tract
GP	Globus pallidus

	,
GPe	Globus pallidus externa
GPi	Globus pallidus interna
GSH	Glutathione
HALF	High-amplitude low frequency
HLA	Human Leucocyte Antigen
HPLC	High performance liquid chromatography
HPRT1	Hypoxanthine-guanine phosphoribosyl transferase gene
HRM	High-resolution manometry
IC	Inhibitory concentration
ICC	Interstitial cells of Cajal
IHC	Immunohistochemistry
IML	Intermediolateral column of the spinal cord
iNOS	Inducible nitric oxide synthase
IP	Intraluminal pressure
IP ₃	Inositol-1,4,5-trisphosphate
IPMC	Ileal peristalsis-like complex
KCI	Potassium chloride
KCNE	Potassium voltage gated channel subfamily E regulatory subunit
KCNQ	Voltage-gated potassium channels of subfamily 7
LAMP1	Lysosomal-associated membrane protein 1

LB	Lewy body
LC3	Microtubule-associated proteins 1A/1B light chain 3B
L-DOPA	L-3,4-dihydroxyphenylalanine
LH	Lateral hypothalamus
LID	Levodopa induced dyskinesia
LNAME	N(gamma)-nitro-L-arginine methyl ester
LPS	Lipopolysaccharide
LRRK2	Leucine rich repeat kinase 2
LUT	Lower urinary tract
LUTS	Lower urinary tract symptoms
МАО-В	Monoamine oxidase B inhibitors
MDS	Movement disorders society
MFB	Medial forebrain bundle
ML-213	N-(2,4,6-Trimethylphenyl)-bicyclo[2.2.1]heptane-2- carboxamide
MLC	Myosin light chain
ММС	Migrating motor complex
MPP+	1-methyl-4-phenylpyridinium
MPTP	1-methyl-4-phenyl-1,2,3,6-tetrahydropyridine
MRI	Magnetic resonance imaging
MSA	Multiple systems atrophy

NADPH	Nicotinamide adenine dinucleotide phosphate
NANC	Non-adrenergic non-cholinergic
NGS	Next generation sequencing
NHP	Non-human primate
NMS	Non-motor symptom
NMSQ	Non-motor symptoms questionnaire
NMSS	Non-motor symptoms survey
nNOS	Neuronal nitric oxide synthase
NO	Nitric oxide
NOS	Nitric oxide synthase
NPY	Neuropeptide Y
OAB	Overactive bladder
OD	Optical density
PAG	Periaqueductal gray
PBS	Phosphate buffered saline
PCR	Polymerase chain reaction
PD	Parkinson's disease
PDE5	Phosphodiesterase type 5
PINK1	PTEN-induced kinase 1
PIP ₂	Phosphatidylinositol-4,5-bisphosphate
РКА	Protein kinase A

PLC	Phospholipase C	
PMC	Pontine micturition centre	
PPL	Home Office Project Licence	
PTM	Post-translational modifications	
PVDF	Polyvinylidene fluoride	
qPCR	Quantitative polymerase chain reaction	
RBD	REM behaviour disorder	
REM	Rapid eye movement sleep	
RIN	RNA integrity number	
RNA	Ribonucleic acid	
ROI	Region of interest	
ROS	Reactive oxygen species	
RT	Room temperature	
RTP	Room temperature and pressure	
SAA	α-Synuclein seed amplification assay	
SEM	Standard error mean	
SHHF	Spontaneously hypertensive heart failure	
SIBO	Small intestinal bacterial overgrowth	
SLT	Speech and language therapy	
SMA	Smooth muscle actin	
SMC	Smooth muscle cells	

SMP	Submucosal plexus	
SN	Substantia nigra	
SNP	Sodium nitroprusside	
SNpc	Substantia nigra pars compacta	
SPECT	Single-photon emission computed tomography	
SRIF	Somatotropin release-inhibitory factor	
STN	Subthalamic nucleus	
ТН	Tyrosine hydroxylase	
TIQ	Time in quiescence	
TRPA	Transient receptor potential	
UK	United Kingdom	
UPDRS	Unified Parkinson's disease rating scale	
UPS	Ubiquitin-proteasome system	
USA	United States of America	
UV	Ultraviolet	
VIP	Vasoactive intestinal peptide	
VIPR	Vasoactive intestinal peptide receptor	
VTA	Ventral tegmental area	
XE-991	10,10-bis(4-Pyridinylmethyl)-9(10H)-anthracenone dihydrochloride	

LIST OF APPENDICES

APPENDIX 1 - SCRIPTS USED IN AUTOMATED IMAGE ANALYSIS (IMAGEJ). 249

Appendix 2 – Scripts used for automated fluctuation analysis (Spike 2 software). 252

1 Introduction

1.1 The history of Parkinson's disease

The term "Parkinson's disease" was suggested in 1872 by Jean-Martin Charcot, in honour of James Parkinson but also to differentiate it from other neurological disorders. Although reports of Parkinsonian symptoms can be found in earlier texts, James Parkinson's "An Essay on the Shaking Palsy" (Parkinson, 1817), was the first clear medical description of the disorder. He described progressive symptoms of rest tremor, postural impairment and others during observation of six subjects. Even in these early works, constipation was mentioned, where expulsion of faeces in a patient required "stimulating medicines of very considerable power" and sometimes "mechanical aid".

He offered with caution his thoughts on causality the of the disease, a theme that echoed throughout his work, referring to it as "opinion" and "conjectural suggestions" only published in order to excite those who; "may point out the most appropriate means of relieving a tedious and most distressing malady" (Parkinson, 1817).

It seems that James Parkinson attributed "lessened muscular power" or weakness to be the cause of the observed difficulty of walking and movement. However, Charcot recognised bradykinesia as a distinct feature of the disease and was resolute, having conducted tests, that PD patients were not particularly weaker than normal people for much of their disease.

"A somewhat attentive examination will enable you to recognise the significant fact that, in such cases, there is rather retardation in the execution of movements than real enfeeblement of the motor powers" (Charcot, 1872).

This, along with observations of a proportion of patients without marked tremor reaffirmed his thoughts to separate the disease from other tremorous disease, such as multiple sclerosis, which it was often grouped with.

1.2 Current knowledge

Parkinson's disease (PD) is a common neurodegenerative disease with varied prevalence worldwide. Europe and North America have a higher prevalence (66-1500 per 100,000) than African, Asian and Middle Eastern countries (10-119 per 100,000). PD is a progressive disease resulting from the loss of dopaminergic neurons in the nigrostriatal tract. Loss of dopamine leads to dysregulation of the activity of the motor circuitry leading to the classical motoric symptoms of tremor, instability, hunched posture and slowness of movement. Cell death in the substantia nigra pars compacta (SNpc) and the presence of Lewy pathology, post-mortem, remains the gold standard for diagnosis of PD as no definitive diagnostic tools exist, although symptomatic diagnosis is used during the lifetime of the patient (Kalia & Lang, 2015).

For the majority, PD is idiopathic or sporadic, in that it has no known cause and occurs in people with no apparent history of the disorder in their family. It is likely that it arises due to the interplay of genetic susceptibility and the environment. There are a proportion of people with PD that have a family history of this disorder. Monogenic familial cases of PD can be caused by mutations in genes which are inherited in a Mendelian fashion. Mutations in some of these genes and others may also

play a role in cases that appear to be sporadic, by modifying the risk or susceptibility of developing PD i.e., genetic risk factors (Kalia & Lang, 2015).

Treatments of the disease are symptomatic, mostly designed to replace dopamine levels within the brain and control the motor symptoms. Currently no disease modifying therapies exist.

1.3 Symptoms of PD

Although PD is associated with increased mortality, there is heterogeneity between studies as to the factor by which it is increased compared to controls (Macleod et al., 2014). Importantly, quality of life is greatly impacted, which progresses with age. Despite the recent development of the SAA assay, diagnosis during the life of a PD patient is based on clinical assessment.

The most recognised symptoms of PD are the movement disorders including bradykinesia, rest tremor, muscular rigidity and postural and gait impairment. These are usually asymmetrical and arise due to the loss of dopaminergic neurones in the nigrostriatal tract. The loss of dopamine leads to dysregulation of the activity of the motor circuitry leading to the classical motoric symptoms.

PD is also associated with a constellation of maladies that do not involve movement which can often precede the motor symptoms (Figure 1). Some important non-motor disturbances are the dysregulation of autonomic functions such as cardiovascular, digestive and urinary dysfunctions. These non-motor symptoms (NMS) are thought to be unrelated to the loss of dopamine as dopamine replacement therapies that improve motor deficits have little or no effect on reversing them (Schapira et al., 2017).

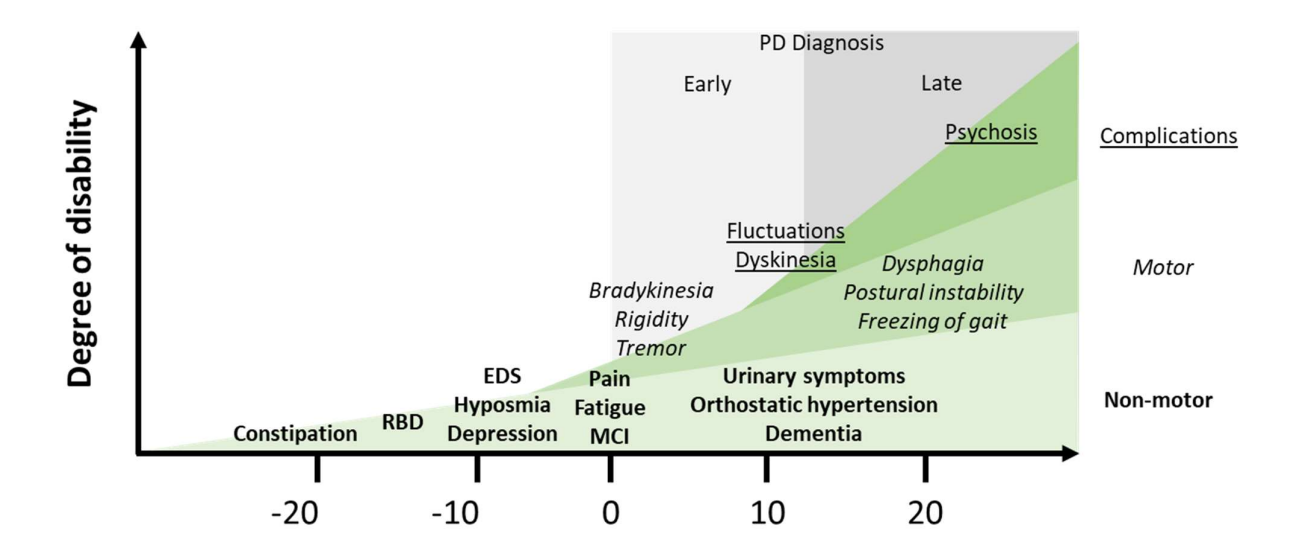


Figure 1 Clinical symptoms and time course of PD progression

"Diagnosis of Parkinson's disease occurs with the onset of motor symptoms (time 0 years) but can be preceded by a premotor or prodromal phase of 20 years or more. This prodromal phase is characterised by specific non-motor symptoms. Additional non-motor features develop following diagnosis and with disease progression, causing clinically significant disability. Axial motor symptoms, such as postural instability with frequent falls and freezing of gait, tend to occur in advanced disease. Long-term complications of dopaminergic therapy, including fluctuations, dyskinesia, and psychosis, also contribute to disability. EDS=excessive daytime sleepiness. MCI=mild cognitive impairment. RBD=REM sleep behaviour disorder". Adapted from Kalia & Lang 2015.

1.3.1 Motor symptoms

The core clinical features of PD and those which diagnosis of the disease rests upon are bradykinesia, rigidity and tremor. Bradykinesia in this case is an umbrella term for the slowness of movement and decreased amplitude of movement (akinesia/hypokinesia). Both bradykinesia and

hypokinesia are present in PD patients even if not exhibited simultaneously and both must occur in the limbs to establish diagnosis, even if they are also present elsewhere. Rigidity appears as resistance to passive movement, which is not solely due to the inability to relax. Rest tremor is present in the majority of patients, it is a tremor in a resting limb that is supressed during the initiation of movement (Postuma et al., 2015). There are also other manifestations of motor symptoms present in patients which affect speech, facial expression, gait and postural instability (O'Gorman Tuura et al., 2018).

Therapies for PD will be discussed in a latter section, but of note the most effective medication Levodopa (L-DOPA), induces motor complications in of itself with continued disease progression. L-DOPA induced complications are of two types, L-DOPA induced dyskinesia and periods of reduced benefit of the therapy termed "off" periods. It is estimated that 10% of patients of patients per year develop motor fluctuations post start of L-DOPA therapy (Ahlskog & Muenter, 2001). Off periods can be predictable or unpredictable in different patients and can manifest as wearing off, worsening of Parkinson's symptoms or sudden switching between states (Aquino & Fox, 2015). Dyskinesias are defined as involuntary movements and can manifest as choreic movements in the limbs and trunk. Although most pronounced in the limbs these can also effect other body parts such as involuntary eye movements (Grötzsch et al., 2007) or respiratory dyskinesia (Calabresi et al., 2010).

1.3.2 Non-motor symptoms

Non-motor symptoms (NMS) of PD have historically been under-recognised, despite mentions of many NMS such as sleep disturbances, autonomic dysfunction and pain in James Parkinson's original description of the disease (Parkinson, 1817). They are now being given more importance highlighted by the revised Movement Disorders Society Unified Parkinson's disease rating scale (MDS-UPDRS), clinical severity criteria for PD, which puts a 'red flag' against diagnosis of PD if non-motor features are absent by 5 years of disease duration (Postuma et al., 2015).

Behavioural abnormalities such as dementia and depression, sleep-related and sensory dysfunction occur in varying forms and degrees in PD patients. Autonomic dysfunction, mainly of the gastrointestinal, cardiovascular and urological systems, may also be present. NMS often appear in the latter stages of the disease but can also appear early, sometimes even preceding the onset of motor symptoms and thus diagnosis by many years (Schapira et al., 2017). Table 1 below describes the commonly known NMS experienced by PD patients, their estimated prevelance and the stages at which they occur within the disease. Research into NMS is necessary not only to aid therepeutic intervention to the debilitating symptoms, but to understand at risk populations and identify biomarkers for progression of disease.

Table 1 Non motor symptoms of PD

Non motor symptom	Estimated prevalence	Stage(s) of disease
Sleep disturbances (REM behaviour disorder, insomnia, restless leg syndrome)	Most patients	Premotor , Early motor
Hyposmia	90%	Premotor , also may present later
Apathy	60%	Premotor , Early motor
Gastrointestinal dysfunction (Constipation, excess salivation, dysphagia)	60%	Premotor , Early motor
Depression	35%	Premotor
Pain	30-85%	Early motor
Bladder dysfunction (nocturia, increased frequency, increased urgency)	30-70%	Early motor, Mid stage
Visual disturbances (diplopia, hallucinations)	78%	Early motor, sometimes pre-motor
Fatigue	50%	Early motor
Anxiety	60%	Mid stage
Cardiovascular dysfunction (orthostatic hypertension, labile hypertension)	30-58%	Late stage
Cognitive decline and dementia	Azim Hassan 83%	Late stage
Psychosis	40%	Late stage

1.4 Gastrointestinal and urinary dysfunction in PD

Gastrointestinal (GI) dysfunction can be seen at all levels of the tract, the most frequent symptoms seen, such as constipation, gastroparesis and dysphagia, are due to motility abnormalities. Our aim is to use different models of PD to discover pathways by which such motility issues may arise at central and peripheral levels. James Parkinson observed GI NMS in patients including constipation and difficulty in swallowing amongst others in his essay, describing the disease (Parkinson, 1817). GI symptoms are amongst the most common domains of NMS, experienced by ~60% of patients (Barone et al., 2009).

1.4.1 Gastrointestinal symptoms in PD

Gastrointestinal symptoms greatly affect the quality of life of patients with PD and present important challenges to the management of the disease as it progresses. In 2021 a new scale for gastrointestinal dysfunction in PD was developed and published by the movement disorders society, after recognition that studies were being performed with different definitions of GI symptoms using various scales. The Gastrointestinal Dysfunction Scale in PD (GIDS-PD) is a self-report scale with a focus on three domains, constipation, bowel irritability and upper GI symptoms but also importantly gathers information on relevant lifestyle factors and comorbidities. The aim is that it will form a standardised tool for the future allowing characterisation and monitoring of GID in PD as well as a potential tool for interventional studies and more optimal management of GID (Camacho et al., 2021). Below we discuss in detail the major GI symptoms prevalent in PD.

1.4.1.1 Drooling

Poor oral control of saliva and excessive pooling can be due to overproduction, known as sialorrhea or defective clearance, due to swallowing difficulties. It can greatly impact quality of life through social embarrassment, poor oral hygiene and an increased risk of aspiration pneumonia but also difficulty eating and speaking (Kalf et al., 2007; Leibner et al., 2010). The estimates of prevalence

in studies vary greatly, ranging from 10 to 84%, due to the different questionnaires and diagnosis methods used (Srivanitchapoom et al., 2014).

Impaired salivary clearance is more likely the cause of drooling rather than overproduction of saliva. Studies show that patients with PD produce less saliva (Bagheri et al., 1999) due to a lower salivary flow rate. Hypomimia, a common symptom of PD characterised by involuntary mouth opening has been shown to be a major factor for drooling allowing accumulated saliva to drip from the mouth. PD patients in this study who suffered from drooling also had stooped posture and less efficient swallowing (Kalf et al., 2011).

1.4.1.2 Dysphagia

Dysphagia is a disorder of swallowing which can arise from dysfunction in the oropharyngeal and or oesophageal phase of deglutition, generally occurring in the later stages of the disease. Even in the early stages some PD patients who do not show clinical manifestations of dysphagia, showed manometric abnormalities (Sung et al., 2010; Suttrup et al., 2017). Like other non-motor symptoms swallowing disorders are underreported. Often quantitative measurements will uncover abnormalities in a patients swallowing even though the patient reports no difficulties in questionnaires (Bird et al., 1994).

Dysphagia is associated with complications such as malnutrition, dehydration and insufficient medicine intake. Aspiration pneumonia, a leading cause of mortality in PD patients, is also associated with dysphagia (Hely et al., 2008).

1.4.1.3 Gastric emptying

Nausea, vomiting, early satiety and bloating are common symptoms experienced by PD patients. These symptoms are characteristic of delayed gastric emptying or gastropareses. The controversy in its definition as a symptom of PD arises because it appears that these symptoms can result from the impact of the disease itself but also due to adverse effects from disease management medication. A systematic review of original articles focusing on gastroparesis and PD estimates that the prevalence of delayed gastric emptying in PD is more than 70% (Heetun & Quigley, 2012).

Healthy volunteers given L-Dopa exhibited significant delays in gastric emptying (Robertson et al., 1992) which recovered when given with the dopamine receptor antagonist, and anti-sickness medication metoclopramide (Berkowitz & McCallum, 1980). Dopamine therapy therefore is likely to contribute to the gastroparesis seen in PD patients, as shown by Hardoff et al. (2001). However, gastric emptying has also been studied in untreated PD patients, wherein it was significantly delayed in both treated and untreated PD with no significant difference between the two patients types (Tanaka et al., 2011; Unger et al., 2011).

These issues not only manifest as symptoms, affecting quality of life but can affect the pharmacokinetics of levodopa. Associations between plasma levels of levodopa and gastric emptying have shown that delayed gastric emptying can be a factor in delayed "on-time" (Doi et al., 2012; Muller et al., 2006).

1.4.1.4 Small Intestinal Bacterial Overgrowth

Small intestinal bacterial overgrowth (SIBO) is a malabsorption syndrome caused by an increase bacterial density as well as the presence of colonic-type species of bacteria within the small bowel. Under normal circumstances various mechanisms contribute to the reduction of bacterial growth potential including, gastric acid secretion, small intestinal motility and the ileocecal valve. Two studies using tomography (Dutkiewicz et al., 2015a) and a 3D magnetic tracking system (Knudsen, Haase, et al., 2017), reported significantly increased small intestinal transit time in PD patients compared to healthy controls. The dysmotility in PD likely causes an increase in colonic bacteria within the small bowel. Studies have shown a higher prevalence of SIBO in PD patients (Fasano et al., 2013; Gabrielli et al., 2011). The PD patients with SIBO had more severe motor fluctuations with longer "off-time" daily and more episodes of "on-time" delay. The motor fluctuation of these same patients significantly improved when administered with antibiotic therapy to eradicate the SIBO. SIBO possibly contributes to motor dysfunction affecting the host immune function by disrupting small bowel integrity and/or affecting L-dopa absorption (Tan et al., 2014).

1.4.1.5 Constipation

The most common gastrointestinal symptom in PD is constipation, which is known as a pro-dromal symptom of PD as its appearance can pre-date the motor symptoms by over a decade (Fasano et al., 2015). Large follow-up population based studies report that reduced frequency of bowel movements and severity of constipation increases the risk of developing PD 3-4.5 fold (Abbott et al., 2001; Lin et al., 2014).

Diagnosis of constipation is by history-taking by the clinician when the patient presents with the symptom, followed by a physical examination. In PD, questionnaires are often used to score a patients symptoms, including specialist questionnaires for non-motor symptoms such as the GIDS-PD and NMSQuest (Chaudhuri et al., 2006). It is argued by Knudsen et al. (2017) that objective measurements reveal far greater prevalence of colonic dysfunction in PD patients than subjective questionnaires. In their study 79% and 66% of patients had significantly increased colonic transit times compared to healthy controls, yet subjective measurement using three different questionnaires only identified prevalence of constipation in the cohort as 3%, 32% and 38% (Knudsen, Fedorova, et al., 2017). The most common definitions of constipation within these questionnaires refer to the frequency of bowel movements and the more recent GIDS-PD also includes questions about straining and stool consistency to hopefully give a more reliable picture of colonic dysfunction.

Constipation can also be presented due to outlet obstruction or "pelvic floor dyssynergia", characterised by difficulty of rectal evacuation due to paradoxical contraction of the sphincter muscles at defectation. This is a rarer occurrence in PD and even when present can be exhibited alongside prolonged colonic transit time (Jost, 2010). Again, such issues may not be picked up in a questionnaire simply on frequency but can be evaluated further if asked about straining and incomplete evacuation.

1.4.2 Urinary symptoms and Parkinson's disease

Similarly to gastrointestinal dysfunction urinary problems were noted by James Parkinson in his original essay, with mentions of in voluntary passing of urine at the late stage of disease in patients

(Parkinson, 1817). The revised MDS-UPDRS contains a question on urinary problems, but it does not go into detail as to the particular symptom and therefore is only useful to inform as to whether a patient has a urinary disturbance and how impactful it is on their daily activities (Martinez-Martin et al., 2015). Other non-motor PD specific questionnaire-based tools go into a little more detail such as the non-motor symptoms questionnaire (NMSQ) and the non-motor symptoms scale for Parkinson's disease (NMSS) but are still limited in the attention given to LUTS. As with GI dysfunction that results in different studies using different scales to make conclusions about prevalence, severity, and efficacy of treatments.

Prevalence of LUTS, dependent on study, ranges in between 30% and 70%. There are many factors as to why the range is so wide. Apart from the different methods of scoring as mentioned above, previous misdiagnosis of PD in patients with multiple systems atrophy (MSA) has skewed older data (Sakakibara et al., 2008). Additionally, understanding the direct effect of PD pathology on urinary dysfunction can be tricky. This is because urinary dysfunction development is especially prevalent in "healthy" men and women over 60 due to benign prostate hyperplasia and idiopathic detrusor overactivity. Nevertheless in all studies to date the incidence of LUTS in PD is significantly higher than the rates in healthy controls (Martinez-Martin et al., 2015; Winge & Fowler, 2006).

LUTS can be split into two categories, storage symptoms and voiding symptoms. Storage symptoms are most common in PD and include nocturia, urgency and frequency. Voiding symptoms consist of slow initiation of urination, prolongation or poor stream and straining.

1.4.2.1 Overactive bladder

Detrusor overactivity (DO) or overactive bladder (OAB) urgency is when a patient has a sudden compelling desire to pass urine which may be difficult to defer. This can occur with or without incontinence and is due to involuntary phasic detrusor contraction (Badri et al., 2014). The key to the storage phase disorders is the low volume thresholds that trigger urgency and the inability to override the urgency, compared to a healthy individual. Although incontinence is usually a marker of severity of OAB, the inability to delay voiding and incontinence can be worsened when the

patient's motor symptoms impact their ability to reach an appropriate space for voiding. Another case where the true extent of LUTS is difficult to determine is nocturia, as PD patients with sleep disturbances may void after waking due to for example RBD, but perceive it is a waking due to nighttime urgency.

1.4.2.2 Weak detrusor and sphincter obstruction

Pressure flow analysis and questionnaire results of PD patients with LUTS revealed up to 60% of patients had weak bladder. Additionally 38% had voiding symptoms of retardation of initiation, intermittency, prolongation, straining and/or the sensation of residual urine (Sakakibara, Hattori, et al., 2001). Like storage symptoms, voiding symptom severity also correlated with disease severity in one study (Sammour et al., 2009) with levodopa showing improvement of voiding symptoms in some patients (Brusa et al., 2007).

1.5 Pathophysiology of PD

The pathological hallmark of Parkinson's disease is progressive neurodegeneration, primarily in the dopaminergic neurons of the substantia nigra. In general, the other hallmark of PD is the presence of intraneural inclusions called Lewy bodies, composed of many different proteins most prominently α -synuclein and ubiquitin.

1.5.1 Neurodegeneration and Motor circuit pathophysiology

Neurodegeneration in the substantia nigra dopaminergic neurons and the motor effects resulting from that loss have been well studied. Loss of dopamine neurons in the SNpc leads to a reduction in dopamine release in the striatum producing an imbalance in motor control pathways in the basal ganglia. The regions within the basal ganglia for the purpose of this discussion connect to form what is known as the "direct", "indirect" and "hyper-direct" pathways. In general, decreasing basal ganglia output (via the direct pathway) leads to the facilitation of movement and increasing basal ganglia output limits or regulates movement (via the indirect pathway) (Albin et al., 1989). Importantly it is believed that the altered activity of these two pathways (and possibly the hyper-

direct pathway), rather than total absence of these two functions, leads to the symptoms of movement disorders.

1.5.2 The basal ganglia and PD

The dopaminergic transmission from the SNpc to the striatum is a key regulation mechanism in the direct and indirect pathways which lead to purposeful movement. The loss of dopaminergic neurons of the SNpc, in MPTP (1-methyl-4-phenyl-1,2,3,6-tetrahydropyridine) treated monkeys, increased the activity of striatal projections to the GPe (the indirect pathway) and reduced activity of the striatal projections to the GPi/SNr (the direct pathway) (Bergman, Feingold, et al., 1998). Additionally, the lack of dopamine transmission to the striatum would leave cholinergic interneurons driving the activity of striatal projections to the GPi/SNr, which are said to favour the indirect pathway, limiting movement (Albin et al., 1989). A similar scenario is likely in the human disease and there are some biochemical and anatomical changes that occur in the human basal ganglia which are partially consistent with this theory.

1.5.3 Extranigral pathology

It is likely that the true situation is more complex in PD, than simply basal ganglia dysfunction, with changes in burst firing and increased oscillatory activity seen in patients within and outside of the basal ganglia (Galvan & Wichmann, 2008). Non-motor symptoms can arise from pathology outside the basal ganglia and will be discussed later but even some of the classical motor symptoms such as, tremor and postural instability, have extranigral pathological correlates (Lim et al., 2009). For example gait decline has been shown to correlate with atrophy in the right hippocampus but not with SNpc atrophy using MRI (Dadar et al., 2020).

1.5.4 Lewy pathology

In PD abnormal inclusions called Lewy bodies (LB) and Lewy neurites accumulate within neurons, in particular neurons of the SNpc but also in other central and peripheral regions. Lewy bodies are mostly composed of insoluble α-synuclein but up to 90 different molecules have been shown in

various immunohistochemical assessments of LBs (Spillantini et al., 1997; Takahashi & Wakabayashi, 2001; Wakabayashi et al., 2013). Lewy bodies are round intraneural inclusions whereas Lewy neurites are abnormal neurites which contain α-synuclein filaments and granular material.

Human α -synuclein is a 140 amino acid protein which contains three major regions, an N-terminal domain, a central domain and a C-terminal tail. The N-terminal domain contains all known disease-linked mutations. The C-terminal domain contains most of the known phosphorylation sites and is the region linked with most of the protein's interactions with other proteins. The central domain of the human protein is prone to aggregate (Burré et al., 2018). The definitive physiological functions of α -synuclein have not been confirmed but deficiency in synaptic transmission when it is knocked down or overexpressed point to an essential role in synaptic function, neurotransmitter release and synaptic plasticity. The structure of native, physiological α -synuclein within a cell is still debated and it is likely that there is not one single form, but that it can exist both as unstructured monomers and tetrameric oligomers in equilibrium in healthy neurons. Disruption of this equilibrium by various triggers, and high levels of oligomers are believed to be the pathogenic state (Wakabayashi et al., 2013). Post-translational modifications (PTM) of α -synuclein can favour oligomerisation. The most well studied PTM is the phosphorylation at the Serine-129 (Ser-129) residue, which has been found to be the most prevalent PTM found in the brains PD patients (Fujiwara et al., 2002).

α-synuclein's distribution is not only intracellular as it can be detected in the plasma and CSF (El-Agnaf et al., 2003). It has been shown to be secreted and taken up by cells, in vitro, in a prion like manner and lead to the formation of LB-like inclusions (Emmanouilidou et al., 2010; Luk et al., 2009). Importantly, potential mechanisms of seeding have been implicated in the human brain, where PD patients transplanted with embryonic mesencephalic tissue were found to have LB and Lewy neurites in the grafted neurons (Kordower et al., 2008; J.-Y. Li et al., 2008). The presence of LB pathology in grafted neurons in itself is not direct evidence of a prion mechanism, as the pathology may arise in response to the toxic environment that the neurons find themselves in within the PD brain. Indeed, other groups have found no LB pathology in grafted neurons of patients up to 16 years after original transplantation (Galvin et al., 2001; Mendez et al., 2008). The progression of

PD as a prion like disease will be discussed later due to links with the enteric nervous system and theories around transmission from the gut to the brain. Whether Lewy pathology can explain the progression and clinical signs of the disease is still up for debate. Ideally, what would be needed to support such statements would be the direct correlation between Lewy pathology, clinical progression and neurodegeneration. For Lewy pathology to be considered causative is also up for debate. There are cases of widespread Lewy pathology without neurological impairment and cases of neurodegeneration preceding Lewy pathology observation, however, in a significant proportion of patients, Lewy pathology does correlate to motor symptoms and/or cognitive decline (Milber et al., 2012; Parkkinen et al., 2008).

Recently an α-synuclein seed amplification assay has been assessed in a large cohort of subjects and been shown to classify people with PD with high specificity and sensitivity. CSF samples from 1100 participants (PD patients, people at risk of developing PD and healthy controls) were run through the Ampiron α-synuclein seed amplification assay (SAA) (Siderowf et al., 2023). Although it was extremely accurate in determining participants with "typical PD", it produced some interesting results when considering α-synuclein and PD. The highest variability in detection of PD using the SAA was in patients that were normosmic and/or patients with the LRRK2 G2019S mutation. For LRRK2 mutations this is not a new phenomenon and has been seen too often to be an anomaly. The proportion of SAA negative LRRK2 PD patients (32.5%) is consistent with previous reports of only one third of PD patients with the G2019S mutation having no Lewy pathology in post mortem examinations (Kalia et al., 2015). Assessment of the prodromal PD participant group, recruited based on hyposmia or REM behaviour disorder (RBD), revealed an interesting set of patients (15/51) that had positive SAA but DAT-SPECT results that did not quite meet the criteria as abnormal, related to PD. This study also revealed a similar SAA positive proportion in nonmanifesting GBA carriers as is documented as the penetrance of GBA mutations for PD. This raises the possibility of a model in which a positive SAA result could precede abnormal dopamine transporter (DAT) imaging, and clinical manifestation. Further work is needed in prodromal participants to truly ascertain the value of this assay in such a context and follow up of the current prodromal cohort will be extremely useful in the continued validation of this assay. Without any

clear associations with clinical phenotype, it is clear that this assay is a marker of α -synuclein pathology and cannot be called a true diagnostic tool for Parkinson's disease, at least with its current definitions. However, it is an important assay to consider for clinical trial design, for stratification or exclusion, dependent on therapeutic target. It again highlights that α -synuclein is important in Parkinson's disease but does not define it always.

1.6 Parkinson's disease therapy

Parkinsons's disease, especially in the early stages can be well managed, however the treatments are only symptomatic. Research into PD therapeutics is focused on the holy grail of treating the symptoms of the disease by slowing the progression of the disease.

1.6.1 Treatment of motor symptoms

Pharmacological interventions that result in enhancement of dopaminergic signalling, via three different mechanisms, are the mainstay of treatment for PD. The three mechanisms of treatment are via the dopamine precursor Levodopa, dopamine receptor agonists and dopamine metabolism inhibitors. Levodopa is converted to dopamine in presynaptic terminals of dopaminergic neurons. In PD the benefit of this treatment occurs when SNpc neurons release this newly synthesised dopamine onto postsynaptic terminals in the striatum. Dopamine receptor agonists, such as Ropinirole, bypass this process and act directly on D1-3 dopamine receptors. The other route to increasing dopaminergic transmission is to inhibit its breakdown via Monoamine oxidase B inhibitors (MAO-B) and Catechol-O-methyl transferase (COMT) inhibitors. MAO-B inhibitors can be used as monotherapy or in combination with Levodopa to potentiate dopaminergic stimulation. COMT inhibitors are used as adjunct therapy to increase the half-life and reduce motor-fluctuations of levodopa.

Tremor as opposed to bradykinesia and rigidity is inconsistently managed by dopaminergic therapy. Even at high levodopa doses tremor may persist, this subtype of patients are said to experience "dopamine-resistant" tremor. In this case anti-cholinergic medication can be effective, but they come with their own drawbacks (Zhong et al., 2022).

Management of PD requires a multifaceted approach where timing and treatment is dependent on the dominance of symptoms at each stage and their impact on quality of life for each individual. Physiotherapy, dedicated to the needs of Parkinsons patients, has been proven to be beneficial for gait and balance as well as speech (Domingos et al., 2018). Surgical interventions such as ablation of the STN and GP, although useful, have been replaced by deep brain stimulation (DBS). DBS involves high frequency stimulation of a region of the brain using electrodes and is less invasive than surgery, reversible and highly effective against the motor symptoms of PD in many patients (DeLong & Wichmann, 2015).

Due to the relative success of symptomatic therapies, the majority of current efforts have focussed on testing potential disease modifying treatments. Reducing inflammation, α -synuclein aggregation/spread and targeting risk factor genes to affect the wider PD population are all strategies being assessed, with the ultimate aim of neuroprotection. Gene therapy, gene silencing, immunotherapy and repurposing of medications have kept the pipelines of pharmaceutical and biotech companies busy, but none have so far been fruitful in translating to the clinic. Hope is at hand with Buntanetap an α -synuclein targeting therapy currently in Phase 2/3 trials but there is no precedent for success, with the previous failures of α -synuclein targeting therapies such as Prasinezumab.

1.6.2 Treatment of non-motor symptoms

The need for disease modifying treatments increases with disease progression as the symptomatic therapies begin to be less effective with increased neurodegeneration and increased involvement of non-dopaminergic systems. The challenge to physicians is differentiating the contribution of the NMS from disease progression, the current medication (motor symptom management) and the emotional state of the patient. Non-motor symptoms are also largely treated currently by symptomatic therapies. Holistic treatments are not possible due to our lack of understanding of the link between pathophysiology of motor and non-motor symptoms. Therefore, each symptom is largely treated individually as a standalone symptom, separate from the underlying cause.

Recommended treatments for drooling are anticholinergics, botulinum toxin injection, radiotherapy and behavioural modification including speech and language therapy (SLT). (Arbouw et al., 2010; Hyson et al., 2002; Marks et al., 2001; Seppi et al., 2011). Dysphagia is also treated with SLTs, to modify and optimize the patients methods of swallowing (Baijens & Speyer, 2009; Bushmann et al., 1989).

Increasing fibre and fluid intake in patients is a simple but effective first step in treatment of constipation. Diet rich insoluble fibre increase (Astarloa et al., 1992) and increased intake of soluble fibre such as Psyllium husks (Ashraf et al., 1997), increased stool frequency and weight in constipated PD patients. However, these measures need to be integrated into the routine of the patient as they do not change colon transit time using objective measurements, and their positive effects on frequency return to baseline levels once the supplement is withdrawn. Probiotics and prebiotic fibre consumption had similar positive effects (Barichella et al., 2016). Prokinetic agents have also been studied in PD and found to be somewhat effective (Liu et al., 2005; Sullivan et al., 2006), but as mentioned, their side effect profile makes their availability limited. The osmotic laxative Macrogol is widely available and has been shown to be well-tolerated and highly effective in PD patients, improving stool frequency, consistency and moderately reducing straining. So far, Macrogol is the preferred agent for management of chronic constipation in PD potentially removing the necessity of rectal laxatives as a rescue remedy, with its continued use (Zangaglia et al., 2007).

Levodopa and dopamine agonists benefit bladder control at least in a subset of patients (Brusa et al., 2007, 2017). Quantitative assessments using NMSS during "on" and "off" states of patients revealed a small but significant group of patients that experience urinary problems only in the "off state", indicating relief during therapeutically beneficial levodopa (Storch et al., 2015). Anticholinergic medications are used as first line therapy in patients with troublesome OAB as they reduce the parasympathetic contractile effect on the bladder (Kapoor et al., 2013). This can be useful for more than one symptom as anticholinergics have been used to combat tremor, but it is necessary to assess and monitor the significant side effects that can occur. Injection of botulinum neurotoxin directly to the detrusor was shown to effectively reduce frequency of urination which lasted up to 6 months (Giannantoni et al., 2011). Stimulating afferent pathways through

neuromodulation is a selectively used, minimally invasive intervention that has shown to be effective in improving symptoms. Deep brain stimulation has been shown to improve LUTS and again highlights the importance of the basal ganglia as well as motor symptoms in LUTS (Kapoor et al., 2013). Surgery is an option where obstruction is the cause of the voiding symptoms, although this is less common in PD (Kapoor et al., 2013). In 2019 Istradefylline was approved by the FDA as an add-on therapy to levodopa to help with "off-state" symptoms. The adenosine A2A receptor antagonist has been shown to be efficacious, long term, in a small trial, to also improve voiding symptoms (weak stream and incomplete emptying) to a greater degree than its modest effects on OAB symptoms (Kitta et al., 2018).

As with motor symptoms, lifestyle changes and physiotherapy should go hand in hand with pharmacological intervention as some "standard" drug treatments can be contraindicated with PD medication or just the disease itself (Church, 2021; Schapira et al., 2017). The current research for therapies of NMS seems to be focused around assessing current symptom standard of care, for their effectiveness in PD patients, with the hope that eventually disease modifying therapies will treat motor and non-motor symptoms.

1.7 Gastroenterology and the Urinary Bladder

The models that we will employ in this thesis will take advantage of the vast knowledge accumulated over the years regarding the function of the GIT and urinary bladder. The general structure and function of these organs are described below to set the tone for our investigations of gastrointestinal and urinary dysfunction in animal models of PD.

1.7.1 The gastrointestinal tract

The gastrointestinal tract is composed of organs that process food, absorb water and nutrients and eliminate waste. Although the gastrointestinal tract contains organs from the oesophagus to the anus this thesis and therefore this section will focus on the workings of the small and large intestine.

Although the anatomy and even the cell types of the colon and small intestine are not the same, a cross section of the two tubular structures for both human and rodent would show similarly distinct layers. The three main layers are the mucosal layer, the submucosa and the tunica muscularis externa. Apart from being the home of the submucosal plexus, the submucosa is known to mostly consist of collagen fibres, connective tissue, lymphatic and blood vessels (Thomson et al., 1986). The role of the mucosa is poorly defined and outside of the scope of this thesis.

Of particular interest are the layers of the muscularis externa which comprise of an inner circular layer and an outer longitudinal layer. Mixing and propulsion rely on the circular layer, whereas transit of a bolus is facilitated by the longitudinal muscle which shortens the gut and increases the diameter of the lumen. The autonomy of gastrointestinal smooth muscle doesn't preclude the need for multiple levels of regulatory mechanisms, to generate purposeful contractile behaviour. Motor function is controlled by smooth muscle cells (SMCs), interstitial cells of Cajal (ICCs), nervous tissues and supporting tissues.

1.7.1.1 Smooth muscle cells

Although the intricate mechanisms of excitation-contraction coupling are poorly understood, depolarisation of SMC's and the resultant increase in cytoplasmic Ca²⁺ activates myosin light chain (MLC) kinase. Phosphorylation of MLC leads to the cross-bridge formation between myosin and actin, leading to force generation (Sanders et al., 2012). Inward currents of Ca²⁺ and/or Na⁺ via voltage dependent calcium channels (VDCCs) or non-selective cation channels cause depolarisation in SMC's. The inward currents are rarely directly regulated in GI SMCs, instead balance is achieved via outward currents, mainly of K⁺, There are a variety of different K+ channels, which stabilise and hyperpolarise the membrane potential, reducing the open probability of VDCCs (Sanders, 2008), of which particular interest to us is the Kv7 channel (discussed later). The inward current itself, and presence of Ca²⁺, does not automatically lead to a contraction as other modulatory events can influence the outcome. Modulation can occur through various routes such as, altering Ca²⁺ sensitivity via neurotransmitters or cyclic nucleotides, or dephosphorylation of myosin. It is important to be aware that although various mechanisms exist to modulate depolarisation and

contractility, most work has been performed by exogenous bath applied modulators on isolated tissues and their effects measured. The physiological situation may differ, and different mechanisms and stimuli may act in intricate pathways that we are just not able to decipher at this time.

1.7.1.2 Nervous tissues

The complex patterns of motility in the intestinal tract such as peristalsis and segmentation are dependent on intrinsic and extrinsic innervation of nervous tissue. The enteric nervous system is the intrinsic neuronal regulator of motility and is made up of motor neurons, interneurons and afferent neurons. Although the submucosal plexus may play some role in the motor reflex the major plexus for myogenic control is the myenteric plexus. Myenteric neurons can loosely be separated into excitatory or inhibitory based on their expression of tachykinins (acetylcholine, substance P, neurokinin A etc) or nitric oxide (NO) and vasoactive intestinal peptide (VIP) (Hasler, 2009). The peristaltic complex was described intricately, over a century ago, as being made up of a coordination of excitation (contraction) above and inhibition (relaxation) below the site of stimulation, usually by a bolus (Bayliss & Starling, 1899). Acetylcholine (ACh) excites smooth muscle cells via muscarinic receptors in part by leading to the inhibition of cyclic adenosine monophosphate (cAMP) dependent relaxation. ACh also leads to the opening of non-selective cation channels and membrane depolarisation (Eglen, 2001; Tanahashi et al., 2021). In the gut NO is now considered the main inhibitory neurotransmitter and acts via activation of guanylyl cyclase, leading to cGMP dependent activation of K⁺ channels as well as decreasing Ca²⁺ sensitivity (Sanders et al., 2012).

Extrinsic innervation via efferent fibres mostly terminate in the myenteric plexus connecting with enteric ganglia. Excitatory efferent parasympathetic cholinergic neurons activate nicotinic receptors on the myenteric neurons. The vagus also contains cholinergic neurons which project to NO and VIP inhibitory enteric neurons promoting relaxation (Berthoud et al., 1991; Chang et al., 2003). Pelvic nerve fibres from the sacral spinal cord innervate the myenteric plexus and can accelerate colonic transit (Andersen et al., 2006). Neuronal activity in the gut is also under sympathetic control which inhibits the excitatory cholinergic transmission of the myenteric plexus. One such path is via preganglionic cholinergic neurons from the spinal cord which project to the prevertebral ganglia,

such as the celiac ganglia. From the celiac ganglia, post ganglionic noradrenergic neurons project to the enteric ganglia, hyperpolarising enteric neurons (Yuyama et al., 2002). Afferent nerves carry sensory information to the CNS. Non-noxious stimuli perception can be mediated by the vagal, splanchnic or pelvic pathways however nociceptive input is mainly carried by the splanchnic nerves to the spinal cord (Hasler, 2009).

1.7.1.3 Interstitial cells of Cajal

The pacemaker cells in the different tracts of the gastrointestinal system do not have a unique site like in the heart. Instead, there are at least six different types of Interstitial cells of Cajal (ICCs) usually defined by their location within the various layers of the gut. Although SMCs generate action potentials, they cannot produce rhythmicity and therefore the co-ordinated slow waves are dependent on ICCs. This has been shown in organ culture from neonatal mice administered with antibodies to c-kit receptors which exhibited a loss of electrical rhythmicity and the abolishment of the slow wave (Ward et al., 1997).

1.7.1.4 The major motor patterns of the small and large intestine

The migrating motor complex (MMC) is a contractile pattern present in the small intestine that propels undigested food, whilst in a fasting state (Szurszewski, 1969). After eating, a faster pattern of intermittent phasic contractions replaces the MMC to mix and propel the contents of the intestine (McCoy & Baker, 1968). The colon consists of a wider variety of different motor patterns some of which are unorganised patterns of local contractions. Some colonic motor patterns are short duration stationary contractions solely for mixing contents to extract water and others are long duration contractions for both mixing and propulsion of faeces (Huizinga et al., 1985; McRorie et al., 1998). The gastrocolonic response, the increase in motor activity of the colon after feeding, is likely regulated predominantly by extrinsic nerves (Tanabe et al., 2002). The mass movement of faeces through the colon is elicited by high amplitude propagated contractions. These can be induced experimentally by distension as well as chemical stimuli and are mediated by cholinergic and nitrergic transmission (M. Li et al., 2002). Motor patterns of the small and large bowel can be

modulated by external factors via central nervous system modulation e.g. by sleep but also via intestinal reflex mechanisms e.g. due to distension or nutrient composition in the lumen.

1.7.2 The urinary bladder

The lower urinary tract is composed of the bladder and the urethra, with the prostate an additional organ in males. The bladder is a muscular organ with two primary functions. They are the storage of urine, produced by the kidneys, and the expulsion of urine at the appropriate time via the urethra. The bladder is composed of two distinct parts, the body or "the dome" and the bladder base, which includes the trigone and the ureterovesical junction. During the filling phase of the micturition cycle, the bladder base contracts, forming a stable structure, this alongside the high outflow resistance from the sphincters allows the relaxed bladder body to file with urine. Voiding is a reversal of this, with the relaxation of the bladder outlet followed by the contraction of the detrusor muscle cells of the bladder body (Andersson & Arner, 2004; Fry et al., 2010).

The bladder wall is made up of four layers, the outermost serosa, the detrusor muscle, the submucosal and mucosal layer. The rest of this chapter will focus on the detrusor muscle but worth noting is the mucosal layer which is commonly known as the urothelium. The urothelium/suburothelium is not only a barrier between the lumen and the detrusor, impermeable to urine, but it is a metabolically active layer that can influence myogenic responses (Ikeda & Kanai, 2008).

1.7.2.1 Detrusor muscle

Smooth muscle cells (SMC) of the bladder are similar in structure to SMCs in other regions of the body and are activated by the same contractile proteins (myosin, actin, myosin light chain kinase and phosphatase) after a rise in intracellular Ca²⁺. In the human bladder, the outer and inner layers of the detrusor have a longitudinal orientation, whereas the middle layer is orientated circularly. They are organised into bundles separated by connective tissue which rearrange and elongate during the filling phase and shorten during voiding (Uvelius, 1976). Action potentials in bladder SMCs are carried by calcium influx and the repolarisation is mediated by potassium efflux through various K⁺

channels (Montgomery & Fry, 1992). The increase in intracellular calcium involved in contraction can be from various sources e.g. extracellular influx via L-type channels or release from intracellular stores.

Within the detrusor muscle there are also cGMP immunoreactive spindle-shaped interstitial cells. They are present in large amounts throughout the detrusor muscle forming an interconnective network. These interstitial cells are proposed to act as pacemakers in the transmission of nerve signals to SMCs, as well as possibly intermediaries in cell to cell communication (Sui et al., 2002).

1.7.2.2 Nerve mediated responses.

Signals of bladder filling are carried by the parasympathetic sensory fibres of the detrusor to the periaqueductal gray (PAG) region. Once these afferent signals exceed a certain threshold and no opposing signals are received to the PAG, the PAG fires to the pontine micturition centre (PMC). The PMC via the sacral spinal cord relaxes the urethral sphincter and contracts bladder dome resulting in voiding. Imaging studies have confirmed this micturition loop in the rat (Tai et al., 2009). The pelvic ganglia is the relay between the preganglionic parasympathetic fibres from the sacral spinal cord and the postganglionic motor nerves which make contact with bladder myocytes. These fibres are mainly cholinergic and it has been suggested that under normal circumstances, at least in the human bladder, contraction is almost exclusively mediated by muscarinic receptor activation. There is a non-adrenergic, non-cholinergic (NANC) mechanism which contributes to contraction in varying degrees dependent on species and pathological state. This NANC contractile response is believed to be mostly due to purinergic stimulation but purinergic desensitisation does not entirely inhibit contractile responses to electrical stimulation (Andersson & Arner, 2004; Fry et al., 2010; Luheshi & Zar, 1990), therefore other neurotransmitters can also play a part in bladder contraction.

Electrical stimulation of adrenergic nerves in the detrusor release norepinephrine. The major relaxatory response of the detrusor is thought to be through cAMP's activation of protein kinase A, (PKA) via β -adrenergic receptor stimulation (Nakahira et al., 2001). Although norepinephrine is not selective and can stimulate α -adrenergic receptors, β -adrenergic receptors predominate in their

expression in the bladder dome (Perlberg & Caine, 1982). Interestingly, the most abundant adrenergic receptor in the bladder base is α_{1D} (Michel & Vrydag, 2006), α -adrenergic stimulation has been shown to cause contractile effects in the bladder, indicating a complimentary role of sympathetic norepinephrine release leading to relaxation of the dome, through β -adrenergic receptor stimulation and maintaining contraction of the base through α -adrenergic receptor stimulation. Physiologically this would serve to minimise reflux and keep the bladder in a storage phase. NANC mediated relaxation is likely mediated by nitric oxide (NO) as all subtypes of NO synthase enzymes have been found in the bladder. Its functional role in the normal healthy detrusor muscle has not been established due to mixed, subtle, responses to NO donors in various species compared to β -adrenergic agonist isoprenaline (Persson et al., 1993; Persson & Andersson, 1992). Similar to the distribution of adrenergic receptors, it has been shown that the bladder base and urethra have a different profile to the dome, when it comes to NO transmission. The major neurotransmitter for relaxation in the bladder base and especially the urethra has been postulated as NO via cGMP (Morita et al., 1992; Robertson et al., 1993).

Alongside neurotransmitter mediated myogenic activity, stretch activated non-specific ion channels are present in detrusor muscle cells, potentially acting as length detectors in the bladder wall. In studies using isolated mouse and rabbit urinary bladder myocytes a 20% mechanical elongation, termed as an increase in slack length, evoked single Ca²⁺ sparks and propagated Ca²⁺ waves. This Ca²⁺ was released from intracellular stores (Ji et al., 2002).

1.8 Pathology of GI dysfunction in PD

The GI tract is a very relevant system to investigate due to recent observations and hypotheses linking the brain and the gut in PD. Based on the distribution of Lewy bodies in postmortem tissue, a staging of the evolution of PD was formed by Braak et al., (2003). Braak's staging system correlates well with the clinical presentation of PD including the pre-motor/prodromal symptoms and identifies the DMV and the olfactory nucleus as the first stage of pathology in PD. The DMV of

the medulla is the site of parasympathetic efferents which innervate the enteric nervous system (ENS) of the GI tract (Phillips & Powley, 2007). Lewy bodies are also seen within the glossopharyngeal parasympathetic efferent projections, as well as their origins, the sacral parasympathetic nucleus. The sympathetic structures are also affected in PD with Lewy bodies observed in the sympathetic ganglia (Greene, 2011) and the intermediolateral column of the spinal cord (IML) (Braak et al., 2007).

Outside the central nervous system (CNS) abnormal α -synuclein has been shown to be present in the plexi and mucosal nerve fibres of the ENS. This has potential as a diagnostic biomarker, however more accessible sites such as the colon are not as sensitive, as studies have shown phosphorylated α -synuclein in healthy individuals. The existence of abnormal α -synuclein seems to follow a rostro-caudal gradient as it is absent in the submandibular gland of healthy individuals but present in the majority of PD patients tested (Visanji et al., 2014). This suggests that proximal tissue may have a more sensitive, disease specific, diagnostic potential.

Although the pathogenicity of Lewy bodies in the ENS is undetermined and even within the CNS controversial, they have been linked with neurodegeneration, whether they be causative or reactionary. Neurodegeneration can be seen in patients in the DMV (Gai et al., 1992) and sympathetic ganglia (Orimo et al., 2005), both areas involved in the control of the GI tract.

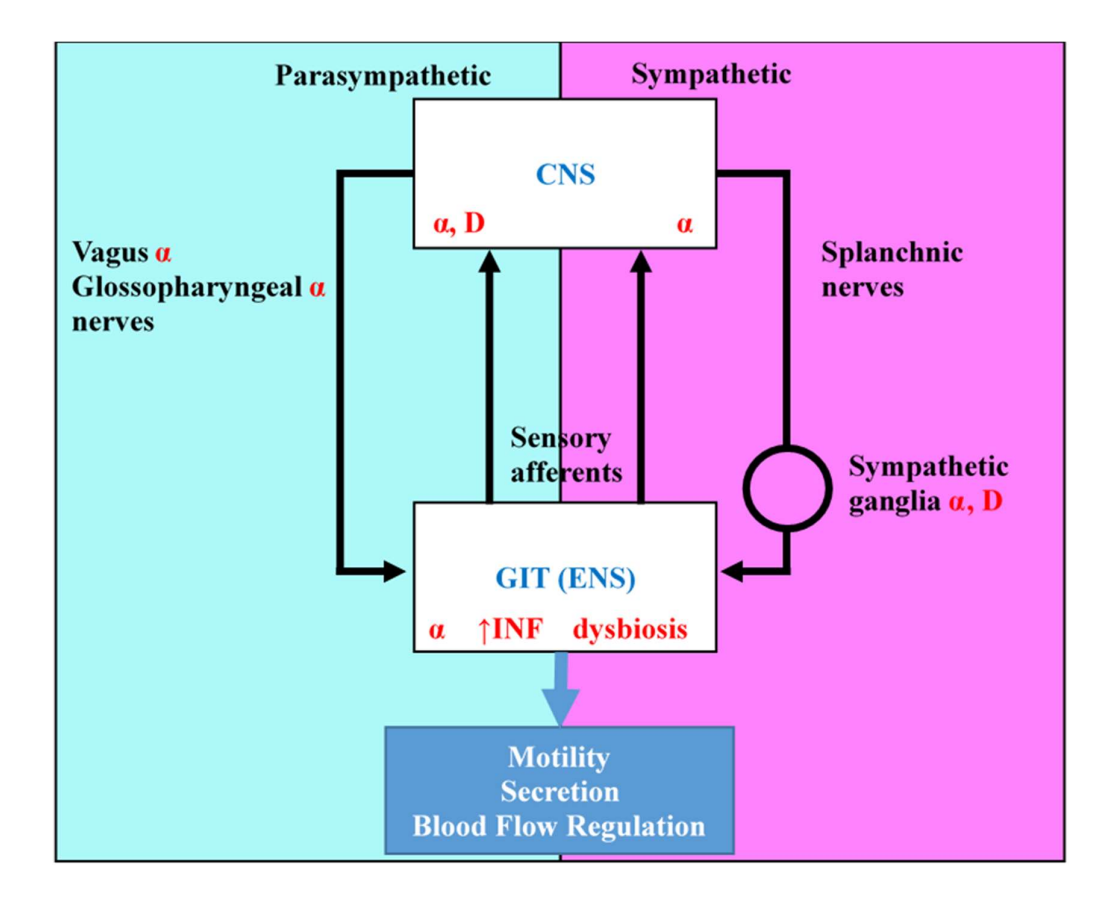


Figure 2 Pathological findings in connections between the CNS and the gastrointestinal tract (GIT) in PD patients.

A summary diagram of the pathology in PD relating to the gastrointestinal tract discussed in this chapter. Figure compiled from original articles and reviewed within Cersosimo & Benarroch, 2012; Warnecke et al., 2022 and Fasano et al., 2015. Abbreviations: ENS, enteric nervous system; α, α-synuclein; D, degeneration; INF, inflammation.

With the pathological evidence mentioned, Braak and colleagues hypothesised that an unknown pathogen initiates sporadic PD via the neurons of the nasal cavity and the neurons in the gut. From there, pathology spreads in a specific manner through the olfactory tract and the vagal nerve,

towards and then within the CNS (Cersosimo & Benarroch, 2012; Hawkes et al., 2007; Warnecke et al., 2022).

Studies in animals add further weight to this hypothesis, particularly the Dresden Parkinson model. Here, intra-gastric administration of the pesticide rotenone induced typical neuropathological changes of PD in mice. These mice were treated daily for 1.5 and 3 months with low doses, to avoid systemic effects. At 1.5 months α-synuclein aggregates were present in the ENS, IML and DMV and by 3 months aggregates were additionally observed in the SN dopaminergic neurons. At 3 months these mice also showed loss of SNpc neurons and motor deficits (Pan-Montojo et al., 2010). Orally administered rotenone has also been shown to induce similar pathology and behavioral deficits in a dose dependent manner (Inden et al., 2007). In another study, daily intranasal inoculation of MPTP led to reduction in tyrosine hydroxylase (TH) in the SNpc, striatal dopamine levels and motor activity with symptoms of tremor (Rojo et al., 2007). The pathology here is similarly distributed to that of Braak's patients.

Regarding the spread of pathology, the group that generated the Dresden model expanded their experiments and disrupted the parasympathetic and sympathetic connection between the ENS and CNS. Hemivagotomy and partial sympathectomy delayed the appearance of motor symptoms and prevented or reduced PD-like pathology in the IML, DMV and SN (Pan-Montojo et al., 2010). Proof of concept for α -synuclein propagation from gut to brain was shown by Holmqvist et al. (2014), in rodents using human PD patient α -synuclein. They injected α -synuclein into the intestinal wall of rats and showed its time-dependent appearance in the vagus nerve and DMV.

A population-based study in Denmark investigated the risk of PD in patients who had undergone a vagotomy, minimum 18 years prior to the follow up. They investigated two types of vagotomy and showed that full truncal vagotomy was associated with a decreased risk for the development of PD. Whereas, patients who underwent "super-selective vagotomy", resection of the nerves supplying the stomach only, had a similar risk to the general population (Svensson et al., 2015). The type of vagotomy is an important distinction for Braak's hypothesis, as super-selective vagotomy preserves

the nerve supply to the majority of the lower GI tract and the results suggest that the vagus nerve participates in the development of PD through the lower GI organs.

In terms of neurodegeneration, differences in neuronal density and differences in the neurochemical subtypes of the ENS remain unclear in PD. Some studies have found no differences in overall density in PD patients compared with controls (Annerino et al., 2012; Lebouvier et al., 2008) yet other studies, sometimes performed by the same group, show a decrease in the number of neurons per ganglia within the submucosal plexus (SMP) (Lebouvier et al., 2010) or a reduction in neurons expressing vasoactive intestinal polypeptide (VIP) in the SMP (Giancola et al., 2017).

1.9 Pathology of urinary dysfunction in PD

The pathology related to lower urinary tract symptoms (LUTS) in PD is thought to be due to the pathophysiology of the disease itself, namely nigrostriatal dopaminergic loss leading to basal ganglia dysfunction. It is proposed that the basal ganglia has an overall inhibitory action on micturition under normal circumstances and that overactivity develops due to basal ganglia impairment in PD. Much of this evidence is gathered from animal studies which will be discussed later but there is some patient correlation data that backs up this theory. Two studies looked at dopaminergic deficit via dopamine transporter single-photon emission computed tomography (DAT-SPECT) and showed a relationship between uptake of the radioisotope [1231]-FP-CIT and LUTS. In both studies, lower striatal [1231]-FP-CIT uptake was seen in groups of patients with urinary dysfunction and PD compared to those with PD but no urinary symptoms. This indicates that increased nigrostriatal degeneration is associated with PD with urinary dysfunction (Sakakibara, Shinotoh, et al., 2001; Winge et al., 2005). Interestingly, the loss of striatal dopaminergic neurones did not predict the effect of medication on bladder control in this study. Although some patients do gain benefit from dopaminergic therapy on their LUTS this does not occur in all patients, indicating that mechanisms elsewhere may be involved.

Although assessed in only a few patients, there are multiple reports of α -synuclein pathology in structures within and around the sacral dorsal roots of the spinal cord that receive afferent signalling

from the bladder and are likely involved in micturition (Del Tredici & Braak, 2012; VanderHorst et al., 2015). In one case degeneration was also observed in Onuf's nucleus which innervates the external urethral sphincter (O'Sullivan et al., 2009). No specific morphological or pathological findings have been assessed or observed in the bladder itself, although pressure-flow analysis has revealed "weak detrusor" during voiding in PD (Sakakibara, Hattori, et al., 2001). Altogether the pathogenesis of LUTS in PD is hypothesised to be nigrostriatal but it is still unclear why many patients do not find relief from dopaminergic therapy. Therefore, more work needs to be done to understand whether other central regions and/or local changes in PD contribute to LUTS.

1.10 Animal models of PD

Experimental models of any disease serve two main purposes; to allow us to gain insight into the mechanisms of the disease and for development of new therapeutic strategies. This is highlighted none more so than in PD, with the reserpine pharmacological animal model leading to the discovery of levodopa (L-DOPA). These seminal findings occurred in the late 1950's, and remains the gold standard until today (Carlsson et al., 1957).

Parkinson's disease research benefits from many different pre-clinical models, induced and developed by various routes, each displaying various aspects of the disease, however none have yet been successful in delivering clinical translation of disease modifying therapies. Here we summarise the most commonly used models, their pathology and their recapitulation of the symptoms of PD. The models that we will focus on in this introduction are in vivo models that can be induced via pharmacological agents or toxins as these are more relevant to our work. Various in vitro models (Slanzi et al., 2020), non-mammalian (Lim, 2010), genetically altered (Breger & Fuzzati Armentero, 2019) and α -synuclein based (Gómez-Benito et al., 2020) models have been useful in aiding our understanding of the disease but are better discussed in the respective review articles.

Table 2 Features of animal models of PD.

Methods of induction	Agents	Neurodegeneration	DA depletion	Motor deficits	Proteinous inclusions	Neuroinflammatory effects
Pharmacological	Reserpine Haloperidol	*	√ √	~	*	×
Neurotoxin	6-OHDA MPTP	* *	√ √	V	* ?	√
Glial activation	LPS	✓	✓	~	*	✓
Proteasomal inhibitor	Lactacystin PSI	✓	✓	√?	√	√
Pesticide	Rotenone	√?	✓	√	√	✓
Genetic Models	α-Synuclein	*	×	√	√	×
	LRRK2	×	✓	√	*	×

Compiled using information obtained from (Duty & Jenner, 2011). Abbreviations: 6-OHDA, 6-Hydroxydopamine; MPTP, 1-methyl-4-phenyl-1,2,3,6-tetrahydropyridine; LPS, Lipopolysaccharide; LRRK2, Leucine-rich repeat kinase 2.

Although there are many different models of PD via various mechanisms, the toxin induced models will be used for our experiments as they have been extensively researched pathology and are well established, reproducible models. As Table 2 shows, they are the model of choice due to their good construct validity and robust behavioural phenotypes.

1.10.1.1 Pharmacological models

The earliest and arguably the most impactful models of Parkinson's disease were those termed the "pharmacological models", in particular the reserpine model. The pharmacological models interrupt dopamine transmission either via depletion of monoamines or by antagonising dopamine receptors

using reserpine or haloperidol. They elicit transient behavioural deficits which when reversed indicate an agent's predicted benefit as a symptomatic therapy for PD. This was exemplified by ground-breaking works in the 1950's, where the "tranquillizing effects" and ptosis of the eyelid, induced by reserpine injection, were completely alleviated by the dopamine precursor L-DOPA, (Carlsson et al., 1957). The majority, if not all, the current dopaminergic therapies used to treat PD are effective in the reserpine model and many have shown efficacy in the haloperidol model, giving pharmacological models predictive validity for symptomatic therapies for PD.

The major drawback of the pharmacological models is the transient nature of the behavioural readouts and the lack of pathology, which means that they are not useful for understanding long term symptomatic relief nor can they be used to assess disease modifying therapies. More recently chronic reserpine dosing regimens have been utilised by a few labs to produce a decrease in the number of TH+ cells in the nigra and sustained motor and olfactory behavioural deficits. This potentially allows for a greater understanding of repeat dosing of symptomatic therapies as well as potential assessment of neuroprotective compounds. The repeat administration pharmacological model has not been widely utilised and leads to widespread, perhaps non-specific, TH+ve cell loss in the brain (Antkiewicz-Michaluk et al., 2014; Santos et al., 2013; Silva-Martins et al., 2021).

1.10.1.2 The 6-OHDA model of PD

6-Hydroxydopamine (6-OHDA), the hydroxylated analogue of dopamine, induces degeneration of dopaminergic neurons of the nigro-striatal tract via inhibition of the mitochondrial respiratory enzymes (Glinka & Youdim, 1995). 6-OHDA has high affinity for DAT and is transported into dopaminergic neurones through this transporter. Impairment of mitochondrial complex I and the uncoupling of oxidative phosphorylation are positively correlated with cell death in 6-OHDA treated animals. This effect appears dose dependent, implying that these are direct mechanisms of the neurodegeneration seen in this model (Kupsch et al., 2014). 6-OHDA can also directly generate reactive-oxygen species (ROS) through its own accumulation and auto-oxidation in the cytosol (Blandini & Armentero, 2012; Mazzio et al., 2004) within the cytoplasm leading to cell death.

Mitochondrial dysfunction, increased ROS, decreased antioxidant enzymes (Kunikowska & Jenner, 2001) and elevated levels of iron (Oestreicher et al., 1994) seen in the 6-OHDA model have also been observed in post-mortem analysis of the human disease (Jenner, 1989). Further similarities with PD include neuroinflammation in the form of nigrostriatal microgliosis and astrogliosis (Cicchetti et al., 2002; Mogi et al., 2000) and striatal dopamine depletion (Thomas et al., 1994). As well as displaying mitochondrial dysfunction, the 6-OHDA model has been shown to have impairment of autophagy, with reduced LAMP1 expression and lysosomal protease activity (He et al., 2018). The model does not capture all the features of PD, in particular the hallmark of PD; Lewy bodies, do not develop after administration of 6-OHDA. Degeneration in PD occurs in other brain regions, such as the noradrenergic neurons of the Locus coeruleus (Braak et al., 2003), however pathology in this model is mostly restricted within the nigrostriatal tract on the whole. (Duty & Jenner, 2011; Vieira et al., 2019). There have been the odd report of increased firing patterns in areas outside the basal ganglia and noradrenergic deficits in the cortex and striatum of a bilateral lesion model but the reports are sparse and likely dependent on injection site and regime (Paredes-Rodriguez et al., 2020; Lama et al., 2021).

6-OHDA cannot cross the blood brain barrier and thus induction of the model requires stereotaxic surgery and injection directly into the brain, which has been highlighted as a drawback. However, this does present the opportunity to study PD with a multifaceted approach in conjunction with peripherally administered toxins (discussed below) and compare to the centrally administered 6-OHDA. Injection is usually performed unilaterally as increased welfare considerations are needed with bilateral lesions due to the development of severe aphagia and adipsia (Ungerstedt, 1971a). Unilateral lesioning also allows for the contralateral hemisphere to be used as an internal control in pathological evaluation and results in several behavioural phenotypes useful for the development of symptomatic therapies. The motor dysfunction exhibited in the 6-OHDA model, when administered unilaterally, is mostly focused on the extent of the lesion. This can be assessed by impaired use of the contralateral forelimb, asymmetric posture and rotational behaviour (Betts et al., 2012). Contralateral rotational behaviour is produced by administration of apomorphine which acts post-synaptically on dopamine (DA) receptors which are hypersensitive in the denervated striatum

(Ungerstedt, 1971b). Ipsilateral rotations can be seen when amphetamine acts pre-synaptically stimulating DA release and blocking its reuptake to a greater degree in the non-lesioned side (Ungerstedt, 1971c). Behavioural readouts that can be attributed to non-motor symptoms of PD also exist within the 6-OHDA model. GI and bladder dysfunction will be discussed in more detail throughout this thesis, but animals lesioned with 6-OHDA have also been shown to exhibit sleep disturbances (Vo et al., 2014), impaired olfactory discrimination (Bonito-Oliva et al., 2014) and cognitive deficits (Grospe et al., 2018).

Ultimately, stereotaxic injection of the toxin causes rapid degeneration of SNpc, which is unlike the slow progression of the human disease. This suits the model more towards pathophysiological evaluation and the development of symptomatic therapies rather than neuroprotective agents, although partial lesions can be produced for this purpose (discussed in more detail in Chapter 5.1).

1.10.1.3 MPTP

1.10.1.3.1 The MPTP mouse model

MPTP was discovered as a toxin which induces parkinsonian symptoms in man when a group of patients were admitted to hospital after using a "synthetic heroin" intravenously. The drug samples were found to contain MPTP amongst other constituents. These patients exhibited classic Parkinsonian features which responded to L-DOPA therapy (Langston et al., 1983). These observations led to its use in rodents and primates as a model of PD. Upon crossing the blood-brain-barrier it is converted to a toxic metabolite 1-methyl-4-phenylpyridinium (MPP⁺) and transported by the Dopamine uptake transporter (DAT) into nigrostriatal dopamine nerve terminals. Accumulation of cytoplasmic MPP⁺ leads to the impairment of mitochondrial respiration and oxidative damage of mitochondria, due to an increased release of glutamate, free Ca²⁺ and reactive oxygen species (ROS). The combination of the reduced adenosine tri-phosphate (ATP), due to mitochondrial damage, and increase ROS leads to apoptosis of the affected neurons (Pfeiffer et al., 2004).

Rats are unaffected by MPTP, however systemic administration in specific strains of mice, particularly the C57 strain, causes bilateral degeneration in the nigrostriatal tract and significant loss

of striatal dopamine. Cell death begins rapidly, 12-72 hours after administration (Duty & Jenner, 2011), again unlike PD. It does however follow a pattern similar to that seen in patients, with the ventral tegmental area (VTA) affected less than the SNpc (Hung & Lee, 1996). Construct validity of this model is shown also by the biochemical features shared with PD including, reduced glutathione (GSH) in the substantia nigra (SN) (Ferraro et al., 1986).

As with the 6-OHDA model, proteinaceous inclusions are not commonly observed in the MPTP mouse model. Of note, two groups have shown α-synuclein aggregates in models with differing administrations of MPTP (Fornai et al., 2005; Meredith et al., 2002), however later studies failed to replicate these findings with the same protocols (Alvarez-Fischer et al., 2008; Shimoji et al., 2005). It also seems that the MPTP mouse model is not useful to model proteasome dysfunction in PD, even though it has been shown to display reduced proteasome activity in some dosing regimens (Fornai et al., 2005). Proteosome inhibitors do not worsen MPTP induced toxicity but in fact in some studies can alleviate it (Kadoguchi, Kimoto, et al., 2008; Kadoguchi, Umeda, et al., 2008; Oshikawa et al., 2009). An important mechanism in the effects of MPTP in the mouse is neuroinflammation, presented as increased microglial activation, astrogliosis, lymphocyte infiltration and an increase in pro-inflammatory cytokines in the SNpc (Furuya et al., 2004; Kurkowska-Jastrzębska et al., 1999, 2009).

MPTP treated mice display hypokinesia measured by a decrease in locomotion tests, such as in pole tests and open-field assays (Arai et al., 1990; Fredriksson et al., 1999). Another indicator of locomotor abnormalities is nest building, a natural behavioural. That has been shown to be impaired in MPTP treated mice (Sedelis et al., 2000). Tremor has also been observed in MPTP mice. One elegant method uses sensor platforms and frequency analysers to distinguish sessions of tremor and session of normal movement (Lee & Lu, 1995). Indications of non-motor symptoms in the MPTP mouse model have been observed in various forms such as, longer latency to buried food retrieval and sniffing time for food, indicating deficits in olfaction (Biju et al., 2018; Han et al., 2021; Schintu et al., 2009). Impaired nesting behaviour can infer distress and lack of motivation and is seen in some studies in MPTP treated mice alongside other indications of anxiety, depressive like

58

behaviours and altered cardiovascular function (Biju et al., 2018; Liu et al., 2020; Santiago et al., 2010; Sedelis et al., 2000).

The main drawback of the MPTP mice model over centrally administered toxin models such as the 6-OHDA model, is its reproducibility and ability to produce behavioural readouts. With so many dosing regimens and variable pathology produced it becomes difficult to compare studies. Even with the same dosing regimen results can sometimes differ.

1.10.1.3.2 The MPTP Primate model

The non-human primate (NHP) is more sensitive to MPTP treatment than lower species, showing reliable efficacy in destruction of dopaminergic neurons in the SN and rapid onset of parkinsonian symptoms. Like the MPTP mouse model, the pathology in the NHP MPTP model is not progressive. Neuroinflammation is active in this model with reactive microgliosis and astrocytosis measured by elevated HLA-DR and glial fibrillary acidic protein (GFAP) intensity and cell number in the substantia nigra (Barcia et al., 2004; Kanaan et al., 2008). Many studies have shown extranigral pathology in the NHP MPTP model, including locus coeruleus lesions, loss of serotonin in various regions (Forno et al., 1986; Mitchell et al., 1985). This can vary depending on the type of NHP and the dosing regimen (Pifl et al., 1991). MPTP treated marmosets do not exhibit Lewy bodies nor do they show degeneration in other regions of the brain, affected in PD, such as the dorsal motor nucleus of the vagus (DMV) and raphe nuclei (Duty & Jenner, 2011).

Classically, the animals have marked motor dysfunction early after MPTP administration including akinesia, bradykinesia rigidity and postural abnormalities, which recover after some weeks to a more stable motor deficit state (Albanese et al., 1988). Motor abnormalities are only significant in animals with substantial lesions, similar to the state in the human (Phillips et al., 2017). Tremor can also be present but only in some species of NHP and the frequency and duration of episodes can be variable (Bergman, Raz, et al., 1998). The advantage of the NHP over the rodent MPTP induced models is the ability to use similar rating scales as those used in human patients for motor and NMS, however this is not uniformly applied or agreed upon in NHP research (Imbert et al., 2000).

Apart from gastrointestinal and urinary dysfunction (discussed in detail later), NMS of PD are also exhibited by the model, with MPTP treated marmosets suffering from sleep disturbances (Barraud et al., 2009), psychosis-like behaviours (Visanji et al., 2006) and cognitive impairment (Pessiglione et al., 2004; Slovin et al., 1999).

Where this model excels, is the pharmacological insights gained from it and its predictive validity. Specifically in relation to dopaminergic therapy, anti-muscarinic agents and combination therapies such as monoamine oxidase type B (MAO–B) and catechol-O-methyl transferase (COMT) inhibitors (Duty & Jenner, 2011).

As well as efficacy, treatment strategies and the pharmacological actions of L-DOPA can be investigated in this model due to the induction of dyskinesia after repeat exposure to L-DOPA. The dyskinesia presents as chorea, dystonia and athetosis, as in man, and can be measured using rating scales validated in man (Langston et al., 2000). The model is responsive to amantadine (Blanchet et al., 1998) and shows that continuous dopaminergic stimulation via alternative therapeutic strategies results in less dyskinesia (Stockwell et al., 2009), as has been shown in humans (Wirdefeldt et al., 2016).

However, due to the models inability to recapitulate the full pathology of the disease, there have been notable failures in translation of efficacy in clinical trials for monoamine uptake inhibitors (Hauser et al., 2007) and non-dopaminergic therapies (Goetz et al., 2007).

1.10.2 Gastrointestinal and urinary dysfunction in animal models of PD

With symptoms which impact so greatly on quality of life and the overwhelming evidence of link of PD to the gut, animal models are sought after to not only expand our knowledge of the pathways of GI dysfunction in PD but to aid discovery of therapeutics.

Currently work is focused on using established animal models of PD to look at functional, neurochemical and molecular alterations in the GI system. With the models initially defined by, or developed based on, motor symptoms and/or pathology, the presence of a second set of symptoms

would provide a more holistic model rather than the "one symptom – one model" approach currently dominating pre-clinical research and therapy as a result.

Being a model of PD, rather than causing PD in an animal, there are various types, with their own advantages and disadvantages, as discussed previously. Furthermore, within the same model different methods are used regarding dosing regimens, concentrations etc. with varied results. Nevertheless, alterations in the gastrointestinal system of PD animal models are present. Apart from the few works with animal models mentioned previously regarding pathology in the oesophagus and stomach, the majority of studies have focused on the bowel, possibly due to constipation being a common debilitating symptom. Findings from animal model studies looking at the small and large intestine are summarised below.

1.10.2.1 The small Intestine

There have been few functional studies undertaken looking at the small bowel. One such study used administration of a dye and monitored the distance travelled at a given time point. It was determined that there was no alteration in transit in an MPTP mouse model of PD (Anderson et al., 2007). In the 6-OHDA model the intensity of labelling and the homogeneity of labelling in the caecum, 10 and 12 hours after BaSO4 gavage, was significantly lower 8 weeks post lesion induction compared to than controls, indicating a slow transit in the small bowel (Fornai et al., 2016).

Changes at the cellular level have been shown, although overall neuron density/ cell number in the ENS segments analysed in both rat and mouse models were maintained (Colucci et al., 2012; Toti & Travagli, 2014). The protein make up of these cells did differ from control samples. In MPTP mice multiple studies observed a significant decrease in dopaminergic neurons positive for Tyrosine Hydroxylase (TH) in immunohistochemical analysis of the ileum (Anderson et al., 2007) and the duodenum (Natale et al., 2010) myenteric and submucosal plexus. To complement this, western blot analysis showed a decrease in TH protein levels in the duodenum (Tian et al., 2008). Another dopaminergic neuron marker is the dopamine transporter protein (DAT). Natale et al. (2010) reported a reduction in DAT positive cells and dopamine monoamine content, in the duodenum of

MPTP treated mice, using HPLC methods. However another study monitored DAT protein expression and found no significant difference to controls, although they did note alteration in the mRNA expression of DAT (Tian et al., 2008). Tian et al., (2008) used a sub-acute protocol over 7days compared to the more aggressive, acute protocol used by Natale et al., (2010) which may be the cause of the different results.

In contrast, the 6-OHDA rat model of PD shows upregulation of dopaminergic neuronal markers in the duodenum of the small intestine. Tian et al. (2008) observed increased TH and DAT positive cells and protein content. With the two models being so different in terms of induction of PD, species and time frame, it is possible that this may lead to such differences in expression. Unfortunately, in the case of TH+ve, neurons others have been unable to find much evidence for their presence in the small bowel (Colucci et al., 2012; Toti & Travagli, 2014) and dopamine concentrations in the ileum were not significantly different to sham-operated controls (Levandis et al., 2015).

When looking for expression of inhibitory neurons, the MPTP model showed no significant changes in the expression of nicotinamide adenine dinucleotide phosphate (NADPH) positive neurons. Neuronal NOS (nNOS) is the responsible isoform of NOS for the production of nitric oxide (NO), one of the major inhibitory neurotransmitters involved in gut motility (Lundberg & Weitzberg, 2013). In the distal ileum 60HDA administration altered the intrinsic inhibitory pathways of the ENS. Although the percentage of cells expressing nNOS decrease, (Blandini et al., 2009; Colucci et al., 2012) those expressing VIP, another inhibitory molecule, significantly increased (Colucci et al., 2012). This suggests that a compensatory mechanism was at play to maintain the inhibitory population of the ENS, with no differences in choline acetyl-transferase (ChAT) positive, excitatory neurons. This change was selective to the distal portion of the ileum but not present in proximal ileum. In fact others have shown an increased percentage of nNOS positive neurons and decrease in ChAT positive cells more proximally, in the duodenum (Toti & Travagli, 2014). This occurred with the total count of neurons in the duodenal myenteric plexus unaltered, meaning that the duodenum may be in a state more prone to inhibition.

Together, this suggest that models of PD have alterations in control of inhibition, however it is dependent on bowel region and model induction. It is an area that is under-researched and although the data is promising it is not entirely consistent.

1.10.2.2 The large intestine

Functional assessments are much more prominent in the literature regarding the large intestine, due to constipation being a prevalent GI symptom in PD. Contrary to PD in humans Anderson et al. (2007) showed a significantly higher stool frequency in a 1-hour stool output assay 3 days after MPTP administration which normalised by 8-10 days similar to controls. However, another MPTP study found a reduction in the total stool output daily, 48 hours post treatment and a reduction in colonic transit using the bead expulsion assay (Natale et al., 2010). The protocol of induction of PD was similar in these two studies, however the subtlety in the different assays of measuring transit may shed light on the opposing outcomes. Additionally, Anderson et al. (2007) points to dysfunction in a subpopulation of inhibitory ENS neurons, in their study, in which the MPTP tissue displayed impaired relaxation when exposed to EFS and incubated with atropine.

The 6-OHDA model shows a degree of consensus between different studies in terms of impaired colonic motility resembling constipation. Daily faecal output has been shown to be significantly reduced in weeks 3 and 4 post lesioning (Blandini et al., 2009). Results of the 1-hour stool assay also showed a decrease in stool weight and water content. This indicates a longer transit time in the large bowel resulting in more absorption of water from the faeces (Zhu et al., 2012). Radiographic examination 10 and 12 hours post BaSO₄ dye administration, showed a delay in transit of the medium within the large intestine 4 weeks post-surgery. This was even more apparent 8 weeks post lesion (Fornai et al., 2016). In response to EFS, colonic tissue displayed reduced contractile activity and efficiency (Fornai et al., 2016). This correlates well with spatiotemporal analysis which show a series of contractions initiating at different sites at the same time rather than the normal well-defined single completed wave. This resulted in multiple, incomplete peristaltic events, with a reduced average peak pressure in one peristaltic period (Colucci et al., 2012). All together this infers that colon emptying requires more time and effort in the centrally lesioned animals, due to

slower, uncoordinated and less-defined peristaltic waves. However, Levandis et al. (2015) found a small but significant increase in the frequency of peristalsis, observing that the threshold volume required to trigger a peristaltic event was significantly reduced.

Following the pattern of the small intestine the colon samples of the MPTP model show decreased TH protein levels (Tian et al., 2008), whereas in the 6-OHDA model an increase in TH positive cells is observed along with more TH protein detected in western blot assays (Tian et al., 2008; Zhu et al., 2012). Likewise, dopaminergic neuron number increases in the 6-OHDA colon measured by an increase in DAT positive cells (Tian et al., 2008). The D₂ dopamine receptor (D2R) when activated, mediates the inhibition of peristaltic activity. However, when Levandis et al. (2015) incubated the colon from 6-OHDA rats with a D2R agonist peristaltic activity did not diminish. This is likely due to the detected lower percentage of D2R expressing cells present in some studies (Colucci et al., 2012; Levandis et al., 2015).

In the proximal colon, central lesioning alters the inhibitory/excitatory balance of the ENS much like that seen in the small bowel. The percentage of cells expressing nNOS decrease, (Blandini et al., 2009; Colucci et al., 2012; Zhu et al., 2012) yet those expressing VIP significantly increased (Colucci et al., 2012), maintaining the inhibitory population of the ENS, with no differences in ChAT positive excitatory neurons (Zhu et al., 2012). The opposite is the case in distal colon, where no differences in the above mentioned inhibitory markers are found but a decrease in the percentage of ChAT positive cells are seen in the myenteric ganglia (Fornai et al., 2016). Functional studies from Fornai et al. (2016) also found reduced ACh release upon EFS and an upregulation of M₂ and M₃ muscarinic receptors, in response to the impaired cholinergic transmission.

Rotenone has been used less extensively to investigate GI dysfunction in PD models. Delayed gastric emptying, decrease in stool frequency and delayed overall gastric transit have been observed in a few studies (Arnhold et al., 2016; Drolet et al., 2009; Greene et al., 2009). Greene et al. (2009) also notes an inhibitory response deficit in the colonic ENS, much like that seen in MPTP treated mice (Anderson et al., 2007). In contrast to the majority of studies in other animal models, ENS neuron density decreased significantly, in one study at 3 days and 6 months (Drolet et al., 2009).

Interestingly, most of the animals showed no sign of motor abnormalities, nor was there any neurodegeneration in the CNS. The presence of gastrointestinal dysfunction and increased α -synuclein pathology (Drolet et al., 2009) within the gut of these rotenone treated mice may relate to the pre-motor phase of PD.

Colonic dysmotility in PD models, is again inconsistent. Regional differences and differences between groups make the overall picture unclear. Differences in chemical coding of neurons and neurotransmission are poorly understood and require further investigation.

1.10.2.3 The bladder

With the focus of the bladder dysfunction in PD regarded mostly as centrally mediated dysfunction, most animal studies have been performed in live, conscious or anaesthetized animals. Not only have they contributed further to our understanding of LUTS in PD but also in understanding micturition physiology e.g. the role of SN in normal micturition.

The first works on bladder function performed in animal models of PD used MPTP treated NHPs. Cystometric assessments in MPTP treated marmosets showed spontaneous contractions during filling of the bladder at very low thresholds compared to control animals, indicating hyperreflexia (Albanese et al., 1988). MPTP treated cynomolgus monkeys also exhibited maximum intravesical pressure (bladder contraction), at a significantly lower volume threshold than control animals. This group showed that in normal animals, D₂ dopamine agonists cause a reduction in bladder volume threshold in both groups however D₁ receptor agonism could increase bladder volume thresholds only in MPTP treated animals (Yoshimura et al., 1993, 1998). Therefore, potentially in the PD state D₁ agonism may be therapeutic for OAB.

Interestingly more recent assessments of bladder function were performed in isolated tissue from MPTP treated marmosets that had an 80% loss of SNpc neurons compared to control treated animals. This study revealed increased spontaneous and electrically induced contractility in tissues from the MPTP treated bladder segments compared to control tissues, for the first time showing that local changes can occur in the bladder upon nigrostriatal neurodegeneration in this model. This was

deemed to be due to an enhanced non-purinergic, non-cholinergic contractile component as desensitization of purinergic receptors and atropine did not abolish the difference seen (Pritchard et al., 2017).

Unilateral or bilateral lesions of 6-OHDA have been used as a popular model of PD with bladder dysfunction. The assessments in the literature have always administered 6-OHDA into the MFB, which as mentioned previously leads to a near complete loss of dopaminergic neurons in the SNpc and the associated fibers in the striatum. Again, most assessments have focused on in life cytometry experiments revealing reduced bladder capacity, voiding volume, voiding efficiency, voiding threshold and various other urodynamic parameters due to increased contractile activity (Praveen Rajneesh et al., 2020; Rajneesh et al., 2023; Soler et al., 2011, 2012; Yoshimura et al., 2003). Additionally one study showed abnormal external urethral sphincter electromyographic activity concurrent with the abnormal bladder contractile responses (Rajneesh et al., 2023). Similarly, to their work in non-human primates Yoshimura et al., 2003 postulate that a D₁ receptor agonist may prove beneficial to reduce OAB in PD. An adenosine A2A receptor antagonist was also shown to suppress bladder overactivity in this model and as mentioned has been subsequently shown to have some efficacy in a clinical trial (Kitta et al., 2012).

One study to date has looked at the local detrusor muscle function from animals treated with 6-OHDA. They saw increased contractile responses of isolated tissues in the presence of high potassium, high concentration of methacholine and ATP and when stimulated via EFS. Some of these changes were attributed to hypertrophy of the bladders of 6-OHDA treated animals in this study but also alterations in cholinergic and purinergic signaling sensitivity, not seen in other studies when assessed previously (Mitra et al., 2015).

Overactivity of the urinary system has been seen consistently in animal models of PD, although the mechanisms by which this occurs is less clear. Changes have been seen which are potentially both locally and centrally driven, although these studies have been performed in animals with established substantial lesions.

1.11 The K_V7 Channel

The Kv7 channels are relatively unexplored in the are of PD but exhibit expression profiles in preclinical species in organs and regions of interest for our investigations in to gastrointestinal and urinary dysfunction in PD.

Voltage-gated potassium channels of subfamily 7 encoded by KCNO genes, the K_v7 family, consists of five members $K_v7.1-5$. First characterised in the 1980's in CNS neurons, they were termed the "M-Channel" as they were responsible for outwardly rectifying K⁺ currents that could be suppressed by muscarinic receptor activation (Brown & Adams, 1980). The "M-current" activates relatively slowly at subthreshold potentials contributing to the resting potential and supressing repetitive firing rather than impacting upon the repolarization of action potentials in the neuronal cell. Neuronally, the inhibition of the M-current via muscarinic receptor activation, acts through G_q stimulation of phospholipase Cβ (PLC) which catalyses the hydrolyses phosphatidylinositol-4,5bisphosphate (PIP₂). PIP₂ hydrolysis produces inositol-1,4,5-trisphosphate (IP₃) and diacylglycerol (DAG) second messenger systems which in their own right could lead to the inhibition of the Mcurrent. However, two elegant studies have shown that PIP₂ itself is required for the K_v7 channels to enter an open state and therefore its removal is inhibitory. In seeking to pin down a specific regulator of KCNQ channels Suh et al., (2006) rapidly depleted PIP2, bypassing PLC, without affecting IP₃ and DAG and Ca²⁺and still observed current suppression. Conversely, a 30% increase of the M-current was shown when PIP₂ was overproduced. Phosphatidylinositol-4-phosphate-5kinase (PI5K) is the final stage in the cascade of PIP₂ production and its overexpression also led to a reduction of the inhibitory action of muscarinic receptor activation on the KCNQ current (Winks et al., 2005, p. 200).

Outside of the CNS, $K_v7.1$ channels play important functional roles in cardiomyocytes and $K_v7.2-5$ are involved in vascular and non-vascular smooth muscle control, in which $K_v7.4$ and $K_v7.5$ predominate. In the heart $K_v7.1$, along with the potassium voltage gated channel subfamily E regulatory subunit (KCNE) encoded auxiliary subunit KCNE1, plays a role in the repolarizing phase of the action potential, underlying I_{ks} (Barhanin et al., 1996; Sanguinetti et al., 1996). The I_{ks}

is responsible for late phase ventricular repolarisation, delays in this current, often caused by mutations of KCNQ1 and KCNE1, lead to severe arrhythmias and sudden death due to the prolongation of the QT interval (Wang et al., 1996).

Pharmacological modulation of K_v7 channels in the vasculature produce changes in smooth muscle membrane potential and vascular tone. Blocking these causes depolarization of the muscle cell and Ca²⁺ influx through L-type Ca²⁺ channels resulting in vasoconstriction (Joshi et al., 2006). Activation of these channels by Retigabine (Kv7.2-5 channel activator), caused membrane hyperpolarisation and relaxation of preconstricted vascular tissue, unless the preconstruction was performed by raised extracellular K⁺ (Joshi et al., 2009). The effects of modulation of these channels have been shown on many rodent vascular tissues (reviewed in Jepps et al., 2013) but importantly this has been translated to human arteries as well. Contraction of human arteries occurred when K_v7 channels were blocked, and activation of the channels relaxed pre-contracted arteries. This effect was reversible by specific K_v7 blockers but not the non-specific K⁺ channel blocker 4-aminopyridine (Ng et al., 2011).

Transcripts of KCNQ and KCNE have been detected in the stomach, small and large bowel with KCNQ4 and KCNQ5 expression dominating in all the tissues as well as KCNE4. These tissues also showed expression of K_v7.4 and K_v7.5 protein through western blot analysis. The same group performed functional assays to examine the effect of the K_v7 channel on gastrointestinal tissue based on contractility of the tissue using a myograph (Jepps et al., 2009). They showed that opening the channels caused a decrease in spontaneous contractile activity and channel blockade increased this activity. Kv7 subtypes have also been visualised and shown to be functionally active in sensory neurons present in human and mouse bowel tissues. Kv7 channel activation attenuated visceral afferent firing evoked by bradykinin and the responses to mechanical stimulation of the bowel following noxious distension (Peiris et al., 2017). This indicates that Kv7 modulation may be useful for treating motility disorders and visceral pain arising from the gastrointestinal organs.

Considerably more work has been performed to understand the role of Kv7 channels in the bladder. In vivo experiments in conscious rats, monitored by cystometry, revealed that administration of the

Kv7 channel activator, Retigabine, inhibits bladder activity. Interestingly this inhibition can occur when Retigabine is administered centrally (intracerebroventricularly) or locally (intravesically). This indicates the Kv7 channel's expression in the CNS and in the bladder has a role in micturition (Streng et al., 2004). The effects on voiding frequency and micturition volume were blocked by Kv7 channel blocker Linopirdine. Assessments in anaesthetised rats revealed that i.v Retigabine reduced the frequency and amplitude of rhythmic bladder contractions via inhibition of afferent nerve fibre firing as well as direct action on the detrusor smooth muscle (DSM) (Aizawa et al., 2017). Protein expression assessments and single cell electrophysiology studies on DSM confirm the functional presence of the various subtypes of Kv7 channels in the rodent, with expression in a similar rank order of expression as in the human DSM (Malysz & Petkov, 2020). This and other evidence has led to interest in Kv7 channel modulation in the treatment of overactive bladder, although the use of current Kv7 channel openers have been hampered due to unexpected side effects in humans (Brickel et al., 2012; Michel et al., 2012).

1.12 Aims of the investigation

Non-motor symptoms of PD have historically been under-recognised and under-researched due to the dominance of the largely dopaminergic clinical presentation of motor symptoms. Understanding whether the NMS are not just due to the adverse effects of medication but also that they have a physiological basis to them and uncover some of these targets will aid new therapies. Research into NMS will aid the development intervention to improve quality of life but also potentially identify biomarkers and increase the understanding of "at risk" populations to enable earlier intervention.

Experimental models can help us to gain insight into the mechanisms of a disease and understand changes that occur due to a pathology which if translatable can aid the pursuit of therapeutics. Whilst not being the disease itself, animal models can show validity when sharing similarities with the human condition. We have chosen to use different models of Parkinson's disease in different animals to see if we can find common changes in their pathology which may lead to GI dysfunction. We have looked at models with differing extents of pathology, as NMSs are present at various stages of the disease. This will hopefully enable future assessments to be performed in human

samples based on our findings and lead to a translational path from pre-clinical to clinical therapeutic interventions.

Literature evidence in this area is often inconsistent and not reproducible even in the same model performed by different groups as illustrated in the introduction. For the most part we have limited our investigations to centre around the characterisation of the Kv7 channel in the urinary and gastrointestinal tract and the assessment of changes in its expression and function in our different models of PD. The interest in the Kv7 channels stems from their expression in dopaminergic neurons of the SNpc combined with their expression in the organs where NMS in PD are observed, namely the bladder and GIT. Our work has focussed on evaluation of overt local adaptive changes that may occur as a result of central dopaminergic loss, using various ex vivo assays. Therefore, we have also explored standard pathways of urinary and gastrointestinal function by interrogating myogenic and neurogenic function such as the cholinergic and nitrergic pathways. As mentioned, previous works have demonstrated changes in the contractile smooth muscle of the gastrointestinal and urinary system in models of PD, without a clear mechanistic link. We hypothesise that the Kv7 channels, may play a role in this dysfunction as they are pivotal channels in the hyperpolarisation of smooth muscle cells.

To address this topic, the aim of each of the following experimental chapters is below:

Chapter 3: Characterisation of the role and distribution of Kv7 channels in gastrointestinal tissues and motility of the mouse.

Chapter 4: To compare ex vivo motility patterns of the ileum and colon from mice treated with MPTP and naïve controls, with a focus on Kv7 modulation.

Chapter 5: To compare ex vivo contractility patterns and protein expression in the bladder, ileum and colon from rats treated with 6-OHDA with sham and naïve controls, with a focus on Kv7 modulation.

Chapter 1: Introduction

Chapter 6: To investigate the expression of Kv7 channels in the brain, GIT and bladder of MPTP treated marmosets compared with naïve controls.

2 METHODS

2.1 Animal Models

2.1.1 MPTP mouse model (Sub-acute MPTP dosing regimen)

All experimental procedures were conducted with the University of Hertfordshire local ethical committee approval and in accordance with the UK Animals (Scientific Procedures) Act, 1986 (National Archives, UK Animals, Scientific Procedures Act, 1986).

Due to MPTP being a highly toxic lipophilic agent, extreme precaution was taken when preparing and dosing the animals with MPTP. Mice were randomly assigned to either the sham group or the treatment group upon arrival.

The experimental group received a sub-chronic dosing regimen of MPTP over 5 days (7x 18mg/kg of MPTP·HCl) (n=10). The sham group received the same number of injections to that of the MPTP group but with saline (0.9% NaCl, 150uL), over the same period (n=8) similar to previously published protocols (Jackson-Lewis & Przedborski, 2007; Tatton & Kish, 1997).

On the first day of dosing mice were moved into a disposable plastic cage on top of a stainless-steel heating bench which had a 50/50 heating element beneath the surface. This heated one half of the cage to 28-31°C, and the other half remained at ambient temperature (23-25°C). Mice could therefore choose to regulate their own body temperature by moving between to different parts of the cage when necessary, thus reducing the possibility of succumbing to MPTP induced hypothermia (Przedborski et al., 2001). After the last dose of MPTP or saline mice were then left in the semi-heated disposable plastic cages for a 5-day washout period to allow for all MPTP to be metabolised or excreted before they were placed back into their original cages. This was to ensure minimal staff contact with MPTP or its metabolites and removal of cages in their entirety as hazardous waste.

2.1.2 6OHDA rat model

All work to generate, maintain and assess this model in life was performed at King's College London by the Neurodegenerative Diseases Research Group, KCL. We were kindly given tissues from these animals at termination for our ex vivo analyses, to further our understanding of Kv7 channels in animal models of PD.

All experimental procedures were conducted with local ethical committee approval (King's College London) and in accordance with the UK Animals (Scientific Procedures) Act, 1986 (National Archives, UK Animals, Scientific Procedures Act, 1986).

Animals were anaesthetised with a mixture of halothane (3–5% for induction, 1–1.5% for maintenance) and 95% $O_2/5\%$ CO_2 . While maintained under halothane anaesthesia, rats were placed in a Kopf stereotaxic frame (Tijunga, USA) with the incisor bars set at -3.3 mm. The animal's body temperature was measured using a rectal probe and the body temperature was maintained at 37 ± 1 °C using a thermostatic heating blanket underlying the animal. After removal of connective tissue, a 2-mm diameter burr hole was made on the appropriate location using a hand drill.

6-OHDA was injected into the left striatum (AP, +0.2mm; ML, +3.0mm; V, -5.5mm from the dura) of rats to create a partial lesion model of PD similar to previously published protocols (Penttinen et al., 2016; Sauer & Oertel, 1994). Four different groups of animals were used in this study uninjected controls, sham treated controls, 12μg 6-OHDA and 24μg 6-OHDA.

2.1.3 MPTP marmoset model

All work to generate, maintain and assess this model in life was performed at King's College London by the Neurodegenerative Diseases Research Group, KCL. We were kindly given tissues from these animals at termination for our ex vivo analyses, to further our understanding of Kv7 channels in animal models of PD.

All experimental work was carried out in accordance with the Animals (Scientific Procedures) Act 1986 approved by the Kings College London Ethical Review Committee. The primate experiments

reported were carried out under a Home Office Project Licence (PPL 70/4986) approved by the King's Ethical Committee which complied fully with the guidelines and recommendations set out in the Weatherall Report 2006 for the use of non-human primates in research (https://royalsociety.org/policy/publications/2006/weatherall-report/).

Marmosets were treated with MPTP (2 mg/kg) subcutaneously administered for 5 consecutive days according to previously published protocols (Jackson et al., 2007; Smith et al., 1996). These animals were used in other studies, where the symptomatic effects of various dopamine agonists were examined. MPTP treatment was administered several years prior to the collection of these samples and therefore any effects seen in the peripheral organs from this study can only be due to long term pathological effects of nigrostriatal degeneration and not acute effects of MPTP on the periphery.

All marmosets were kept in home cages in pairs with dimensions: $166 \times 140 \times 90$ cm at an ambient temperature of $25^{\circ} \pm 1^{\circ}$ C. Animals were housed in a 12h light/dark cycle and were fed once daily with a diet of bananas, oranges and apples with free access to food pellets (Mini Marex–E; Special diet Services) and drinking water. The animals were originally housed and used at the Neurodegenerative Disease Research Centre at King's College London.

The animals' environment was enriched by installation of a viewing turret on top of the cages to mimic height as would be the case in a normal habitat. Enrichment also included wooden ladders/perches, hammocks, swings, nesting boxes, multiple feeding platforms and saw dusted floors for forage feeding as approved by the Home Office inspectorate at King's College London facilities.

2.2 In vitro colonic and ileal motility bioassay

The methodology has been described in detail previously (Abdu et al., 2002; Keating et al., 2014), Briefly, after confirmation of euthanasia a midline laparotomy was immediately performed and the exposed abdomen bathed in Krebs solution [in mM: 119 NaCl, 4.7 KCl, 1 NaH2PO4, 1.2 MgSO4, 25 NaHCO3, 2.5 CaCl2, 11 glucose] pre-gassed with carbogen [95% O2, 5% CO2]. The

gastrointestinal segment was removed and immediately placed into a beaker of Krebs solution. In experiments using ileum segments, 6 cm segments of ileum were harvested, for the colon the entire organ was used. Using a syringe, the lumen of the intestinal segments were cleared of any contents by gentle flushing with Krebs solution. An adapted standard organ bath procedure was used. Segments of colon (whole) or ileum (6 cm length) were placed into the organ bath (20 mL volume) and perfused continuously (10 mL min⁻¹) with 37°C Krebs solution, gassed with carbogen, and equilibrated to pH 7.4. The oral and aboral ends of the intestinal segments were securely attached to an input and output port of the organ bath respectively (Figure 3 a). The input port was connected to a reservoir and syringe set-up, which allowed the controlled perfusion of Krebs solution through the lumen of the segment. The output port was attached in series to a pressure transducer (BD DTX PlusTM, Oxford, UK). Motor activity was initiated in the intestinal segments by an infusion of Krebs from the syringe into the lumen until a constant intraluminal pressure was reached. In the colon this was approximately 5 mmHg and the ileum segments were held at ~1 mmHg. These figures were determined in preliminary experiments as adequate to produce regular motor patterns without inducing over-stretching of the tissue, which could induce rupture.

Under these conditions, regular aborally propagating waves of contraction developed spontaneously in the segments and persisted over time. These contractile waves were recorded as changes in intraluminal pressure (Figure 3 b & c) and were termed colonic peristaltic motor complexes (CPMCs), or ileal peristaltic motor complexes (IPMCs). After an equilibration period of 40 minutes activity had reached a consistent pattern, in terms of amplitude and frequency, then experimental procedures were started. These movements are more physiologically relevant than contractile responses in a traditional organ bath and can give us a better insight into the physiological role of different in vivo mechanisms related to peristalsis.

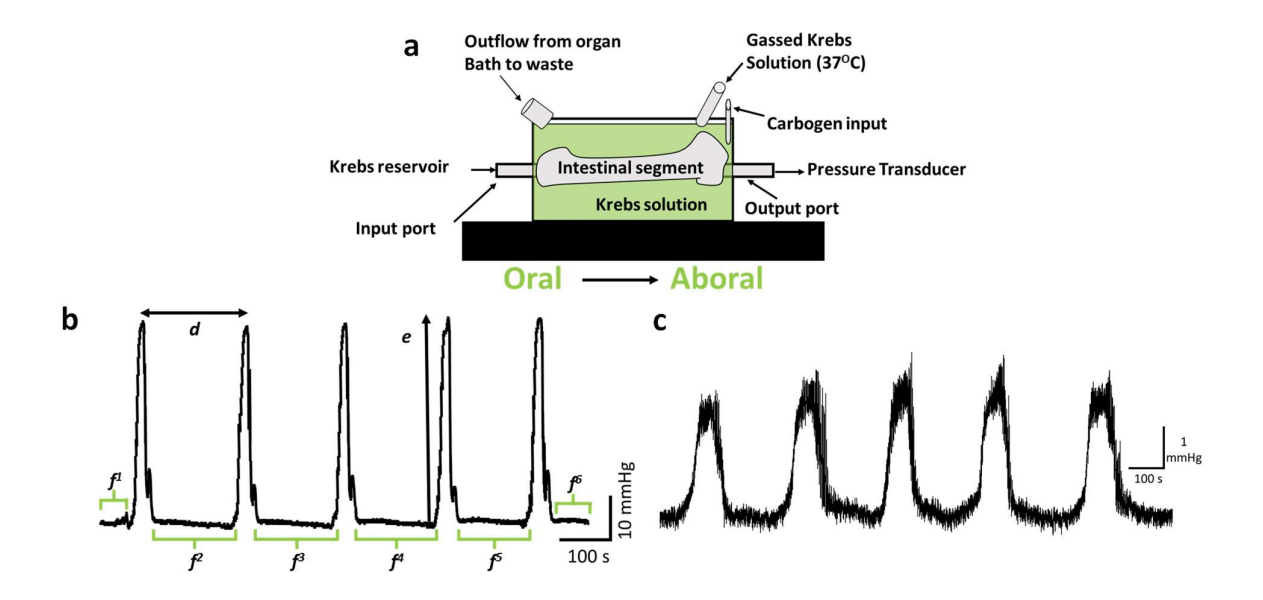


Figure 3 Luminal distension of intestinal segments in a motility organ bath leads to peristaltic like motor complexes.

Schematic diagram of the in vitro organ bath experimental apparatus (a). An illustrated CPMC trace (b), IPMC trace (c). The parameters used to evaluate changes in motility were; interval between successive PMCs (d); amplitude of individual CPMC (e); time in quiescence (TIQ) (f1+f2+etc.). Adapted from Keating et al., 2014.

2.2.1 Experimental Procedure

Test compounds were bath applied using a cumulative concentration response protocol consisting of four successive 15-minute perfusion periods, starting with the vehicle and 3 incremental concentrations of a drug, followed by a washout period to assess the reversibility of the effects. Preliminary experiments were performed to determine a suitable dose response range for each compound. Compounds were tested at 0.1, 0.3 and 1 μ M and their effects upon CPMC/IPMC parameters were noted. If a compound gave rise to significant excitatory or inhibitory effects at the

lowest concentration tested (0.1 μ M), the concentration range was reduced, and experiments repeated using a cumulative dosing procedure at the lower concentration range. This strategy was repeated until a cumulative concentration response effect for each drug had been obtained.

2.2.2 Data analysis

Changes in intraluminal pressure generated by peristaltic like motor activity were amplified (Digitimer, NL108, Welwyn Garden City, UK) and subsequently acquired to a computer through a CED 1401 interface and Spike2 software (Cambridge Electronic Design, Cambridge, UK). Intraluminal pressure was sampled at 100 Hz. Analysis was performed off-line using the software applications contained in the Spike2 software package. AUC was calculated using an in-built script in the Spike2 software. Raw data are expressed as means ± SEM and compared by one-way analysis of variance (ANOVA) for repeated measures followed by Dunnett's test as appropriate. P<0.05 was taken as significant. Fluctuation assessments were measured using a script created by the author (available in Appendices) which measures the distance between the peak and trough of each fluctuation over a given distance.

2.3 Organ bath contractility

After perfusion of the animal the bladder, ileum and colon were excised and placed in a container of carbogen aerated (95% O₂/5% CO₂, pH 7.4) Krebs buffer and transported to the organ bath laboratory in our institution (approximately 1.5-hour journey).

Once in our laboratory all tissues were flushed, cleaned and trimmed of connective tissue prior to suspension in the Bennet organ bath in a carbogenated Krebs solution at 37°C. The strips of gastrointestinal and bladder tissue were suspended in individual organ baths and attached to an FT-100 force transducer held at 1g tension. The force transducer was connected to an iWORKS amplifier which used the Labscribe (v1.817) software to record tissue responses.

To assess neurogenic responses of the tissues, the strips were contracted indirectly by electrical field stimulation (EFS) delivered through a pair of platinum electrodes placed either side of the

tissue in the organ bath. The electrodes were connected to the Digitimer D330 MultiStim System (Digitimer, UK) which provided EFS pulses.

2.3.1 Experimental Procedure

Once the tissue strips were secured in the organ bath, they were allowed to equilibrate for 20 minutes. A test EFS pulse of 20Hz frequency or 1 µM Carbachol was applied to the tissue to assess tissue viability. Any tissue that did not show significant responses were discarded and replaced if possible. The tissue was then washed three times and left again to equilibrate for at least 5 minutes before commencing the experiments.

Compound additions were made directly to the bath at concentrations that lead to the desired final bath concentrations. EFS stimulations were performed at varying frequencies dependant on experimental requirements however all other parameters remained constant (pulse width: 0.5 seconds; pulse duration: 10 seconds; max voltage: 35V; interval; 5 minutes).

2.3.2 Data analysis

Data analysis from the organ bath work was performed offline in the Labscribe software. The response of treatments in grams was calculated using the V2-V1 function in the software where V2 is the value of the peak response and V1 is the baseline response. For concentration response experiments (cumulative dosing), V1 (the baseline) was determined as the tension (in g) prior to the first concentration of the compound and V2 was the recorded at the peak response of each concentration. For single dose and EFS treatments V1 was calculated as the baseline immediately prior to each administration or pulse and V2 at the peak of the response.

2.4 Immunohistochemistry

2.4.1 Gut and Bladder Tissue

2.4.1.1 Stretch preparations

Segments of ileum and colon were immersed for 15 minutes in 0.1M phosphate buffered saline (PBS) pH 7.2 containing 1µM nifedipine (Sigma-Aldrich, UK), as a muscle relaxant to allow the tissue to be stretched without tearing. Sections were then opened along the mesenteric line and washed with PBS to remove the content of the lumen. Subsequently, the ileum and colon preparations were stretched on a Sylgard based dish with the mucosa layer facing upwards and fixed overnight in 4% paraformaldehyde at 4 °C. Following fixation, the tissues were washed in DMSO followed by three 10 min washes in PBS and then stored at 4 °C in PBS containing 0.1% sodium azide (Sigma-Aldrich). Specimens were processed as longitudinal muscle-myenteric plexus stretch preparations (LMMPs) by peeling away the different layers (i.e. mucosa, submucosa and circular muscle) as previously described (Blandini et al., 2009).

Prior to immunostaining, stretch preparation samples were permeabilised for 1 h at room temperature in blocking buffer containing 0.1% Triton X-100 in animal free blocking buffer (Vector Laboratories, UK) to reduce non-specific binding. Stretch preparations were then incubated for 72 hours in mixtures of primary antibodies diluted in the blocking buffer, at 4°C. Stretch preparations were then washed with PBS and incubated with secondary antibodies diluted in the blocking buffer for 1 h at room temperature. The tissue preparations were then washed 3 x 10 min in PBS and mounted onto slides.

2.4.1.2 Whole mount immunohistochemistry

To determine the expression of the $K_v7.4$ protein, tissues were fixed in 4% paraformaldehyde and embedded in paraffin. Sections, $8\mu m$ in thickness, were deparaffinised with xylene and dehydrated so that artifacts of water droplets or binding of reagents to paraffin did not occur. Permeabilization of the tissues was achieved by placing the slides in a Decloaking ChamberTM (Biocare Medical LLC) in a tri-sodium citrate, Tween 20 solution for antigen retrieval. Prior to incubating the

sections with primary antibody for three days at 4°C, endogenous peroxidase activity was quenched by 30-minute exposure to 0.3% H₂O₂. Immunoreactivity (ir) was observed by Avidin-biotin peroxidase complex immunohistochemistry, using 3,3-diaminobenzidine as the chromogen (Vector Laboratories Ltd, Peterborough, UK).

2.4.2 Brain tissue

Directly after perfusion of the of the animals, brains were removed and placed in 4% paraformaldehyde and fixed for 48 hours, washed in 0.1 M PBS, and cryoprotected in 30% sucrose solution for 4–6 days. Coronal sections from the blocks containing substantia nigra were cut at 30µm using a Leica freezing microtome and these were kept free-floating in 0.1 M PBS containing 0.01% sodium azide until processed for immunohistochemistry.

Sections were incubated in primary antibodies for three days at 4°C and then in an appropriate secondary for 2 hours at RTP or visualised via the avidin-biotin peroxidase complex immunohistochemistry, prior to mounting on slides.

2.4.2.1 Serial brain tissue sectioning

Directly after perfusion with Krebs solution, the brains were removed and placed in 4% paraformaldehyde and fixed for 48 hours a 4°C. They were then washed in 0.1 M PBS and placed in 30% sucrose solution (in PBS Azide (0.01%)) for 2–4 weeks. These were embedded in OCT cryoembedding matrix (Thermo Fisher, UK) and coronal sections from the blocks containing substantia nigra and DMV were cut at 30 µm using a Leica freezing microtome. Using the rat brain atlas (Paxinos & Watson, 2009) as a guide, serial coronal sections of substantia nigra were collected from each animal with one section processed for TH immunohistochemistry every 300 µm from the start of the substantia nigra pars compacta (Figure 4 a) until the end (Figure 4 b). Sections of the DMV from each animal were taken to correspond with areas at which the DMV was at its largest (Figure 4 c). These were kept free-floating in 0.1 M PBS containing 0.01% sodium azide until processed for immunohistochemistry. The sections were stained with primary antibodies against TH (ab112, Abcam, UK) and ChAT (ab178850, Abcam, UK) overnight on a rocker (RT). The

following day the sections were incubated with the appropriate secondary antibodies for 2 hours at RT. ChAT labelling was used as a marker of cholinergic neurons. Immunoreactivity (ir) was observed by Avidin-biotin peroxidase complex immunohistochemistry, using Vector VIP substrate kit (Vector Laboratories Ltd, Peterborough, UK) as per manufacturer's instructions.

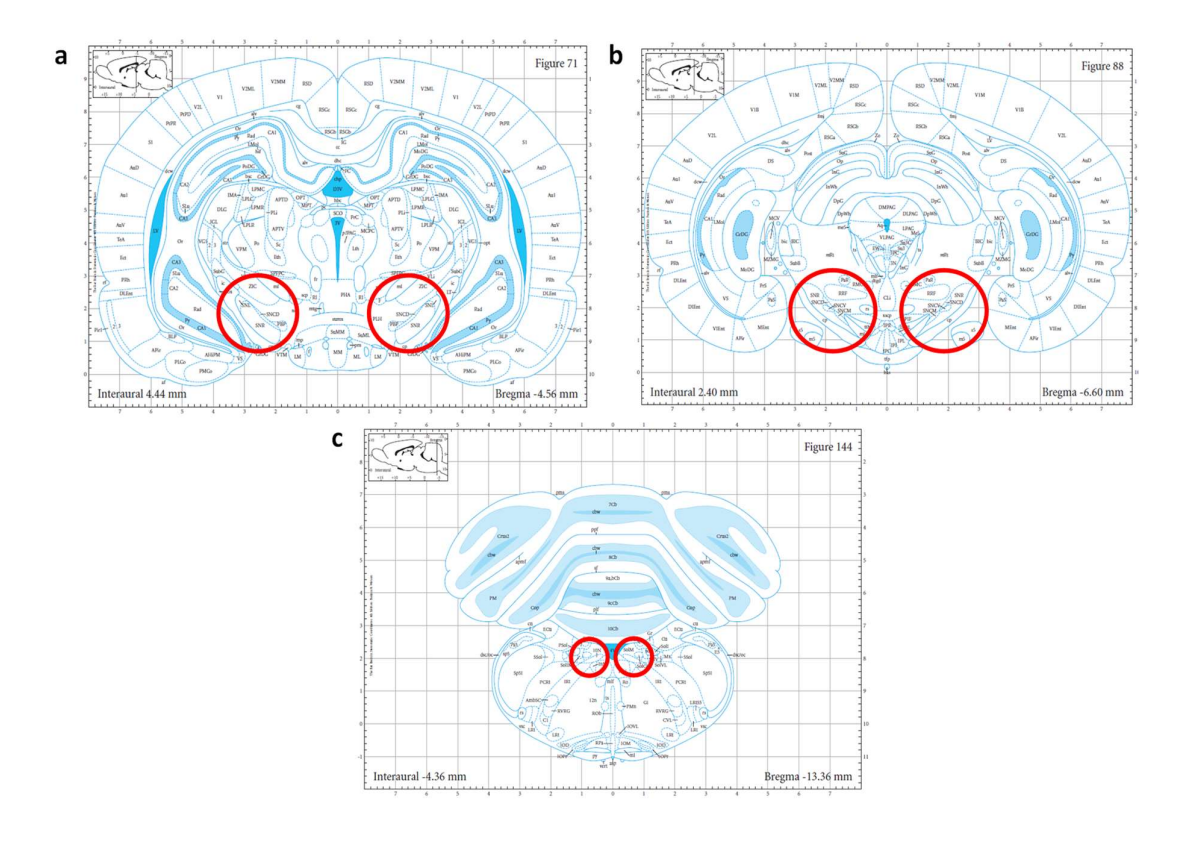


Figure 4 Representative images of sections used in brain immunohistochemistry.

Images from the rat brain atlas (Paxinos & Watson, 2009) used to identify sections containing the start of the SNpc (a), the end of the SNpc (b) and the DMV (c).

2.4.3 Image analysis

Images were acquired using a Nikon TE2000-U microscope and NIS Elements software (Nikon, Cambridge, UK). Where possible automation of analysis was employed using the Fiji plugin (Schindelin et al., 2012) of the ImageJ image analysis software (Schneider et al., 2012). This was performed to remove bias from the analysis of images. Automation included adoption of colour deconvolution and auto thresholding of all the images to remove background and reduce bias (script in appendix). The mean cell count, and optical density were calculated from multiple areas analysed on each image.

2.5 qPCR

100mg of cryopreserved segments of isolated colon, ileum and bladder tissue were homogenised in 1ml of TRIzol® Reagent (Thermo Fisher, UK), according to the lysate preparation protocol provided, using a FastPrep-24[™] (MP Biomedicals, USA) bead homogeniser. The addition of chloroform and centrifugation (12,000 x g, 4oC, 15 mins) resulted in a separation of an upper aqueous phase containing RNA. This upper phase was transferred to a new tube, ethanol was added and centrifuged as per kit instructions. The sample was then transferred to a PureLink™ RNA Mini Kit Spin Cartridge (Thermo Fisher, UK), and purification of RNA was performed, as per kit instructions.

RNA concentration was measured using a nanodrop 1000 (Thermo Scientific, UK). Genomic DNA removal and cDNA synthesis was performed using QuantiTect Reverse Transcription Kit (Qiagen, UK).

100ng of cDNA was used in a PCR mix containing TaqMan[™] Fast Advanced Master Mix (Thermo Fisher, UK) and appropriate the Custom TaqMan[™] Gene Expression Assay for the reference gene (HPRT1) and the gene of interest (KCNQ4) (Thermo Fisher, UK). Real-time PCR was performed on the Quantstudio 7 Flex (Applied Biosystems, UK) with the following conditions: 50°C for 2 min, 95°C for 10 min, 40 cycles of 95°C for 15 sec, 57°C for 20 sec and 60°C for 30 sec. The data

was exported as comparative Ct and analysed using the $2^-\Delta\Delta$ CT method normalised against the housekeeping gene.

In an attempt to increase the number of animals within our sample size, RNA extraction and qPCR was attempted with formalin fixed paraffin embedded (FFPE) tissue sections. This was unsuccessful and a comparison between frozen and FFPE tissue is detailed in chapter 2.5.1.

2.5.1 Comparison of the use of FFPE and frozen tissue for qPCR studies

2.5.1.1 Introduction

Some samples in our inventory of marmoset tissues were only available in paraformaldehyde fixed paraffin embedded (FFPE) blocks. To make the most of these precious samples and add to the power of our study but also correlate our protein results with mRNA expression we attempted to perform qPCR from FFPE tissue sections. Tissue samples, whether from a clinical or pre-clinical setting, are routinely fixed in formalin or paraformaldehyde and embedded in paraffin wax to facilitate stable, easy, cost effective, long-term storage for further research. Such fixation methods cause cross-linking of proteins and enable immunohistochemical studies to be performed even years later. The usage of fixed tissue for other downstream applications can be challenging due to degradation and fragmentation of proteins, DNA and RNA (Choi et al., 2017). The ability to develop biomarkers in formalin fixed paraffin embedded tissue would open the door to a wealth of samples from pathology departments all over the world. Such methods would be not only useful for "basic" research purposes but can be integrated into routine for clinical biopsies to gain a better understanding from each diagnosis in the personalised medicine era.

Purity and integrity of the starting RNA is critical for the success of any accurate evaluation of gene expression. For qPCR, total RNA once extracted should ideally be free of protein, genomic DNA, any other contaminants and be undegraded (Fleige & Pfaffl, 2006). Successful extraction of intact RNA from fixed paraffin embedded tissues for different assays can be variable. There have been reports of next generation sequencing (NGS) and qPCR successful, in some studies, with samples that had been stored for 22 years (Carrick et al., 2015), but unsuccessful in others that were only 10

years old (Choi et al., 2017). Great care must be taken in tissue preparation for such assays and time is of utmost importance to prevent degradation of RNA upon tissue excision. RNA has been shown to be sensitive to degradation by inadequate storage and sample handling (Angela Pérez-Novo et al., 2005) as well as time. RNA extraction for quantification assays was judged to be optimum in samples that are diced into small fragments prior to being flash frozen tissue and then homogenised using a bead homogeniser (Bustin et al., 2005).

Several kits and methods have been produced in order to attempt to extract RNA via different methods based around the same deparaffinization and rehydration steps used in immunohistochemistry. Studies have shown that short amplicon mRNA (~60bp) are more stable in fixed paraffin embedded tissue and can be detected by quantitative reverse-transcriptase polymerase chain reaction (RT-PCR) (Abrahamsen et al., 2003; Choi et al., 2017).

Here we attempted to quantify the KCNQ4 mRNA content in our marmoset model of PD using qPCR. These samples are from a set of FFPE tissues, in which KCNQ4 expression was assessed via immunohistochemistry in chapter 6.3.2. We attempted to extract mRNA from these samples to be able to correlate its expression with immunoreactivity of the protein in the same sample. Such assessments can be important in structures such as the colon and other parts of the gastrointestinal tract which are not just homogenous tubes but have differences in protein expression and neurochemical differences in different portions of the same organ (Noorian et al., 2011). Therefore, where possible, the same segments should be collected and compared to each other. In this chapter we show that RNA extracted from our FFPE tissue resulted in poor quality and poor integrity mRNA compared to that extracted from freshly frozen tissue.

2.5.1.2 Methods

An FFPE RNA Purification Kit (Cat. 25300, Norgen Biotek, Ontario, Canda) was used to extract RNA from sections from FFPE ileum and colon tissue from the common marmoset PD model.

Approximately 25mg of microtome cut sections were departaffinised and incubated in xylene for 5

minutes at 50°C with routine vortexing. Between each step the solution was centrifuged at 14000 x g for 6 minutes and supernatant discarded. Rehydration was then performed with reducing concentrations of ethanol (100%-70%), with vortexing and centrifugation between each incubation. The resultant pellet was air dried for 10 minutes to completely remove ethanol. Digestion was performed using a digestion buffer provided in the kit, containing Proteinase K, for 30 mins at varying temperatures, as per manufacturer's instructions.

Another proprietary buffer from the kit manufacturer was added to the mixture along with ethanol and the lysate was passed through a column for extraction of RNA. On-column DNA removal was also performed using DNAse1, prior to elution of RNA, to remove contamination of DNA fragments in quantification and amplification steps.

The RNA extraction procedure from freshly frozen tissue is mentioned in chapter 6.2.3.

The simple quantification of RNA was performed using a NanoDrop 1000 spectrophotometer (Thermo Scientific, UK) as nucleic acids absorb UV light at 260 nm. The RNA integrity was measured using the Agilent 2100 bioanalyzer system using the Agilent RNA 6000 Pico kit (Agilent, UK). The samples were kindly run by Dr Steve Sheardown, Cerevance, UK. 1µl of sample is placed on the bioanalyser chip along with a ladder according to manufacturer's instructions and read on the bioanalyser to produce an RNA Integrity Number (RIN).

2.5.1.3 Results

2.5.1.3.1 Extraction from FFPE tissue produces low yield, contaminated RNA.

RNA extracted using the above methods showed that samples from FFPE tissue had lower absorbance (Figure 5 a) at 260nm than those from freshly frozen tissue (Figure 5 b), indicating low yield. Relative to the absorbance at 260nm, high absorbance at other wavelengths indicates contamination of a sample. The absorbance at 280 nm is measured because this is typically where proteins and phenolic compounds have a strong absorbance. Organic compounds often have absorbance at ~225nm and other contaminants such as phenol and peptide bonds absorb light at 200-230nm. The ratio between 260nm and 280 is used to determine protein contamination of a

sample. Pure RNA should have a ratio between 2.1 and 1.8. Our data shows the majority of the FFPE extracted mRNA samples have high protein contamination (Figure 5 c) and this coincides with low yield. Only one sample from the freshly frozen tissues had protein contamination and the yield and purity of the rest of the samples were high (Figure 5 d).

Samples with 260/230 ratios under 1.5 are considered to have a significant amount of organic contaminants (Figure 5 e). Again, many of our FFPE samples show very high contamination, with only the one freshly frozen sample showing high contamination (Figure 5 f).

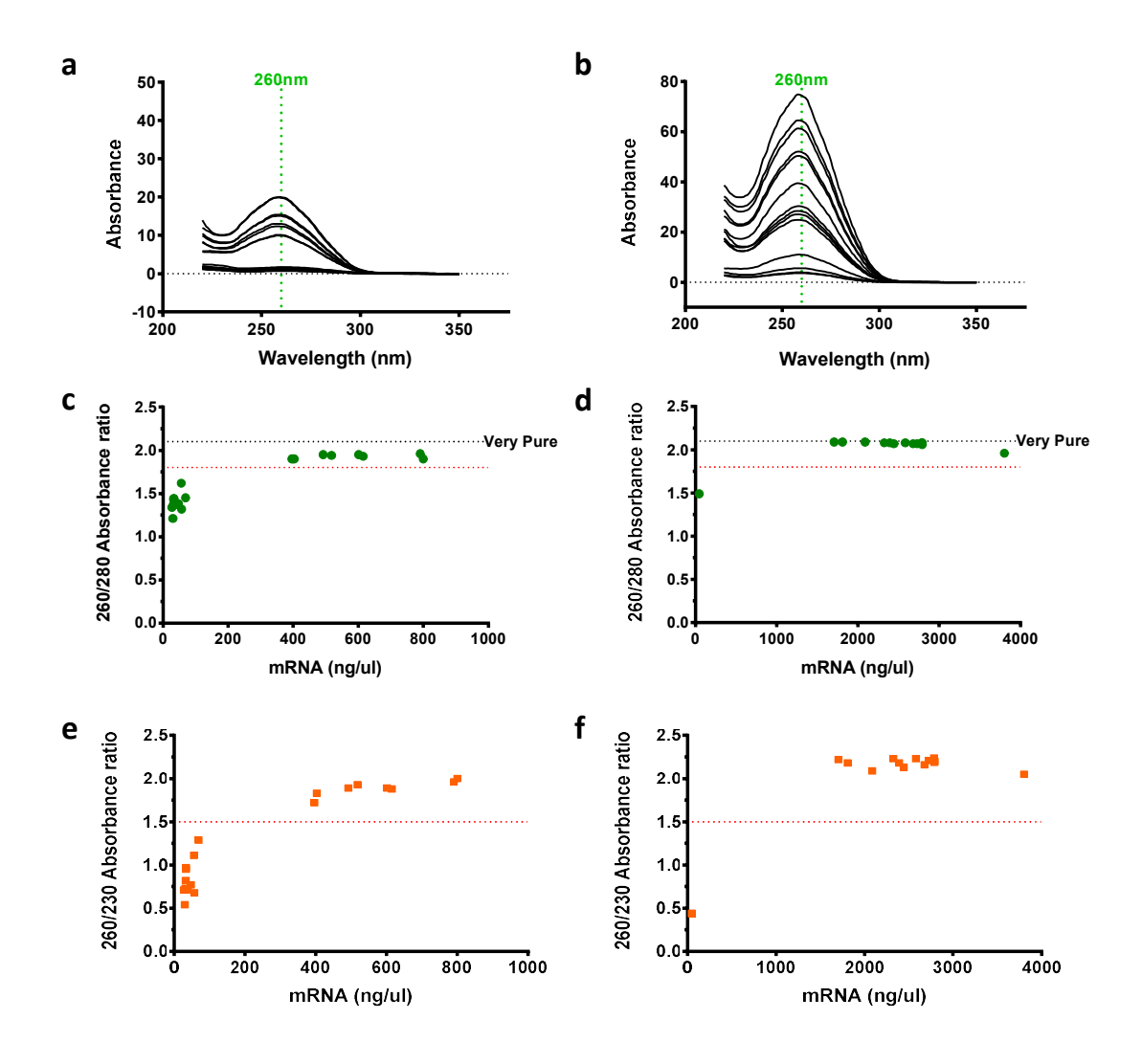


Figure 5 Nanodrop results from FFPE vs Frozen tissue mRNA extraction.

Raw data absorbance values and ratios from RNA extracted from FFPE tissue (a,c,e) and flash frozen tissue (b,d,f). RNA yield is measured at 260nm of which there is less RNA recovered in FFPE (a) compared to frozen (b) tissue. Absorbance ratios of 260/280 nm and 260/230 nm against yield indicate higher contamination in FFPE (c, e) compared to frozen (d, f) tissue.

Freshly frozen tissue yielded significantly higher mRNA than tissue taken from FFPE blocks (Figure 6 a). The preparations had significantly higher scores when measured for purity using the 260/280 (Figure 6 b) and 260/230 ratios (Figure 6 c). Despite the low yield and contaminants, the FFPE samples were assayed for detection of the housekeeping gene and gene of interest (KCNQ4) using qPCR. The majority of Ct values were above acceptable limits to believe that any real amplification had occurred (Ct > 35) for both KCNQ4 and HPRT1. There were some samples which had detectable level of mRNA for the housekeeping gene (Ct ~32), however these were a lot higher than the Ct values in the freshly frozen tissue (Ct ~25) (Figure 51).

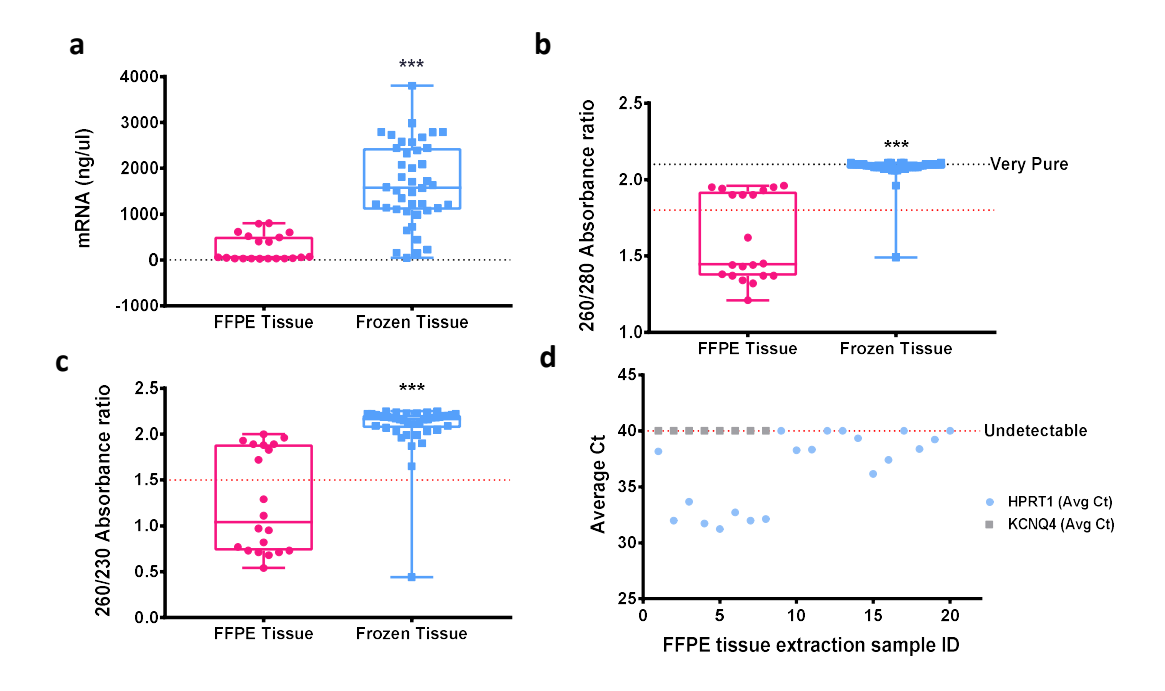


Figure 6 Summary box plots of comparison of FFPE vs frozen Tissue and qPCR data of FFPE tissue.

RNA yield is significantly lower in extraction from FFPE tissue compared with frozen (a) tissue. The ratio of mRNA to contamination by protein (b) and guanidine salt/phenol (c) is significantly lower in FFPE tissue extracted RNA samples. qPCR analysis (d) showed that KCNQ4 was undetectable in all FFPE samples, and the housekeeping gene was very lowly detected in only a few samples. Data are expressed as mean, SEM; ***p < 0.0001; vs freshly frozen tissue by unpaired t-test ($n \ge 20$).

2.5.1.3.2 mRNA from FFPE tissue samples show poor RNA integrity.

The RNA extraction from FFPE tissue yielded low quantity, contaminated samples which did not show detectable levels of our gene of interest. The ribosomal ratio of the RNA is an indicator of the quality and integrity of the of the RNA. The Agilent bioanalyzer allows a visual inspection of RNA integrity and generates ribosomal ratios to give a "RNA Integrity Number" (RIN) for each sample.

All samples from FFPE tissue had a poor RIN score where scores were available (Figure 7 a), when compared to the manufacturers guide on RIN (Figure 7 b). This showed that all the RNA samples that were extracted from FFPE tissue were strongly degraded.

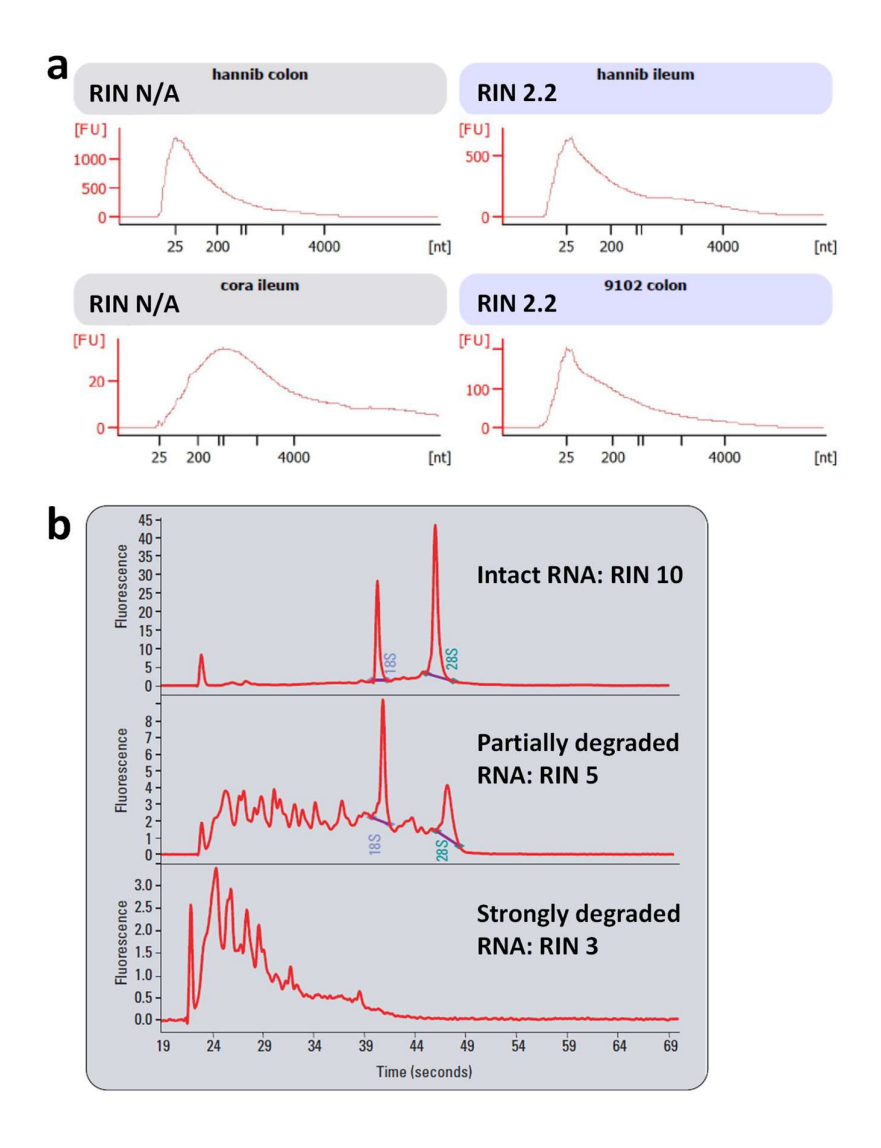


Figure 7 Bioanalyser traces showing RNA degradation in FFPE tissue.

Example bioanalyser electropherogram of RNA samples from FFPE colon and ileum tissue from MPTP treated and naïve marmosets (a). Manufacturer's (Agilent, UK) guide on integrity of RNA detectable by bioanalyser (b).

2.5.1.4 Discussion

Detecting gene expression through quantifying mRNA levels has become an important tool in scientific research. Having this information especially in comparisons of disease vs healthy tissue can lead to target identification for therapeutics and give rise to biomarkers, to understand disease progression and therapeutic efficacy. As the functional biomolecule, proteins are, rightly so, valued more in terms of their quantification. They also happen to be easier to preserve, even though they are not always easier to detect. RNA preservation requires more care as it is rapidly digested by RNAse enzymes which are ubiquitously present. Although it has been proven to not always correlate with protein expression in a cell or tissue (Greenbaum et al., 2003), quantifying mRNA does reflect how much transcription has occurred in a particular sample. Poorly understood post transcriptional mechanisms and *in vivo* half-lives of proteins can be reasons for a lack of correlation between mRNA and protein but also methods of quantification of both protein and mRNA contain significant noise and error which may cloud this picture.

The ability to analyse the exact same sample for both mRNA and its translated protein would remove some of the noise in the corelation. Integration of results from multiple approaches is essential in disease such as cancer where a single tumour is not always just a homogenous lump but contains genetic, phenotypic, and functional heterogeneity (Meacham & Morrison, 2013). Different parts of the same organ can have different sub-functions and therefore have varied expression of genes and protein. This is especially true of structures within the gastrointestinal system, which often have clearly defined names despite having less clear boundaries such as the small intestine (Karaosmanoglu et al., 1996). Therefore, we attempted to quantify both protein and RNA in the same fixed paraffin embedded sample from our MPTP treated marmoset model of PD. Motivated by the possibility of a wealth of global clinical samples to conduct research on, many successful methods have been optimised for performing such assessments in fixed embedded tissue. Such corelations from the same sample are not common place due to the high variability between processing of clinical samples between different facilities leading to varied reliability in extraction and quantification of proteins and RNA (Carrick et al., 2015; Choi et al., 2017; Wolff et al., 2011).

In this chapter we focus on mRNA detection. The integrity and purity of the mRNA is paramount to its successful extraction and quantification in downstream assays such as qPCR. Ideally, the extraction and purification process should yield RNA that is free of protein, genomic DNA, enzymatic inhibitors or co-factors and undegraded (Fleige & Pfaffl, 2006). The best yield has been found to be obtained from tissue that has been cut up into small pieces quickly upon removal, frozen in liquid nitrogen and homogenised using an automated homogenisation method (Bustin et al., 2005).

Our samples were historic samples from the MPTP marmoset model, fixed in paraformaldehyde and embedded in paraffin blocks for the purpose of immunohistochemical detection of proteins. Even in the best experimental settings fixed tissue have been shown to produce 30 times lower yield of RNA, with more impurities than tissue preserved using specific methods for RNA preservation (Matsuda et al., 2011). We used proprietary kits and reagents purchased for the purpose of extracting the highest quality RNA from these FFPE sections and compared the quality of RNA to that extracted from freshly frozen tissue. The first noticeable difference in the comparison was the peak absorbance measured using the nanodrop at 260nm. This was significantly higher in the frozen tissue than in the samples from the FFPE tissue (Figure 5 a & b). The absorbance at 260nm is specific for nucleic acids and indicates the yield of the extraction. The nanodrop also measures the absorbance of proteins at 280nm and organic compounds at 230nm. Ratios can be used between the absorbance at 260nm/280nm and 260nm/230nm to indicate purity of the sample. For pure RNA 260/280 ratios ideally are between 2.1 and 1.8. Lower ratios indicate protein contamination which may influence downstream applications. Samples with 260/230 ratios below 1.8 are thought to have a significant organic compound contaminants and a value close to 2.0 is considered pure (Fleige & Pfaffl, 2006). Many of our FFPE samples had extremely low RNA yield and contamination below acceptable levels (Figure 5 e & f). This was significantly different from the samples extracted from frozen tissue which had significantly higher yield (Figure 6 a), and most samples were free from protein and organic contamination (Figure 6 b and c).

These were major indications that our assessment of gene expression in these samples would not be successful, nevertheless we attempted to run qPCR on these samples. Use of normalisation to an

internal reference gene is commonplace in such assays and this has been shown to be even more important when RNA integrity is called into question. Previous work shows that quantification of a gene of interest may change due to the integrity of the RNA extracted, but this also is the case with a similar trend for a housekeeping gene, Therefore, relative quantification aims to correct for variations in qPCR efficiency due to sample contamination (Pfaffl, 2001). The housekeeping gene that we used for our samples was HPRT1 mentioned in chapter 6.2.3. It was shown to be a suitable reference gene for quantification studies of mRNA in common marmoset tissues, as it has stable expression in gastrointestinal tissues as shown by two different measures of expression stability (Shimamoto et al., 2013).

Most of our samples did not give Ct values with the housekeeping gene in a range that would give confidence of a real amplification (Figure 6 d). There were some samples which had detectable level of mRNA for the housekeeping gene (Ct ~32) however these were a lot higher than the Ct values in the freshly frozen tissue (Ct ~25) (Figure 51). Higher gene quantification variation has been shown to occur in reference genes from degraded RNA (Angela Pérez-Novo et al., 2005). Although the Ct value of the reference gene for FFPE samples were high, we attempted to also probe for our gene of interest KCNQ4. The primer was chosen to amplify on a short product that was specific for KCNQ4 and not other KCNQ subtypes. Amplification of a short product (70-250bp) is less dependent on RNA quality (Fleige & Pfaffl, 2006). Studies have shown that short amplicon mRNA (~60bp) are the most stable in fixed paraffin embedded tissue and can be detected by quantitative reverse-transcriptase polymerase chain reaction (RT-PCR) (Abrahamsen et al., 2003; Choi et al., 2017). The lowest predicted product primers that we were able to construct which maintained specificity to KCNQ4 was 100bp in length. Unfortunately, this did not yield a product in our FFPE sections (Figure 6 d) but was successful in the frozen tissue where RNA was more intact (Figure 51).

The original methods of assessing RNA integrity such as the nanodrop ratios and 28S:18S ribosomal RNA ratios, have been questioned for their accuracy and objectivity. A value of 1.8 for a 260/280nm ratio corresponds to 60% contamination and traditional 28S:18S ratios are subject to human interpretation of images on a gel (Bustin et al., 2005). More sophisticated, automated

methods are now available which use the "lab on chip" technology and integrate the assessment of ratios and shapes of curves on an electropherogram to produce an RNA Integrity Number (RIN). The number is produced based on machine learning where the system has "learned" the patterns of different grades of degraded and non-degraded RNA. There is still variability in the system stemming around the sample type, but it is a high throughput, reliable system which is being used widely to assess RNA integrity. We used the bioanalyser to confirm degradation in our FFPE samples (Schroeder et al., 2006). We saw very low RIN numbers, if any were given at all, and the shape of our electropherogram showed no separation of ribosomal RNA, implying that the RNA in the FFPE samples was strongly degraded.

In summary, we attempted to quantify mRNA levels of KCNQ4, our gene of interest, from the same FFPE samples that we had seen differences in protein expression previously. The RNA that we were able to extract from the FFPE samples was low in yield, highly contaminated and too degraded for us to quantify. As we cannot be sure of the processing of the samples prior to embedding it is likely that the duration of fixative or processing for embedding as well as the time that the samples have been kept, have contributed to the lack of quantifiable RNA. This has been shown to be very important in the success of RNA based assays from FFPE samples.

2.6 Western blot

Tissue segments were homogenised in Tissue Extraction Reagent 1 (FNN0071, Thermo Fisher Scientific, UK) containing HaltTM Protease Inhibitor Cocktail (87786, Thermo Fisher Scientific, UK) using a FastPrep -24TM Tissue Homogeniser (MP BiomedicalsTM, UK). The tissue to lysis buffer ratio was 100mg to 1ml of buffer. Western blot was performed using the Mini gel tank system, BoltTM 4 to 12%, Bis-Tris graded gels and the iBlot 2 Dry Blotting System (Thermo Fisher Scientific, UK). We used graded gels as they allow optimal separation of proteins for both high and low molecular weight and allow multiple proteins of interest to be visualised on the same membrane. Briefly, Total protein (20μg) from homogenized colon, ileum and bladder was separated on graded gels using gel electrophoresis (160V, 35m). Proteins were transferred onto a PVDF membrane, blocked with milk (RT, 1 hour) and incubated overnight (4°C) with primary antibodies.

The membranes were then incubated in the appropriate secondary antibodies (RT, 1 hour) in milk or BSA, where appropriate. Details of the antibody combinations and dilutions are listed in

Table 3. The bands were visualized using chemiluminescence (Radiance Plus chemiluminescence substrate, Azure biosystems, UK) and quantified using Image Lab software (Bio-rad, UK) against a β-actin loading control.

3 K_V7 CHANNEL REGULATION OF GASTROINTESTINAL MOTOR ACTIVITY IN A MURINE MODEL OF PERISTALSIS

3.1 Introduction

The functional role of the K_v 7 channels in gastrointestinal organs have not been fully characterised in any species. Therefore, this chapter will look at K_v 7 channel openers and blockers on colonic and ileum motility-like behaviour in tissues from mice.

Several members of the potassium channel family are expressed within the gastrointestinal tract but one family, the K_v7 family of voltage-gated potassium channels (K_v7.1 to K_v7.5) encoded by the KCNQ genes, have been shown to be critically involved in regulating GI function including nociceptive behaviour and spontaneous contractility of smooth muscle cells (Ipavec et al., 2011; Jepps et al., 2009; Peiris et al., 2017). Furthermore, studies have shown that mutations in KCNQ genes give rise to hereditary disease states such as cardiac long QT syndrome, atrial fibrillation, epilepsy and deafness (Kubisch et al., 1999; Singh et al., 1998; Wang et al., 1996). As such there is growing interest in targeting K_v7 channels for pharmacological intervention. Retigabine, a first in class activator of KCNQ channels was an effective anti-epileptic approved by the FDA in 2011, but it was later withdrawn due to limited use and declining numbers of patients initiating therapy (Kuersten et al., 2020). Interestingly, extracts from plants which have traditionally used by indigenous people of the Americas as analgesics and gastrointestinal therapeutics have been shown to increase KCNQ currents (Abbott et al., 2021).

Most studies to date have focused on studying K_v7 expression in cardiac myocytes, epithelia, neurons, and the bladder. These studies have revealed a tissue specific expression profile of these channels where Kv7.1 channels predominate in epithelial cells and cardiac myocytes (Barhanin et al., 1996; Sanguinetti et al., 1996) while K_v7.2 to K_v7.3 have a more neuronal expression pattern (Brown & Adams, 1980; Selyanko et al., 1999; Wang et al., 1996). In the human bladder K_v7.4 and K_v7.5 channels are essential regulators of detrusor smooth muscle and there is evidence that these channels can form heteromeric complexes (Bientinesi et al., 2017; Svalø et al., 2015). Human arteries express all subtypes of Kv7 channels except KCNQ2 and modulation of Kv7 channels affects arterial tone (Ng et al., 2011).

KCNQ channels were first investigated in tissues of the gastrointestinal tract when KCNQ1-3 transcripts were found to be expressed in various parts of the rat stomach and isolated smooth muscle cells (SMC) from the stomach (Ohya et al., 2002). Building upon that study, all Kv7 subtypes were found to be expressed in the rat gastric fundus and found to lead to increased contraction of the strips when blocked by Kv7 channel blocker XE-991 and relaxed in a concentration dependent manner with Kv7 activators. Interestingly, XE-991 reduced VIP induced relaxation of the strips indicating its involvement in VIPs relaxation mechanisms (Ipavec et al., 2011). These results were corroborated in the guinea pig gastric corpus, and a role of Kv7 channels in the cholinergic and adrenoceptor response postulated, due to impaired responses of acetylcholine and adrenaline in the presence of Retigabine (Apostolova et al., 2017).

In the mouse intestine K_v7 channel expression has been located in extrinsic afferent neurons of the colon, where sensory nerve excitability was attenuated by using K_v7 channel openers and augmented with K_v7 channels blockers (Peiris et al., 2017). Also, K_v7.4 and K_v7.5 channel mRNA was found to be expressed most abundantly, of the five subtypes, in smooth muscle from various organs of the gastrointestinal tract. Pharmacological studies demonstrated a role for these channels in controlling the contractile activity of intestinal smooth muscle (Jepps et al., 2009). Jepps et al., (2009) mounted one-centimetre segments of the mouse colon into a wire myograph and measured contractility of the colonic segments in response to different Kv7 channel modulators. Kv7 channel blockers Linopirdine and XE-991 increased spontaneous contractile activity in the mouse colon,

and the Kv7 activator Retigabine inhibited contractile activity. As well as smooth muscle, Jepps et al., (2009) using immunohistochemistry found some labelling of Kv7 channels within the myenteric plexus region. Interstitial cells of Cajal (ICC) within the muscular plexus near the submucosal surface of the circular muscle layer of the mouse small intestine have also been shown to express Kv7 channels, in particular Kv7.5 (Chen et al., 2007). Murine colonic ICCs also express Kv7 channels and with addition of XE-991, intramuscular ICCs depolarise, leading to activation of a large inwardly rectifying current (Wright et al., 2014). Crucially similar expression patterns and functional observations were found in the human taenia coli (Adduci et al., 2013). In those studies XE-991, produced irreversible concentration dependent contractions and Kv7 activator Retigabine produced concentration dependent relaxations of precontracted human taenia coli strips.

The Kv7 channels have been shown to be expressed on many of the major cell types involved in the motor function of the gastrointestinal tract, in many species. Despite this, the characterisation of the role of K_v 7 channel activity in controlling gastrointestinal motility-like behaviour has not been performed.

This study set out to determine the role of K_v7 channels in regulating motility-like behaviour in the mouse intestine. Since motility is a complex interaction between neurogenic and myogenic properties within the gut wall we chose to perform this study using a well characterised *in-vitro* model of murine intestinal motility that utilises segments of murine intestine (Abdu et al., 2002; Keating et al., 2014). The advantage of this model is that regular contractile activity can be invoked in these tissues, and the effects of compounds can be quantified on their ability to block motor patterns in these tissues both at the neuronal or myogenic level. The contractile activity in this model is produced by distension of the lumen of large segments of intestinal tissue mounted on to an organ bath. The stimulus of the distension to a threshold level induces powerful contractions of the muscle which propagate aborally. This can be used to model the reflexes of ascending excitation and descending relaxation that occur when moving a bolus along the gastrointestinal tract (Brookes et al., 1999).

We used this ex vivo model and IHC techniques to:

Test the effects of K_v7 channel openers and blockers on colonic and ileum motility-like behaviour.

Understand the expression profile of Kv7.4 channels across different cell types in the in gastrointestinal tissues.

Our results show the first functional evidence that K_v 7 channels play an important role in regulating intestinal motility, and that K_v 7channel activity occurs within both myogenic and neurogenic circuitry within the gastrointestinal tract.

3.2 Methods

3.2.1 Animals

All experimental procedures were conducted with local ethical committee approval and in accordance with the UK Animals (Scientific Procedures) Act, 1986 (National Archives, UK Animals, Scientific Procedures Act, 1986). 24 wildtype C57BL/6J male mice (Charles River, UK) 10 to 12 weeks of age and weighing 25-30 g were used in this study. Animals were housed under controlled ambient temperature (21 ± 2oC), light-dark cycle of 12:12 hours and were allowed free access to food and water. They were euthanised by exposure to a rising concentration of CO₂ with confirmation via cervical dislocation. We used mice for two reasons, apart from non-human primates, mice are susceptible to MPTP and therefore will be used to model PD following this initial characterisation. Secondly, our in vitro motility organ bath is set up for and validated using tissues from mice.

3.2.2 In vitro colonic and ileal motility bioassay

Further details of the bioassay methods are mentioned in 2.1.3.

3.2.3 Drugs

For K_v 7 channel activation, tissues were incubated in rising concentrations of Ethyl [2-amino-4-[[(4-fluorophenyl)methyl]amino]phenyl]carbamate (Retigabine) and N-(2,4,6-Trimethylphenyl)-

100

bicyclo[2.2.1]heptane-2-carboxamide (ML213) in dimethylsulfoxide (DMSO) dissolved in Krebs solution.

For inhibition of Kv7 channels the pan-Kv7 blocker 10,10-bis(4-Pyridinylmethyl)-9(10H)-anthracenone dihydrochloride (XE-991) was dissolved directly in Krebs solution. All compounds were purchased from Tocris Biosciences, Bristol, UK.

3.2.4 Immunohistochemistry

3.2.4.1 Stretch preparations

Further details of the methods are mentioned in 2.4.1.1.

To analyse the presence of K_v7.4 channels in the enteric neurons of the myenteric plexus of the LMMPs, double staining was performed using anti-KCNQ4 (ab6579, Abcam, Cambridge, UK; 1:200) and the pan-neuronal marker, anti-PGP9.5 (ab10410, Abcam, Cambridge, UK; 1:200) and appropriate secondary antibodies.

3.2.4.2 Whole mount immunohistochemistry

Further details of the methods are mentioned in 2.4.1.2.

Wholemount sections were also collected and incubated with Anti-KCNQ4 for 72hrs at 4°C. Immunoreactivity (ir) was observed by Avidin-biotin peroxidase complex immunohistochemistry, using 3,3-diaminobenzidine as the chromogen (Vector Laboratories Ltd, Peterborough, UK) as per manufacturer's instructions. Double labelling was also performed with Anti-PGP9.5 antibody and Anti-KCNQ4 as above.

3.3 Results

3.3.1 Peristaltic motor complexes of the ileum and colon show different motility pattern profiles in our system.

Six cm segments of colon or ileum were placed into the motility organ bath and distended with Kreb's solution. Kreb's infusion into ileal segments invoked rhythmic contractile activity in these tissues which had a different profile to those seen in colonic segments. The ileal contractile activity, consisted of small, localised waves of contraction (Figure 8 a), which led to a gradual change in IP. Infusion of Krebs solution into the lumen of colonic segments initiated large rhythmic contractile activity in which periods of contraction were interspersed with periods of quiescence (Figure 8 b), termed colonic peristaltic motor complexes (CPMC).

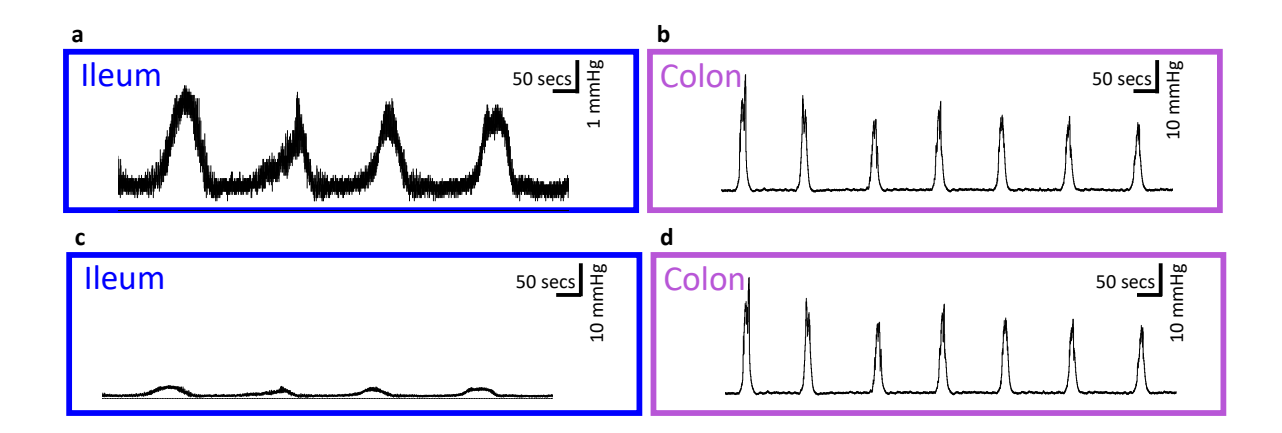


Figure 8 Peristaltic motor complexes of the ileum and the colon.

An exemplar trace of IPMC activity during distension of the lumen in the absence of any other stimuli or compounds (a). An exemplar trace of CPMC activity during distension of the lumen in the absence of any other stimuli or compounds (b). IPMC and CPMC traces shown on the same scale (c & d).

When comparing the ileum and the colon segments in the motility organ bath there are differences in all parameters that are measured. Within a 15 minute period the colon exhibits a higher frequency (Figure 9 c) of motor complexes, which are larger in amplitude (Figure 9 d) and resultantly have a larger area under the curve (Figure 9 e). The motor complex width indicates the time at which the tissue is active. The amount of time that the colon spends at rest (TIQ) is significantly longer than the TIQ of the ileum (Figure 9 g) due to the shorter width of each complex (Figure 9 h). The average time between one complex to the next was observed to be significantly shorter in the colon than the mean IPMC interval (Figure 9 i) in the ileum.

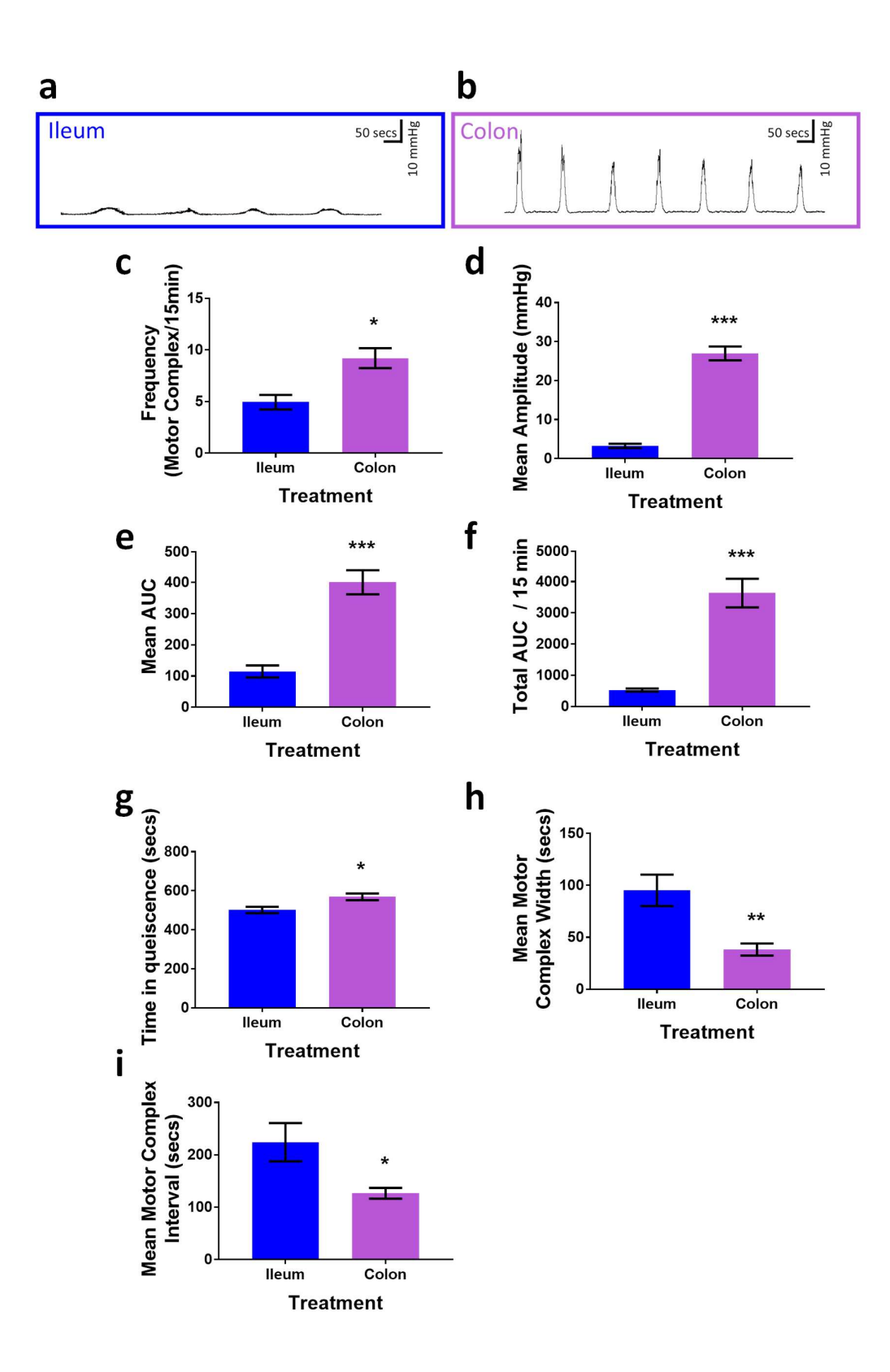


Figure 9 A comparison of colonic and ileum motor complexes.

An exemplar trace of IPMC activity (a) and CPMC activity (b) during luminal distension, in the absence of any external stimulus or compound. Summary bar charts comparing the complexes of the ileum to the colon for; the average frequency of motor complexes over the 15 minute period (c), the mean motor complex amplitude (d), the mean AUC of a complex (e) and the total AUC over the 15 minute period (f), the TIQ over the 15 minute period (g) the mean motor complex width (h) and the mean motor complex interval (i). Data are expressed as mean, SEM; *p < 0.05; **p < 0.01; ***p < 0.001; versus ileum by unpaired t-test.

A single IPMC is longer in duration than a CPMC and is formed of gradual increases in intraluminal pressure which returns to baseline after its peak (Figure 10 a). The intrinsic contractility of the ileum is consistent when at rest and during active periods (Figure 10 e). A CPMC consists of large increases in contractility which build upon each other until the peak of the CPMC and then a decline back to the rest state (Figure 10 b & f).

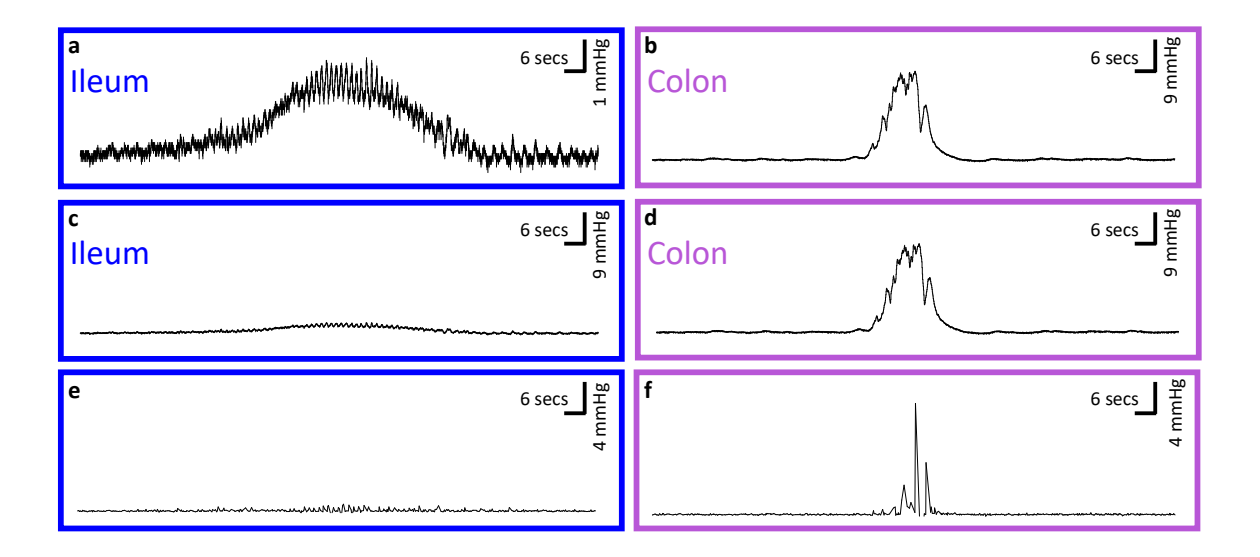


Figure 10 Individual peristaltic motor complexes of the ileum and the colon.

An exemplar trace of a single IPMC during distension of the lumen in the absence of any other stimuli or compounds (a). An exemplar trace of a single CPMC during distension of the lumen in the absence of any other stimuli or compounds (b). An IPMC and CPMC at the same scale (c & d). A trace of contractility changes during an IPMC (e) and a CPMC (f).

Fluctuations of contractility in the ileum do not increase in amplitude (Figure 11 c) but reduce in frequency (Figure 11 d) during a motor complex. In the colon the mean fluctuation amplitude (Figure 11 c) significantly increases, indicative of the jumps in IP seen in individual CPMCs (Figure 10 b). There is a significant reduction in frequency of fluctuations in the active phase of the colon (Figure 11 d). This reduction in frequency is greater in the colon than that of the ileum despite the frequency being similar between the tissues at rest.

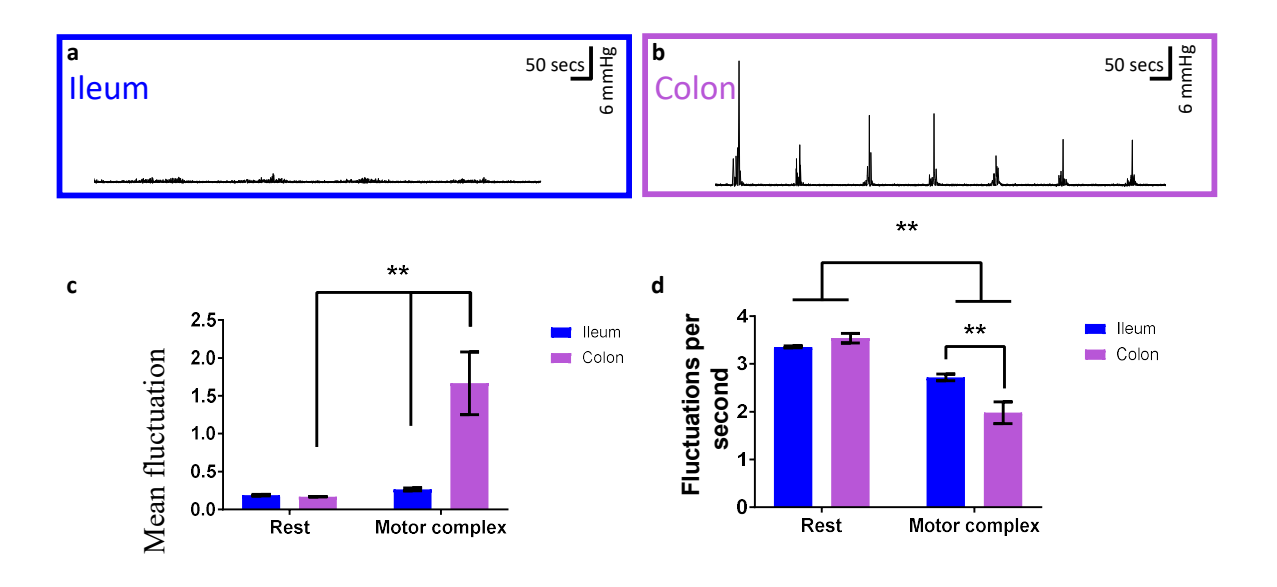


Figure 11 Assessment of contractility in the ileum and the colon.

An exemplar trace of contractility in the ileum (a) and colon activity (b) during luminal distension, in the absence of any external stimulus or compound. Summary bar charts comparing contractility in the ileum and colon; measured as fluctuation amplitude (c) and fluctuation frequency (d). Data are expressed as mean, SEM; $n \ge 4$; **p < 0.01; using two-way ANOVA.

3.3.2 Kv7 Channel activators reduce CPMC and IPMC activity.

To investigate the physiological effects of activating $K_{\nu}7$ channels in colonic segments we applied Retigabine and ML213 to the tissue using a cumulative dosing strategy. Bath application of the $K_{\nu}7$ channel opener retigabine (0.1- 1 μ M) caused a dose dependant decrease in CPMC activity (Figure 12a). Retigabine significantly decreased CPMC frequency and increased TIQ at 1 μ M compared to vehicle (Figure 12 b, f). Both the frequency and TIQ changes were fully reversible upon washout of retigabine. We found that retigabine had a more potent inhibitory effect upon CPMC amplitude than

on CPMC frequency or TIQ. Retigabine caused a dose dependent decrease in CPMC amplitude observed at all three doses tested (Figure 12 c).

The amplitude and width of each motor complex contribute to the area under the curve (AUC), a marker for the strength or magnitude of the complex. Retigabine diminished the average amplitude of each CPMC at all concentrations but did not significantly alter their width (Figure 12 g). Resultantly the Mean AUC per CPMC was reduced at all concentrations (Figure 12 d) as was the total power output (Total AUC) over the 15 minute test period (Figure 12 e). The vehicle DMSO had no significant effect when compared to the initial control period in which the tissue was bathed in carbogenated Krebs solution, alone (control).

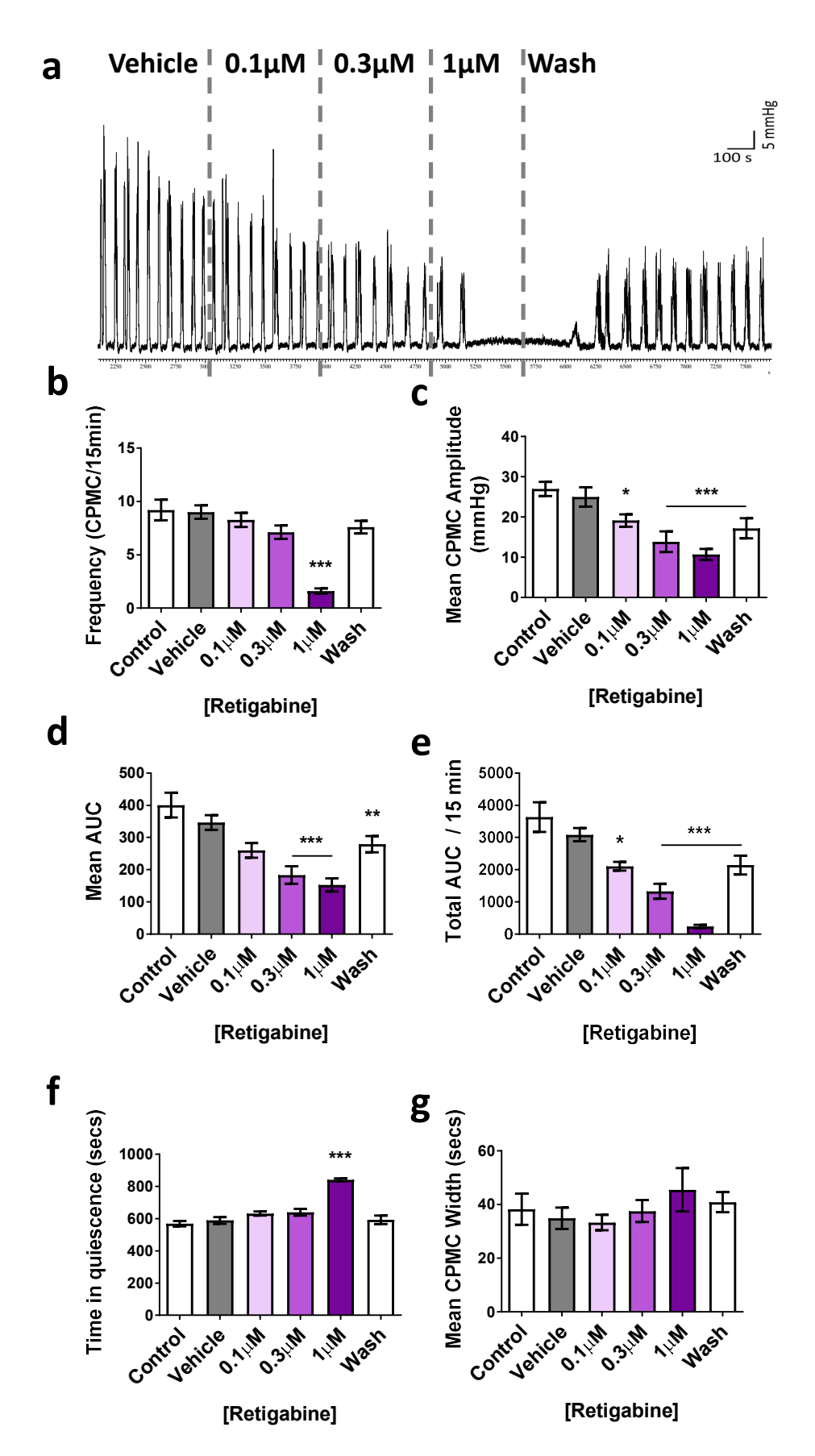


Figure 12 The effect of the Kv7 opener Retigabine on CPMC activity

An exemplar trace of CPMC activity during the Retigabine incubation experiment (a) Summary bar charts for; the average frequency of motor complexes over the 15 minute period (b), the mean motor complex amplitude (c), the mean AUC of a complex (d) and the total AUC over the 15 minute period (e), the TIQ over the 15 minute period (f) the mean motor complex width (g) and the mean motor complex interval (h) in the presence of Retigabine. Data are expressed as mean (n=5), SEM; *p < 0.05; **p < 0.01; ***p < 0.001; versus vehicle/control by repeated measures one-way ANOVA followed by Dunnett's test.

Next, we investigated the effects of ML213 upon CPMC activity (Figure 13). The partially selective Kv7.2/7.4 compound, ML213, was more potent in decreasing CPMC activity than Retigabine. Bath application of ML213 (0.03- 0.3 μ M) significantly decreased CPMC frequency, amplitude, and increased TIQ at doses of 0.1 & 0.3 μ M ML213. The effects of ML213 upon frequency and TIQ reversed upon washout of ML213. The changes in amplitude were irreversible over the 40-minute washout period assessed.

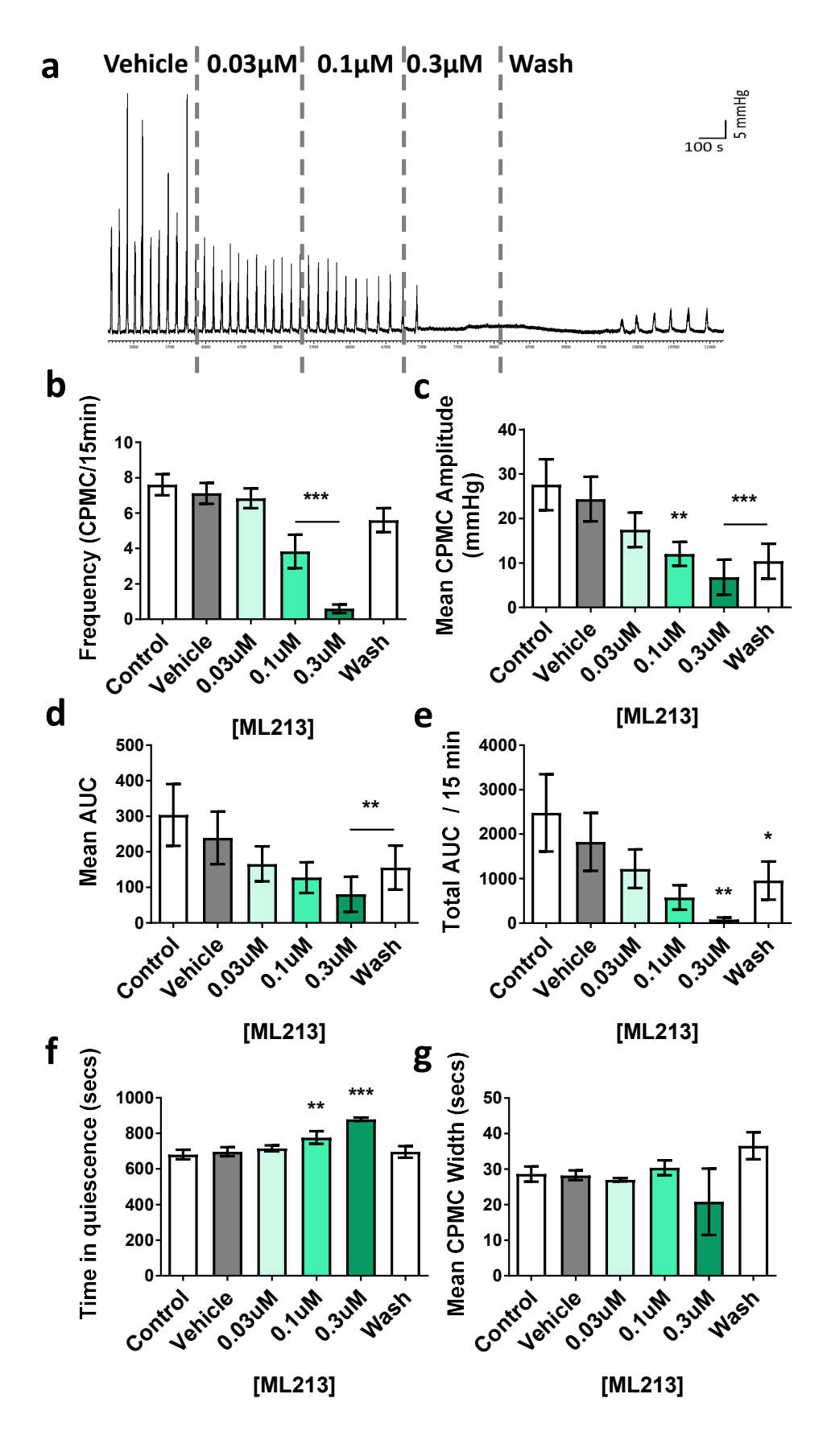


Figure 13 The effect of Kv7 opener ML213 on CPMC activity

An exemplar trace of CPMC activity during the ML213 incubation experiment (a) Summary bar charts for; the average frequency of motor complexes over the 15 minute period (b), the mean motor complex amplitude (c), the mean AUC of a complex (d) and the total AUC over the 15 minute period (e), the TIQ over the 15 minute period (f) the mean motor complex width (g) and the mean motor complex interval (h) in the presence of ML213. Data are expressed as mean (n=5), SEM; *p < 0.05; **p < 0.01; ***p<0.001; versus vehicle/control by repeated measures one-way ANOVA followed by Dunnett's test.

Bath application of retigabine (0.1 -1.0 μ M) caused a decrease in ileal peristaltic motor complexes (Figure 14a). At 1 μ M retigabine IPMC frequency was decreased from 4.6±0.2 IPMCs/900 s (vehicle) to 1.25 ± 0.5 IPMCs/900 s (1 μ M retigabine, p<0.001 versus vehicle, Figure 14b) and TIQ was increased from 479±39 s (vehicle) to 815±33 s (1 μ M retigabine, p<0.001 versus vehicle, (Figure 14 f). Both the frequency and TIQ changes were fully reversible upon washout of retigabine. Retigabine also caused a dose dependent decrease in IPMC amplitude, in which significant decreases in amplitude were observed at 0.3 and 1.0 μ M Retigabine (Figure 14 c). The distension evoked IPMCs of the ileum were different to those produced in the colon but were still affected in a similar fashion by Kv7 activators.

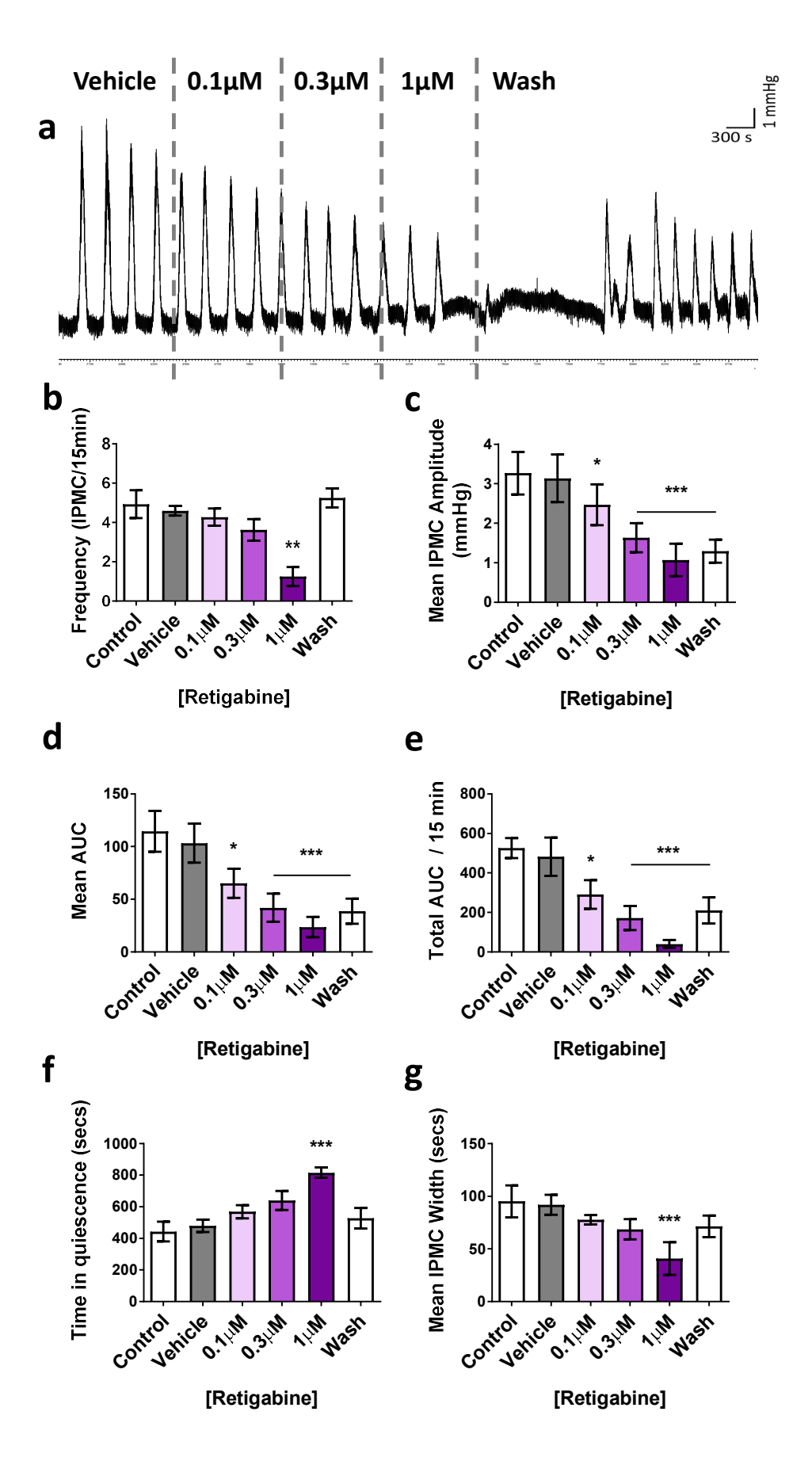


Figure 14 The effect of the Kv7 opener retigabine on IPMC activity

An exemplar trace of IPMC activity during the Retigabine incubation experiment (a) Summary bar charts for; the average frequency of motor complexes over the 15 minute period (b), the mean motor complex amplitude (c), the mean AUC of a complex (d) and the total AUC over the 15 minute period (e), the TIQ over the 15 minute period (f) the mean motor complex width (g) in the presence of Retigabine. Data are expressed as mean (n=4), SEM; *p < 0.05; **p < 0.01; ***p < 0.001; versus vehicle/control by repeated measures one-way ANOVA followed by Dunnett's test.

3.3.3 XE-991, A Kv7 Channel blocker, increases CPMC and IPMC activity.

Inhibition of the Kv7 channels with the addition of XE-991 (0.1 -1.0 μM) caused an increase in CPMC activity (Figure 15 a). At 0.3 and 1 μM XE-991 CPMC frequency was increased compared to vehicle control. At 1 μM XE-991 CPMC frequency was increased from 7.6±0.7 CPMCs/900s (vehicle) to 12.8±1 CPMCs/900s (1μM XE-991, p<0.001 versus vehicle) (Figure 15 b) and TIQ was decreased from 678±13 s (vehicle) to 572±23 s (1μM XE-991, p<0.001 versus vehicle) (Figure 15 f). Changes in the frequency were irreversible during the 40-minute washout of XE-991. XE-991 also caused a dose dependent increase in CPMC amplitude in which significant increases in amplitude were observed at 0.3 (32.9±1.3) and 1.0 μM (35.9±1.8) XE-991, compared to vehicle (27.1±0.9, p<0.001 versus vehicle) (Figure 15 c). During the periods of incubation with drug there was only a significant effect on mean AUC per CPMC in the presence of 1 μM XE-991 (Figure 15 d). However, the total power output, Total AUC (Figure 15 e), was increased by 0.3μM and 1μM XE-991. The mean CPMC interval measures the mean time from the beginning of one CPMC to the next within the 15-minute period. Again, here there is a significant decrease in this time from 0.3 μM XE-991 onwards, in line with the increase in frequency (Figure 15 h).

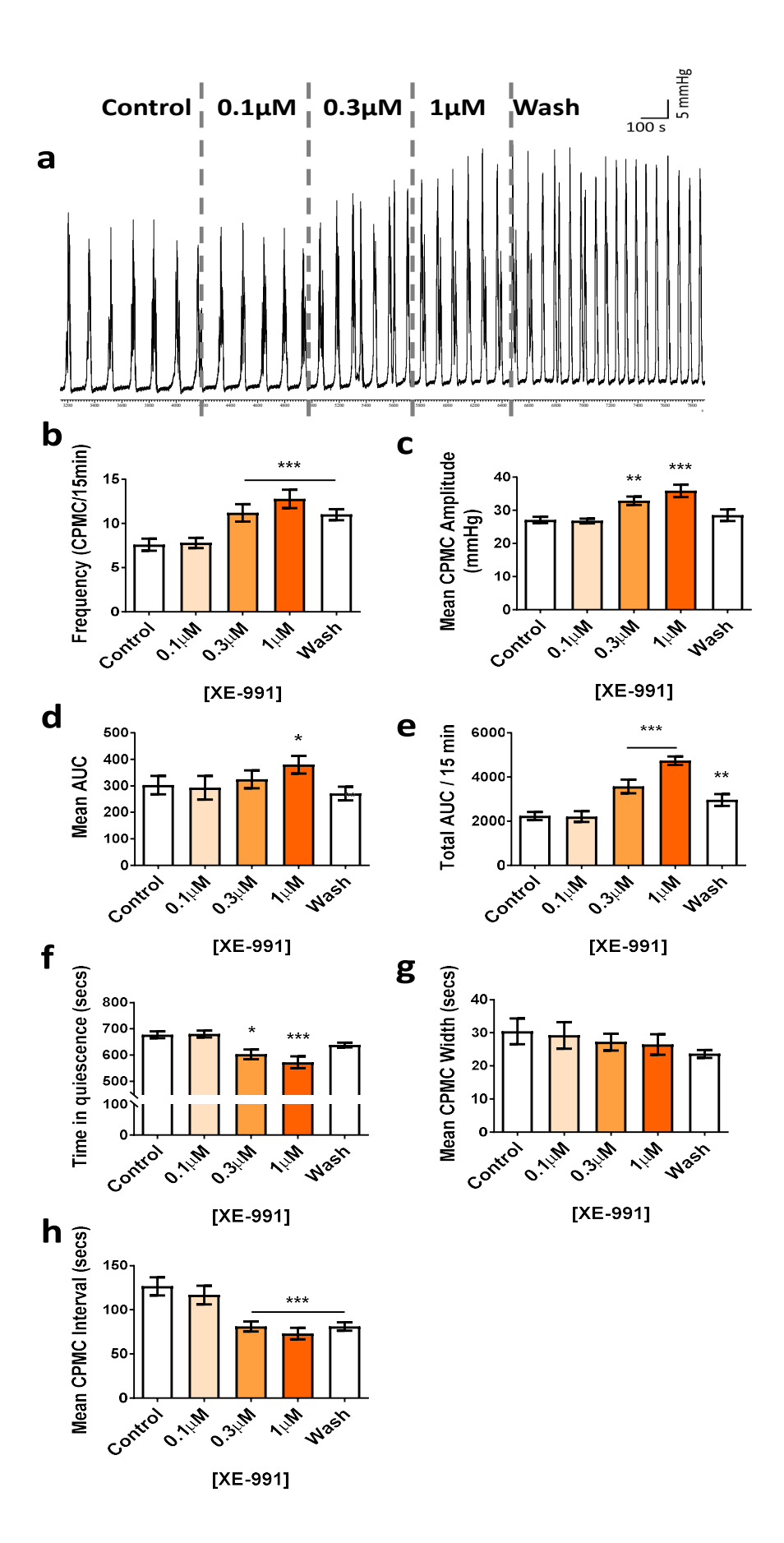


Figure 15 The effect of the Kv7 blocker XE-991 on CPMC activity

An exemplar trace of CPMC activity during the XE-911 incubation experiment (a) Summary bar charts for; the average frequency of motor complexes over the 15 minute period (b), the mean motor complex amplitude (c), the mean AUC of a complex (d) and the total AUC over the 15 minute period (e), the TIQ over the 15 minute period (f) the mean motor complex width (g) and the mean motor complex interval (h) in the presence of XE-991. Data are expressed as mean (n=5), SEM; *p < 0.05; **p < 0.01; ***p<0.001; versus vehicle/control by repeated measures one-way ANOVA followed by Dunnett's test.

Bath application of XE-991 (0.1 -1.0 μ M) caused increased activity in ileal peristaltic motor complexes (Figure 16). At 1 μ M XE-991 the IPMC frequency was increased from 4.6±0.8 IPMCs/900 s (vehicle) to 6.5 ± 0.8 IPMCs/900 s (1 μ M XE-991, p<0.001 versus vehicle) (Figure 16 b) and TIQ was decreased from 501±16 s (vehicle) to 330±43 s (1 μ M XE-991, p<0.001 versus vehicle) (Figure 16 f). Changes in the frequency were irreversible during the 40-minute washout of XE-991. XE-991 did not caused an increase in IPMC amplitude (Figure 16 c) during XE-991 application but a reduction in mean AUC was observed at 1 μ M (Figure 16 d). The mean interval between IPMCs was reduced by XE-991 in a dose dependent manner (Figure 16 h).

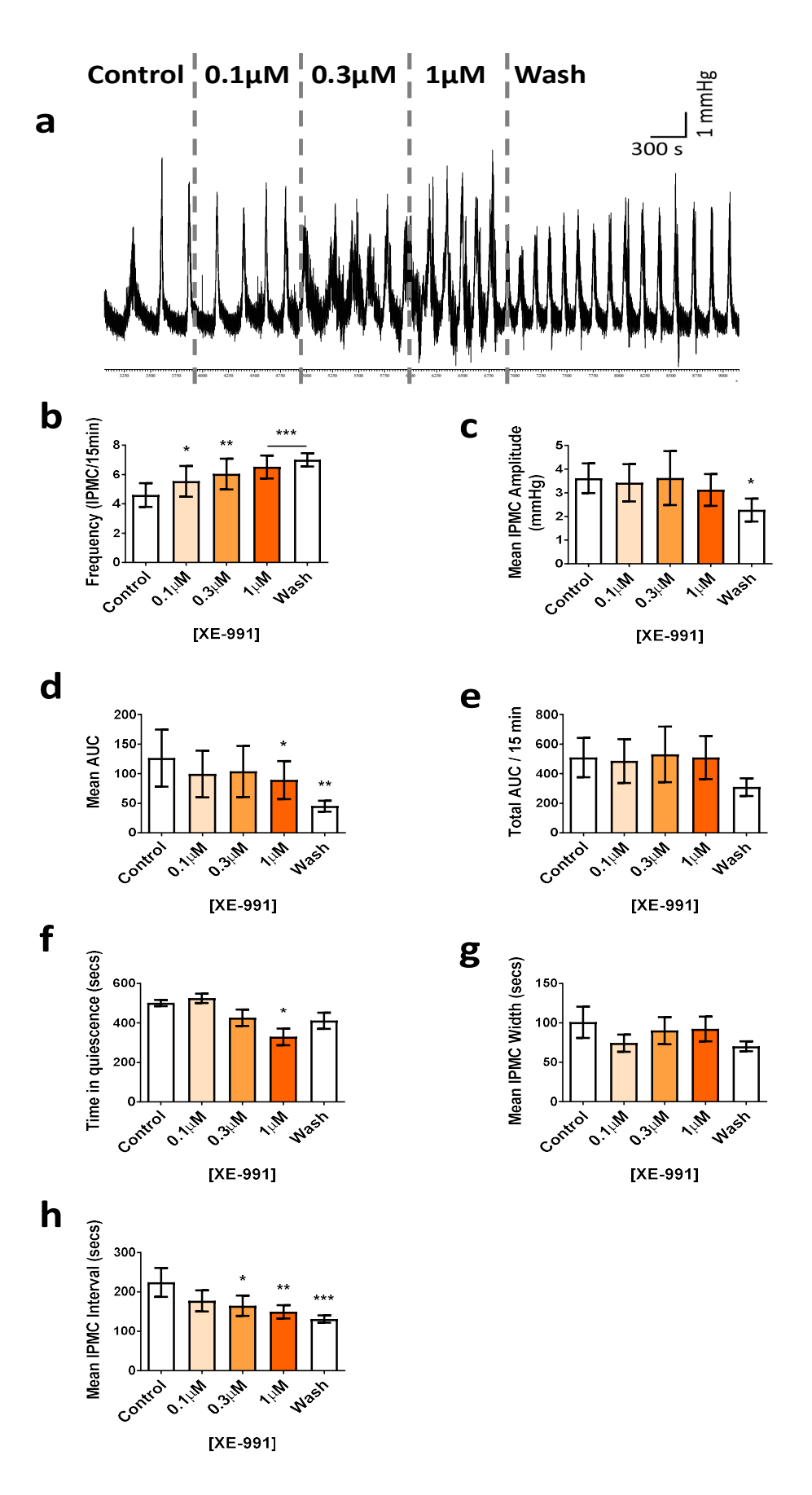


Figure 16 The effect of the Kv7 blocker XE-991 on IPMC activity

An exemplar trace of IPMC activity during the XE-911 incubation experiment (a) Summary bar charts for; the average frequency of motor complexes over the 15 minute period (b), the mean motor complex amplitude (c), the mean AUC of a complex (d) and the total AUC over the 15 minute period (e), the TIQ over the 15 minute period (f) the mean motor complex width (g) and the mean motor complex interval (h) in the presence of XE-991. Data are expressed as mean (n=5), SEM; *p < 0.05; **p < 0.01; ***p<0.001; versus vehicle/control by repeated measures one-way ANOVA followed by Dunnett's test.

3.3.4 The Retigabine induced decrease in CPMC activity is inhibited by $K_{\nu}7$ channel blocker XE-991

To ensure that the compounds in this set up were acting through the KCNQ channels, we incubated Retigabine in the presence of KV7 blocker XE-991. The effects of Retigabine on frequency (Figure 17 a) and TIQ (Figure 17 e) were counteracted in the presence of the Kv7 blocker XE-991. The reduction in amplitude due to retigabine (Figure 17 b), and as a result AUC (Figure 17 c, d), is shifted by XE-991, indicating action at the same site.

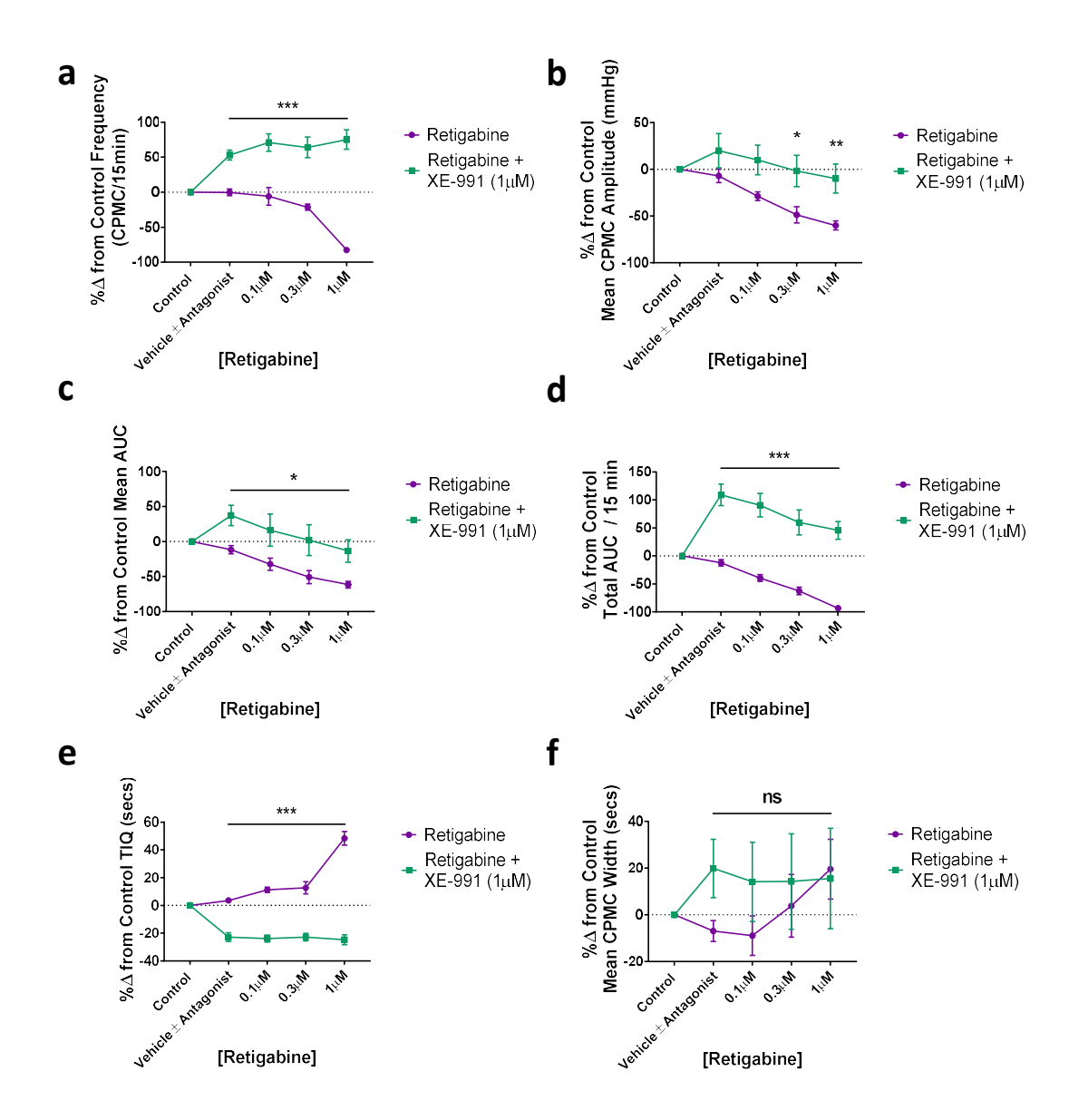


Figure 17 Kv7 blockade has an inhibitory effect on Retigabine induced decrease of CPMC activity.

Summary dose response charts comparing the average frequency of CPMCs over 15 minutes (a), CPMC amplitude (b), Mean AUC (c), Total AUC over the 15 minute period (d), TIQ over the 15 minute period (e) and mean CPMC width (f) in response to increasing concentrations of Retigabine in the presence (\bullet) and absence (\bullet) of XE-991. Data are expressed as % mean (n=4) to the control response, SEM; *p < 0.05; **p < 0.01; ***p<0.001; mean Retigabine + XE-991 versus mean Retigabine alone at corresponding concentrations by repeated measures one-way ANOVA followed by Dunnett's test.

3.3.5 Immunohistochemistry confirms the presence of Kv7.4 positive structures in the smooth muscle layers and the myenteric plexus.

Using immunohistochemistry, we determined the expression of KCNQ4 encoded protein in the colon. The colon comprises of different layers and here we show KCNQ4-ir using different preparations of the tissue. Within the wholemount sections (Figure 18 a-e) there is staining of structures within the longitudinal and circular muscles, the myenteric plexus as well as the epithelial layer. With the stretch preparations (Figure 18 f-h) we were able to focus more on the myenteric region alone and here show KCNQ4 expression on cells that also express the neuronal marker PGP9.5.

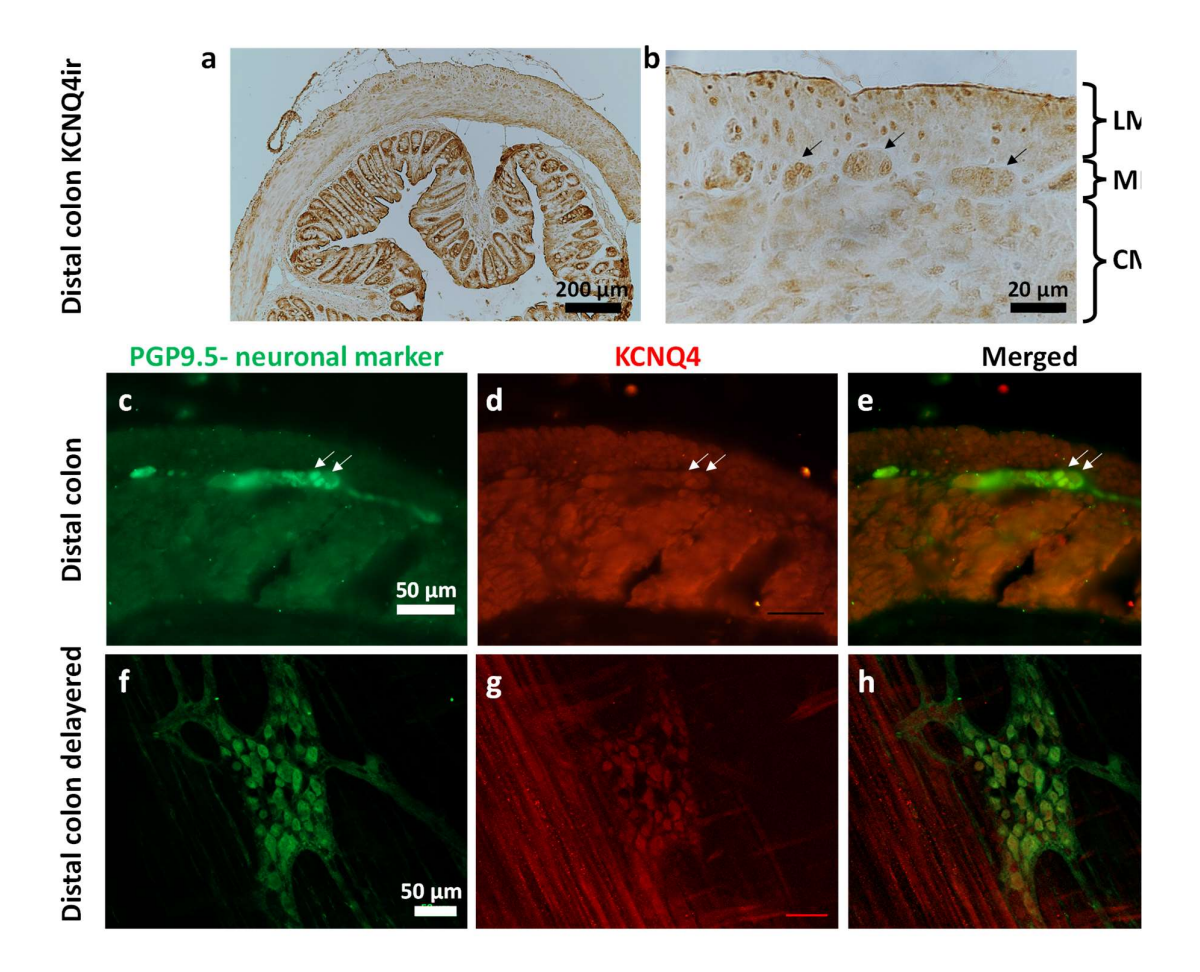


Figure 18 Expression of KCNQ4-ir in the smooth muscle layers and myenteric plexus of the murine colon

Wholemount colon shows high levels of KCNQ4 expression (a). At higher magnification (b) distinct structures with KCNQ-ir can be seen in the longitudinal (LM) and circular muscle (CM) layers as well as the myenteric plexus (MP). PGP9.5 staining highlights the neurons of the myenteric plexus in wholemount (c) and stretch preparation (f) colon tissue. KCNQ4 staining (d and g) and double labelling shows co-localisation between these two markers (e and h). Arrows indicate Kv7.4 expression within the myenteric plexus.

3.4 Discussion

Firstly, we have shown that distension evoked motor complexes of the large intestine differ from that of the small intestine. The complexity and completeness of the ENS mean that even in the absence of extrinsic CNS innervation, such isolated segments generate patterns of peristaltic-like motor activity ex vivo. In this instance the IPMCs of the ileum consist of small, fast contractions building upon each other to produce waves of increases in IP followed by periods of quiescence. The colon, when distended, produces regular more pronounced increases in IP due to proximal contractions which propagate aborally (Figure 8). When comparing periods of activity and periods of rest in the tissues, the colon produces more frequent periods of activity, than the ileum within a given time. The colonic motor complexes on average have almost a 10-fold larger amplitude and resultantly have greater area under the curve. As mentioned, the ileal motor complexes consist of small, fast contractions building upon each other. This pattern means that the active phase of the ileum for each motor complex lasts much longer than that of the colon, as the width of the ileal motor complexes are significantly larger than those of the colon. The interval between each motor complex is also larger in the ileum. Despite this, the time that the ileum spent at rest, TIQ, was slightly but significantly lower than that of the colon, despite the colon's higher frequency of motor complexes (Figure 9).

We attempted to characterise the differences further by looking at the inherent fluctuations of the tissue which can also be termed as contractility. This can be viewed when stretching out the traces to view an individual motor complex, with rest periods either side. (Figure 10). At rest both the colon and the ileum have comparable amplitude of contractility. In the active phase, contractility of the ileum remains similar in its amplitude, even though IP in the organ as a whole increases. The amplitude of this contractility in the colon during an active motor complex are significantly increased, indicative of the large "jumps" in IP that are seen in the CPMC. The number of fluctuations per second in both tissues is again similar at rest but decreases significantly in both when the tissues are in the active phase. The number of fluctuations per second is significantly lower in the colon compared to the ileum during the active phase. This is likely as a consequence of the larger amplitude of contractility during the colon's "jumps" in IP (Figure 11), when active.

The differences in motor patterns between the two tissues are likely to be indicative of the differences in structure and functional roles between the colon and small intestine.

This study builds upon the work of Jepps et al. (2009), in showing a more physiologically relevant effect of modulation of the K_v7 channels in gastrointestinal smooth muscle structures. We have confirmed that ongoing K_v7 activity is present in this *in-vitro* model and is critical in gastrointestinal motility in the colon and ileum. Activation of Kv7 channels brings peristalsis-like movements to a halt and Kv7 channel inhibition induces an increase in the frequency and magnitude. With this apparatus we were able to house a complete segment of the organ, with a fully functional network of the different cell types. This allows us to investigate mechanisms involved in basal activity and tease apart the consequences of impacting one cell type or the other.

As mentioned, distension of the lumen of intestinal segments in our bioassay induces regular peristaltic like complexes which have periods of activity, measured as increases in intraluminal pressure, separated by periods of rest. This pattern is continuous in the absence of any other external stimulus, as long as the distension of the lumen is maintained. The control system of this basal activity and, peristalsis as a whole, is a complex motor pattern that involves the interplay of neurogenic, myogenic and pacemaker mechanisms. Ion channels can be present on these cell types but not be involved in the basal distension evoked peristalsis- like complexes. Our previous work has shown that although TRPA1 channel activation can regulate motility, they do not contribute to generation or regulation of basal motor activity induced by distension. We concluded this as TRPA1 antagonists had no effect on baseline CPMC measurements (Hassan et al., 2020). Blockade of Kv7 channels using XE-991 increased the activity of colonic and ileal peristaltic-like motor complexes, indicating their involvement in this basal activity. Baseline activity was also effected by XE-991 in myograph mouse colonic preparations (Jepps et al., 2009), human taenia coli (Adduci et al., 2013) and the rat gastric fundus (Ipavec et al., 2011). This suggests that the Kv7 channel plays an important role in setting the intrinsic basal tone of the organs of the GIT (Adduci et al., 2013).

We first looked at K_v7 channel modulation in the colon due to it being the site of highest expression of KCNQ channels in the GI tract (Jepps et al., 2009) and this bioassay's ability to produce robust

consistent peristaltic like motor complexes. Increasing the opening probability of the $K_\nu 7$ channels using compounds, Retigabine and ML213, abolished the colonic peristaltic like motor complexes. The inhibitory effects on peristaltic motor complexes by $K\nu 7$ channel openers in our study were seen at lower concentrations (0.3 μ M-1 μ M) than in previous publications using gastrointestinal tissue (Jepps et al., 2009; Peiris et al., 2017). This is likely due to the completeness of our system and the expression of $K_\nu 7$ channels throughout the different layers and cell types of the tract. The inhibitory effects of Retigabine were also present in the same dose dependent manner in the ileum. Neuronally, the KCNQ "M-current" activates relatively slowly at subthreshold potentials contributing to the resting potential and supressing repetitive firing rather than impacting upon the repolarization of action potentials in the neuronal cell (Suh et al., 2006). In vascular smooth muscle activation of these channels by Retigabine, caused membrane hyperpolarisation and relaxation of preconstricted vascular tissue (Joshi et al., 2009). Our results show that the activation of $K_\nu 7$ channels by Retigabine works to both effect the frequency of CPMCs by suppressing action potentials and neurotransmitter release by neurons and effects the amplitude by causing relaxation in the muscle, via hyperpolarisation of smooth muscle cells.

At the effective concentrations in this study $(0.3\mu\text{M}-1\mu\text{M})$ Kv7 channel blocker, XE-991 has not been shown to inhibit other ion channels (Greenwood & Ohya, 2009). XE-991 has an IC50 at $K_v7.1-7.4$ at ~1-5 μM but is less potent at $K_v7.5$ at ~60 μM . From Jepps et al., 2009, we see that $K_v7.4-7.5$ dominate in their expression in the GI tract above other K_v7 channels. With as little as 0.3 μM effective at causing an increase in frequency and amplitude of the CPMC, we believe that much of the effect of K_v7 modulation in the GI tract is $K_v7.4$ driven. In the ileum XE-991 has similar effects on frequency and TIQ as in the colon, however, amplitude does not increase. During the wash phase (25-40 minutes after XE-991 removal) amplitude is unexpectedly decreased compared to the first 15 minutes post equilibration. From our observations, the ileum is a much more sensitive organ within this set up and often did not last much longer than the 1.5-hour experiment. It was less robust in its ability to produce constant regular contractions for that period. When removed from the apparatus, on most occasions it had lost its structure and often degraded, shedding its mucosa. This decrease is more likely due to time in the organ bath at distension than any delayed effects of XE-

991. Retigabine decreased the CPMC amplitude (Figure 12) and IPMC amplitude (Figure 14) at all tested concentrations but only showed significant effects on TIQ at the highest concentration (1µM). Blockade of the Retigabine response with XE-991 showed a shift in response in parameters that are influenced by amplitude. There was also a total blockade of any Retigabine response in frequency and its related measurements. Therefore, the modulation of activity seen with these compounds is due to their action on Kv7 channels. With the multitude of cell types potentially expressing Kv7 channels and therefore involved in these responses as well as the limited concentrations of the modulators tested, it is difficult to tease apart any other pharmacological interpretations.

A novel activator partially selective for $K_v7.2$ and $K_v7.4$, ML213 (Figure 13), was shown to be more potent in effecting CPMCs amplitude and frequency than Retigabine (Figure 12). Due to the low expression of KCNQ2 in gastrointestinal smooth muscle (Jepps et al., 2009), it may be suggested that this increased potency is due to its selective binding of K_v7.4. This again implies its position as the critical subtype of K_v7 channels involved in smooth muscle motility. However a more recent study (Brueggemann et al., 2014), showed a revised selectivity where, ML213 was an effective activator which cannot distinguish between K_v7.4, K_v7.5 and K_v7.4/7.5 heteromers. These two activators, along with many others, share a binding site on the pore domain of K_v7 channels. A mutation in an essential tryptophan in the s5 transmembrane domain of the K_v7.5 channel, which renders the Retigabine response ineffective, also greatly reduced the increase in current in response to application of ML213 (Brueggemann et al., 2014; Yu et al., 2010). In vascular tissue the EC50 of many K_v7 activators were assayed showing that ML213 had an 8-fold increase in potency over Retigabine in producing vasorelaxation (Jepps et al., 2014). Such assays, like our studies, cannot draw conclusions as to whether this is due to specificity, affinity or other factors of the two compounds, especially as in the gastrointestinal tract we believe that multiple cell types are involved the functional outcomes.

All compounds had a lasting effect on the tissue. Retigabine caused the amplitude of contractions to remain almost one third below the original amplitude even after removal of the drug and a considerable wash period. XE-991 irreversibly decreased the interval between complexes and

increased the frequency per 15-minute interval when no drug was present. ML213 also diminished the magnitude of CPMCs even during a 40-minute wash period. This may be due to irreversible binding, the drugs causing a permanent conformational change to the channel or an insufficient washout period. It is more likely that this is not due to irreversible binding as the complexes during the last wash period are not the same in terms of magnitude or frequency as they are when in the presence of the highest drug concentrations. However, as these compounds are acting on multiple cell types and we are limited on time of each experiment we cannot pinpoint the reason for these apparent irreversible effects. Similar to our findings, the contractile effects of XE-991 did not return to baseline up to 45 minutes after washout from human taenia coli preparations (Adduci et al., 2013). In the same study Retigabine induced a dose dependent relaxation of bethanechol preconstricted taenia coli strips, however after washout of the compounds from the organ bath, the strips continued to relax beyond their original tone. This did not occur with bethanechol preconstriction and DMSO vehicle control alone. Retigabine induced relaxation of nonpreconstricted strips took 2 hours post washout to return to basal muscle tone (Adduci et al., 2013). Had we monitored our preparations 2 hours after washout we may have seen similar observations of slow dissociation kinetics, which have been observed with these modulators in other tissues (Ipavec et al., 2011; Wladyka & Kunze, 2006; Yeung & Greenwood, 2005).

This is similar to the action of K_v7 channel modulation in neurons of the CNS (Brown & Passmore, 2009), and there is a temptation to attribute the effects that we see, entirely to the action of the enteric nervous system. Jepps et al. (2009), implied that the channels were not on neurons, as the neuronal blockade by toxins completely abolished what they termed as high-amplitude low frequency (HALF) contractions. Within this contraction type, prior to toxin administration, they saw changes in frequency in the presence of XE-991. At lower toxin concentrations HALFs were present and again increased in frequency with XE-991 administration. Differences in amplitude of the complexes indicate an effect on smooth muscle cells yet changes in frequency are likely to result from action on a different cell type, neurons or the Interstitial Cells of Cajal (ICC). As well as smooth muscle, Jepps et al., (2009) using immunohistochemistry found some labelling of Kv7 channels within the myenteric plexus region however double labelling with a neuronal marker was

not performed. Interstitial cells from the guinea pig bladder have displayed KCNQ currents that play a role in the resting membrane potential and excitability of the cell (Anderson et al., 2009). In the gastrointestinal system Kv7 channels in the ICC have not been fully characterised but their expression has been shown in small intestine (Chen et al., 2007). In the cultured ICCs from the mouse colon, electrophysiological studies have shown K+ currents that are active at the resting membrane potential that are blocked by XE-991 (Wright et al., 2014). The channels have been proposed to be involved in the pacemaker activity of colonic ICCs.

Somatostatin [somatotropin release-inhibitory factor (SRIF)] is present in a subpopulation of interneurones that project within the myenteric plexus but not into the muscle layers of the intestine. When SRIF was administered into the same preparation as we have used, it increased the interval between peristaltic events but not the magnitude or duration of the individual contractile events. This fits well with co-localisation and fibre tracing studies, in pinning its actions to within the enteric circuitry rather than being myogenically driven (Abdu et al., 2002).

Our immunohistochemical characterisation (Figure 18) shows that the $K_{\nu}7.4$ channel is present on the smooth muscle layers and within the myenteric plexus. The functional effects on frequency and amplitude of $K_{\nu}7$ drugs in our system confirm this, with frequency primarily governed neuronally and amplitude driven myogenically. A lack of double labelling of $K\nu7.4$ with a marker of ICCs means that we cannot confirm any expression on ICCs, which if present may also contribute to the functional effects on frequency by $K\nu7$ modulation.

The functional roles of Kv7 channels in enteric neurons have not been studied to our knowledge, hopefully the evidence that we have provided in this study of their expression will lead to that. Should Kv7 channels in enteric neurons function in vivo as Kv7 channels do in other neuronal cells they would contribute to the resting membrane potential and afterhyperpolarisation of the cell. Consequently they would regulate excitability of the neuron and consequently the release of neurotransmitters such as acetylcholine (Brown & Passmore, 2009; Martire et al., 2004; Nickolson et al., 1990). This seems highly likely considering the effects we observed, where blocking the channel led to an increase in frequency of peristaltic like motor complexes, yet without dedicated

studies this cannot be confirmed. Kv7.5 positive ICCs have been shown to be present in the mouse colon in regions abundantly innervated by cholinergic neurons. Inhibition of the Kv7 channels on ICC preps caused depolarisation of ICCs and enhanced excitability (Wright et al., 2014). In vivo, cholinergic transmission as well as membrane potential, may modulate Kv7 channels on ICCs to regulate or generate pacemaker activity in the gastrointestinal system. The mechanism of Kv7 channel's regulation of small or large intestine smooth muscle excitability has not been investigated but smooth muscle of other tissues have been looked into. Addition of Kv7 activators reduced excitability of smooth muscle cells (SMC) via hyperpolarisation of isolated mesenteric artery SMCs (Jepps et al., 2014) and bladder detrusor SMCs (Provence et al., 2015). In Detrusor SMCs addition of the Kv7 activators led to a decrease in intracellular calcium levels (Provence et al., 2015) and conversely the vasoconstriction of pulmonary artery preparations by Kv7 blockers required calcium influx (Joshi et al., 2006). The NO donor, Sodium nitroprusside (SNP) and the phosphodiesterase-5 (PDE5) inhibitor, Sildenafil induced relaxations of the rat penile artery and corpus cavernosum were impaired in the presence of Kv7 blocker Linopirdine, implicating the Kv7 channels in the NOcGMP pathway (Jepps et al., 2016). Similarly, relaxation of rat aorta and renal artery preparations by natriuretic peptides were impaired by Linopirdine. Natriuretic peptides work directly on the smooth muscle via cGMP. Kv7.4 expressing human embryonic kidney cells were used to show that K+ currents increased with cGMP stimulation and this effect was abolished by addition of a Kv7 blocker (Stott et al., 2015). Unlike vascular smooth muscle, relaxation of precontracted gastric fundus strips exposed to the NO donor, acidified sodium nitrite, were not altered with Kv7 inhibition. However, the effect of another known relaxation mechanism, vasoactive intestinal peptide (VIP), was impaired by approximately 25% in the presence of XE-991, implicating the Kv7 in the signal transduction of VIP in SMCs of the stomach (Ipavec et al., 2011). VIPR2 receptors are activated by VIP leading to relaxation of the gastric fundus through an increase in intracellular cyclic adenosine monophosphate (cAMP) and activation of protein kinase A (PKA). Our experiments cannot conclude whether the mechanisms at play in this experiment of Kv7 modulation are NO (cGMP) or VIP (cAMP) mediated, this requires further pharmacological investigation.

The cAMP pathway has also been implicated in the physiological regulation of the M-current in myenteric and renal myocytes which showed increased Linopirdine sensitive currents when incubated with an exchange protein directly activated by cAMP (EPAC) activator (Stott et al., 2016). A phosphodiesterase 4 inhibitor, Rolipram, activated Kv7 current in A7r5 cells which express Kv7.5 channels as did β-adrenoceptor agonist isoprenaline via enhanced PKA dependent phosphorylation of the channel (Mani et al., 2016). Blockade of Kv7 channels significantly reduce relaxation in both mesenteric and renal artery preparations induced by an EPAC activator and isoprenaline, indicating the channels involvement in this pathway (Stott et al., 2016). In Guinea pig gastric corpus strips, isoprenaline had reduced effects in strips pre-incubated with Retigabine, further indicating its central role in β-adrenoceptor induced relaxation (Apostolova et al., 2017).

In conclusion, we have demonstrated that that ongoing K_v7 activity is present in this *in-vitro* model and is a critical regulator of gastrointestinal motility in the colon and the ileum. K_v7 activity is important in limiting peristaltic activity and inhibition of these channels has an excitatory effect on the small and large intestine, increasing the frequency and magnitude of peristaltic-like complexes. Of the various K_v7 channels, our results show that $K_v7.4$ potentially plays a central role in these actions. More specific compounds may allow us to have a better understanding of the mechanism by which excitation of the gastrointestinal tract can be manipulated using K_v7 modulators with a view to potential treatment of motility disorders such as constipation.

Gastrointestinal and urinary dysfunction in animal models of Parkinson's disease

4 K_V7 CHANNEL REGULATION OF GASTROINTESTINAL MOTOR ACTIVITY IN AN MPTP MOUSE MODEL

4.1 Introduction

Early assessments of gastrointestinal dysfunction in MPTP treated mice focused on the acute, likely peripherally mediated effects of the toxin. MPTP administered 45 minutes prior, caused delayed transit of a charcoal mixture in a dose dependent manner (Haskel & Hanani, 1994). This timepoint and dose is unlikely to have led to any central effects of MPTP, as MPTP often requires multiple doses over time to achieve neurodegeneration. The authors did not assess nigral dopaminergic loss, but the impaired gastrointestinal transit was not alleviated by the co-administration of the monoamine oxidase inhibitor pargyline, indicating that the effects were likely due to the parent molecule, MPTP, rather than its neurotoxic metabolite MPP+. The inhibition of transit by MPTP in this study was postulated to be mediated via β -adrenoceptors and dopamine receptors, as propranolol and haloperidol both diminished the inhibitory effects. Neither drug effected motility significantly when administered in the absence of MPTP (Haskel & Hanani, 1994). More sensitive measurements of gastrointestinal function showed similar effects via electrodes surgically placed on the small intestine of MPTP treated rats. These rats showed no sign of nigral dopaminergic neuron loss, as they are resistant to the neurotoxic effects of MPTP, but MPTP injection decreased small intestinal activity significantly. Although, the frequency of the migrating motor complexes returned to normal frequency within 24 hours of injection, they returned in a disrupted manner with

significant prolonged duration of an irregular spiking phase. Pargyline recovered some of this chronic disruption but not the acute inhibition. Significantly lower levels of dopamine were detected in the in the small intestine but in the highest dose group only (Eaker et al., 1987). MPTP in isolated mouse colon preparations caused muscle relaxation at low concentrations but higher concentrations elicited multiple contractile events (Hanani, 1990). It is clear that MPTP can have peripheral effects on GIT, which is something for us to consider in our studies.

The variable effects of MPTP on transit and gastrointestinal motility is also apparent in studies in vivo, where dopaminergic neuron loss occurs in the SNpc. Monitoring the distance travelled of an orally administered dye at a given time point, it was determined that there was no alteration in small intestinal transit at day 3 and day 10 post MPTP treatment compared to vehicle treated animals (Anderson et al., 2007). In the same study Anderson et al. (2007) showed a significantly higher stool frequency in a 1-hour stool output assay 3 days after MPTP administration which normalised by 8-10 days. However, similar dosing regimens, by other groups have resulted in reduced stool frequency, stool weight and increased colonic transit time, as measured by the bead expulsion assay. This lasted for the duration of the experiment, which was 7 days post final MPTP dose (Natale et al., 2010; Sampath et al., 2019) but has been shown to continue for up to 53 days (Lai et al., 2018). Probenecid can be used to limit renal excretion of compounds and has been used in PD mouse models to increase the exposure of the MPTP. In this dosing regime, treated mice again display increased colonic transit time and reduce faecal water content (Han et al., 2021).

Isolated segments of the colon from MPTP treated mice showed more robust contraction and impaired relaxation after electric field stimulation (EFS) (Anderson et al., 2007). This is postulated to be in part due to a reduction in the dopaminergic transmission within the ENS. Multiple studies have shown decreased dopamine content, TH+ve, DAT positive cells in the small and/or the large intestine of PD animal models (Anderson et al., 2007; Lai et al., 2018; Natale et al., 2010; Tian et al., 2008). Dopamine's role in the gastrointestinal tract is largely inhibitory regarding contractility and overall transit time. Loss of dopaminergic neurons has been observed in the myenteric plexus of a small number of PD patients (Lebouvier et al., 2008; Singaram et al., 1995) and therefore, the MPTP model is useful to investigate this particular mechanism in GI dysfunction of PD.

Other mechanisms have also been shown to be altered in the MPTP model. Nitrergic relaxation assessed by EFS was shown to be severely diminished in colon tissue from MPTP treated mice, with a significant reduction in neuronal nitric oxide synthase expression (nNOS) (Lai et al., 2018). Increases in α-synuclein in the small intestine (Natale et al., 2010) and colon (Han et al., 2021; Sampath et al., 2019) as well as gut inflammation and dysbiosis (Lai et al., 2018) have been reported in tissue from MPTP treated animals. Interestingly, these alterations have also been observed in patients, however their, use as early biomarkers and causality in slow transit time is yet to be determined (Fasano et al., 2015).

Most studies of the gastrointestinal tract discussed so far, have used gross behavioural readouts such as stool output or expulsion assays. Whilst being very translatable, functional readouts, from those types of assays it is not easy to distinguish changes in different organs of the gastrointestinal tract and to discern whether the dysfunction is due to local or central changes. The assays in isolated tissues have been mostly using conventional organ baths, which is useful for looking at transmission of different contractile and relaxant mechanisms but not motility or peristalsis per se. One exception to this is a recent study by Gries et al., (2021), where spatiotemporal maps were used to visualise motility, real time in a whole organ system using isolated mouse small and large intestine from human α-synuclein expressing A30P mice. Here they showed a reduction in motility in both intestines of A30P mice, preceding motor symptoms. Interestingly they also found a panel of proteins and miRNAs that were altered locally in the tissues compared to control mice, of which a significant portion were also found to be dysregulated in human PD (Gries et al., 2021).

Our model of intestinal motility (discussed in chapter 3.2.2), has the advantage of being able to accommodate large sections of the intestinal tract and measure peristaltic like complexes, with all relevant cell types in sync including muscle cells and enteric neurons. Having characterised motility patterns of the different segments of the gastrointestinal tract and the effects of Kv7 channel modulators (Chapter 3) on naïve tissue.

We used this ex vivo model and IHC techniques to:

Monitor whether basal peristaltic like motor complexes differ between MPTP-treated and sham-treated mice.

Test whether differences are present in the effects of K_v 7 channel openers and blockers on colonic and ileum motility-like behaviour between MPTP-treated and sham-treated mice.

In this study MPTP treatment resulted in a significant decrease in TH+ve neurons in the substantia nigra, and abnormal shaped peristaltic like motor complexes in the ileum. There were no obvious functional differences in colon motility nor any robust differences in the responses to Kv7 modulation in either tissue. We did observe hyperactivity in the motility pattern of the small intestine in our MPTP treated mice, however it was likely not due to Kv7 channel disruption.

4.2 Methods

4.2.1 Animals

All experimental procedures were conducted with local ethical committee approval and in accordance with the UK Animals (Scientific Procedures) Act, 1986 (National Archives, UK Animals, Scientific Procedures Act, 1986). 16 wildtype C57BL/6J0laHSd male mice (Envigo, UK), 12 weeks of age and weighing 21-25 g were used in this study. Animals were housed under controlled ambient temperature (21 ± 2 oC) and an even light-dark cycle of 12:12 hours. The animals were allowed free access to food and water. They were euthanised by exposure to a rising concentration of CO₂ and transcardially perfused with Krebs solution.

The experimental group received a sub-chronic dosing regimen of MPTP over 5 days (7x 18mg/kg of MPTP·HCl) (n=10). The sham group received the same number of injections to that of the MPTP group but with saline (0.9% NaCl, 150uL), over the same period (n=8). Further details of the methods are mentioned in 2.1.1.

Animals were euthanised one a day, 6-8 weeks post treatment. This time point post dose was chosen to minimise the impact of any acute, transient, peripheral effect on the GIT, which may influence

our findings. Once euthanised, the brains were processed for immunohistochemistry and the gut tissues were used in the motility bioassay.

4.2.2 In vitro colonic and ileal motility bioassay

The methods for this bioassay are as above in, using tissues from MPTP and sham dosed animals.

4.2.3 Experimental Procedure

The experimental procedure and data analysis for this bioassay is as above in chapter 2.1.3, using tissues MPTP and sham dosed animals.

4.2.4 Drugs

For K_v 7 channel activation, tissues were incubated in rising concentrations of Ethyl [2-amino-4-[[(4-fluorophenyl)methyl]amino]phenyl]carbamate (Retigabine) in dimethylsulfoxide (DMSO) dissolved in Krebs solution.

For inhibition of Kv7 channels the pan-Kv7 blocker 10,10-bis(4-Pyridinylmethyl)-9(10H)-anthracenone dihydrochloride (XE-991) was dissolved directly in Krebs solution. All compounds were purchased from Tocris Biosciences, Bristol, UK.

The MPTP used for dosing the animals was purchased from Sigma Aldrich, UK (M0896).

4.2.5 Immunohistochemistry

Further details of the Immunohistochemistry methods are mentioned in 2.4.2.

Substantia nigra containing sections were incubated in a primary antibody against tyrosine hydroxylase (TH) (ab112, Abcam, UK; 1:500) at RTP overnight and with an appropriate secondary antibody for one hour (RT). Immunoreactivity (ir) was observed by Avidin-biotin peroxidase complex immunohistochemistry, using 3,3-diaminobenzidine as the chromogen (Vector Laboratories Ltd, Peterborough, UK), as per manufacturer's instructions.

4.2.5.1 Image analysis

Images were acquired using Nikon T£2000-U microscope and NIS Elements software (Nikon, Cambridge, UK). Manual cell counts of dopaminergic neurons were performed from multiple areas analysed within regions of interest and extrapolated to the total area of the region.

4.3 Results

4.3.1 MPTP administration to mice led to a bilateral lesion due to a significant loss of dopaminergic neurons in the SNpc.

MPTP dosing of mice (7 x 18mg/kg) over 5 days resulted in a small statistically significant loss of bodyweight on day 1 post dose of approximately 1g (Figure 19 e, Day 0: $22.61g \pm 0.28$ vs Day 1: $21.6 g \pm 0.43$, mean \pm SEM). This returned to baseline levels by day 2 and continued to increase in the same manner as sham animals over the next 5 days (Figure 19 d & e). Analysis was performed on SNpc sections from sham and MPTP treated animals. Counts of TH+ve cells revealed an approximate 35% loss of dopaminergic neurons in the SNpc of mice injected with MPTP (Sham: 83.3 ± 4.9 vs MPTP: 53.3 ± 6.2 , cells per section, mean \pm SEM).

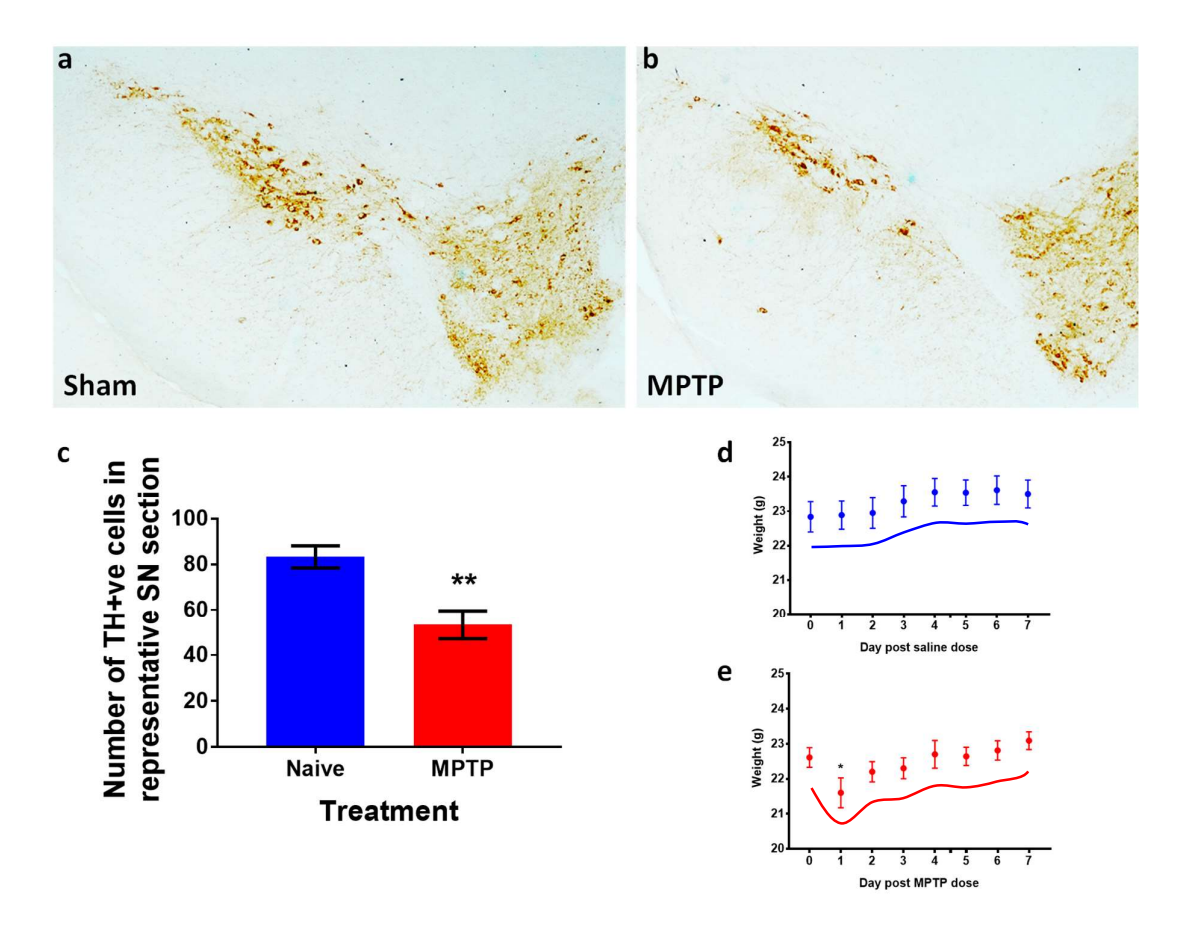


Figure 19 The effect of MPTP administration on the SNpc and mouse body weight.

Representative images of the SNpc of sham (a) and MPTP (b) dosed mice, stained for TH+ve neurons. Summary bar chart of TH+ve neuron counts in SNpc sections from sham and MPTP treated groups (c). MPTP treatment significantly reduced the number of TH+ve neurons in the SNpc, (mean \pm SEM, $n \ge 7$, ** p = < 0.01, unpaired t-test). Average body weight prior to and post dose of sham (d) and MPTP treated mice (e). MPTP treatment led to a small reduction in the average bodyweight of mice on the first day after dosing, (mean \pm SEM, $n \ge 7$, * p = < 0.05, one way ANOVA).

4.3.2 The ileum of MPTP treated mice displays an altered motility profile to that of sham treated mice.

Six-centimetre segments of ileum was placed into the motility organ bath and distended with Kreb's solution. This resulted in rhythmic contractile activity in these tissues. The ileum tissues from sham treated (Figure 20 a) animals had a different profile to those from MPTP treated animals (Figure 20 b).

When comparing the segments from the two treatment groups in the motility organ bath the major difference that can be observed is an increased amplitude in the IPMCs of MPTP treated mice (Figure 20 d). There were no differences between the treatment groups in terms of frequency, time in quiescence, IPMC width or interval between IPMCs (Figure 20). From that we can conclude that the increases seen in AUC (Figure 20 e & f) are driven by the increase in mean amplitude of the IPMCs from MPTP treated mice.

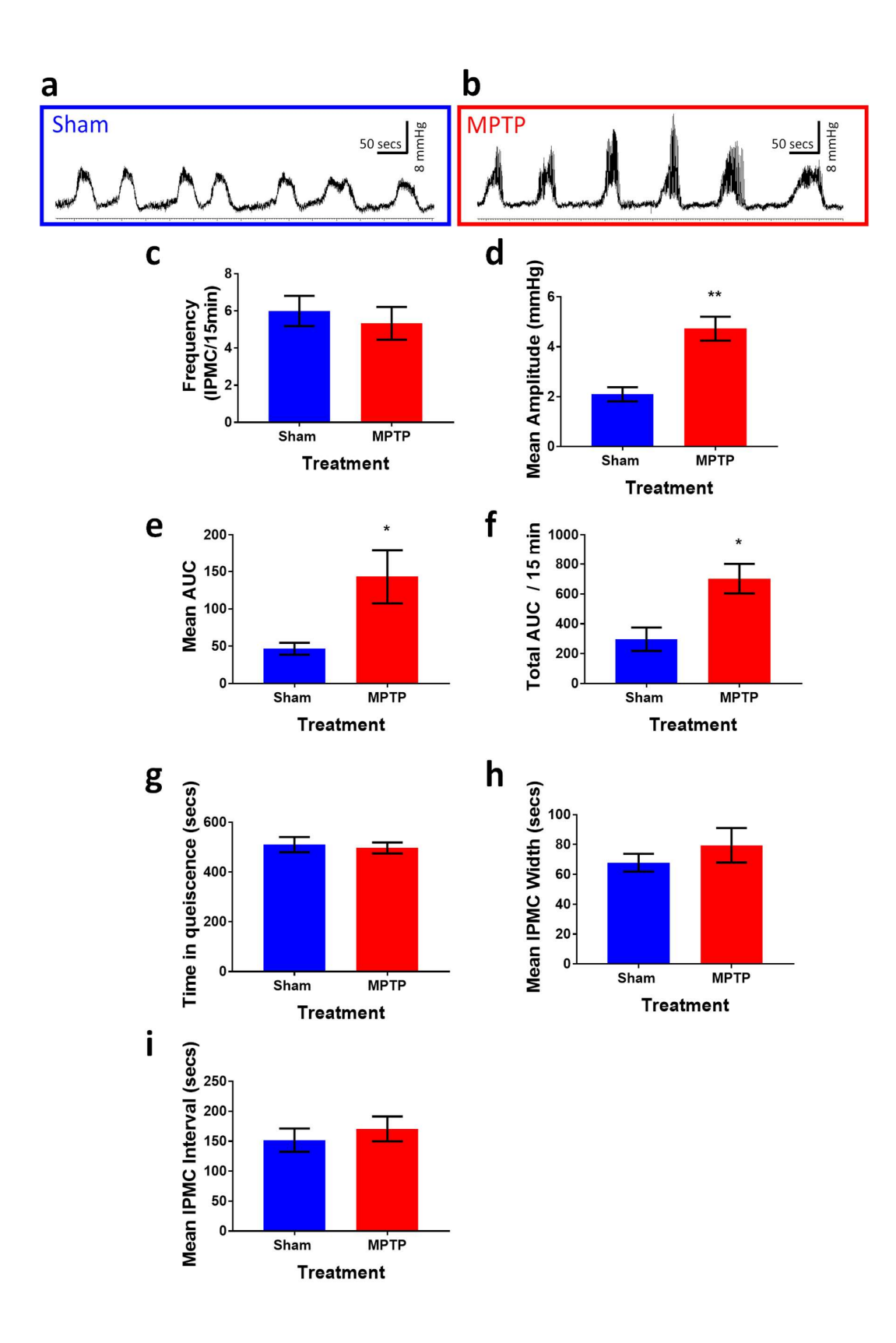


Figure 20 A comparison of IPMC activity in sham and MPTP treated mice.

An exemplar trace of IPMC activity of the ileum of a sham (a) and MPTP treated animal (b) during luminal distension, in the absence of any external stimulus or compound. Summary bar charts comparing the IPMCs of the ileum from sham and MPTP treated animals for; the average frequency of motor complexes over the 15 minute period (c), the mean motor complex amplitude (d), the mean AUC of a complex (e) and the total AUC over the 15 minute period (f), the TIQ over the 15 minute period (g) the mean motor complex width (h) and the mean motor complex interval (i). Data are expressed as mean, $n \ge 3$, SEM; *p < 0.05; **p < 0.01; ***p < 0.001; versus sham by unpaired t-test.

Upon closer inspection of individual motor complexes between the two groups it was evident that the increase in the amplitude of the MPTP IPMCs were due to increased contractility fluctuations (Figure 21 b & d) during the active phase, rather than a regular definition of higher amplitude. From our previous work defining ileal peristaltic motor complexes (chapter 3.3.1) we showed that IPMCs exhibit fluctuations or small localised waves of contraction which maintain a consistent amplitude during both the rest and active phase of the complex (Figure 11 c also seen in Figure 21 a). Removal of the regular localised waves from our traces, as a baseline removal, shown in Figure 21 c & d revealed that tissues from MPTP treated animals (Figure 21 c) exhibited greater amplitude of the fluctuations during the active than those in tissues from the sham animals (Figure 21 d), which showed very little fluctuation during the active phase.

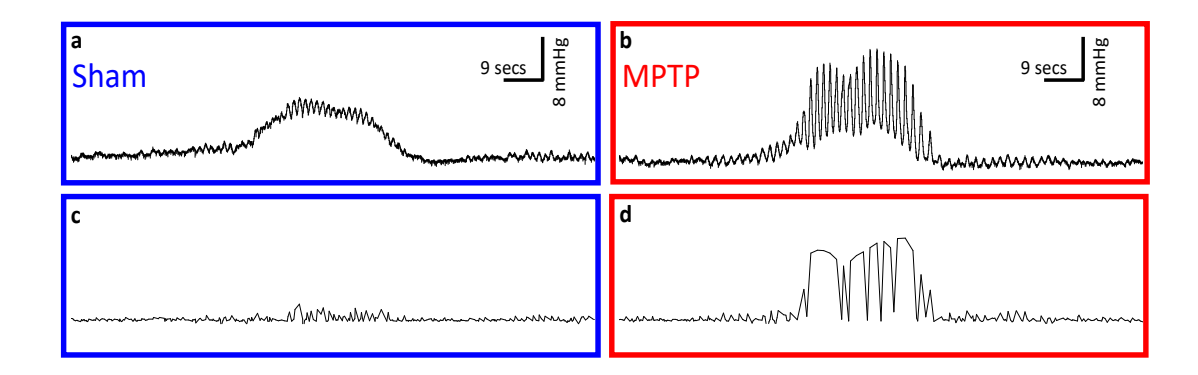


Figure 21 Traces of a single IPMC of a sham and MPTP treated animal.

An exemplar trace of a single ileal peristaltic motor complex from a sham (a) and MPTP treated animal (b) during luminal distension, in the absence of any external stimulus or compound. A trace of contractility changes visualised by removal of baseline fluctuations during an IPMC from a sham (c) and an MPTP treated animal (d).

This contractility was quantified from a 15-minute period in which no drug was present in ileum tissue from sham and MPTP treated mice (Figure 22 a & b). Fluctuations in the tissues from MPTP and sham treated mice were similar in frequency and amplitude during the periods that the tissue was at rest (Figure 22 c & d). During the active phase, fluctuation amplitude was significantly higher in the ileum tissues from MPTP treated animals compared to those from sham treated animals $(0.68 \pm 0.04 \text{ vs } 0.26 \pm 0.02 \text{ mmHg}, \text{p}<0.001)$ (Figure 22 c). As expected, the number of fluctuations per second were reduced during the active phase of the IPMC. However, the ileum from MPTP treated animals showed a significantly greater reduction in frequency compared to ileum tissue from sham treated animals $(1.93 \pm 0.36 \text{ vs } 2.72 \pm 0.14 \text{ mmHg}, \text{p}<0.01)$ (Figure 22 d). This is likely due to the vast increase in amplitude of each fluctuation in the active phase of the IPMC of MPTP treated animals compared to those from sham treated controls (Figure 22 c).

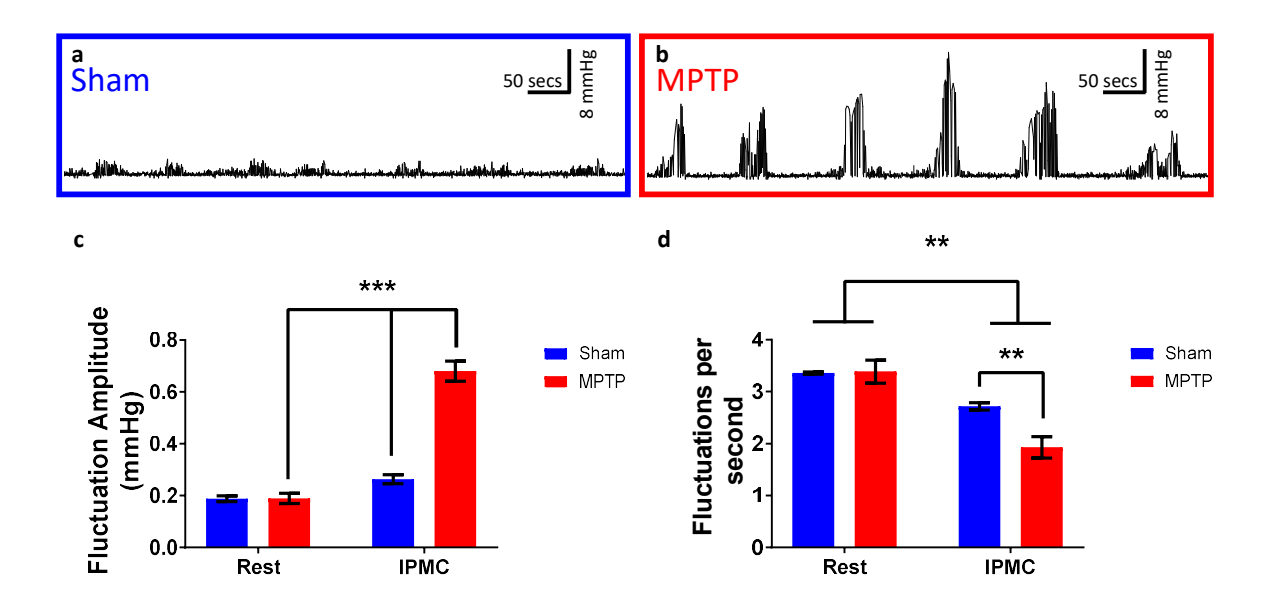


Figure 22 Assessment of contractility in the ileum of sham and MPTP treated mice.

An exemplar trace of contractility in the ileum from a sham animal (a) and an MPTP treated animal over a 15-minute period (b) during luminal distension, in the absence of any external stimulus or compound. Summary bar charts of contractility measured as fluctuation amplitude (c) and fluctuation frequency (d) in the ileum of sham and MPTP treated mice. Data are expressed as mean, SEM; $n \ge 3$; **p < 0.01; ***p < 0.001; using a two-way ANOVA.

4.3.3 Kv7 channel modulators effect IPMC activity similarly in the isolated ileum of MPTP treated and sham mice.

Activation of K_v 7 channels in segments of ileum cause a dose dependent reduction in IPMC activity, measured by various parameters as shown previously (Figure 14). Here, we applied Retigabine to tissue from sham and MPTP treated tissue using the same cumulative dosing strategy. Bath application of the K_v 7 channel opener Retigabine (0.1- 1 μ M) caused a dose dependant decrease in IPMC amplitude (Figure 23 b), frequency (Figure 23 c) and AUC (Figure 23 d & e).

There was a dose dependent increase in TIQ compared to that of vehicle control (Figure 23 a). Importantly, the percentage change from vehicle control was not significantly different and followed a similar pattern in ileum tissues from sham and MPTP treated mice apart from in one isolated instance in the TIQ at $0.3\mu M$.

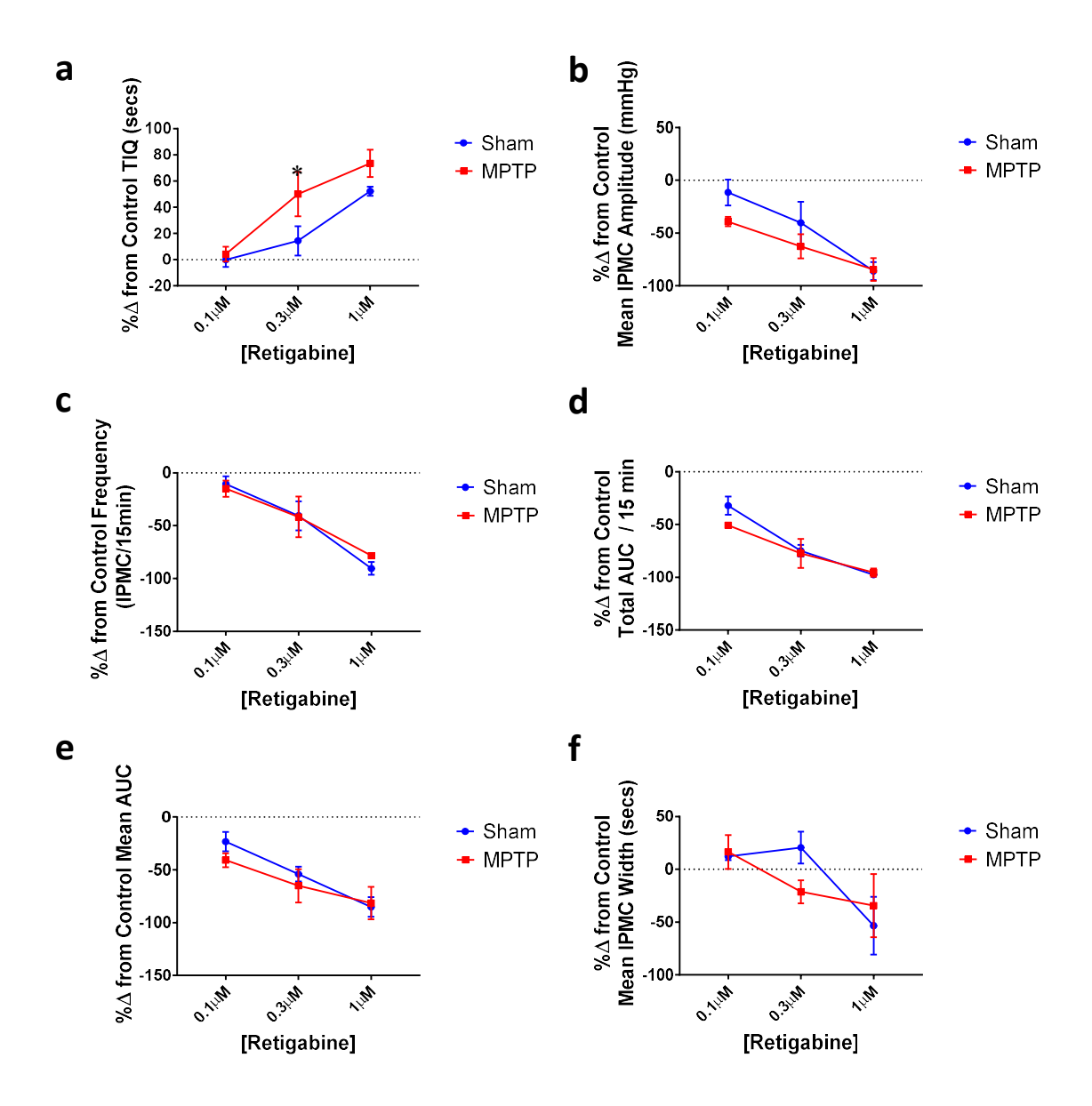


Figure 23 Kv7 activation decreases IPMC activity similarly in tissues from sham and MPTP treated mice.

Dose response to increasing concentrations of Retigabine in the isolated ileum from sham ($\stackrel{\bullet}{\bullet}$) vs MPTP ($\stackrel{\bullet}{\bullet}$) treated mice. Mean TIQ over 15 minutes (a), mean IPMC amplitude (b), frequency (c), Total AUC over 15 minutes (d) mean AUC (e), and mean IPMC width (f) in the presence of Retigabine are not significantly different between tissues from sham and MPTP treated mice. Data are expressed as mean ($n \geq 3$), SEM; % change from vehicle control. Statistical analysis by two-way ANOVA followed by Sidak's post hoc test, *p < 0.05 versus sham.

Blockade of K_v7 channels in segments of ileum caused a dose dependent increase in IPMC activity, in various parameters, as shown previously (Figure 16). XE-991 was applied to the motility bath containing tissue from sham and MPTP treated tissue using the same cumulative dosing strategy as previously used. Bath application of the K_v7 channel blocker XE-991 (0.1- 1 μ M) caused a dose dependant increase in IPMC frequency (Figure 24 c). There was a dose dependent decrease in TIQ (Figure 24 a) and mean interval between IPMCs (Figure 24 g) compared to that of vehicle control. The percentage change from vehicle control was not significantly different and followed a similar pattern in ileum tissues from sham and MPTP treated mice for all parameters assessed, except for a significant difference in frequency at the highest concentration only (Figure 24 c & g). Mean amplitude (Figure 24 b) and AUC (Figure 24 d & e) did not change or were negatively impacted. As discussed previously this is likely an artifact resulting from the time that the tissue is under experimentation, rather than a drug effect.

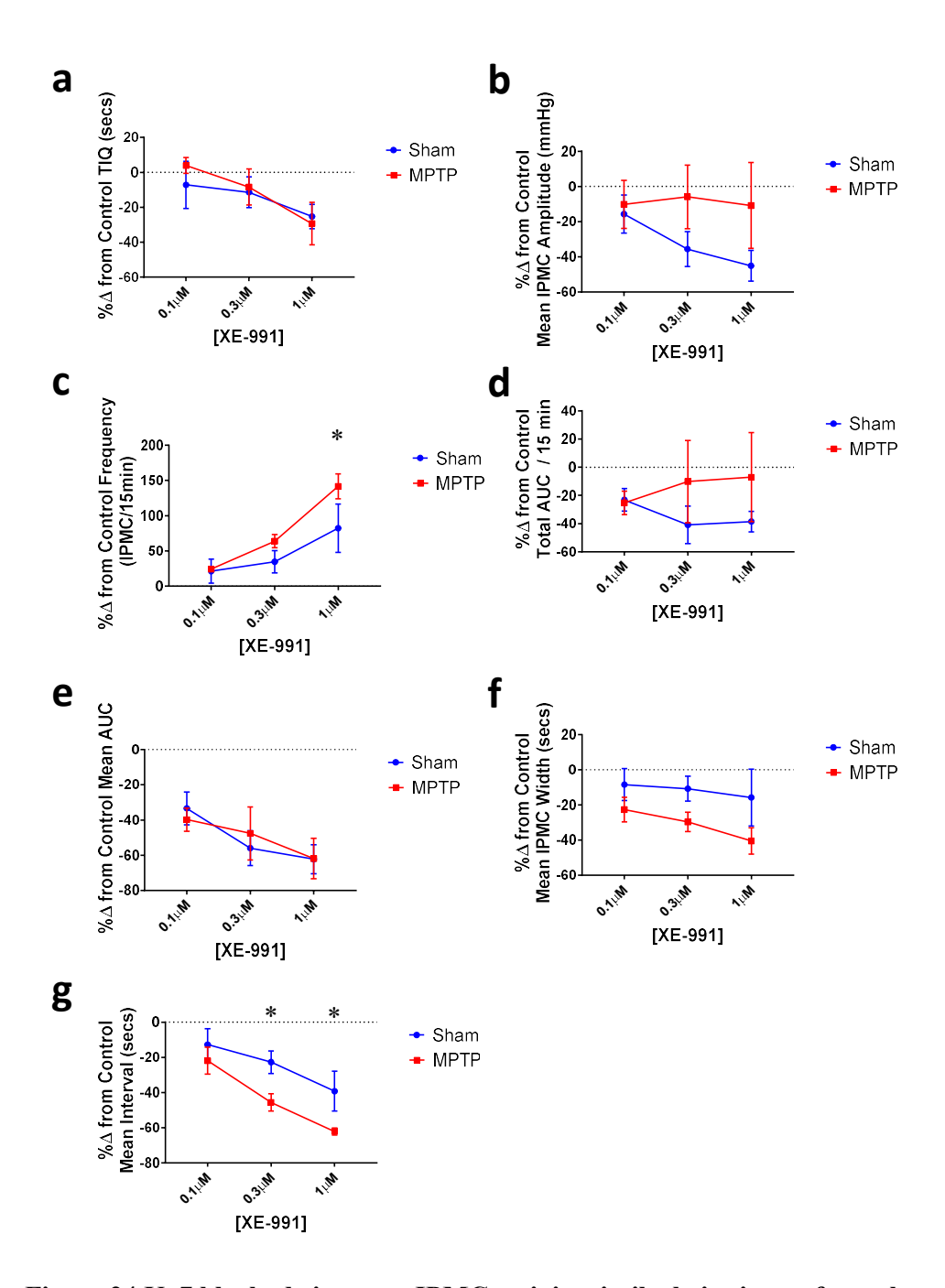


Figure 24 Kv7 blockade increase IPMC activity similarly in tissues from sham and MPTP treated mice.

Dose response to increasing concentrations of XE-991 in the isolated ileum from sham ($\stackrel{\bullet}{\bullet}$) vs MPTP ($\stackrel{\bullet}{\bullet}$) treated mice. Mean TIQ over 15 minutes (a), mean IPMC amplitude (b), frequency (c), Total AUC over 15 minutes (d) mean AUC (e), and mean IPMC width (f) in the presence of XE-991 are not significantly different between tissues from sham and MPTP treated mice. Data are expressed as mean ($n \geq 3$), SEM; % change from vehicle control. Statistical analysis by two-way ANOVA

4.3.4 Colon motility in MPTP treated mice is similar to that of sham treated mice.

The colon tissues from sham treated (Figure 25 a) animals had a similar profile to those from MPTP treated animals (Figure 25 b). When comparing the segments from the two treatment groups in the motility organ bath there were no significant differences observed in amplitude, frequency, time in quiescence, or any of the other parameters measured.

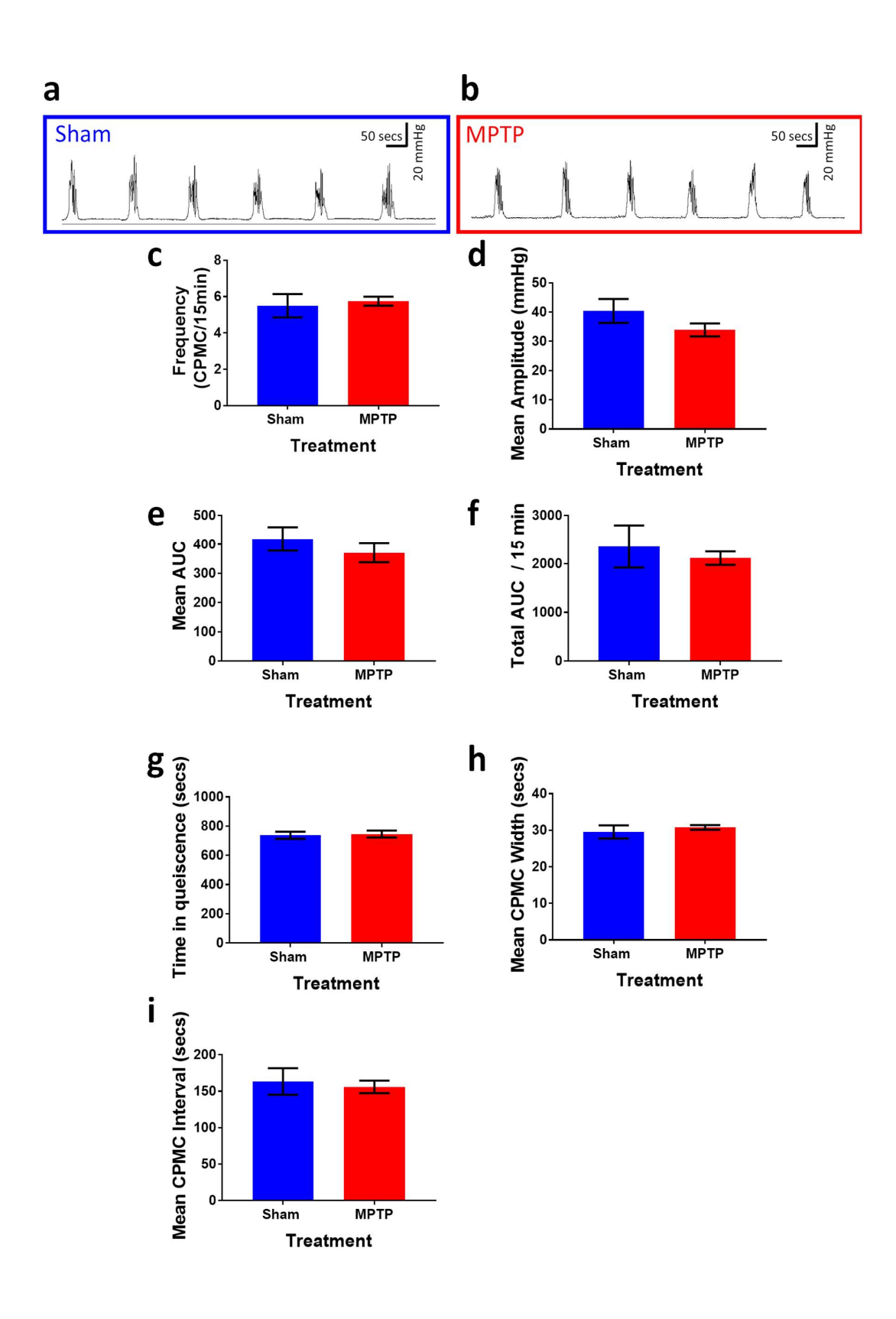


Figure 25 A comparison of CPMC activity in sham and MPTP treated mice.

An exemplar trace of CPMC activity of the colon of a sham (a) and MPTP treated animal (b) during luminal distension, in the absence of any external stimulus or compound. Summary bar charts comparing the CPMCs of the colon from sham and MPTP treated animals for; the average frequency of motor complexes over the 15 minute period (c), the mean motor complex amplitude (d), the mean AUC of a complex (e) and the total AUC over the 15 minute period (f), the TIQ over the 15 minute period (g) the mean motor complex width (h) and the mean motor complex interval (i). Data are expressed as mean, n=4, SEM; *p < 0.05; **p < 0.01; ***p < 0.001; versus sham by unpaired t-test.

From our previous work defining colonic peristaltic motor complexes (3.3.1) we showed that CPMCs exhibit fluctuations or small localised waves of contraction which increase in amplitude but decrease in frequency during the active phase of the complex (Figure 11 c & d). This was also true in this set of experiments (Figure 26).

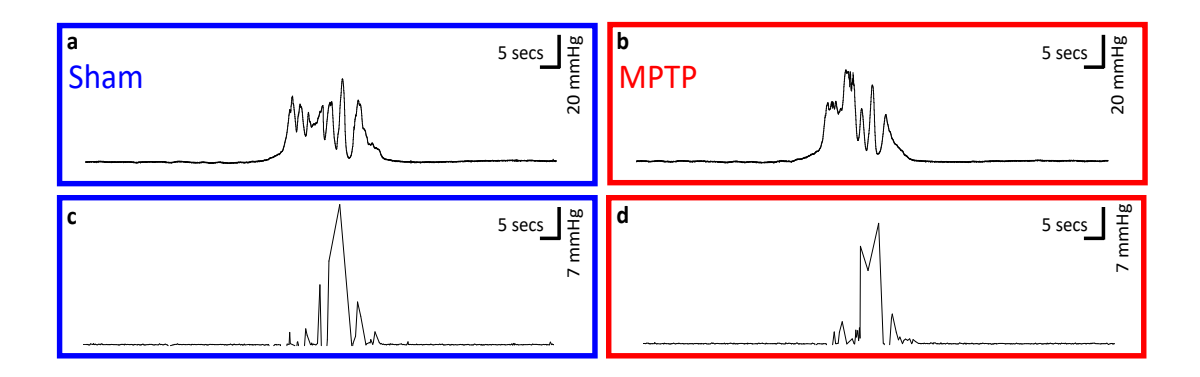


Figure 26 Traces of a single CPMC of a sham and MPTP treated animal.

An exemplar trace of a single colonic peristaltic motor complex from a sham (a) and MPTP treated animal (b) during luminal distension, in the absence of any external stimulus or compound. A trace of contractility changes during a CPMC from a sham (c) and an MPTP treated animal (d).

This contractility was quantified from a 15-minute period in which no drug was present, in colon tissue from sham and MPTP treated mice (Figure 27 a & b). Fluctuations in the tissues from MPTP and sham treated mice were similar in frequency and amplitude during the periods that the tissue was at rest and during the active phase (Figure 27 c & d). No significant differences were observed.

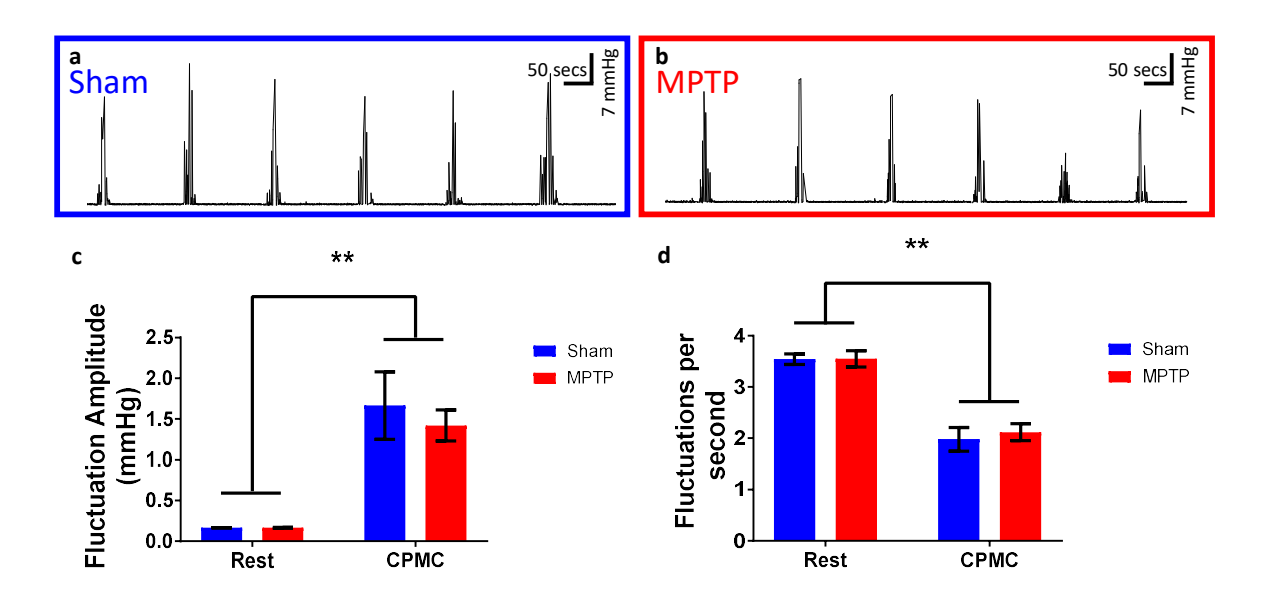


Figure 27 Assessment of contractility in the colon of sham and MPTP treated mice.

An exemplar trace of contractility in the colon from a sham animal (a) and an MPTP treated animal over a 15-minute period (b) during luminal distension, in the absence of any external stimulus or compound. Summary bar charts of contractility measured as fluctuation amplitude (c) and fluctuation frequency (d) in the colon of sham and MPTP treated mice. Data are expressed as mean, SEM; n = 4; **p < 0.01; ***p < 0.001; using a two-way ANOVA.

4.3.5 Kv7 channel modulators effect CPMC activity similarly in the isolated colon of MPTP treated and sham mice.

Activation of K_v 7 channels in segments of colon caused a dose dependent reduction in CPMC activity, measured by various parameters as shown previously (Figure 12). Here, we applied Retigabine to tissue from sham and MPTP treated tissue using the same cumulative dosing strategy. Bath application of the K_v 7 channel opener Retigabine (0.1- 1 μ M) caused a dose dependant decrease in CPMC amplitude (Figure 28 b), frequency (Figure 28 c) and AUC (Figure 28 d & e).

There was a dose dependent increase in TIQ compared to that of vehicle control (Figure 28 a). There was no effect to CPMC width at any concentration of Retigabine in tissue from either treatment group (Figure 28 f). Importantly, the percentage change from vehicle control was not significantly different and followed a similar pattern in colon tissues from sham and MPTP treated mice in all parameters assessed except for one isolated point of a significantly increased response to Retigabine for TIQ (Figure 28 a) only at the lowest dose $0.1 \mu M$.

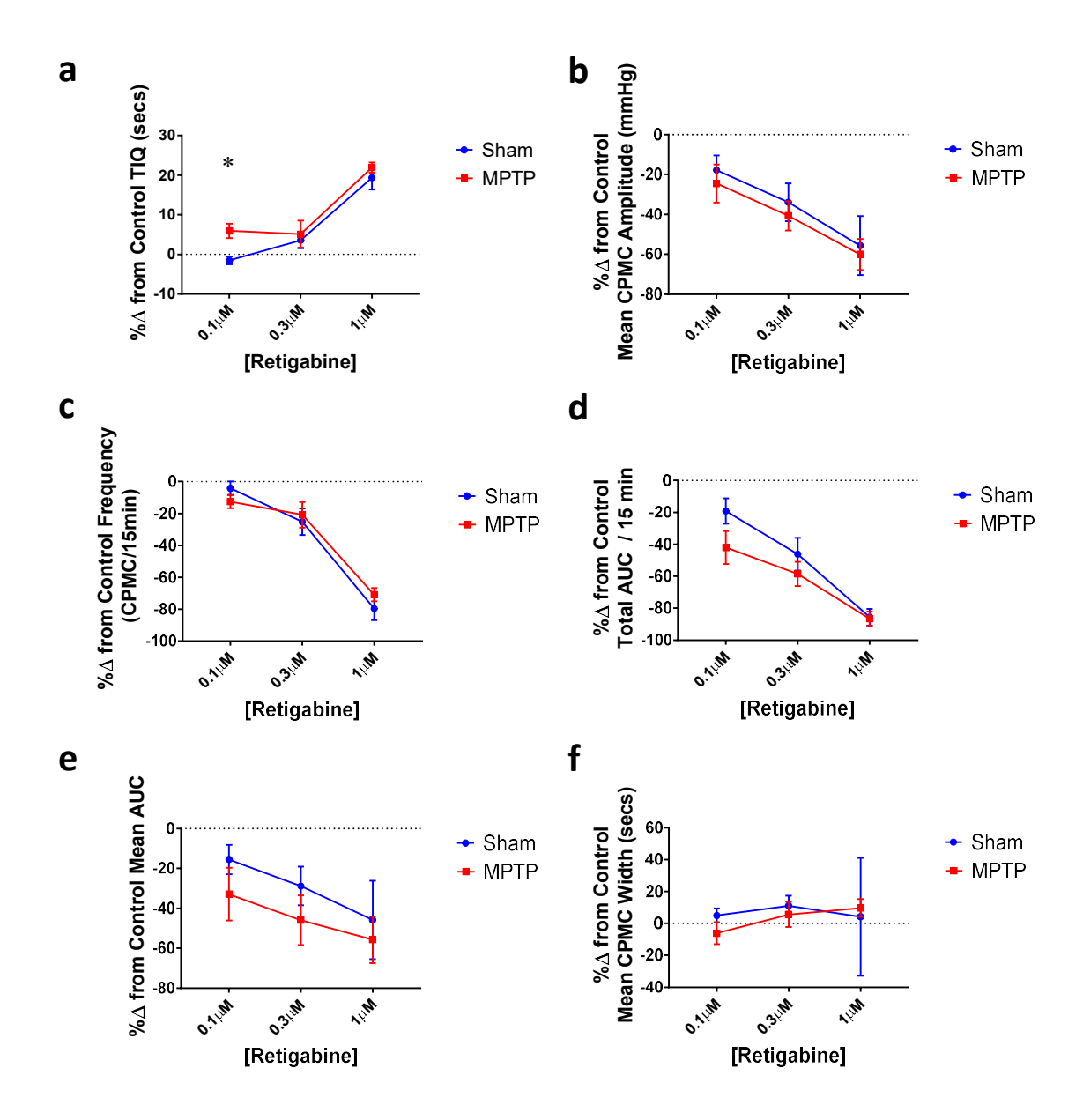


Figure 28 Kv7 activation decreases CPMC activity similarly in tissues from sham and MPTP treated mice.

Dose response to increasing concentrations of Retigabine in the isolated colon from sham ($\stackrel{\bullet}{\bullet}$) vs MPTP ($\stackrel{\bullet}{\bullet}$) treated mice. Mean TIQ over 15 minutes (a), mean CPMC amplitude (b), frequency (c), Total AUC over 15 minutes (d) mean AUC (e), and mean CPMC width (f) in the presence of Retigabine are not significantly different between tissues from sham and MPTP treated mice. Data are expressed as mean (n =4), SEM; % change from vehicle control. Statistical analysis by two-way ANOVA followed by Sidak's post hoc test, *p < 0.05 versus sham.

Blockade of K_v7 channels in segments of colon cause a dose dependent increase in CPMC activity, measured by various parameters, as shown previously (Figure 15). XE-991 was applied to the motility bath containing tissue from sham and MPTP treated tissue using the same cumulative dosing strategy as previously used. Bath application of the K_v7 channel blocker XE-991 (0.1- 1 μ M) caused a dose dependant increase in CPMC amplitude (Figure 29 b), frequency (Figure 29 c) and AUC (Figure 29d & e). There was a dose dependent decrease in TIQ (Figure 29 a) and mean interval between (Figure 29 h) CPMCs compared to that of vehicle control. Importantly, the percentage change from vehicle control in all parameters was not significantly different and followed a similar pattern in colon tissues from sham and MPTP treated mice.

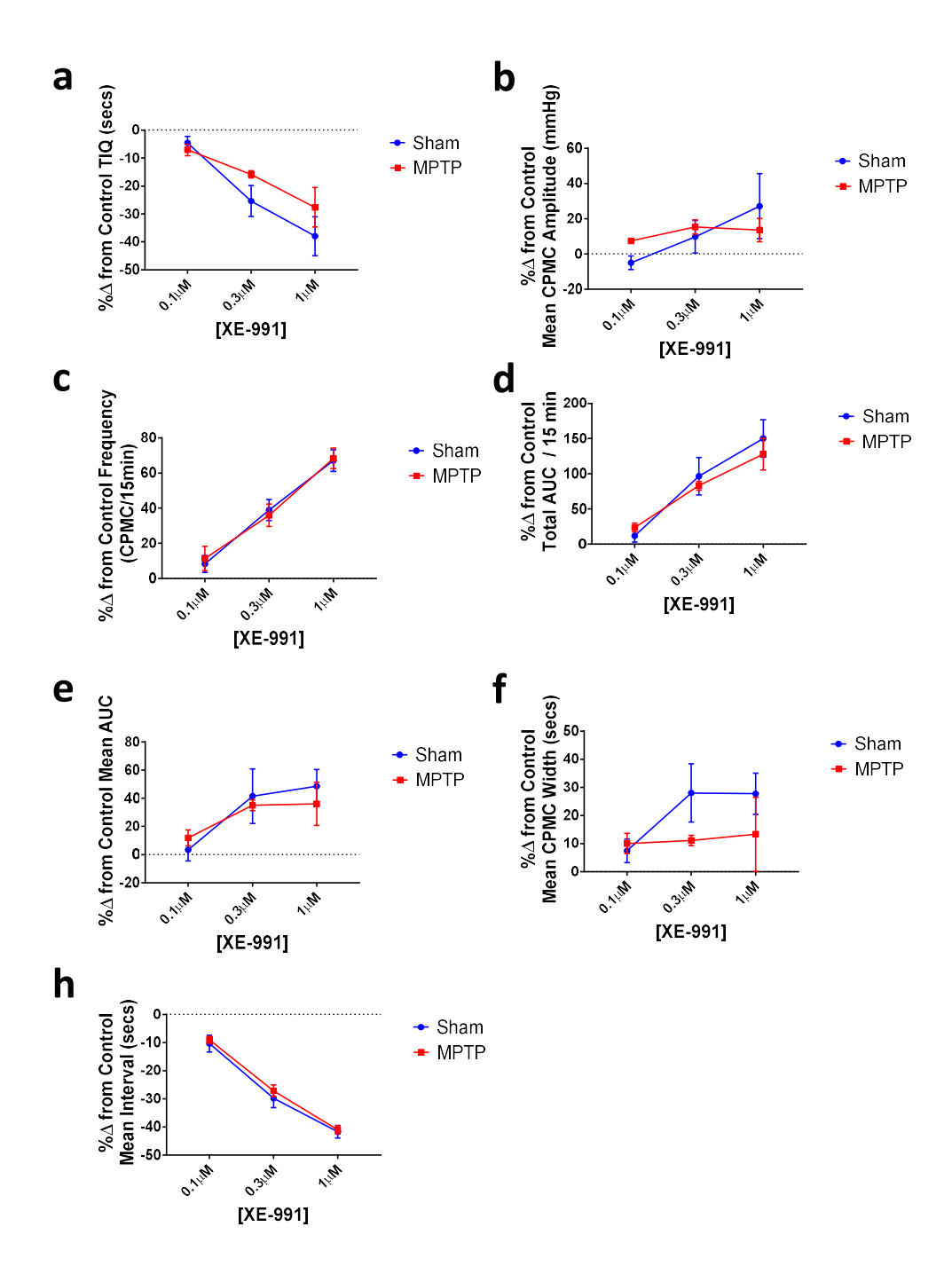


Figure 29 Kv7 blockade increase CPMC activity similarly in tissues from sham and MPTP treated mice.

Dose response to increasing concentrations of XE-991 in the isolated colon from sham () vs MPTP () treated mice. Mean TIQ over 15 minutes (a), mean IPMC amplitude (b), frequency (c), Total AUC over 15 minutes (d) mean AUC (e), and mean IPMC width (f) in the presence of XE-991 are not significantly different between tissues from sham and MPTP treated mice. Data are expressed as mean (n

4.4 Discussion

Animal models of Parkinson's disease have been used to try to understand the dysfunction in the gastrointestinal system of PD patients as mentioned in chapter 1.10.2. This is the first time, to our knowledge, that tissues from a model with neurodegeneration in the nigra have been put through this type of organ bath system to measure motility. Here we show that in the ileum of MPTP treated animals, these basal complexes, although still regular in frequency, have increased amplitude and magnitude (measured as AUC) compared to the ileum tissue from sham treated controls (Figure 20). There were no differences in the basal activity of the colon and the effects of Kv7 channel modulation were similar between MPTP and saline animals in both tissues.

Mouse models of PD have for the most part shown to have increased transit time and impairment of inhibitory and relaxation mechanisms (Arnhold et al., 2016; Gries et al., 2021; Haskel & Hanani, 1994; Natale et al., 2010; Rota et al., 2019; Sampath et al., 2019). The toxin induced models have shown this to be in part, due to local impairment as well as linked to central pathology (Greene et al., 2009; Haskel & Hanani, 1994; Natale et al., 2010; Rota et al., 2019). Our dosing regimen led to the successful generation of animals with lesions in the substantia nigra with an average of ~36% loss of dopaminergic neurons in the SNpc. This led to dysfunction in the gastrointestinal system of MPTP treated animals in the form of hyperactivity of the ileum.

As mentioned previously the horizontal organ bath produces regular peristalsis like motor complexes in gastrointestinal tissue upon distension. The distension here mimics a bolus in the lumen and the motor complexes are produced by the tissue as a reaction, in an attempt to move the bolus aborally. In the presence of this distention these motor complexes follow distinct patterns which are different in the ileum compared to the colon, as mentioned in chapter 3.3.1. In this study the basal complexes in the ileum of MPTP treated animals, with no drug incubation, were regular in frequency but exhibited increased amplitude and magnitude (measured as AUC) compared to the ileum tissue from sham treated controls (Figure 20). This was measured in a 15-minute period, in which an average of 6 IPMCs were quantified from at least three animals from each treatment group.

In the normal situation, as mentioned in 3.3.1, the contractility of the ileum is the same during the active phase of the IPMC as it is during rest. In this model the small fluctuations of the tissue, referred here as contractility, maintain frequency and amplitude regardless of the tissue's peristaltic state. The active phase of an IPMC is only caused by an increase in intraluminal pressure, not increases in contractility. When looking at this increase in amplitude, in the tissues from the MPTP treated animals, there is a difference in this contractility more so than a change in total intraluminal pressure (Figure 21). This also resulted in an increase in AUC. Measurement of the fluctuations in the ileum from MPTP treated animals shows increases in amplitude that are approximately three times greater than those from the ileum of sham treated animals. The total time of the active phase (IPMC width) is not significantly different between the treatment groups. Therefore, we postulate that the MPTP treated tissues have a lower frequency of fluctuations, due to the increased time needed to reach the heightened amplitude (Figure 22).

With the mice here treated with MPTP and showing some form of hyperactive basal activity in the ileum we incubated the segments of ileum with Kv7 modulators. Kv7 activation and blockade in ileum segments from both MPTP and sham treated animals behaved in a similar way. Activation of Kv7 by Retigabine led to a reduction in activity of the ileum via various parameters and blockade led to an increase in IPMC activity in a dose dependent manner. Although there were a few isolated events of significant differences in our motility assessments of the ileum and colon with Kv7 modulators, they were not consistent enough, with a dose response to conclude a real difference between the sham and MPTP tissue. With a larger sample size we may have been able to gain greater confidence in whether this was a real effect. However, currently the lack of a difference between tissues from MPTP treated mice and sham treated mice to Kv7 modulators lead us to believe that the hyperactivity seen in the MPTP treated ileum segments is due to impairment of a different mechanism.

Other studies using MPTP treated mice have shown impairment of protein expression involved in dopaminergic transmission within the ENS of the small intestine and functional slowness of transit (Anderson et al., 2007; Natale et al., 2010; Tian et al., 2008). Diminished relaxation mechanisms have been noted in the colon of MPTP treated mice, believed to be due to impairment of the

nitrergic system (Lai et al., 2018). Our investigations did not stretch to assessing these neurotransmitters and their related proteins in our samples; however, impairment of either system could lead to the hyperactivity observed in our ileum preparations from MPTP treated mice.

The study which has used a setting most similar to ours does not assess this contractility, however exemplar traces from the paper do not appear to show differences in this contractility. Abdu et al., (2002) used bath addition of somatotropin release-inhibitory factor and nitric oxide synthase (NOS) inhibitor L-NAME and showed differences in both frequency and in amplitude of motor complexes in the rat jejunum. The ileum assessments in our study from MPTP treated mice only had altered amplitude of IPMCs but the frequency remained similar to tissue from control animals. Therefore, it may be that the difference in our study is not to do with these two pathways and is likely not neuronally driven. From exemplar traces it is difficult to tell but atropine and nifedipine were assessed at high concentrations and initially showed some effects on amplitude only but quickly caused global silencing of complexes. The L-type calcium channel antagonist, nifedipine, at lower concentrations has been shown to reduce amplitudes of peristaltic like complexes in the guinea pig ileum without effecting frequency, in other studies (Spencer et al., 2001).

Effects on amplitude can be multifaceted and in these experiments we also assessed the contractility of the segments from MPTP treated mice. Contractility is where the most obvious effects can be seen in our study. Without further pharmacological manipulation, we were unable to determine the molecular basis for this contractility and for the differences observed. Looking at various pharmacological agents of different neurogenic and myogenic pathways and allowing for washout periods is particularly difficult in this set-up, with the small intestine, as the tissue starts to lose integrity and different layers start to degrade (Schreiber et al., 2014). We were only able to assess our initial aims looking at basal differences and any functional differences using Kv7 modulators in tissue from naïve and MPTP treated mice. It is very likely that this contractility is simply the basic electrical rhythm of the tissue, but it is difficult to determine as the small intestine movements are made up of various types, such as slow waves, longitudinal oscillations and peristaltic movements. Longitudinal oscillations are continuous throughout recordings in most studies and occur independent of circular muscle movements. It is thought that they correspond to pendular

158

movements, which are "sleeve" like contractions that occur in the longitudinal muscle and produce a "to and fro" movement of the contents (Hennig et al., 1999; Seerden et al., 2005). Anecdotally we observed such movements continuously in our preparations, but our apparatus and readouts are not sensitive enough to distinguish between different movement types and the different muscle types responsible for them.

Spatiotemporal maps are used frequently for such motility assessments. Although they include similar organ bath apparatus to ours, they use video recording equipment and frame by frame analysis of the movement of the segments. This was the method used by Gries et al., (2021), to conclude that isolated small intestine tissue from pre motor alpha-synuclein transgenic mice had fewer and slower contractions than those from naïve mice (Gries et al., 2021). This is not something which we observed in the segments from MPTP tissue, however using video recording analysis would be a more sensitive method and may unearth more differences between the treatments. The hyperactivity or overactivity that we saw did not translate to any alteration in frequency of peristaltic movements. This doesn't necessarily contradict the significantly increased small intestinal transit time seen in PD patients compared to healthy controls (Dutkiewicz et al., 2015a; Knudsen, Haase, et al., 2017), or that in animal models (Natale et al., 2010; Sampath et al., 2019). Intestinal transit requires co-ordinated activity between the various muscle groups and movement types. Any disruption of this co-ordination between contraction and relaxation can impair the movement of a bolus forward. Spatiotemporal maps have also revealed distension evoked movements which can travel in both directions (Schreiber et al., 2014). Again, our assessments of intraluminal pressure do not give directionality and therefore the proportion of forward (oral to aboral) movements to backward (aboral to oral) are key determinants in intestinal transit.

So far there has been very little literature on functional effects of MPTP on the isolated colon in such an organ bath setting. In this study dysfunction in the colon due to neurodegeneration caused by MPTP were not seen. Basal activity levels, measured using multiple parameters, were very similar in both groups. During the 15-minute period where basal activity and CPMC parameters were measured, colon tissue from MPTP treated animals showed no differences compared to saline treated animals (Figure 25). The assessment of fluctuations during the rest phase and active phase of

colonic activity also did not differ between the two treatment groups. Contractility followed the same pattern of increased amplitude and decreased frequency during the active phase of a CPMC (Figure 27).

Proximal colon from MPTP treated animals assessed in the conventional organ bath has been shown to have impairment of relaxation mechanisms (Anderson et al., 2007). Other studies using MPTP treated mice have assessed colonic transit, stool frequency and water content in vivo and shown impairment (Natale et al., 2010; Sampath et al., 2019). Such measurements although extremely relevant are not able to differentiate whether the impairment is due to local changes to the colon or due to impairment of central transmission to the colon, nor whether the effects are due to MPTP's peripheral effects or its central effects. Our studies were performed on tissue from animals 6-8 weeks post treatment, allowing plenty of time for washout of the toxin, neurodegeneration to occur and any local changes due to neurodegeneration to manifest. Transient effects, such as the accelerated defecation seen in Anderson et al., (2007) would likely not have affected our studies due to the extended period post treatment that our assessments took place.

As well as the lack of a difference in the basal motor complexes we saw no difference between the treatment groups in CPMC activity when the colon segments where exposed to Kv7 modulators. As seen previously, Kv7 activators reduce CPMC activity (Chapter 3.3.2) and the Kv7 blocker XE-991 increases CPMC activity (Chapter 3.3.3). Both colon segments from sham and MPTP responded similarly to these modulators of the Kv7 channel in a dose dependent manner. Reduced Kv7 channel expression or KCNQ mutations have been associated with developmental and epileptic encephalopathy (Beck et al., 2021) and Hirschsprung's disease patients (O'Donnell et al., 2017) with GI dysfunction. However, there have been no literature reports of Kv7 deficiency in the colon of patients with PD or in animal models of PD. Here there was a lack of effect in the colon with these compounds therefore, we can conclude that MPTP administration in mice does not lead to Kv7 dependent dysfunction of the colon.

Here we have shown a long-term effect of MPTP induced neurodegeneration on the contractility of the gastrointestinal tract, specifically in the ileum. The ileum of MPTP treated animals were more active in our assay compared to the ileum tissue from sham treated controls. Although still regular in frequency, ileum segments from MPTP treated animals exhibited increased amplitude and magnitude (measured as AUC) (Figure 20). The limitations of our assay did not allow us to fully characterise the functional effect of these local changes to the ileum. Video recording of the intestinal segments whilst in the organ bath would add sensitivity to the system and allow us to view the direction of peristaltic movements. Insertion of a small bead, into this preparation, would mimic the movement of a bolus through the segment. This would allow us to see whether the impairments of contractility, that we see, alter transit. Protein or RNA quantification of samples from these animals, may allow us to better understand the mechanisms behind these changes. We also assessed the impact of Kv7 modulators on the gastrointestinal tract segments of MPTP treated and naïve animals. We found no differences in the effects on motility when opening or closing these channels in either treatment group, despite previously observing reduced expression of Kv7.4 channels in the ileum of the marmoset MPTP model. Ultimately, studies on human tissue from PD patients will inform on whether Kv7 channel plays a role in the gastrointestinal dysfunction in PD.

5 CONTRACTILITY IN THE GASTROINTESTINAL AND URINARY SMOOTH MUSCLE IN A PARTIAL LESION MODEL OF PARKINSON'S DISEASE.

5.1 Introduction

The 6-hydroxydopamine (6-OHDA) induced rodent model of neurodegeneration is a preferred option by many authors when investigating the peripheral consequences of dopaminergic loss due to its central administration. 6-OHDA's inability to cross the blood brain barrier, require it to be injected directly into distinct locations in the brain to cause neurodegeneration within the nigrostriatal tract. The low doses required to achieve a lesion in the CNS mean that is perfectly placed as a model to assess the effects of a truly central insult on pathology, behaviour and peripheral outcomes such as gastrointestinal dysfunction.

Three target sites have been widely used in rodents, the medial forebrain bundle (MFB), the substantia nigra pars compacta (SNpc) and the caudate-putamen complex/striatum. Injection into the MFB leads to an almost complete lesion of DA neurons in the SNpc and total depletion of DA in the ipsilateral striatum (Blandini et al., 2009; Levandis et al., 2015). In fact, it is a more extensive loss than is seen in human PD, from a unilateral lesion perspective. Bilateral lesions using this injection site result in difficulty in drinking and eating in the treated animals, which reduce its use on welfare grounds (Deumens et al., 2002). Administration of 6-OHDA into the SNpc has a more

moderate effect on the DA neurons but still achieves ~90% loss. With this administration, ventral tegmental area (VTA) dopaminergic neurons are also vulnerable to cell death. This was initially thought to be a drawback of the model as the VTA was thought to be spared in PD, however studies have shown that the VTA does degenerate in the human condition (Alberico et al., 2015). Intrastriatal delivery of 6-OHDA has been used to asses a more progressive DA pathology (Stott & Barker, 2014). Intrastriatal administration represents a "dying back" mechanism of axons prior to neuronal loss, as is believed to occur in human PD (Grosch et al., 2016). Striatal administration usually produces rapid degeneration of the dopaminergic nerve terminals close to the injection site, which achieves a partial retrograde lesion of dopaminergic neurons in the SNpc. This can be useful for modelling the early stages of PD (Blandini et al., 2007).

The DMV is another brain region effected in the 6-OHDA model. Administration of 6-OHDA into the SNpc has been shown to lead to a reduction in the number of ChAT positive neurons in this region and delayed gastric motility (Anselmi et al., 2017; Toti & Travagli, 2014; Yang et al., 2019; Zheng et al., 2014).

With the popularity of this model for assessment of peripheral consequences of nigrostriatal dopaminergic pathology, numerous studies have looked at gastrointestinal dysfunction in rodents, via various 6-OHDA administration regimes.

Functionally, 6-OHDA treated animals have shown slow GI transit compared to sham treated animals, measured by slower expulsion in a colorectal bead expulsion assay (Chai et al., 2020). Interestingly, the same group looked at bead expulsion using the same methods but in a mouse model of 6-OHDA and saw no difference in bead expulsion time compared to sham mice (McQuade et al., 2021). 6-OHDA treated rats have been shown to have delays in the intestinal transit of the liquid meal test (Albuquerque et al., 2021) and of BaSO4 from at least 4 weeks post 6-OHDA injection (Feng et al., 2019; Fornai et al., 2016). Functional, in life assays although very informative, have many contributing factors, which can lead to alterations in transit. Measuring faecal output is a relatively simple assessment but is also dependent on a wide variety of processes. Food and water consumption, gastric emptying, motility and absorption irregularity can all impact

faecal output. Nevertheless, 6-OHDA treated rats often exhibit reduced faecal output and reduced water content in the faeces (Albuquerque et al., 2021; Blandini et al., 2009; de Moraes Thomasi et al., 2022; Feng et al., 2019; Zhu et al., 2012), this was again not apparent in the assessment in the mouse model (McQuade et al., 2021). Mucosal integrity and intestinal permeability have also been shown to be affected in the 6-OHDA model. This was assessed by increased FITC-dextran permeability and decreased transepithelial resistance in the small and large bowel (Feng et al., 2019).

As previously mentioned, isolated segments of the gastrointestinal tract can be excised and assessed in an organ bath type preparation to understand local changes that occur after central insults. The colon is the most studied part of the gastrointestinal tract, in organ bath systems, due to the prevalence of constipation in PD. Peristaltic like movements can be measured in the horizontal organ bath, measuring changes in intraluminal pressure and using spatiotemporal maps. It is not clear whether unilateral 6-OHDA injection leads to alterations in peristalsis like motor complexes as similar injection protocols into the MFB have had contrasting results. Colucci et al.; (2012) showed that segments of the distal colon from 6-OHDA treated rats had irregular, uncoordinated and slower peristaltic waves than control animals. Conversely, Levandis et al.; (2105) saw a significant increase in peristalsis frequency and decreased threshold volume in 6-OHDA distal colon preparations compared to controls. Oddly, both studies attributed these effects to decreased dopamine 2 receptor expression (D2R).

Electrically evoked motor patterns from 6-OHDA have been shown to be reduced assessed using electric field stimulation (EFS) in the traditional organ bath (Fornai et al., 2016; Pellegrini et al., 2016). This decrease was postulated to arise from an observed reduction in ChAT positive neurons and acetyl choline release during EFS. Interestingly, the studies noted this despite upregulation of muscarinic receptors, substance P and tachykinin NK₁ receptors in the colon from 6-OHDA animals (Fornai et al., 2016; Pellegrini et al., 2016). Examinations of molecular changes in the gastrointestinal system after 6-OHDA lesioning have focused on neuronal populations in the ENS. Most have found no significant changes in the total number of neurons in a given area of both the small and large bowel but various differences in the composition of the subpopulations of neurons

(Blandini et al., 2009; Colucci et al., 2012; Fornai et al., 2016; Sinen et al., 2021; Toti & Travagli, 2014; Zhu et al., 2012).

Investigations into the small intestine are variable. Some groups observed increases in the number of dopaminergic neurons, nNOS positive neurons and a reduction in ChAT positive cells in the duodenum (Colucci et al., 2012; Tian et al., 2008; Toti & Travagli, 2014). Conversely, other studies show a reduction in nNOS positive cells (Blandini et al., 2009; Colucci et al., 2012) in the ileum with one showing a perceived compensatory change in the form of upregulation of VIP positive neurons (Colucci et al., 2012). Another study points to a small but significant reduction in the number of neurons per ganglion, no change to the proportion of nNOS positive cells. This groups also determined that there was damage to the enteric neurons which was assessed by translocation of RNA binding protein Hu, from the cytoplasm to the nucleus (Chai et al., 2020). Importantly in the human condition, only one study has investigated ENS cell loss in the small intestine, the authors showed no myenteric neuron loss nor change in phenotypes of subpopulations (Annerino et al., 2012). Further work in human tissue will help to determine if any of these studies in 6-OHDA animal models are translationally relevant.

The colon has received more attention in the human with several small biopsy studies also yielding mixed results. Some studies have found no differences in overall ENS density in PD patients compared with controls (Annerino et al., 2012; Barrenschee et al., 2017; Lebouvier et al., 2008). Other studies, sometimes performed by the same group, show a decrease in the number of neurons per ganglia within the submucosal plexus (SMP) (Lebouvier et al., 2010). Subpopulations within the colonic ENS often do not differ in terms of the proportion of various neurotransmitter positive cells (Annerino et al., 2012; Corbillé et al., 2014; Lebouvier et al., 2010). Here again other studies show a reduction in neurons expressing vasoactive intestinal polypeptide (VIP) in the SMP (Giancola et al., 2017) or an increase VIP mRNA (Barrenschee et al., 2017). Colon tissue from 6-OHDA lesioned animals, for the most part, exhibit increased proportion of dopaminergic neurons, VIP positive neurons and decreased proportion of nNOS and ChAT positive cells in the myenteric plexus in various studies (Blandini et al., 2009; Chai et al., 2020; Colucci et al., 2012; Fornai et al., 2016; Levandis et al., 2015; McQuade et al., 2021; Tian et al., 2008, 2008; Zhu et al., 2012). In

terms of total number of neurons only one study from all of these showed a reduction in the number of myenteric plexus neurons per ganglia, with an increase in the number of ganglia per given area observed. This work was performed in colon tissue from a mouse that had been lesioned with 6-OHDA rather than a rat (McQuade et al., 2021). The variability in assessments of GI tissue in the human disease highlight the heterogeneity of GI dysfunction in PD. This makes it trickier to model it in animals, translate the findings and ultimately treat in patients. Opposing changes in animal models due to the plethora of methodology increase the difficulty of this even more. Other changes that are conserved in the majority of models may prove to be the most useful approach for assessment in patient samples.

In PD patients lower urinary tract symptoms (LUTS) occur in up to 65% of patients, with the onset for the majority occurring after clinical diagnosis of PD (Sakakibara et al., 2018). Overactive bladder is the most common urinary symptom of PD and presents as nocturia, urinary urgency, incontinence and increased urinary frequency. Voiding symptoms such as difficulty in initiation, also occur in PD and although less common, have been shown to correlate to the stage of the disease also (Araki & Kuno, 2000). Partially due to the correlation between disease stage and LUTS as well as the fact that micturition is largely a CNS controlled action, the majority of animal and human studies have focused around central manipulations and in life interventions (Titova et al., 2017).

Stereotaxic injection of 6-OHDA in rats has been shown to lead to a reduction in voided volume of urine per micturition, however total urine volume over 24 hours is not different between 6-OHDA lesioned animals and controls. This was more akin to a "storage disorder" than a "voiding symptom" as 6-OHDA animals had reduced bladder capacity, smaller volume threshold to induce contractions but voiding pressure and residual urine after voiding was not different to sham lesioned animals. Agonism of supraspinal D1/D5 dopamine receptors inhibited this overactivity (Yoshimura et al., 2003). A larger study showed similar symptoms in 6-OHDA treated animals but crucially comparisons were also made to uninjected naïve controls. In this study sham animals also exhibit some significant cystometric abnormalities although to a lesser extent than the 6-OHDA animals, again pointing towards sensitivity towards central injury on micturition (Soler et al., 2011). An

adenosine A2A receptor antagonist has been shown to suppress by overactive bladder symptoms in rodents (Kitta et al., 2012) and PD patients (Kitta et al., 2018) believed to be through a supraspinal site of action. This shows promise for the translational potential of this model. Stem cell transplantation into the 6-OHDA lesion site in rats also alleviated some of the LUTS in the short term (Campeau et al., 2014; Soler et al., 2012).

Local alterations have also been assessed in the bladder of 6-OHDA lesioned animals in one study. Tissue strips from sham lesioned and 6-OHDA lesioned animals euthanised 26-29 days post lesioning were placed in a traditional organ bath for evaluations of contractility. Tissue from the 6-OHDA animals had significantly higher contractile response in the high K⁺ viability test, baseline EFS frequency response and during direct muscarinic and purinoceptor activation. It is worth noting that the authors saw some level of hypertrophy in animals that received 6-OHDA lesions and when some of these responses were normalised to tissue weight the differences between the treatment groups were lost (Mitra et al., 2015). They also performed injection of 6-OHDA into the MFB, producing a maximal lesion.

In this study we chose to induce nigral lesions via striatal injection to mimic an earlier stage of disease, with lesser dopaminergic loss to assess gastrointestinal and urinary dysfunction. We used this ex vivo model and molecular techniques to:

Assess neuropathology in the DMV upon striatal 6OHDA administration. Investigate overt local changes in the contractility of the colon, ileum and bladder of 6OHDA-treated and sham-treated rats via electrical and pharmacological manipulation as well as protein expression studies.

Understand whether differences are present in the functional effects and molecular expression of $K_{\nu}7$ channels in the colon, ileum and bladder of 6OHDA-treated and shamtreated rats.

This is the first such work investigating local autonomic dysfunction in a partial lesion model and therefore we first characterised the neuropathology, including observations of a loss of cells in the DMV. With our increasing interest in Kv7 channels in models of PD, we show for the first time that a partial lesion model of 6-OHDA had increased expression of the Kv7.4 channel in the bladder which manifested as functionally as increased hyperpolarisation. We also observed alterations in the relaxation mechanisms of the bladder and the ileum tissues from 6OHDA treated animals when compared to control tissue.

5.2 Methods

5.2.1 Animals

All experimental procedures were conducted with local ethical committee approval (King's College London) and in accordance with the UK Animals (Scientific Procedures) Act, 1986 (National Archives, UK Animals, Scientific Procedures Act, 1986). 18 wildtype Wistar male rats (Charles River, UK) weighing 250-310 g were used in this study. Animals were housed under controlled ambient temperature (21 ± 2 oC) and an even light-dark cycle (12:12 hours). Animals were allowed free access to food and water. 6-OHDA was injected into the left striatum (AP, +0.2mm; ML, +3.0mm; V, -5.5mm from the dura) of rats to create a partial lesion model of PD. Four different groups of animals were used in this study uninjected controls (n=6), Sham treated controls (n=4), 12μg 6-OHDA (n=7) and 24μg 6-OHDA (n=7). The tissues were distributed to different parts of the study, n numbers are stated for each result where appropriate. Due to the number of animals on the study and the length and number of experiments, animals were euthanised 6-12 weeks post lesion at an average rate of three animals per week. They were euthanised by exposure to a rising concentration of CO₂ with confirmation via exsanguination. The animals were transcardially perfused with ice-cold oxygenated (95% O2 plus 5% CO2) Krebs-Henseleit solution [in mM: 118 NaCl, 4.7 KCl, 1.2 KH2PO4, 1.2 MgSO4, 25 NaHCO3, 2.5 CaCl2, 11 glucose] to remove any remaining blood from the circulation and vessels of organs.

5.2.2 Organ bath contractility

After perfusion of the animal the bladder, ileum and colon were excised and placed in a container of carbogen aerated (95% O₂/5% CO₂, pH 7.4) Krebs buffer and transported to the organ bath laboratory in our institution (approximately 1.5-hour journey).

Once in our laboratory all tissues were flushed, cleaned and trimmed of connective tissue prior to suspension in the Bennet organ bath in a carbogenated Krebs solution at 37°C. The strips of gastrointestinal and bladder tissue were suspended in individual organ baths and attached to an FT-100 force transducer held at 1g tension. The force transducer was connected to an iWORKS amplifier which used the Labscribe (v1.817) software to record tissue responses.

Further details of the organ bath methods, experimental procedure and data analysis are mentioned in 2.32.1.3.

5.2.2.1 Data analysis

NOTE: With no significant differences in any of the CNS readouts between 12µg and 24µg 6-OHDA treatment and no correlation between loss of TH-ir cells in the SN and response to 10Hz EFS, all subsequent comparisons are performed with three groups, naïve sham and 6-OHDA only (12µg and 24µg combined).

Data analysis from the organ bath work was performed offline in the Labscribe software. The response of treatments in grams was calculated using the V2-V1 function in the software where V2 is the value of the peak response and V1 is the baseline response. For concentration response experiments (cumulative dosing), V1 (the baseline) was determined as the tension (in g) prior to the first concentration of the compound and V2 was the recorded at the peak response of each concentration. For single dose and EFS treatments V1 was calculated as the baseline immediately prior to each administration or pulse and V2 at the peak of the response.

5.2.3 Drugs

6-OHDA hydrochloride (Sigma-Aldrich, H4381) was dissolved in 0.9% saline containing 0.1% ascorbic acid for the stereotaxic injection, prepared at a concentration of 14.58μg/μL.

For K_v 7 channel activation, tissues were incubated in rising concentrations of Ethyl [2-amino-4-[[(4-fluorophenyl)methyl]amino]phenyl]carbamate (Retigabine) in DMSO. The compound was purchased from Tocris Biosciences, Bristol, UK.

Carbachol (Cch, Carbamoylcholine chloride, C4382) - a cholinergic agonist, L-NAME (Nω-Nitro-L-arginine methyl ester hydrochloride, N5751) - a nitric oxide synthase inhibitor, Sildenafil (Sildenafil citrate, SML3033) - a phosphodiesterase 5 inhibitor, Atropine (Atropine sulphate salt monohydrate, A0257) - a muscarinic receptor antagonist, ATP (Adenosine 5'-triphosphate disodium salt hydrate, A2383) - a purinergic agonist, were all purchased from Sigma-Aldrich, UK.

5.2.4 Immunohistochemistry

5.2.4.1 Brain tissue

Using the rat brain atlas (Paxinos & Watson, 2009) as a guide, serial coronal sections of substantia nigra were collected from each animal with one section processed for TH immunohistochemistry every 300 µm from the start of the substantia nigra pars compacta (Figure 4 a) until the end (Figure 4 b). Sections of the DMV from each animal were taken to correspond with areas at which the DMV was at its largest (Figure 4 c). and sections were stained with primary antibodies against TH (ab112, Abcam, UK) and ChAT (ab178850, Abcam, UK). Immunoreactivity (ir) was observed by Avidin-biotin peroxidase complex immunohistochemistry, using Vector VIP substrate kit (Vector Laboratories Ltd, Peterborough, UK) as per manufacturer's instructions. Further details of the immunohistochemistry methods are mentioned in 2.4.2.1.

5.2.4.2 Gut tissue

To determine the expression of the Kv7.4 protein, ileum and colon tissues the sections were incubated with Anti-KCNQ4 (ab6579, Abcam, Cambridge, UK; 1:200) for three days at 4°C.

Immunoreactivity (ir) was observed by Avidin-biotin peroxidase complex immunohistochemistry, using 3,3-diaminobenzidine as the chromogen (Vector Laboratories Ltd, Peterborough, UK) as per manufacturer's instructions. Further details of the sectioning and immunohistochemistry methods are mentioned in 2.4.1.2.

5.2.5 Western blot

Tissue segments from naïve, sham injected or 6-hydroxydopamine (6-OHDA) treated rats were assessed for protein expression of various proteins relevant to the contractile and relaxatory mechanisms of the gut and bladder. Details of the antibody combinations and dilutions are listed in

Table 3. Further details of the western blot methods are mentioned in 2.6.

Table 3 Antibodies used in protein detection from rat tissues.

Marker	Primary Antibody	Dilution	Secondary Antibody	Dilution
Neuronal nitric oxide synthase (nNOS)	sc-5302	1:200	ab97040	1:10000
Phosphodiesterase 5A (PDE5A)	sc-398747	1:1000		
β-actin	ab6276	1:5000		
Choline Acetyltransferase (ChAT)	ab178850	1:1000	ab6721	1:3000
Guanylyl Cyclase (GC)	ab50358	1:5000		
KCNQ4	ab65797	1:500		

5.3 Results

5.3.1 Unilateral injection of 6-OHDA into the striatum led to a loss of TH+ cells in the Substantia Nigra

Animals were culled 21-40 days post 6-OHDA injection into the striatum. Using our stereology-like technique we performed cell counts on 7 different sections from the start of the nigra (Figure 4 a) to the end (Figure 4 b). This allowed us to build up a full picture of the dopaminergic loss throughout the structure. Manual counts were performed as mentioned in chapter 2.4.2. The images show a clear loss of TH-ir throughout the nigra on the ipsilateral side in 6-OHDA treated animals compared with uninjected naïve and sham treated rats (Figure 30). Our counting method produced consistent numbers through a total of 24 animals in the contralateral side (Figure 31 c). This gave us confidence in the lesion size estimation. There was no significant difference in the contralateral side of any of the treatment groups (Figure 31 c) yet the same animals showed significant loss in cell counts in the side ipsilateral if injected with 6-OHDA injection (Figure 31 d). The ipsilateral side counts were Naïve: $17921 (\pm 1963) > \text{Sham}$: $15594 (\pm 710) > 12 \mu \text{g}$: $9273 (\pm 1077) > 24 \mu \text{g}$: $6207 (\pm 1360)$, mean ($\pm \text{SEM}$). When comparing loss in 6-OHDA treated animals to their respective contralateral hemispheres the mean ($\pm \text{SEM}$) loss for $12 \mu \text{g}$ dosed animals was $50.5\% (\pm 5.8)$ which was not significantly different from the $24 \mu \text{g}$ dosed animals which had a $66.7\% (\pm 6.4)$ loss of TH-ir neurons (Figure 31 b).

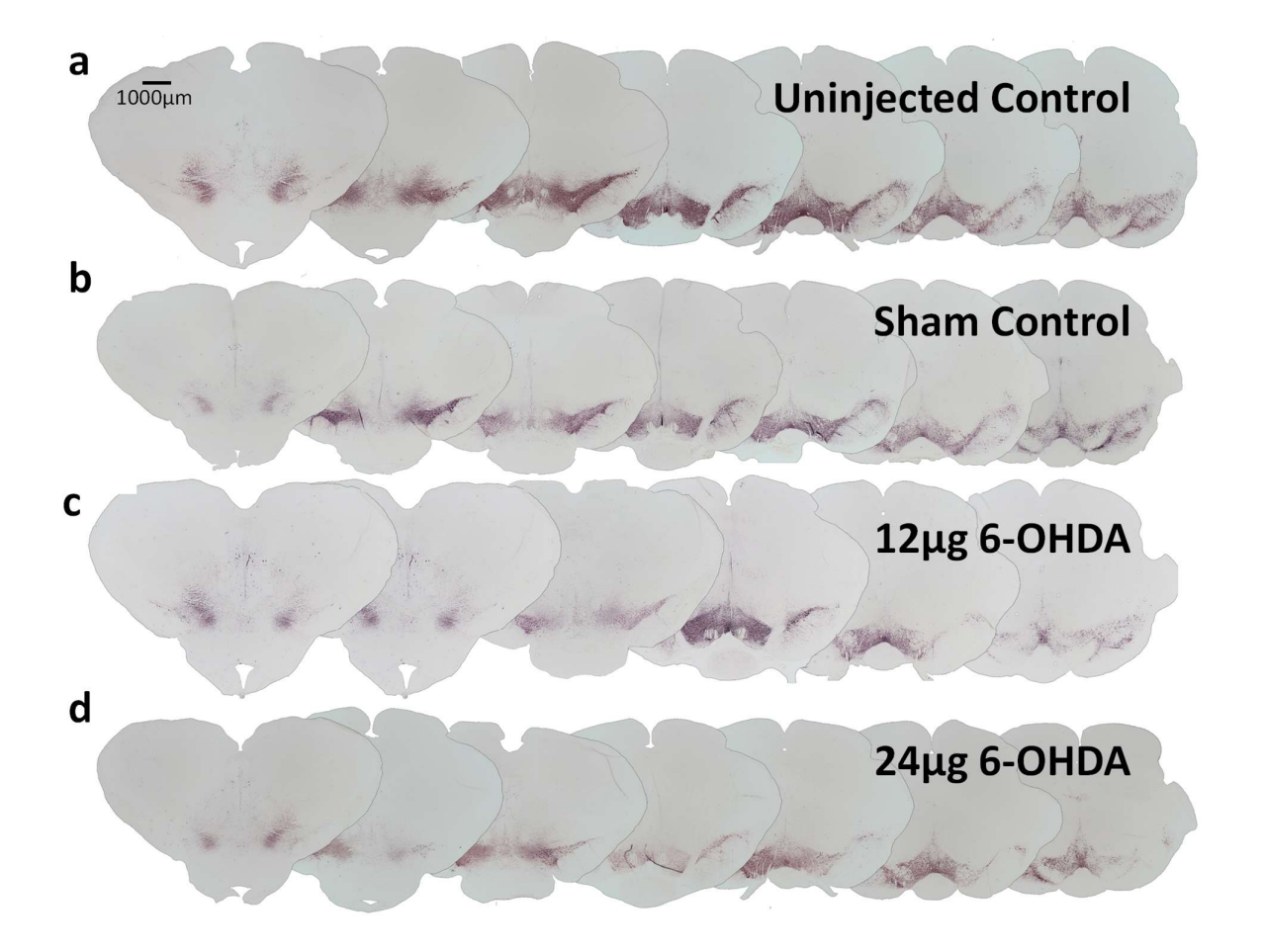


Figure 30 Series of tyrosine hydroxylase immunostained sections showing loss in the substantia nigra of 6-OHDA treated rats.

TH-ir staining in ventral midbrain sections from an uninjected naïve rat(a), a sham injected rat(b), and a rat injected with $12\mu g(c)$ and $24\mu g(d)$ of 6-OHDA into the left striatum. Each section is $30\mu m$ in thickness and $300\mu m$ apart from the section that precedes it. There is a marked reduction of TH immunoreactivity in the left hemisphere (lesioned side) of $12\mu g(c)$ and $24\mu g(d)$ 6-OHDA treated rats.

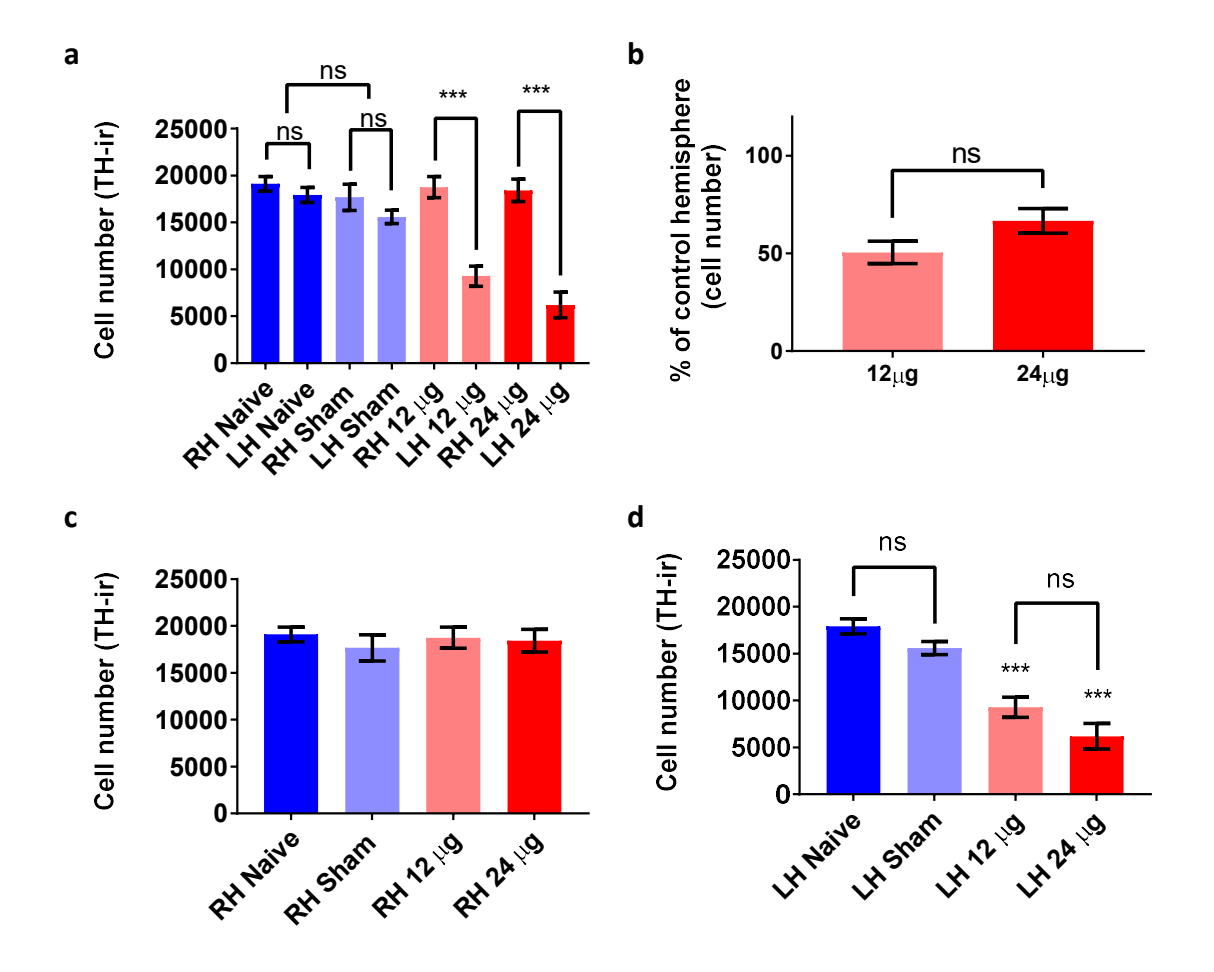


Figure 31 Quantification of the loss of TH-ir neurones in the SN of 6-OHDA treated rats.

Summary bar graphs of TH-ir neuron counts comparing both hemispheres of naïve, sham treated, and rats treated with $12\mu g$ and $24\mu g$ of 6-OHDA (a). The ipsilateral side (left hemisphere) had significant loss of TH-ir when compared to the contralateral internal control (right hemisphere) in $12\mu g$ and $24\mu g$ 6-OHDA treated rats. The % loss in $12\mu g$ and $24\mu g$ 6-OHDA treated animals were not significantly different (b). Cell number counts were consistent in the ipsilateral side of all treatment groups (c). The $12\mu g$ and $24\mu g$ 6-OHDA treated rats had significant loss of TH-ir neurons in the side contralateral to the injection site compared to naïve and sham animals (d). Each bar represents mean \pm SEM ($n \ge 4$) ***P < 0.001.

5.3.2 The ipsilateral DMV of 6-OHDA treated rats show loss of ChAT+ve neurons and TH-ir fibres.

Manual counts were performed as mentioned in chapter 2.4.2 for ChAT+ve neurons and OD was measured from an average of 10 different regions. Adjacent sections were used corresponding to the region shown in Figure 4 c. Although our aim was to multiplex and quantify TH-ir and ChAT-ir from the same section, quantification of TH-ir fibres had to be performed on adjacent single plex sections as colour separation was not sufficient in the software used. Duplexing did allow us to visualise that TH-ir fibres and ChAT+ve neurons occupy the same region in the hindbrain (Figure 32). The percentage of ChAT+ve cells in the ipsilateral DMV of the 6-OHDA treated animals were significantly lower than those in the sham treated and naïve DMV (Figure 33). The percentage of neurons on the ipsilateral side were Naïve: 94% (± 2) > Sham: 82% (± 7) > 12μ g: 44% (± 9) > 24μ g: 39% (± 5), mean (\pm SEM). When comparing the percentage loss between $12~\mu$ g and $24~\mu$ g 6-OHDA treated animals to their respective contralateral hemispheres there was no significant difference. OD measurements of TH-ir in the DMV was also significantly lower in the 6-OHDA treated animals but again there was no significant difference between $12~\mu$ g and $24~\mu$ g treated animals.

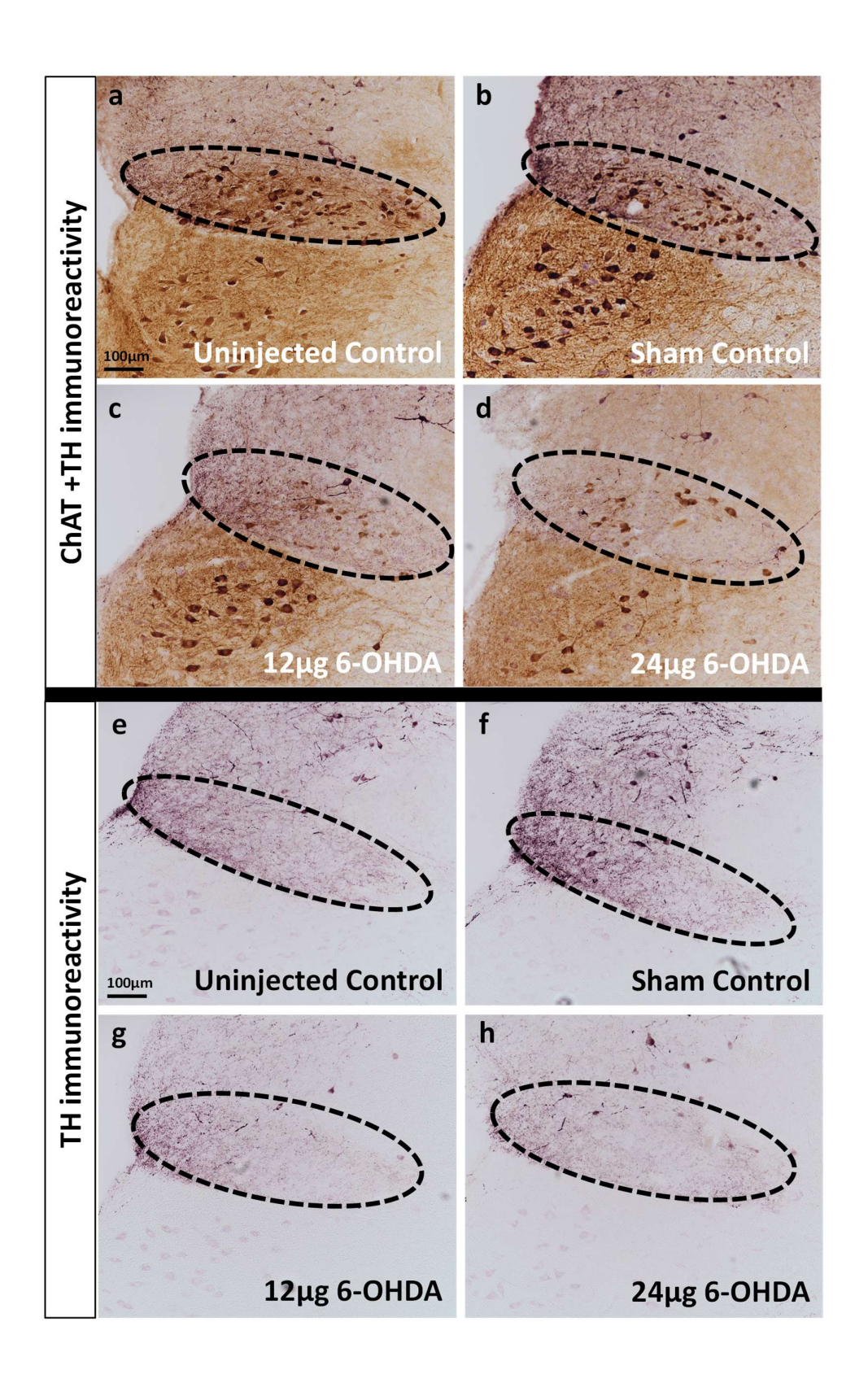


Figure 32 Corresponding sections of the DMV show loss of ChAT+ve neurons and TH-ir fibres in 6-OHDA treated rats.

Exemplar images from ChAT-ir (brown) and TH-ir (purple) staining in DMV sections from an uninjected naïve rat(a), a sham injected rat(b), and rats injected with $12\mu g$ (c) and $24\mu g$ (d) of 6-OHDA into the left striatum. There is a marked reduction of ChAT immunoreactivity in the sections from $12\mu g$ (c) and $24\mu g$ (d) 6-OHDA treated rats. TH-ir single stained sections of DMV from an uninjected naïve rat(e), a sham injected rat(f), and rats injected with $12\mu g$ (g) and $24\mu g$ (h). Again, there is a marked reduction of TH immunoreactivity in the sections from $12\mu g$ (g) and $24\mu g$ (h) 6-OHDA treated rats.

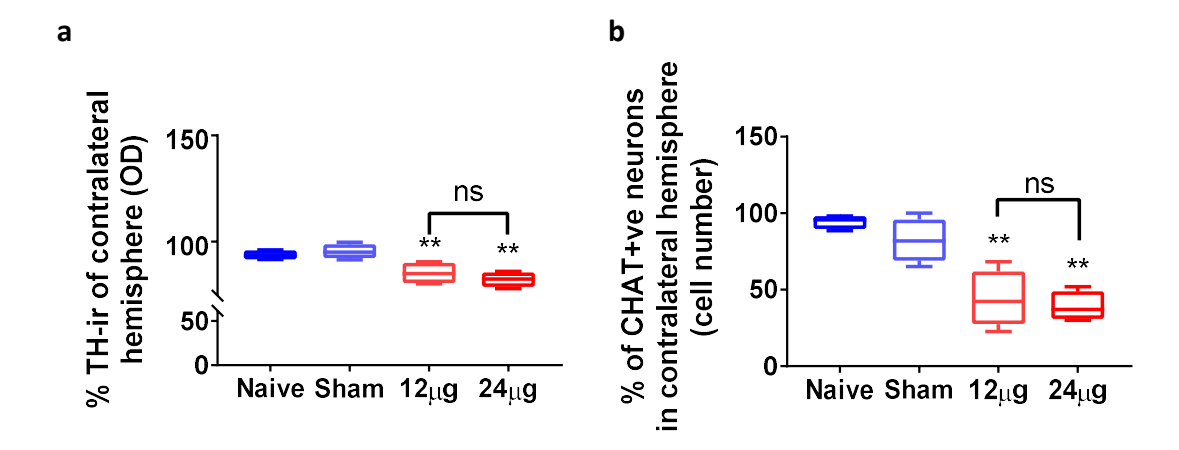


Figure 33 Quantification of the loss of TH-ir fibres and ChAT+ve neurons in the DMV of 6-OHDA treated rats.

Summary box plot of TH-ir (a) fibre optical density (OD) and ChAT+ve (b) neuron number compared against the contralateral hemisphere of naïve, sham treated, and rats treated with $12\mu g$ and $24\mu g$ of 6-OHDA. The ipsilateral side (left hemisphere) had significant loss of TH-ir fibres (a) and ChAT+ve (b) neurons when compared to the contralateral internal control (right hemisphere) in $12\mu g$ and $24\mu g$ 6-OHDA treated rats. The % loss between $12\mu g$ and $24\mu g$ 6-OHDA treated animals were not significantly different, $n \ge 4 **P < 0.01$.

5.3.3 The extent of TH+ve cell loss in the SN did not correlate with response to EFS in the gastrointestinal tract and the bladder in this model of PD.

Where a tissue did not show any response to an EFS and a Carbachol viability test it was discarded. The strips of gastrointestinal and bladder tissues that were viable were subjected to EFS stimulation at 10 Hz. This was plotted against the extent of the % ipsilateral TH loss values (Figure 34 a-c) gained from immunohistochemical analysis performed in chapter 5.3.1 and compared between 6-OHDA treatments (Figure 34 d-f). There was no correlation between loss of TH-ir cells in the SN

and response to 10Hz EFS in any of the tissues we tested. Nor was there any significant difference between $12\mu g$ and $24\mu g$ 6-OHDA treated rats in the EFS response.

With no significant differences in any of the CNS readouts between $12\mu g$ and $24\mu g$ 6-OHDA treatment and no correlation between loss of TH-ir cells in the SN and response to 10Hz EFS, all subsequent comparisons are performed with three groups, naïve sham and 6-OHDA only ($12\mu g$ and $24\mu g$ combined).

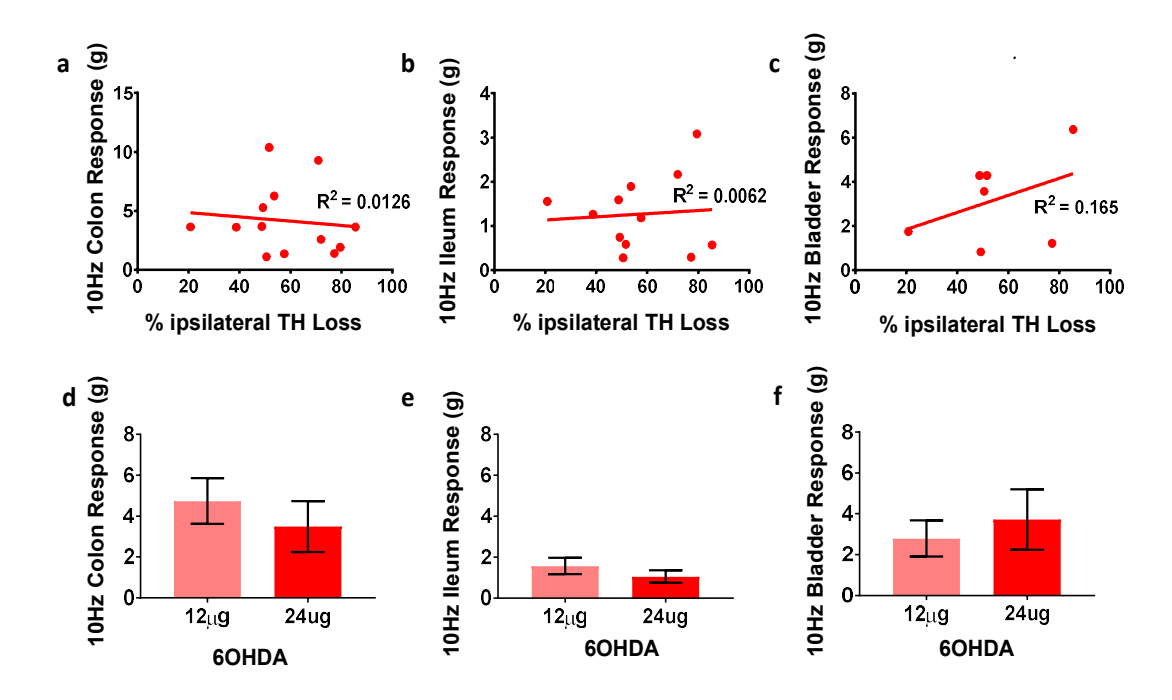


Figure 34 Comparison of 6-OHDA treatment and effects with response to EFS

Plot of % ipsilateral TH-ir loss in SN against response to 10Hz electric field stimulation (EFS) ($n \ge 7$) in the conventional organ bath for the colon (a), ileum (b) and bladder (c). The extent of the lesion did not correlate well with an increase or decrease in response to EFS at 10Hz in any tissue. Summary bar charts ($n \ge 4$) also show no significant difference between 12µg and 24µg 6-OHDA treated rats in the response to 10Hz EFS in the colon (d), ileum (e), or bladder (f).

5.3.4 Electrical field stimulation (EFS) and carbachol (CCh) stimulation of isolated gastrointestinal and urinary bladder strips revealed no differences in treatment groups.

There was no significant difference in the concentration-dependent contraction to carbachol in the isolated tissue segments from naive, sham and 6-OHDA treated rats (Figure 35 a, c, e). Cumulative application of carbachol led to a concentration dependent contraction in the colon, ileum and bladder to varying degrees. The maximal response to CCh in tissues from naïve animals was seen in the colon; $3.58g~(\pm 0.16)$, followed by the bladder; $3.21g~(\pm 0.09)$ and then lastly the ileum; $1.56g~(\pm 0.18)$; mean $(\pm SEM)~n \geq 3$. The carbachol concentration response curve produced LogEC50 values which were similar across the different tissues and treatment groups (Table 4) with no significant differences observed.

The values for the sham ileum are stated as ambiguous in the non-linear regression analysis and the curve is irregular (Figure 35 c). This is due to one outlier, where one tissue responded maximally at 1µM and with a very large increase in tension, compared to the others which responded maximally at 3µM with half the increase in tension. Such responses exist within ileum tissues from the naïve and 6-OHDA groups but with a n=9 in those groups such outliers are balanced by the other values. The sham group only had n=3 in the ileum and therefore the outlier has a bigger impact on the mean data. For the bladder, no sham tissues were available for assessment, so all comparisons are made to naïve treated rat tissue only.

Table 4 Log EC50 contractile response to CCh in different tissues from naive, sham and 6-OHDA treated rats.

	Naïve	Sham	6-OHDA
Colon	-6.35 (±0.11)	-6.35 (±0.33)	-6.61 (±0.24)
Ileum	-6.64 (± 0.20)	-6.50 (±0.12)	~ -6.52 (±0.07)
Bladder	-5.82 (±0.05)		-5.65 (±0.13)

In response to EFS at increasing stimulation frequencies (50V, 0.2 ms pulse width and 0.25 to 40Hz trains of 20 pulses), increases in contractile tensions were observed in all tissues (Figure 35 b, d, f). Again, there were no significant differences in each tissue between the different treatment groups. In this case the largest maximal response in naïve animals was produced by the bladder > colon > ileum. The sham ileum looks to be more active than the naïve and 6-OHDA, but this is still non-significant and as mentioned likely due to outliers and a lower sample size.

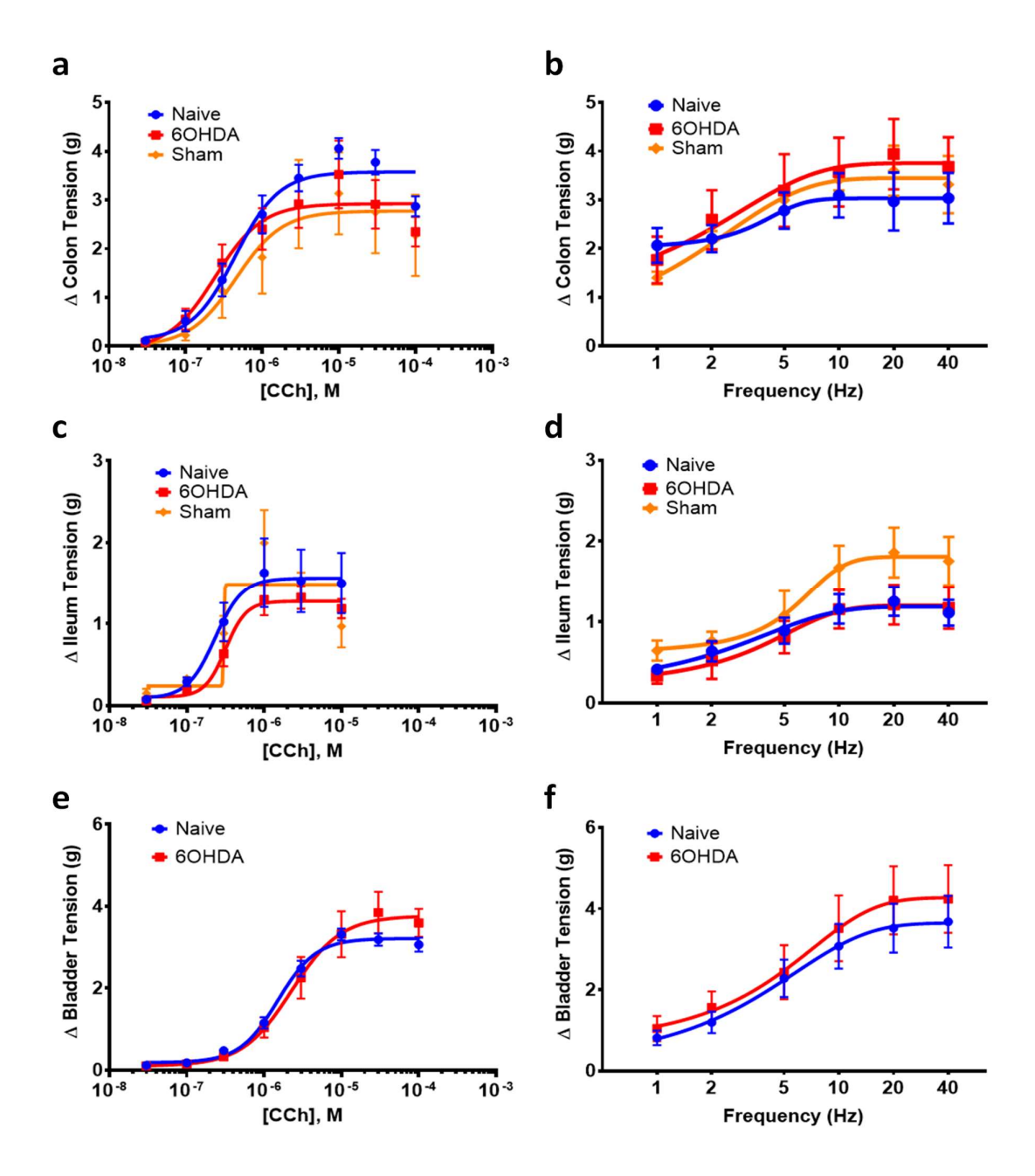


Figure 35 Dose response curves to Carbachol and EFS frequency response curves in various tissues from control and 6-OHDA treated rats.

Administration of carbachol evoked a concentration dependent contraction of the isolated colon (a), ileum (c) and bladder (e). There were no significant differences in the carbachol concentration response curves of the tissues from the naïve, sham and 6-OHDA treated rats. Colon (b), ileum (d) and bladder (f) tissues from the same groups showed no significant differences in contractile responses to EFS frequencies ranging 1-40Hz. Analysis by two-way ANOVA, mean \pm SEM (n \geq 3).

5.3.5 The effect of K_v 7 activator Retigabine on isolated segments and K_v 7.4 expression was not significantly different between treatment groups in gastrointestinal tissue.

Cumulatively increasing concentrations of Retigabine resulted in a reduced contraction in response to 10Hz EFS in both colon (Figure 36 a) and ileum (Figure 36 c) segments from naïve tissue. In the colon (Figure 36 a) this reduction was only significant in the presence of $10\mu M$ Retigabine for the colon with a reduction of 22.6% (± 6.5). At $3\mu M$ and $10\mu M$ Retigabine concentration in the ileum (Figure 36 c) there was a significant reduction in 10Hz contraction of 13.3% (± 2.5) and 34.9% (± 4.1) respectively, from vehicle control, (mean (SEM); one way ANOVA). When comparing the different treatment groups, no significant difference was observed in the response to 10Hz EFS in the presence of the Kv7 activator Retigabine, between, naïve, sham or 6-OHDA treated animals in isolated colon (Figure 36 b) or ileum (Figure 36 d).

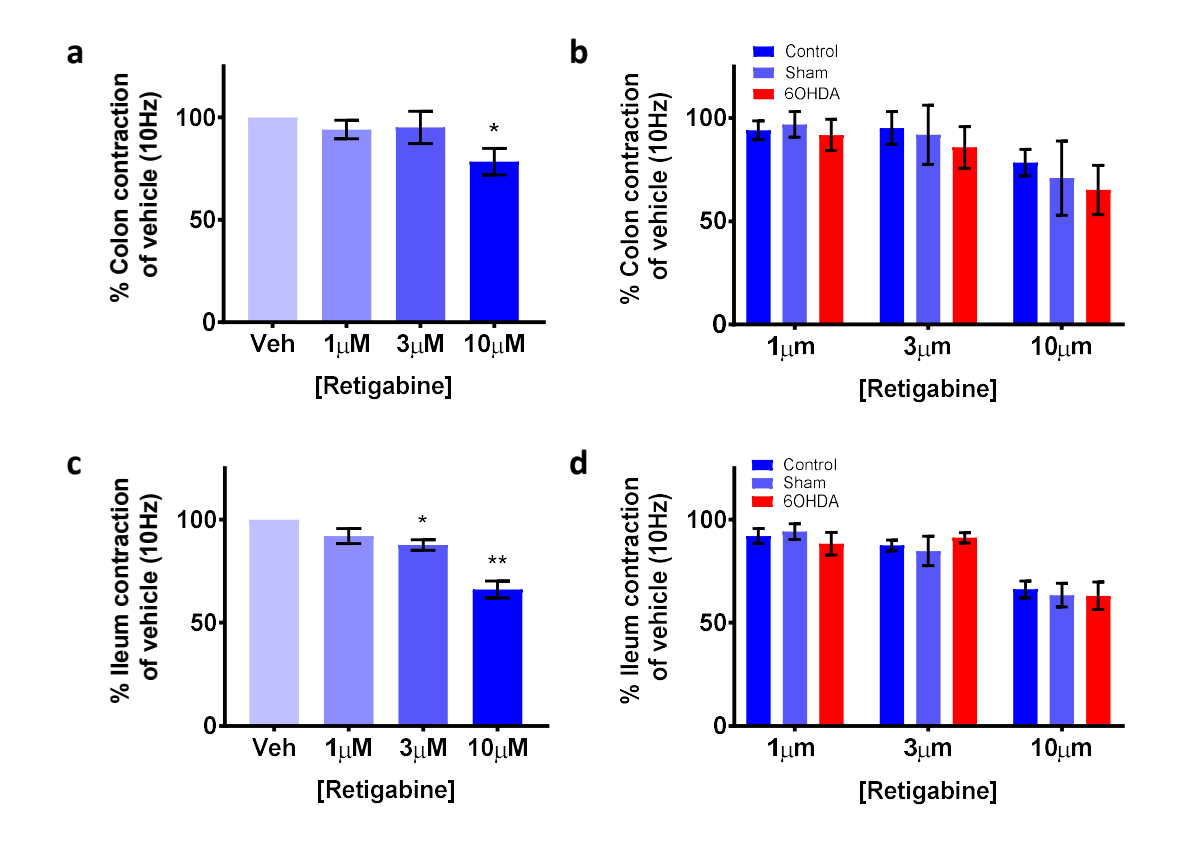


Figure 36 Responses of gastrointestinal tissues from treated and untreated rats to 10Hz EFS, in the presence of Kv7 channel activator Retigabine.

Summary bar charts of response to 10Hz EFS in the presence of increasing concentrations of Kv7 channel opener Retigabine. Incubation of Retigabine resulted in a significant reduction in 10Hz response in the naïve colon (a) in the naïve ileum tissue (c) (n=5, *p=<0.05, **p=<0.01, one-way ANOVA). Comparison of tissues from different treatment groups revealed no significant difference in the Retigabine effect on 10Hz EFS responses in the colon (b) or ileum (d) from naïve, sham or 6-OHDA treated rats.

185

Immunohistochemistry revealed numerous KCNQ4-ir punctate structures in the longitudinal layers and elongated strands in the circular layer of the smooth muscle of the naïve colon (Figure 37 a) and ileum (Figure 38 a). Optical density was quantified (using Image J) and compared in the three main segments where KCNQ4 staining was present: the longitudinal muscle, circular muscle and the mucosa. The optical density of the staining was not different in between any of the treatment groups in the colon (Figure 37 e) or ileum (Figure 38 e). Automated counting of the number of KCNQ4 positive cells, % coverage of an area and cell size in the longitudinal muscle layers was performed using the methods set out in chapter 2.4.1.2. there was no statistical difference in the expression of KCNQ4-ir structures in the colon (Figure 37 f, g and h) and the ileum (Figure 38 f, g, and h) between naïve, sham and 6-OHDA treated rats, for any of the parameters measured.

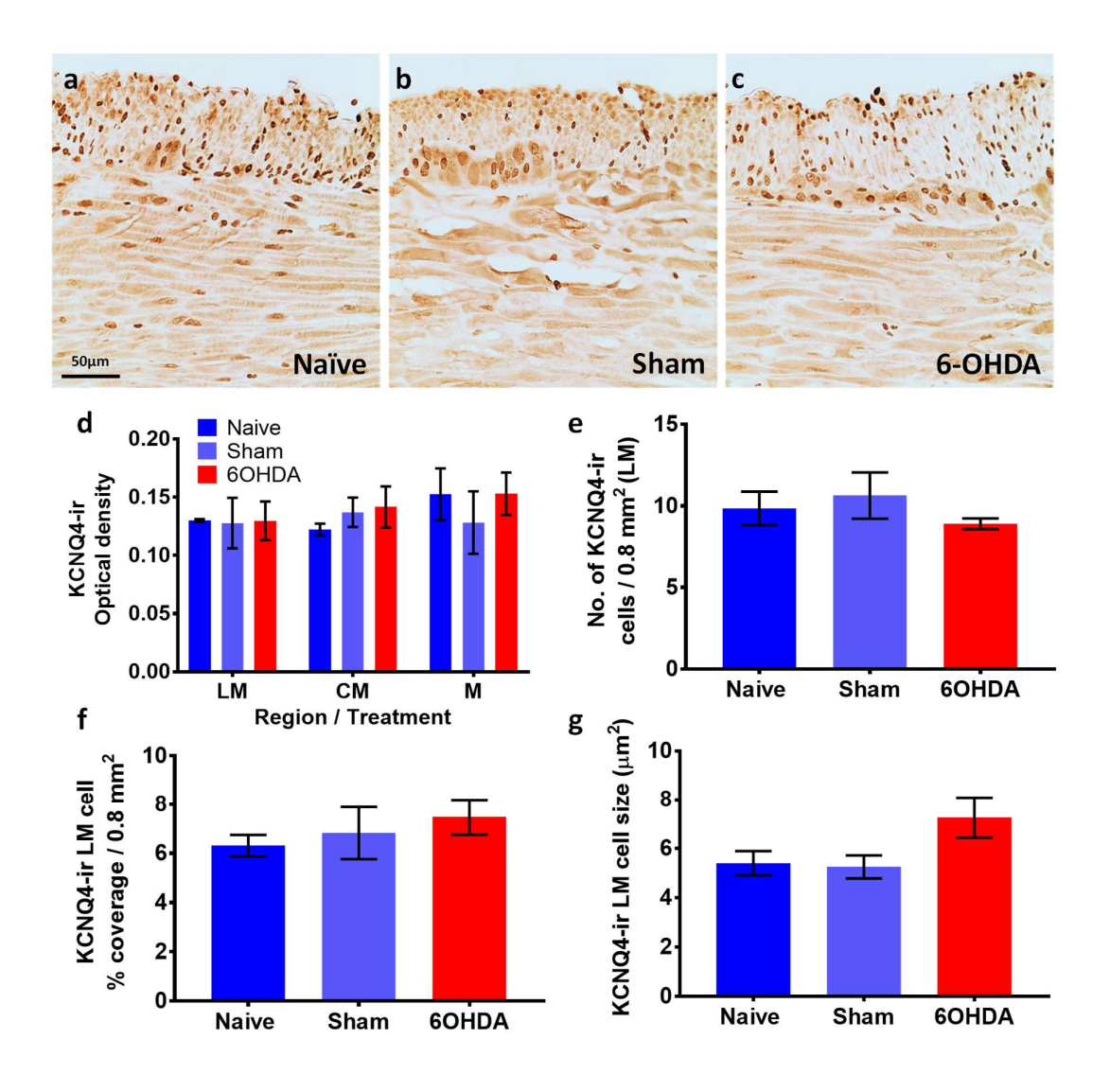


Figure 37 KCNQ4-immunoreactivity in the colon of 6-OHDA treated and untreated rats.

Representative images of KCNQ4-ir in the colon of naïve (a), sham (b) and 6-OHDA (c) treated rats. Summary bar charts showing the comparison between treatments for average optical density of KCNQ-ir in the different tissue regions; LM = longitudinal muscle, CM = circular muscle, M = mucosa (d), the number of KCNQ-ir cells (e), percentage coverage of staining (f) per $0.8 mm^2$ region of interest and mean cell size in μm^2 (g). No significant differences were found in the expression of KCNQ4-ir in the colon between treatment groups. The data are expressed as mean, SEM; vs naïve tissue by one-way ANOVA followed by Sidak post hoc test.

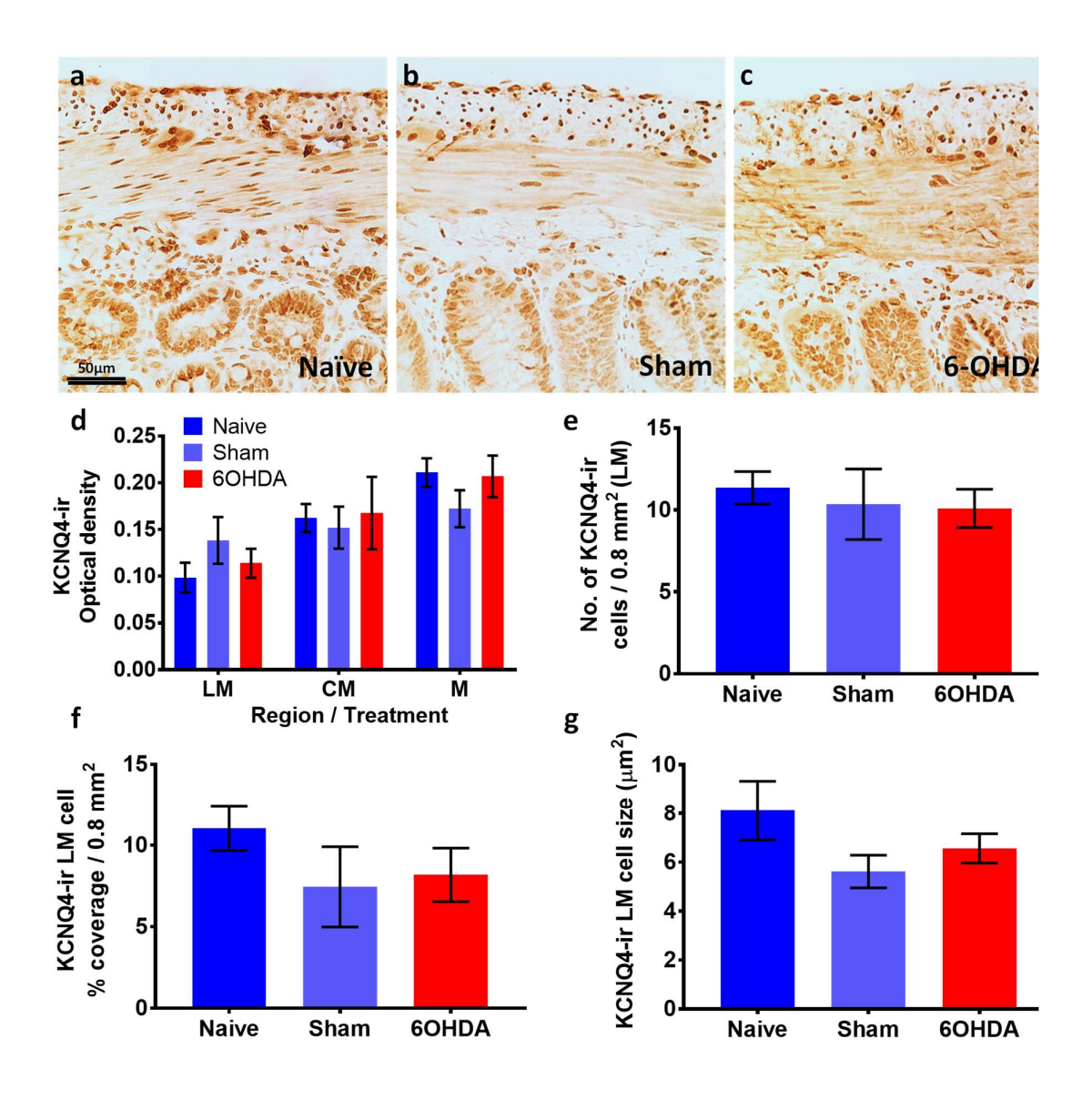


Figure 38 KCNQ4-immunoreactivity in the ileum of 6-OHDA treated and untreated rats.

Representative images of KCNQ4-ir in the colon of naïve (a), sham (b) and 6-OHDA (c) treated rats. Summary bar charts showing the comparison between treatments for average optical density of KCNQ-ir in the different tissue regions; LM = longitudinal muscle, CM = circular muscle, M = mucosa (d), the number of KCNQ-ir cells (e), percentage coverage of staining (f) per $0.8mm^2$ region of interest and mean cell size in μm^2 (g). No significant differences were found in the expression of KCNQ4-ir in the colon between treatment groups. The data are expressed as mean, SEM; vs naïve tissue by one-way ANOVA followed by Sidak post hoc test.

5.3.6 The isolated segments of bladder from 6-OHDA treated rats show increased response to the Kv7 activator Retigabine and increased Kv7.4 expression.

Cumulatively increasing concentrations of Retigabine resulted in a reduced contraction in response to 10Hz EFS in the naïve bladder strips (Figure 39 a). This reduction was significant in the presence of $10\mu\text{M}$ Retigabine with a reduction of 9.7% (± 2.0). In bladder tissues from 6-OHDA animals, $10\mu\text{M}$ Retigabine resulted in a much larger reduction of contraction compared to the vehicle 10Hz contraction in the same tissues. The 10 Hz contraction in the presence of Retigabine was reduced by 55.8% (± 11.9) compared to the vehicle 10Hz contraction (Figure 39 b) (mean ($\pm\text{SEM}$). When comparing the different treatment groups (Figure 39 c), the Retigabine effect was significantly greater in the bladder from the 6-OHDA treated animals. This is further strengthened by our expression data. Bladder tissue from animals lesioned with 6OHDA had significantly greater expression of Kv7.4 protein (relative to β -actin) than bladder tissues from uninjected naïve animals (Figure 39 d).

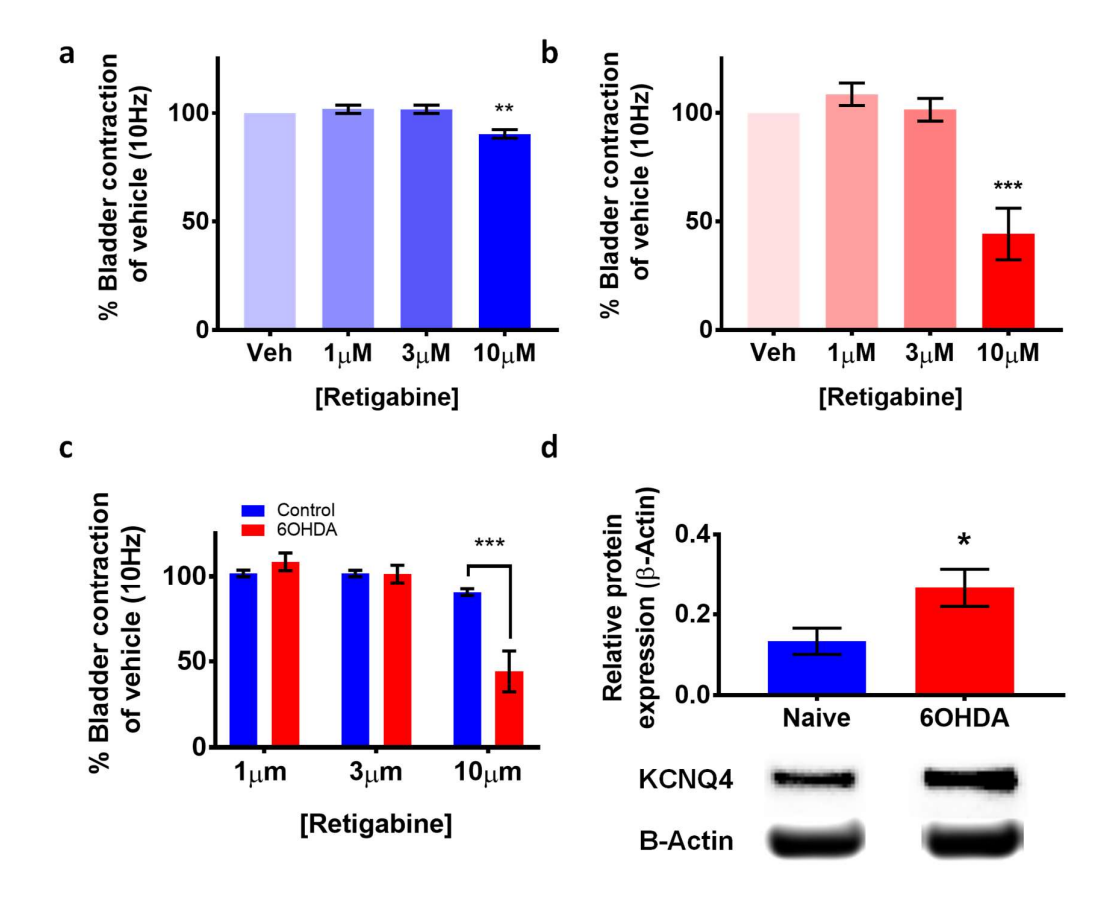


Figure 39 Retigabine has a larger effect on bladder tissue from 6-OHDA treated animals due to increased KCNQ4 expression.

Summary bar charts of response to 10Hz EFS in the presence of increasing concentrations of Kv7 activator Retigabine and mean KCNQ4 expression in naïve and 6-OHDA bladder strips. Incubation of Retigabine resulted in a significant reduction in 10Hz response in the naïve bladder (a) and in 6-OHDA bladder tissue (b) at the $10\mu M$ concentration. The data are expressed as mean (\pm SEM) 10Hz contraction as a % of vehicle, vs vehicle ($n\geq 5$, ** p=<0.01, ***p=<0.001, one-way ANOVA). Comparison of tissues from the different treatment groups (c) revealed a larger reduction in 10Hz contraction in 6-OHDA tissues in the presence of Retigabine. The data are expressed as mean (\pm SEM) 10Hz contraction as a % of vehicle, vs naïve tissue ($n\geq 5$, ** p=<0.01, ***p=<0.001, two-way ANOVA). Summary bar chart and exemplar image of western blot experiments (d), in which, bladder strips from 6-OHDA treated animals have significantly higher expression of Kv7.4 protein than tissues those from naïve animals. The data are expressed as mean (\pm SEM) Kv7.4 expression relative to β -actin, vs naive ($n\geq 5$, * p=<0.05, unpaired t -test).

5.3.7 Impairment of relaxation mechanisms in the gastrointestinal tract of the partial unilateral lesion 6-OHDA model

To look at the effects of modulating the NO-cGMP pathway, we performed EFS in the presence of cumulatively increasing concentrations of Sildenafil. Sildenafil resulted in a reduced contraction in response to 10Hz EFS in both colon (Figure 40 a) and ileum (Figure 40 c) segments from naïve tissue. In the colon (Figure 40 a) this reduction was only significant in the presence of $10\mu M$ Sildenafil with a reduction of 14.8% (± 6.1). When $3\mu M$ and $10\mu M$ Sildenafil was incubated with the ileum (Figure 40 c) there was a significant reduction in 10Hz contraction of 18.9% (± 3.9) and 30.9% (± 3.5) respectively, from vehicle control, (mean (\pm SEM). When comparing the different treatment groups, no significant difference was observed in the response to 10Hz EFS in the presence of the phosphodiesterase 5 (PDE5) inhibitor, Sildenafil, between, naïve, sham or 6-OHDA treated animals in isolated colon (Figure 40 b). In the ileum segments (Figure 40 d), no significant reduction was seen in 10Hz contraction at any concentration of Sildenafil in tissue from 6-OHDA treated rats. This meant that there was an impairment of the response to Sildenafil that was significantly different in the tissues from the 6-OHDA treated rats from the naïve and sham tissues at $3\mu M$ and $10\mu M$.

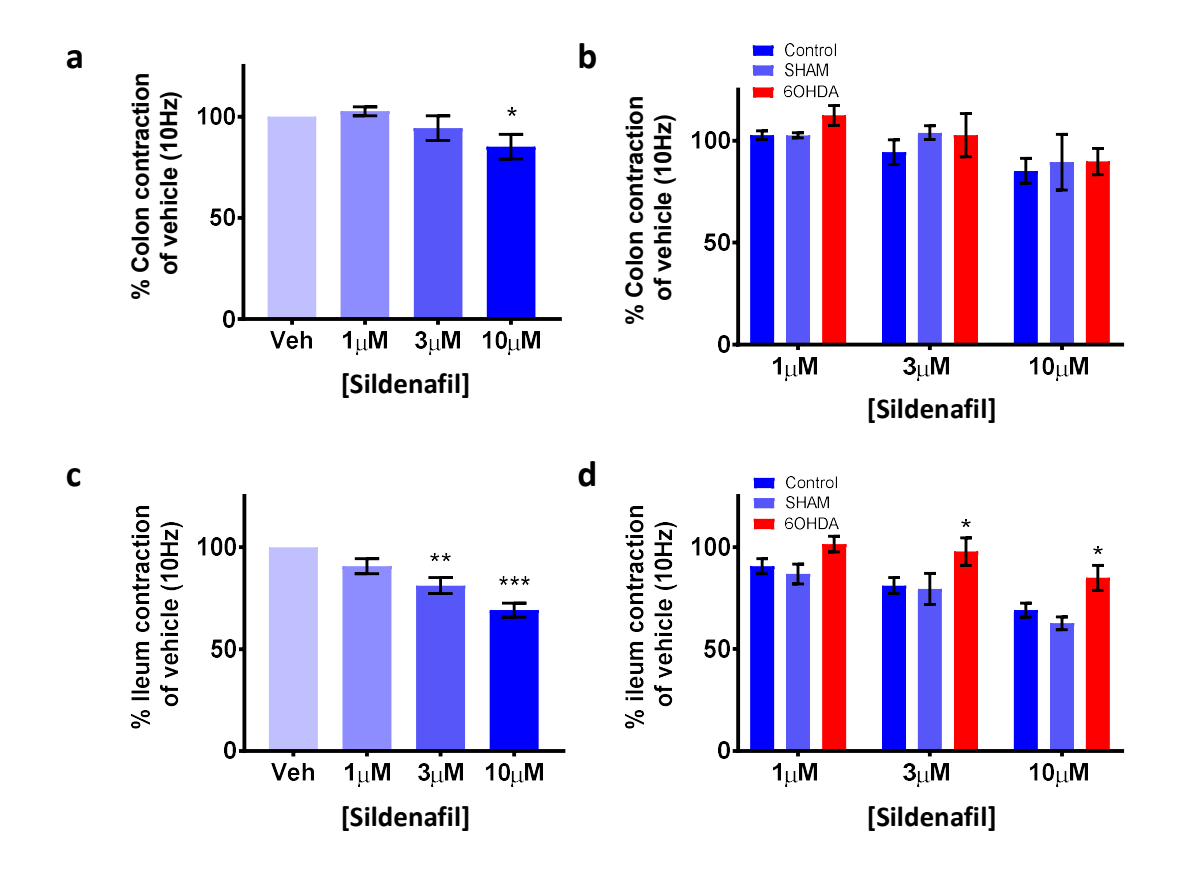


Figure 40 Responses of gastrointestinal tissues from treated and untreated rats to 10Hz EFS, in the presence of Sildenafil.

Summary bar charts of the response to 10Hz EFS in the presence of increasing concentrations of PDE5 inhibitor Sildenafil. Incubation of Sildenafil resulted in a significant reduction in the 10Hz EFS response in the naïve colon (a) at $10\mu M$ and at $3\mu M$ and $10\mu M$ in the naïve ileum tissue (c). The data are expressed as mean (\pm SEM) 10Hz contraction as a % of vehicle, vs vehicle ($n \ge 5$, * p = <0.05, **p = <0.01, ***p = <0.001, one-way ANOVA). Comparison of tissues from different treatment groups revealed no significant difference in the Sildenafil effect on 10Hz EFS responses in the colon (b) however there was a significantly reduced response to Sildenafil in the ileum from 6-OHDA treated rats. The data are expressed as mean (\pm SEM) 10Hz contraction as a % of vehicle, vs naïve and sham tissue ($n \ge 5$, * p = <0.05, two-way ANOVA).

Segments of the colon from the different treatment groups were analysed by western blot to determine expression of various proteins. Although there was a trend towards reduced expression of nNOS in the colon of 6-OHDA treated rats compared to naïve and sham tissues (Figure 41 a) this difference was not significant. Also, within the nitrergic pathway the relative expression of guanylyl cyclase (GC) was significantly reduced in the colon of 6-OHDA rats vs naïve rats (Figure 41 d). However, when compared to sham treated animals this was not significant, possibly due to the low number of sham samples and larger variability between them. There was no difference found in expression of PDE5 (Figure 41 b), which confirms the lack of difference in treatment groups to Sildenafil seen previously (Figure 40 b). ChAT expression within the colon tissue is also not different between treatment groups (Figure 41 c).

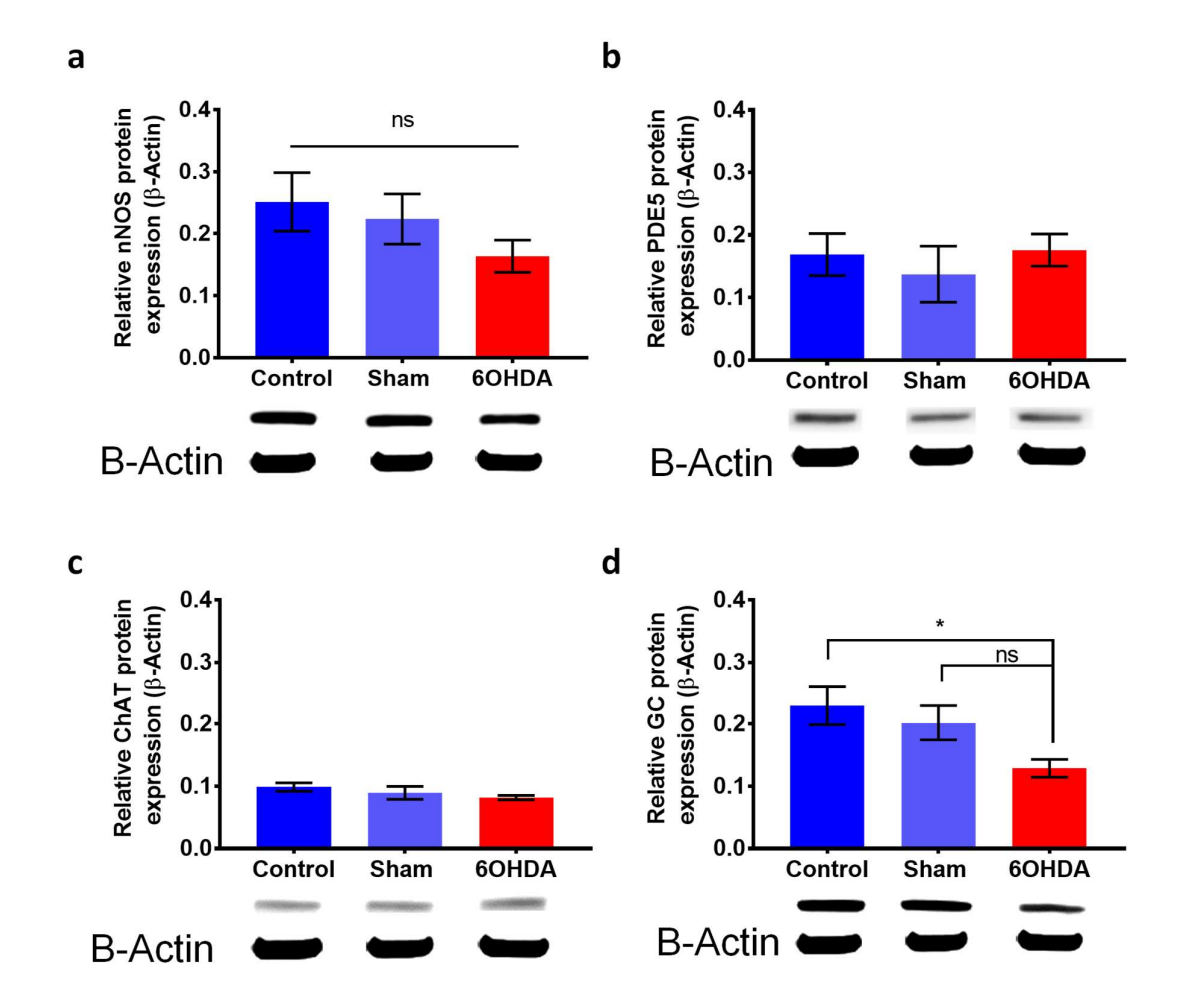


Figure 41 Expression of proteins relevant to the nitrergic and cholinergic system in the colon of 6-OHDA treated and untreated rats.

Summary bar charts and representative images of expression data from western blot analysis of colon tissue segments from naïve, sham and 6-OHDA treated rats. There is no significant difference in the expression of nNOS (a), PDE5 (b) or ChAT (c) between any of the treatment groups. GC expression was significantly reduced in colon segments from 6-OHDA treated animals vs naïve animals, but the difference was not significant when compared to sham treated animals ($n \ge 3$, *p = < 0.05, oneway ANOVA).

Segments of the ileum from the different treatment groups were analysed by western blot to determine expression of various proteins. Only two out of the four antibodies of interest gave any signal. These were ChAT (Figure 42 a) and GC (Figure 42 b) and there was no significant difference between the treatment groups. The results from these ileum segments are not reliable due to the fractionation of proteins even when probing for β-actin (Figure 42). We attempted adding double the amount of protease inhibitors to the lysate and trying multiple homogenisation methods, however these extra bands still appeared. It is likely that this fragmentation is due to improper storage of these samples as they were not flushed of their contents prior to transit. The ileum lumen naturally contains endogenous proteases, nor were they flash frozen immediately after dissection.

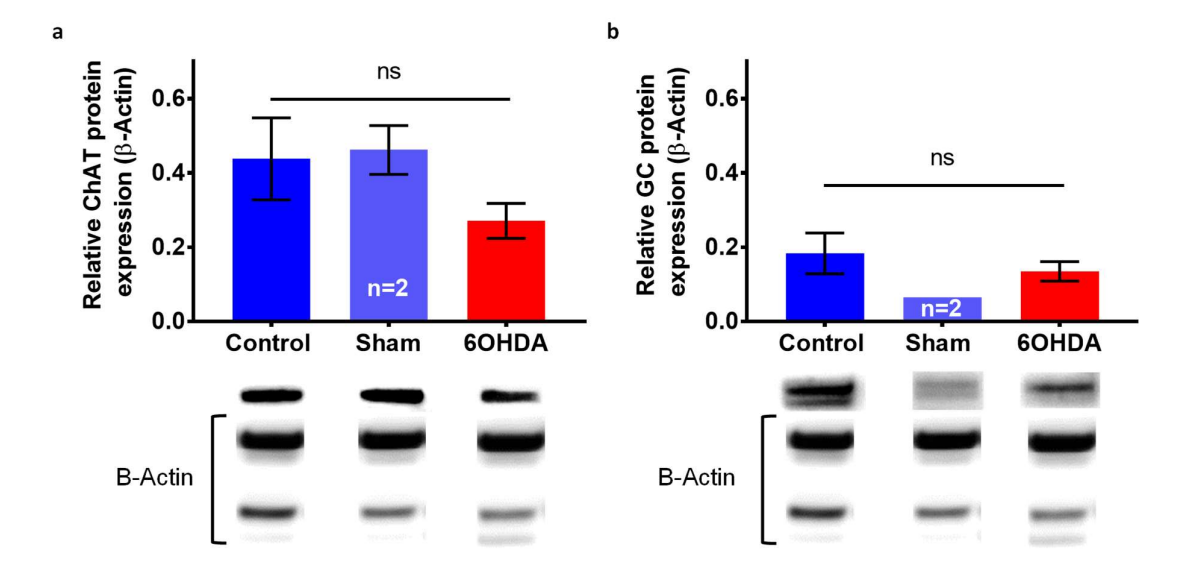


Figure 42 Expression of proteins relevant to the nitrergic and cholinergic system in the ileum of 6-OHDA treated and untreated rats.

Summary bar charts and representative images of expression data from western blot analysis of ileum tissue segments from naïve, sham and 6-OHDA treated rats. There is no significant difference in the expression of ChAT (a) and GC (b) between any of the treatment groups. The representative images show multiple bands when stained with anti- β -actin antibody indicating fragmentation of proteins ($n \ge 2$, one-way ANOVA).

5.3.8 Striatal 6-OHDA administration leads to impairment of the nitrergic system in the bladder.

Inhibition of nitrergic transmission by L-NAME resulted in significantly increased EFS evoked contractions in naïve detrusor (Figure 43 a). This potentiation was significant in the presence of 1mM L-NAME with an increase to 112.2% (± 4.4). 6-OHDA tissues were more sensitive to nitric oxide synthase blockade as contractions were significantly increased from 10 μ M to 114% (± 3.1) up

to 121.4% (±4.2) at 1mM (Figure 43 b). When comparing the responses to L-NAME between the two treatment group (Figure 43 d), although there is increased potentiation at lower concentrations in tissues from 6-OHDA treated rats, this is not significantly different from bladder strips from naïve animals. Western blot analysis showed no differences between the detrusors from the control and 6-OHDA lesioned animals in the expression of ChAT (Figure 43 e) or PDE5 (Figure 43 d). Neuronal nitric oxide synthase (nNOS) expression was significantly reduced in detrusor strips from 6-OHDA rats (Figure 43 d). Soluble guanylyl cyclase (GC), the receptor of NO, had significantly reduced expression in bladder tissue from 6-OHDA treated animals compared to the expression in naïve tissue (Figure 43 d).

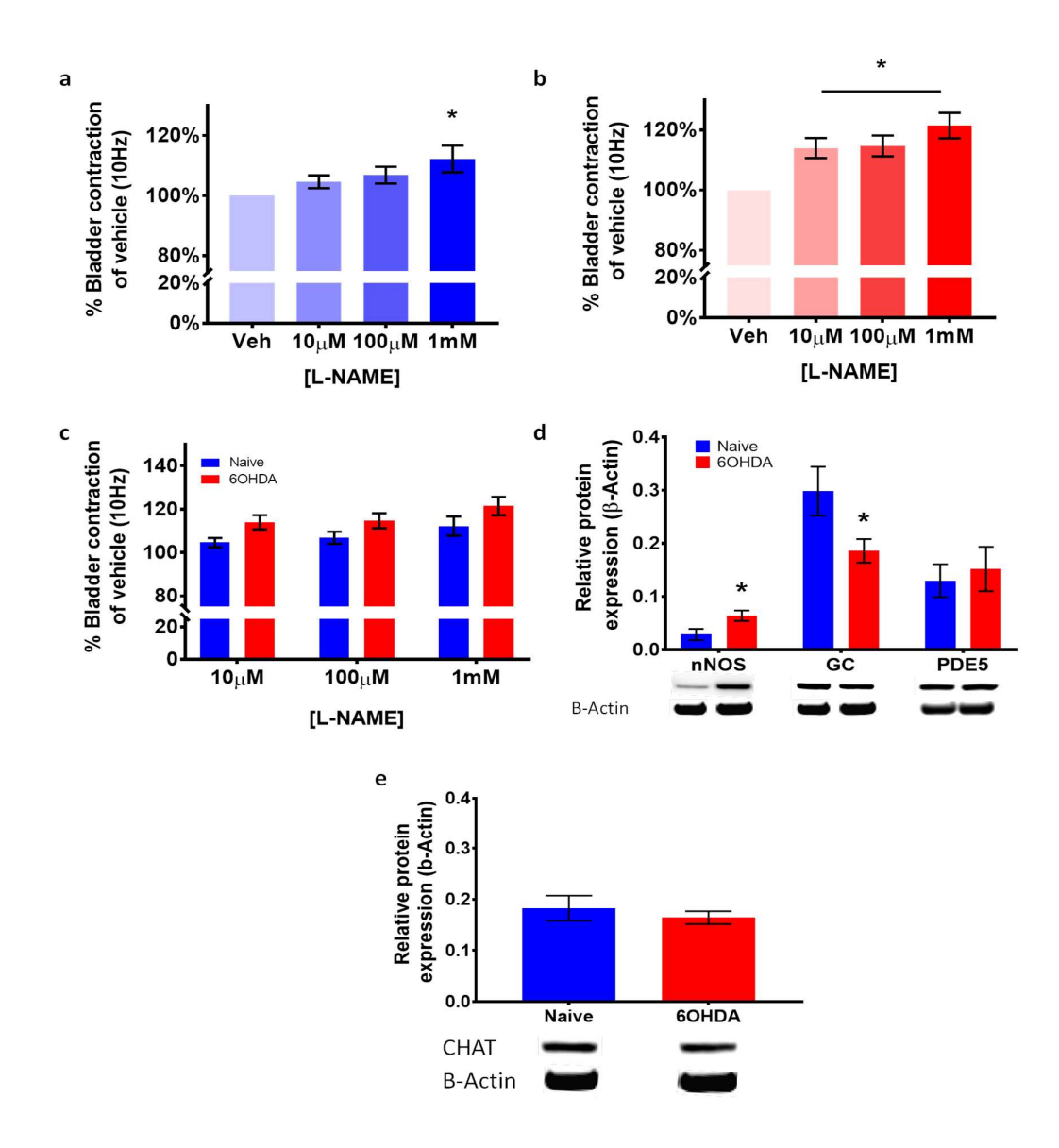


Figure 43 Contractile responses in bladder tissue from 6-OHDA treated animals are larger due to altered expression of proteins involved in the nitrergic system.

Summary bar charts of response to 10Hz EFS in the presence of increasing concentrations of L-NAME and mean protein expression in naïve and 6-OHDA bladder strips. Incubation of L-NAME resulted in a significant increase in 10Hz response in the naïve bladder at 1mM (a) and in 6-OHDA bladder tissue (b) at concentrations $\geq 10\mu M$ (n ≥ 5 , * p=<0.05, one-way ANOVA). Comparison of tissues from different treatment groups did not reveal a significant difference in the 10Hz contraction (n ≥ 5 , * p=<0.05, two-way ANOVA). Bladder strips from 6-OHDA animals showed significantly higher expression of nNOS but reduced expression of GC (d) compared to naïve tissue. There is no difference between the treatment groups in expression of PDE5 (d) or ChAT (e) (n ≥ 5 , * p=<0.05, unpaired t -test).

5.3.9 A reduction in the non-cholinergic, non-purinergic EFS evoked contraction is seen in bladder tissues from 6-OHDA rats.

In the detrusor strips from the naïve and 6-OHDA rats, 1µM atropine reduced the peak EFS-evoked contractile responses at all frequencies (Figure 44 a, purple) but the level of reduction was statistically significant only at stimulation frequencies ≥ 5Hz in naïve (•) animal tissue and 10Hz in 6-OHDA tissue (■). When comparing the tissue from the different treatments and their responses in the presence of atropine there was no significant difference. To evaluate the purinoceptor response in the bladder strips we administered 1mM ATP while these tissues were still incubated with atropine. A contraction was observed which diminished with each subsequent administration of ATP and on all three administrations there was no significant difference between tissue from naïve and 6-OHDA animals (Figure 44 c). The EFS response range was then run again under conditions of muscarinic block and ATP desensitisation (Figure 44 a, brown). This resulted in a significant reduction in EFS response (from Atropine alone) at all frequencies which was statistically significant at stimulation frequencies \geq 2Hz in naïve (•) and 6-OHDA tissue (\blacksquare). When comparing the different tissues responses in this setting (Atropine + ATP desensitisation) a difference can be observed in the non-cholinergic, non-purinergic EFS evoked contraction of 6-OHDA tissues which are much smaller than those from naïve tissues. This difference is observed at all frequencies but is only significantly reduced at 40Hz (Figure 44 b).

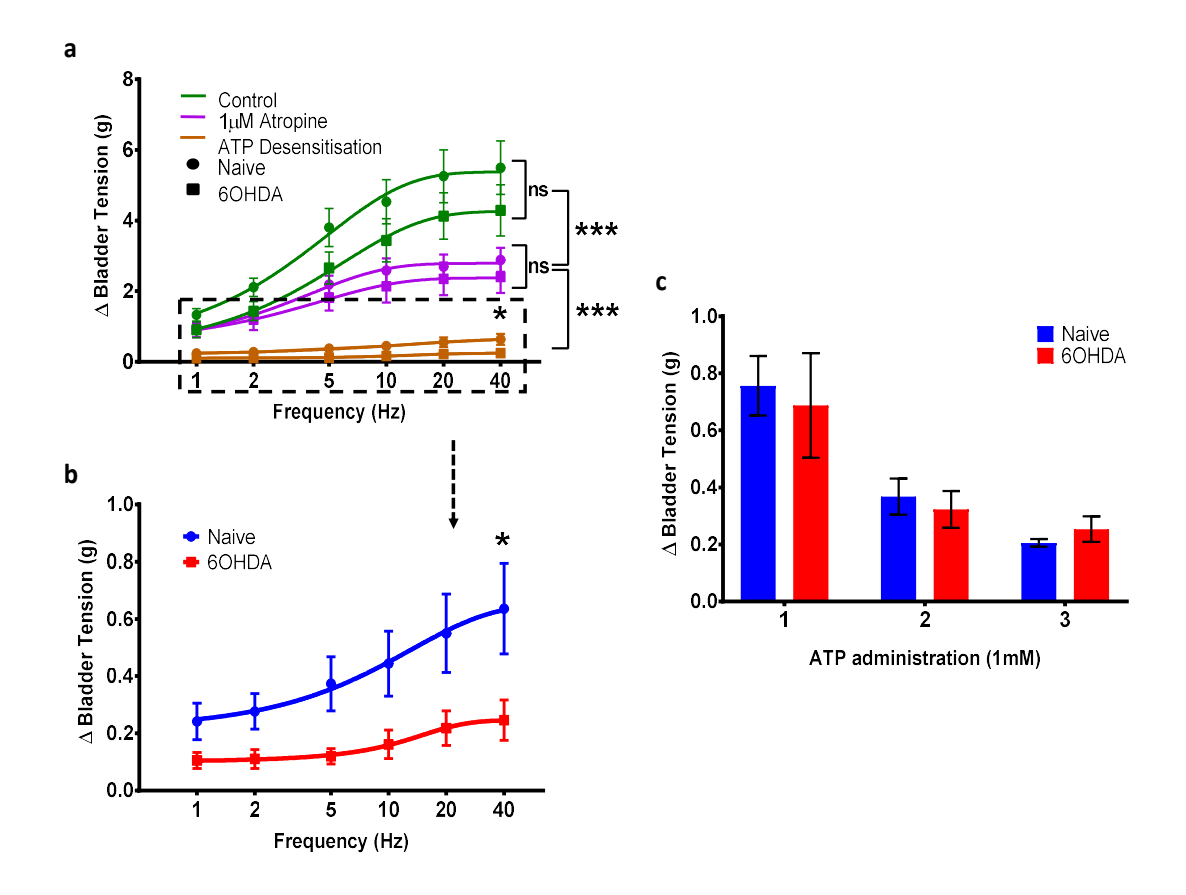


Figure 44 Responses of bladder tissues to EFS, in the presence of atropine and ATP desensitisation.

EFS frequencies ranging 1-40Hz (a) were significantly reduced in the presence of atropine (purple) similarly in the naïve (\bullet) and 6-OHDA (\blacksquare) bladder. Post desensitisation with repeated ATP administration (brown) a further reduction in response was seen. When comparing the EFS response after that a small but significant non-cholinergic, non-purinergic, neurogenic alteration in the 6-OHDA detrusor was revealed (b). The response to 1mM ATP administration was not significantly different between bladder strips from naïve and 6-OHDA treated rats $(n \ge 5, *p = <0.05, ***p = <0.001, two-way ANOVA)$.

5.4 Discussion

Administration of 6-OHDA into the striatum of rats in this study was used to mimic the "dying back" mechanism thought to be the pathway of dopaminergic neuron loss in PD. It also allowed us the opportunity to understand neuropathology and peripheral changes that may occur earlier in the disease as the lesion that occurs from this regime is partial. In this study we show for the first-time that 6-OHDA administration into the striatum leads to significant changes in the DMV and alterations in nitrergic transmission in the bladder and ileum. We also observed functional consequences of altered Kv7 channel expression in the bladder, in a unilateral partial lesion animal model of Parkinson's disease.

The unilateral injection of 6-OHDA caused significant neurodegeneration in the injected side as assessed when using the contralateral hemisphere as an internal control (Figure 31). Although two different doses ($12\mu g$ and $24\mu g$) of 6-OHDA were administered into the striatum there was no significant difference between the cell numbers counted in the injected side or the percentage loss when compared to the contralateral control hemisphere. The extent of dopaminergic loss was quite variable ranging from 20% - 80% loss on the ipsilateral side but this did not correlate with any real difference in response of colon, ileum, or bladder to EFS (Figure 34 a-c). It is worth remembering that this was a unilateral partial lesion model and so all neuropathology was restricted to one hemisphere. With intrastriatal injection of 6-OHDA, greater dopaminergic loss leading to behavioural deficits is seen with multiple injections over multiple sites within the striatum (Deumens et al., 2002). We have shown that simply increasing the dose at one site is not sufficient to induce increased neuropathology in the SNpc or the DMV, at least with the concentrations that we have used.

Dopaminergic projections from the SNpc modulate vagal efferent outputs of cholinergic neurons in the DMV to regulate gastric function. Whether the region is directly innervated by the SNpc or indirectly is still a source of controversy. In rodent studies two groups have focused efforts into looking at the connectivity of the SNpc and the DMV using tracer studies and neuronal

manipulations. The contrast in these findings are still puzzling as Anselmi et al., (2017) describes a direct pathway of dopaminergic neurons that project to the DMV from the SNpc and effect gastric motility via dopamine receptors present on ChAT positive neurons in the DMV. Another group show no direct projections from the SNpc to the DMV and instead postulate that various indirect connections are present, most prominently between the SNpc's projections to Orexin A neurons in the lateral hypothalamus (LH), which in turn project to the DMV and modulate gastric motility (Wang, Lian, et al., 2014; Yang et al., 2019). The DMV is a region that has been shown to display pathology in both the 6-OHDA and paraquat models of Parkinson's disease (Anselmi et al., 2017, 2018; Bove et al., 2019; Toti & Travagli, 2014; Yang et al., 2019; Zheng et al., 2014). To understand if the partial lesion model that we have generated here, also has pathology in the DMV, we performed staining to quantify the number of ChAT+ve neurons present and assessed TH+ve fibres by measurements of optical density. Again, here we found a significant decrease in both markers but not a significant difference between the dosing groups. The loss of ChAT positive neurons confirms and builds upon previous studies, showing for the first time that striatal neurotoxin administration can also lead to neurodegeneration in the DMV. This was previously shown only with SNpc administration of 6-OHDA (Anselmi et al., 2017; Toti & Travagli, 2014; Yang et al., 2019; Zheng et al., 2014) and provides confirmation of a nigrostriatal link to the DMV. The functional effects of this are likely to be mostly evident in assessment of gastric motility, which we did not perform. Such effects have been seen consistently with neuronal loss in the DMV, in rodents. Alongside the stomach, vagus nerve efferent's stemming from the DMV project to the entire GI tract including the myenteric ganglia of the small and large intestine. Different parts of the GI tract are innervated by different branches of the vagus nerve (Berthoud et al., 1991). The neurons in the DMV have heterogenous morphological and electrophysiological properties and distinct populations of these neurons project to distinct locations in the GI tract (Browning et al., 1999). Therefore, it is difficult to state the extent functional implications of the loss we have observed. That notwithstanding, truncal vagotomy has led to disruption in motility patterns in the small intestine of animals and could theoretically lead to local compensatory changes in the gastrointestinal tract (Weisbrodt et al., 1975). In vivo assessments of transit would further shed light on the functional effects of the DMV neurodegeneration on the GIT.

Our staining of the same region in the DMV with anti-TH antibodies revealed the presence of dopaminergic fibres. In 6-OHDA treated animals there was a significant reduction in the anti-TH staining indicating loss of these fibres. Injection of an anterograde dextran tracer by Anselmi et al., (2017) into the SNpc was the first piece of evidence of direct projections from the SNpc to the Dorsal vagal complex. These projections were in close proximity of cholinergic neurons of the DMV and catecholaminergic neurons of the A2 area. The projections that we observed in our studies where in various regions although we only measured the projections apposed to cholinergic neurons in the DMV. Although these projections have been mapped previously by others, to our knowledge this is the first time they have been characterised as TH positive and shown to be reduced in a model of PD. This loss of TH positive projections is likely due to the loss of dopaminergic cell bodies in the SNpc in our partial lesion model. This finding supports the idea that there is a direct connection between neurons of the SNpc to the DMV rather than an indirect connection via the LH, which is postulated to function through Orexin A neurotransmission rather than dopamine. The effects seen in the DMV although significant were small and restricted to the ipsilateral side. We did not assess the in vivo effect of the loss of projections in the DMV that we observed, but further investigation may uncover further insights into PD pathology and gastrointestinal dysfunction.

The neuropathology of the two different dosing regimens were not significantly different and nor were the responses of the peripheral tissues from each group to EFS (Figure 34 d-f). Due to the number of assays that were performed in freshly isolated tissue, not all tissues were available to all studies. As a result of the lack of neuropathological differences in the two dosing regimens tissue were assessed going forward as 6-OHDA regardless of dose, compared to sham and untreated naïve animals.

A handful of work by others have shown local changes in contractility of peripheral tissue as a result of neurotoxin administration to model Parkinson's disease. Overt changes can be monitored by performing frequency response curves to EFS and dose response curves to the muscarinic receptor agonist, carbachol in the organ bath. Cholinergic transmission is the major contractile pathway in gastrointestinal tissues and the urinary bladder. We did not see any difference in the

responses of any of the tissues to increasing concentrations of carbachol nor increasing frequencies of EFS in either treatment group. The responses were particularly variable in the ileum and colon, and no shifts in EC50 were observed to carbachol. In the bladder this is at odds with work by another group, that showed hypersensitivity to muscarinic stimulation and EFS in the bladders from 6-OHDA animals (Mitra et al., 2015). Our partial lesion model is different to theirs as they injected 6-OHDA into the medial forebrain bundle (MFB), which produces a fuller lesion. It is worth noting that in that study the authors omitted two animals in their study from further analysis as they only had partial striatal lesions of ~67% and 48% compared to the intact side. They only used data from animals that had lesions greater than 95%. They also mention that the 6-OHDA bladders on dissection appeared inflamed, which we did not notice in any of our tissue. Differences in the appearance of the bladder after neurotoxin administration, has also been observed in the MPTP treated marmoset, and although Pritchard et al., 2017 do not show any difference in the bladder tissue response to carbachol between the treatment groups they show hyperactivity in the bladder in response to EFS (Pritchard et al., 2017). As mentioned, none of the tissues in our study showed any significant differences to EFS stimulation from 1-40Hz.

In other studies with the MPTP marmosets no differences were noted in the carbachol response in the colon (Coletto et al., 2021) but contrary to our findings, the ileum of the MPTP treated marmosets showed hyperactivity in response to high frequency EFS (Coletto et al., 2019). The MPTP marmoset in those studies have bilateral dopaminergic loss of approximately 70%, therefore it may be that our partial lesion model is not sufficient to show the overt changes that the MFB 6-OHDA (Mitra et al., 2015) and MPTP marmoset studies do (Coletto et al., 2019, 2021). A unilateral lesion model is already limited by only inducing a maximum of 50% loss of the total dopaminergic cell bodies in the nigra when looking at the whole animal. Reduced EFS responses in colon tissue from 6-OHDA have been observed but again those studies used injection in to the MFB to produce a maximal lesion (Fornai et al., 2016; Pellegrini et al., 2016). Even when looking for a correlation between ipsilateral loss and EFS response none of the three tissues showed any real correlation with increased dopaminergic loss (Figure 34). Here also there were no significant differences between 12µg injected animals and 24µg in their response to a 10Hz EFS stimulation. Therefore, it is likely

that in, animal models at least, larger dopaminergic loss is needed to elicit overt differences in contractility of the colon, ileum and bladder measurable via cholinergic and electric field stimuli.

Our interest in the Kv7 channel in models of PD led us to investigate the effects of Retigabine incubation on the 10Hz EFS response in gastrointestinal tissue segments. Retigabine caused a dose dependent decrease in contraction in response to EFS in the colon and ileum tissues of naïve and sham treated animals (Figure 36). To our knowledge this is the first time that Kv7 channel activation has been shown to reduce EFS responses in the rat colon and ileum, although our previous work (chapter 3) and the work of others have shown similar results via different methods in the mouse colon (Jepps et al., 2009). The reduction in EFS response in the presence of Retigabine was seen equally in the tissues dissected from 6-OHDA injected animals indicating that Kv7 channels are not affected in the GIT in this model. We used immunohistochemistry and an automated analysis method for quantifying the $K_V7.4$ expression in cross sections of ileum and colon. We looked at expression in the different layers of these tissues but found no significant differences between treated, sham, and naïve tissue (Figure 37 and Figure 38) in cell number, size or staining. We can therefore conclude that striatal 6-OHDA injection resulting in partial dopaminergic loss does not lead to effects on Kv7 function or Kv7.4 expression in the colon or ileum.

As previously mentioned, most studies focus on central changes with 6-OHDA that cause LUTS and supraspinal manipulations, rather than assessing whether changes occur locally in the urinary bladder. Most of the research into the Kv7 channel and the bladder detrusor muscle have been performed in the guinea pig, however some work has been performed in rats. Interestingly, on a whole tissue level it appears that the expression levels of different subtypes of the Kv7 channel in the rat more closely resemble the human than the guinea pig (Malysz & Petkov, 2020). In an in life setting, Kv7 channel manipulation using Retigabine administered i.v. or i.c.v to rats increases micturition intervals (Streng et al., 2004). Retigabine was also administered to anaesthetised rats and shown to decrease rhythmic bladder contractions through a reduction of afferent nerve firing but also possibly through direct action at the level of the detrusor muscle (Aizawa et al., 2017). Very few studies have been performed in isolated rat detrusor with pharmacological manipulation

of the Kv7 channel. Two studies were performed using small segments of tissue in a myograph, and confirmed the channel's functional potential, as Kv7 activators Retigabine and ML-213 both inhibited contractility of the detrusor muscle (Rode et al., 2010; Wang, Tar, et al., 2014).

Our work was performed using larger strips of rat bladder in an organ bath (approximately one quarter of the bladder). In our studies with bladder strips from control animals we saw a decrease in EFS stimulated contractile responses in the presence of 10µM Retigabine. In tissue from naïve rats this reduction was small, only by $\sim 10\%$ from the vehicle response. When looking at bladder strips from 6-OHDA rats there was a significantly greater effect of 10µM Retigabine leading to a ~65% reduction in contractile response to 10Hz EFS compared to vehicle response (Figure 39). In this case we did not have bladder from Sham treated animals to compare to naïve and 6-OHDA animal tissue. The lack of sham bladder tissue is a limitation of our work as LUTS have been shown to occur even in sham injected animals, although in that case the LUTS were likely centrally driven, due to injury, as they were transient (Soler et al., 2011). Expression data using frozen bladder segments from the same sets of animals showed a \sim 50% increase in K_V7.4 expression by western blot. With such a dramatic increase in expression and difference in response at 10µM Retigabine, we would expect to see some sort of dose response in the 6-OHDA animal bladder strips. Although this experiment does not contain enough concentrations to understand a dose response relationship, it is unclear why there is not at least some response at 3µM Retigabine in the 6-OHDA bladder strips.

In Parkinson's disease nocturia, urinary urgency, incontinence and increased urinary frequency can be grouped as a symptom of overactive bladder (Araki & Kuno, 2000). In vivo cystometric measurements in the 6-OHDA rodent, with full unilateral lesions, also show that these animals to have overactive bladder (Yoshimura et al., 2003). The increased expression of Kv7.4 channels would likely lead to a local reduction in detrusor activity. This could potentially be an early compensatory mechanism initiated to counteract overactive bladder as has been seen with other Kv7 channels in patients with Bladder outflow obstruction (BOO) (Svalø et al., 2015). Alternatively, the increase in Kv7 channel expression in a PD bladder may lead to increased relaxatory effects or lower basal tone. This may also lend itself to a cause of voiding symptoms

such as retardation of initiation, intermittency or prolongation, observed in patients with PD (Sakakibara, Hattori, et al., 2001). It remains to be seen whether patients with PD also have changes in expression in Kv7 channels in the bladder and how that progresses with disease and LUTs.

Like other smooth muscle, a part of the relaxatory mechanism of the bladder detrusor muscle occurs via an increase cGMP through the generation of nitric oxide (Chung et al., 1996). LNAME is a nitric oxide synthase inhibitor often used to investigate the NO-cGMP relaxation pathway in tissues such as the bladder (Santoso et al., 2011). The detrusor strips from 6-OHDA animals in the presence of LNAME exhibited a significant enhancement of the contraction to 10Hz EFS at concentrations as low 10µM LNAME. In the tissue from naïve animals, we were only able to see a significant enhancement at 1mM, 100-fold higher concentration (Figure 43). When these results were analysed together in an ANOVA there was no significant difference between the naïve and the 6-OHDA tissues, but the trends can be seen. The differences are relatively small particularly at the lower concentrations and the experiment is likely not powered to detect such a change, nor is it set up to determine a dose response relationship. The basis of this impairment seems to be due to differences in expression of the major proteins in this pathway. Western blot experiments were performed to assess the expression of nNOS, partly responsible for NO generation in the urinary bladder (Fathian-Sabet et al., 2001) and its receptor soluble guanylyl cyclase, the enzyme that catalyses the production of cGMP from guanosine triphosphate. The expression of nNOS is increased in the bladder tissues from 6-OHDA animals which strengthens our finding in our functional assay of increased effects of the NOS inhibitor LNAME. Interestingly the levels of GC are significantly reduced in 6-OHDA bladder tissues. ChAT and PDE5 are expressed similarly in naïve and 6-OHDA tissues. Although we do not see overt hyperactivity in our EFS response curves (Figure 35), the expression patterns of proteins we see in nNOS and GC and the sensitivity to LNAME indicate impairment of the nitrergic system. Other studies in animal models with greater dopaminergic loss have shown hyperactivity in the bladder tissue in similar settings (Mitra et al., 2015; Pritchard et al., 2017) and what we have found may be a precursor to this. Hypothetically 6-OHDA's reduction in guanylyl cyclase may lead to hyperexcitability which at this stage is compensated by the increased production of NO due to the increase in nNOS observed. With our

study only a partial lesion model and leading to such local changes in the bladder, it is possible that with increased dopaminergic loss the apparent compensatory increase in nNOS may dimmish or fail to counteract the reduced GC, leading to the presentation hyperactivity. To understand whether this is the case in PD, future studies would need to look into patients at different severity stages of the disease, to understand if there are temporal changes in these proteins.

Sildenafil is famously a vasodilator through phosphodiesterase type-5 (PDE5) inhibition used as a treatment in male erectile dysfunction. PDE5 is expressed throughout the gastrointestinal tract from the stomach to the colon in the rat (Sopory et al., 2004). Inhibition of PDE5 has been shown to increase intestinal fluid accumulation, reduce the amplitude of spontaneous contractions of the duodenum and increase colonic cGMP levels in rodents, as well as restore normal transit time and water content in preclinical models of constipation (Clemente et al., 2008; Sharman et al., 2017; Sopory et al., 2004). Conversely, administration of Sildenafil intraduodenally in a small human trial has been shown to inhibit motility in subjects (Lee et al., 2003). In our experiments, with segments of gastrointestinal tissue, incubation with Sildenafil caused an expected decrease in magnitude of contraction to 10Hz EFS. Although the dose range was limited there were trends of this occurring in a dose dependent manner and significant effect at 10μM in the naïve colon. Contractility was also significantly reduced at 3µM and 10µM in the naïve ileum (Figure 40). In colon segments from sham and 6-OHDA treated animals the response to sildenafil is the was not different. However, the ileum tissue from 6-OHDA tissue did not show any reduction due to Sildenafil at any concentration and the response was significantly different to that of the ileum segments from sham and naïve animals.

Unfortunately, the frozen ileum samples from the same animals could not be reliably analysed for protein expression due to degradation of the proteins, potentially during initial processing. The majority of the antibodies tested yielded no positive signal on the ileum whilst producing consistent signal in the colon. Furthermore, the β -actin housekeeping blot revealed multiple bands not seen on other tissues using the same antibody. Other ileum samples from our experience do not show this degradation with β -actin (Figure 42). A possible reason for this degradation is that during transport of the samples, and freezing, the chyme of the ileum, which contains proteases was still present

within the organ. Although protease inhibitors were included in the sample during homogenisation, potentially the proteases had sufficient time to continue to degrade the proteins in the sample. We do have expression data from the colon tissues processed in the same way, which would not contain chyme causing degradation. We did not see any functional differences in the effect of sildenafil on the colon between the treatment groups and nor did we see any differences in PDE5 expression via western blot (Figure 41). ChAT expression was also not different between the treatment groups. With cholinergic neurotransmission seemingly intact in the 6-OHDA colon it is no surprise that we found no differences in contractility in our experiments to EFS or the cholinergic agonist, carbachol, in any tissue. It is therefore likely that the upregulation in muscarinic receptors seen in other studies (Fornai et al., 2016) does not occur in our partial lesion model. There were trends towards reduced expression of nNOS and guanylyl cyclase, but better powering of future experiments will give a more definitive answer (Figure 41). In the papers mentioned in this discussion, studies are being performed with a sample size greater than 9 per group, whereas our study on occasions only contained 2 or 3 usable tissues for some groups.

Without expression data we can only speculate on the reasoning behind the lack of Sildenafil response in 6-OHDA ileum segments. The simplest conclusion would be that this is due to reduced expression of PDE5 in the 6-OHDA ileum. There is no evidence of this in literature but data from the MPTP marmoset also shows impairment of relaxation mechanisms in organ bath data. One group observed a lack of potentiation of contractile response to EFS in the presence of LNAME (Coletto et al., 2019). The authors showed no significant changes in expression of NOS-ir neurons in the myenteric plexus of the ileum but did not investigate PDE5 expression. Although Sildenafil's is a specific inhibitor of PDE5, it is merely one regulator of the complex NO-cGMP pathway which is regulated by multiple proteins. Arterial vasodilation and cardiac β-adrenergic reserve have been shown to be regulated by PDE5's targeting of cGMP from soluble GC stimulation (Nagayama et al., 2008). Reduced expression of soluble GC has been seen in other rodent studies and leads to reduced cGMP in the aorta of the aged Spontaneously hypertensive rats, these tissues have a decreased relaxation response to PDE5 inhibition (Ruetten et al., 1999). Although the colon and ileum are different structures, which display different protein expression patterns (Noorian et al.,

2011), if as we see in our expression data from the colon there is reduced expression in guanylyl cyclase in the ileum also, that could also explain the lack of effect of Sildenafil. That is a large extrapolation but nevertheless we have at least shown an impairment of Sildenafil induced relaxation mechanisms of the ileum in 6-OHDA treated rats for the first time. This may be important in treatment strategies for patients with constipation as Sildenafil has been shown to increase faecal water content and decrease transit time in pre-clinical models of constipation (Sharman et al., 2017). However, if the effects seen in our model translate then this may not be a suitable therapy.

The contractile response of the bladder is a result of cholinergic and non-cholinergic transmission. Most of the non-cholinergic component of neural excitation is purinergic and has been shown to be enhanced in animal models of PD (Mitra et al., 2015; Pritchard et al., 2017). To investigate the differences in the bladder tissue from 6-OHDA and naïve rats in the purinoceptor response we used the purinergic agonist ATP in an EFS frequency response paradigm (Figure 44). By incubating the tissues in 1 µM Atropine we were able to remove the cholinergic responses to get a better resolution of purinergic responses to EFS. The EFS responses in the presence of atropine were not significantly different between tissues from 6-OHDA and naïve animals. At lower frequencies the response to EFS in the presence of atropine was similar to the response in its absence, however at higher frequencies (>5Hz) the atropine incubated responses were significantly reduced. This indicates that non-cholinergic transmission is responsible for the EFS response at lower frequency stimulation but cholinergic, atropine sensitive, co-transmission occurs in higher EFS frequency stimulated contractions, as seen by others (Brading & Williams, 1990). Administration of ATP (1mM) caused a contraction in bladder tissues, but again there was no difference in the magnitude of contraction between the treatment groups each time we administered ATP. Desensitisation of the purinergic by repeated administration of ATP, a technique used by others (Brading & Williams, 1990; Luheshi & Zar, 1990; Pritchard et al., 2017), again showed that there was no difference between tissues from 6-OHDA and naïve animals, in multiple ATP induced contractions. However, an EFS train of increasing frequency stimulation from 1-40Hz in the presence of atropine and purinergic desensitisation revealed a small but significant impairment of the non-cholinergic, nonpurinergic contraction in tissues from 6-OHDA animals. This response has been postulated to be mediated via neuropeptide Y (NPY) (Iravani & Zar, 1994). Our investigations of this via western blot were not successful as we could not detect bands with commercially available antibodies in any tissue including positive control tissues for NPY. However, Iravani & Zar, (1994), have shown that rodent bladder detrusor muscle has an abundance of NPY-ir nerve fibres. They also showed that administration of NPY potentiated EFS contractions even in the presence of atropine.

Adrenoceptors are also expressed in the detrusor muscle and α₁-adrenoceptor agonist phenylephrine produces a weak contraction of the detrusor (Michel & Vrydag, 2006). The impairment that we have seen in non-cholinergic, non-purinergic responses to EFS may be due to adrenergic transmission, in particular α₁-adrenoceptors, as it appears to play a minor functional role in detrusor contractility. Further work would be needed to confirm the mechanisms of the deficiencies of the non-cholinergic, non-purinergic responses to EFS observed in the bladders of this partial lesion model of PD.

In this study we used a striatal injection of 6-OHDA to investigate gastrointestinal and urinary dysfunction in a partial lesion model of Parkinson's disease. Although we saw no significant dose dependency in our model, we were able to observe neuropathology in the form of significant dopaminergic neuron loss in the SNpc and subsequent loss of cholinergic neurons and TH+ve fibres in the DMV. This treatment did not lead to overt deficits in gastrointestinal or urinary function when isolated segments were assayed in the organ bath, however we were able to find local changes in these tissues when assessing protein expression and using pharmacological manipulation. This work brings together the first evidence of functional and expression changes in the urinary bladder of the Kv7 channel and of proteins involved in nitrergic relaxation mechanisms, in a partial lesion model of PD. Impairment of relaxation mechanism was also observed in our experiments with ileum tissue from 6-OHDA tissue when using Sildenafil. In a partial lesion, unilateral, model one would not expect the results to be so pronounced that they would affect overall motility, however impaired relaxation and hyperactivity in peripheral tissues has been a theme throughout our works and in animal models of PD. The mechanisms that we have uncovered here require further

validation, to assess their role in the human condition, and understand whether they can be targeted to alleviate some of the autonomic symptoms of PD.

6 CHANGES IN KCNQ4 ENCODED K_v7.4 CHANNEL IN THE MPTP TREATED PRIMATE MODEL OF PARKINSON'S DISEASE

6.1 Introduction

The MPTP primate model, covered previously (1.10.1.3.2), is considered the gold standard for a model of PD, due to its reliable pathology, biochemistry and predictive validity, at least in terms of dopaminergic therapies (Duty & Jenner, 2011). Most studies in animal models focus on the motor symptoms and dopaminergic pathology however an animal as a whole organism has so much more to offer. Once it is clear that the model displays aspects that are recognised as a hallmark of a disease, other symptoms and pathologies that are associated with the disease should also be investigated. Due to the expense and ethical issues around non-human primate work, the use of the model is rarer than PD models in other species.

Assessments of the gastrointestinal tract in the MPTP treated marmoset started with early work looking at alterations in the neuronal population of the ENS. A higher number of neurons were observed per ganglion in the myenteric plexus of the ascending colon of MPTP treated marmosets as a result of an increase in nNOS-immunoreactive (-ir) neurons, despite decreased TH-ir neurons. In the submucosal plexus there was a reduction of TH-ir neurons but no loss in total number of neurons (Chaumette et al., 2009). Although no functional studies were performed with these animals or with the tissues, there have been observations of increased NOS-ir neurons in the myenteric plexus of PD patients with slow transit constipation (Wattchow et al., 2008). Coletto et

al. (2021) assessed colon tissue from MPTP treated marmosets in ex vivo assays as well as via immunohistochemical analysis of the myenteric plexus. They showed alterations in ion transport ability across the mucosal epithelia of the colon from MPTP treated marmosets. Interestingly, in an organ bath preparation, the colonic segments showed increased frequency and reduced amplitude of the contractions of the longitudinal muscle segments of the colon. Neurochemical alterations were also seen in the myenteric plexus with an increase in VIP-ir and a decrease in ChAT-ir neurons in the proximal colon but no difference in nNOS-ir neurons. Most VIP-ir neurons co-localise with nNOS-ir and therefore this finding also points to alterations in the inhibitory system as with Chaumette et al. (2009).

The small intestine has been shown to also have reduced transit time in PD patients (Dutkiewicz et al., 2015a); (Knudsen, Haase, et al., 2017). To our knowledge only one study has investigated dysfunction in the small intestine of the MPTP marmoset model. Similar to the colon, investigation by the same group revealed that the ileum from MPTP treated marmosets showed increased frequency of spontaneous contractility, which correlated positively with the in-life assessments of increased motor disability. Responses to EFS in segments of the ileum showed potentiation of contractile responses in tissue from MPTP treated marmosets and a significantly impaired relaxation phase. Despite no significant differences of nNOS-ir in the myenteric plexus, a lack of significant potentiation of EFS responses was observed in the presence of the nitric oxide synthase inhibitor L-NAME in the ileum segments from MPTP treated marmosets (Coletto et al., 2019). The lack of potentiation by L-NAME, the lack of a relaxation phase, the increased EFS response and enhanced basal contractility points to dysregulation in the relaxation pathway and nitrergic transmission in the ileum in this study.

Urinary dysfunction in PD is associated with detrusor hyperreflexia and can manifest as nocturia, urgency and urge incontinence. Other works in MPTP treated NHPs have shown hyperreflexia in an in vivo setting present in the form of reduced contraction volume thresholds (Albanese et al., 1988; Yoshimura et al., 1993). Potentiated responses to EFS and increased spontaneous activity is a theme of tissue from MPTP treated marmosets and has been seen in bladder segments also (Pritchard et

al., 2017). This was shown to be due to increased non-cholinergic/purinergic transmission, likely from presynaptic alterations.

In the gastrointestinal tract, a range of physiological processes such as the release of neurotransmitters, contractility of smooth muscle and epithelial function are controlled by K+ channels (Sanders, 2008). Opening of K+ channels result in hyperpolarisation of the resting membrane potential leading to reduction in cellular excitability. Importantly, it has been shown that the KCNQ-4 gene encoded Kv7.4 channels play a complex role in cGMP mediated relaxation in various tissues (Stott & Greenwood, 2015).

Voltage-gated potassium channels encoded by KCNQ genes, the K_v7 family, consists of five members $K_v7.1$ -5. First characterised in the 1980's in CNS neurons, they were termed the "M-Channel" as they were responsible for outwardly rectifying K^+ currents that could be suppressed by muscarinic receptor activation (Brown & Adams, 1980). The "M-current" activates slowly at subthreshold potentials contributing to the resting potential and supressing repetitive firing rather than impacting upon the repolarization of action potentials in the neuronal cell.

In the periphery along with K_v7.5, K_v7.4 is the most abundantly expressed in the muscular layers of human taenia coli (Adduci et al., 2013) and the mouse gastrointestinal tract (Jepps et al., 2009) including all parts of the mouse small intestine. In studies with human taenia coli strips a Kv7 channel blocker, XE-991, produced irreversible concentration dependent contractions. Retigabine, a Kv7 channel activator, produced concentration dependent relaxations of precontracted human taenia coli strips. This effect was only very slowly reversible and the strips after washout were observed to have a reduced baseline tone for up to two hours. This suggests that the Kv7 channel plays an important role in setting the intrinsic basal tone of the human taenia coli (Adduci et al., 2013).

Similarly, in mouse colon segments Retigabine caused a reduction in contractility and conversely inhibition of the channels caused an increase in the amplitude and frequency (Jepps et al., 2009). Studies in the rat aorta with the NO donor, sodium nitroprusside (SNP), showed that incubation with the K_v7 channel blocker, Linopirdine, can prevent SNP induced arterial relaxation (Stott et al.,

2015). Further evidence to suggest that Kv7 channels also contribute to vasorelaxations mediated by the NO-cGMP pathway come from work in rat penile artery, where SNP and sildenafil mediated relaxations were inhibited by Linopirdine (Jepps et al., 2016).

Kv7 channels, Kv7.4 and KV7.5 in particular, have also been implicated in similar regulation of bladder smooth muscle excitability in various species including guinea pig (Provence et al., 2018), rat (Rode et al., 2010) and crucially human detrusor muscle (Svalø et al., 2015).

Of particular interest for PD, the subtype K_v7.4, has been shown to be expressed in very few regions of the mouse brain, including nuclei of the central auditory pathway, cells of the ventral tegmental area (VTA) and the SNpc (Kharkovets et al., 2000). Pharmacological activation of K_v7 channels in the 6-OHDA model of PD have been shown to reduce the severity of L-DOPA induced dyskinesia, without effecting the antiparkinsonian effects of L-DOPA (Sander et al., 2012, 2013). Blockade of these channels has been shown to increase striatal dopamine synthesis and protect dopaminergic neurons of the substantia nigra pars compacta (SNpc) (Liu et al., 2018).

Up to now no study has investigated the expression of KCNQ4-encoded Kv7.4 channels in a primate model of PD. K_v7.4 channels are expressed in the primary site of neurodegeneration in PD, the substantia nigra (Kharkovets et al., 2000), and the GI tract. GI dysfunction in PD is potentially a result from the aberrant contractile response of the GI smooth muscle (Knudsen, Fedorova, et al., 2017) but so far with no obvious nitrergic or cholinergic cause. Our aim was to investigate whether K_v7.4 channels are altered in the central nervous system and peripheral tissues, in a relevant model of PD and whether this may point to a mechanism of gastrointestinal and urinary dysfunction in PD.

In this preliminary study we investigated the expression Kv7.4 in the brain, the gastrointestinal smooth muscle and urinary bladder using immunohistochemistry and quantitative PCR in drug naïve and MPTP-treated common marmosets.

To our knowledge this the first study to show expression of Kv7.4 channels in the CNS and the periphery of the common marmoset. We have also shown differences in expression of the Kv7.4

channel in various regions, between marmosets treated with MPTP, which may contribute to central and peripheral dysfunction.

6.2 Methods

6.2.1 Animals

Two treatment groups of normal, control (drug and toxin naïve) (n = 10; 5 male and 5 female, 366-444g) and MPTP (Sigma, Poole, UK)-treated (n = 14, 7 males and 7 female 348-480g) adult common marmosets (*Callithrix jacchus*, Harlan, UK) were used in this study. The MPTP-treated (2 mg/kg subcutaneously administered for 5 consecutive days) animals were prepared according to previously published protocols (Jackson et al., 2007; Smith et al., 1996) and were used in other studies, where the symptomatic effects of various dopamine agonists were examined. Further details of the methods are mentioned in 2.1.3.

The marmosets were euthanised using an overdose of pentobarbital sodium (60 mg/kg; Euthatal, Merial Animal Health Ltd.). Upon cessation of foot and corneal reflexes, the thoracic and abdominal cavities were opened. The animals were transcardially perfused with ice-cold oxygenated (95% O₂ plus 5% CO₂) Krebs-Henseleit solution (composition mM: NaCl 118, KCI 4.7, CaCl₂ 2.5, MgSO₄ 1.2, NaHCO₃ 25, KH₂PO₄ 1.2, glucose 11). Perfusion was performed to remove as much blood from the tissues to reduce autofluorescence and non-specific binding of antibodies when performing immunohistochemistry.

Samples were collected and processed differently dependent on their downstream use. For some animals only frozen tissues were collected and analysed in this study, for other animals only fixed paraffin embedded blocks were available.

6.2.2 Immunohistochemistry

6.2.2.1 Gut and Bladder Tissue

To determine the expression of the K_v7.4 protein, tissues were fixed in 4% paraformaldehyde and embedded in paraffin. Sections were incubated with Anti-KCNQ4 (ab6579, Abcam, Cambridge, UK; 1:200) for three days at 4°C. Immunoreactivity (ir) was observed by Avidin-biotin peroxidase complex immunohistochemistry, using 3,3-diaminobenzidine as the chromogen (Vector Laboratories Ltd, Peterborough, UK).

Double labelling was also performed in the gut tissue with polyclonal Anti-KCNQ4 (ab6579, Abcam, Cambridge, UK; 1:200) and anti-Smooth muscle γ & α-actin antibody (MAB1522, Sigma, Poole, UK; 1:10,000) for three days at 4°C. This was performed to assess whether KCNQ4 channels are present on smooth muscle cells of the GIT. Immunofluorescence was detected using VectaFluor Duet Immunofluorescence Double Labelling Kit (DK88-28; Vector Laboratories Ltd, Peterborough, UK) as per manufacturer's instructions. Further details of the methods are mentioned in 2.4.1.2.

6.2.2.2 Brain tissue

Substantia nigra containing sections were incubated in primary antibodies against tyrosine hydroxylase (TH) (T1299, Sigma, Poole, UK; 1:1000) and Anti-KCNQ4 (ab6579, Abcam, Cambridge, UK; 1:200) for three days at 4°C. TH is an enzyme in the pathway for biosynthesis of dopamine and therefore is a cellular marker for dopaminergic neurons. Further details of the methods are mentioned in 2.4.2.

6.2.3 qPCR

Further details of the qPCR methods are mentioned in 2.5.

The KCNQ4 primer was a custom sequence designed based on the sequences available in the ensemble database

(https://www.ensembl.org/Callithrix_jacchus/Gene/Summary?db=core;g=ENSCJAG00000002997; r=NTIC01036611.1:80676654-80735124). It was designed for a region that is conserved between

the splice variants of the KCNQ4 gene but dissimilar to sequences on the other KCNQ subtypes (Fwd: GGTAGCCCCTGCCG, Rev: GGAGGAGCGCTGGCC).

The housekeeping gene, HPRT1, sequence was derived from Shimamoto, et al., 2013 (Fwd: TTGGAAAGGGTGTTCATTCCTC, Rev: CCTCCCATCTCCTTCATCACA). Both primers were Custom TaqManTM Gene Expression Assays produced by Thermofisher, UK.

6.2.4 Image analysis

Details of the Image analysis methods are mentioned in 2.4.3.

6.2.5 Data analysis

All statistical analysis was performed using Prism 6.0 software (GraphPad, San Diego, CA USA). Analysis of the immunohistochemical and qPCR data was compared using the Student's unpaired t-test. Analysis of the bright-field microscopy images of gut and bladder sections for optical density (OD) and cell counts, utilized two-way ANOVA statistical analysis followed by Sidak *post hoc* test.

6.3 Results

6.3.1 A reduction in KCNQ4-ir, TH positive neurons is observed in the SNpc of MPTP treated marmosets.

A proportion of dopaminergic neurons of the substantia nigra pars compacta express KCNQ4 encoded Kv7.4 channels (Figure 45). As expected, there is a marked reduction in TH+ve neurons in the MPTP treated animals and resultantly a reduction in KCNQ4-ir neurons.

We analysed the number of TH+ve KCNQ-ir cells in the SNpc, to investigate the extent of degeneration following MPTP treatment. There was on average, a 71.6% reduction of TH+ve

dopaminergic neurons observed in the SNpc of MPTP treated marmosets (Figure 46 a). The number of KCNQ4-ir cells also decreased significantly in the treatment group (Figure 46 b), however this was not proportional to the general degeneration (Figure 46 c). The proportion of KCNQ4-ir, TH+ve cells in the SNpc of MPTP treated marmosets $(8.30\% \pm 2.86)$ was significantly lower than the proportion in the naïve SNpc $(16.74\% \pm 1.55)$.

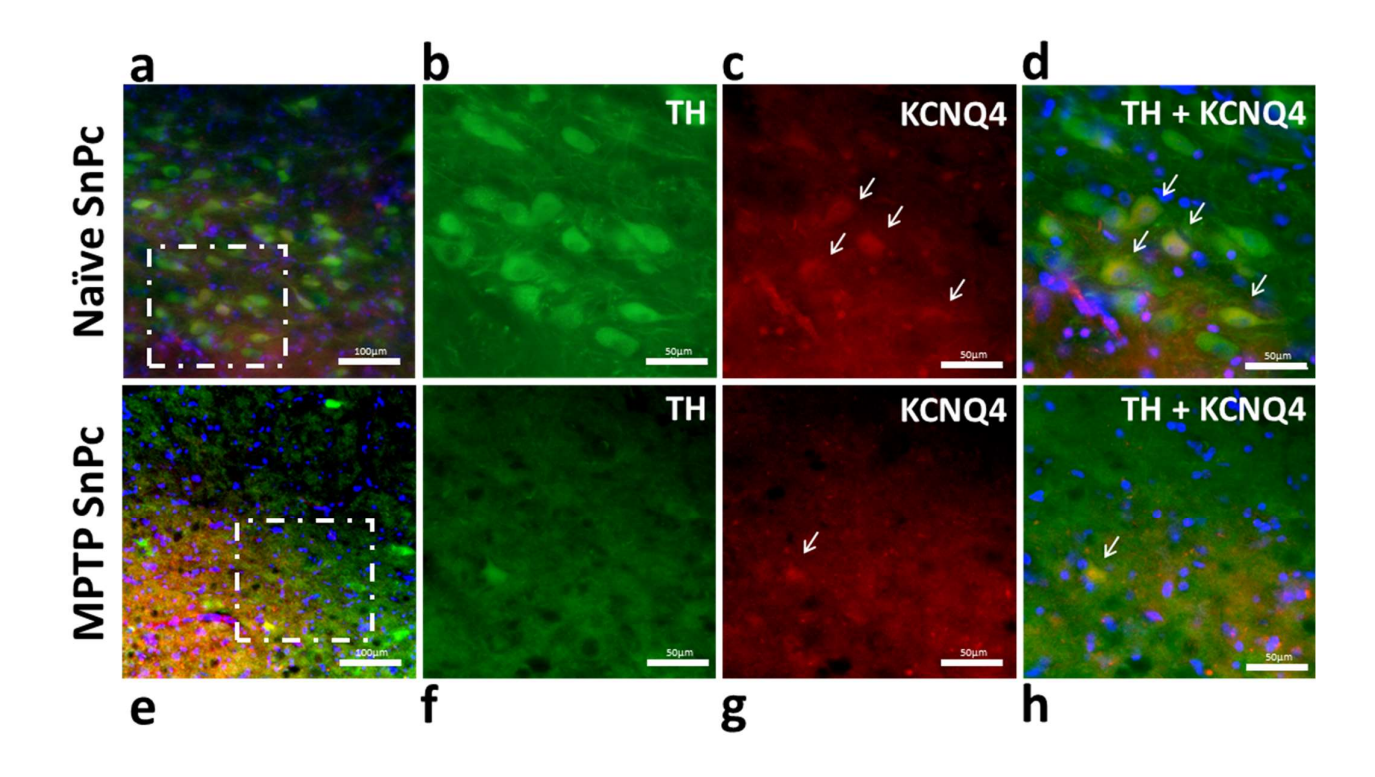


Figure 45 Immunofluorescent staining for KCNQ4 in TH+ve neurons of the SNpc

Immunofluorescent staining for KCNQ4 and TH in the SNpc of Naïve (a-d) and MPTP (e-h) treated marmosets. Higher magnification images shown in b-d and f-g. An anti-TH antibody (green) was used to detect dopaminergic neurons in SNpc (b & f), anti-KCNQ4 (red, c & g) and merged images showing co-localisation (d & h). White arrows indicate TH+ve cells with KCNQ4 expression.

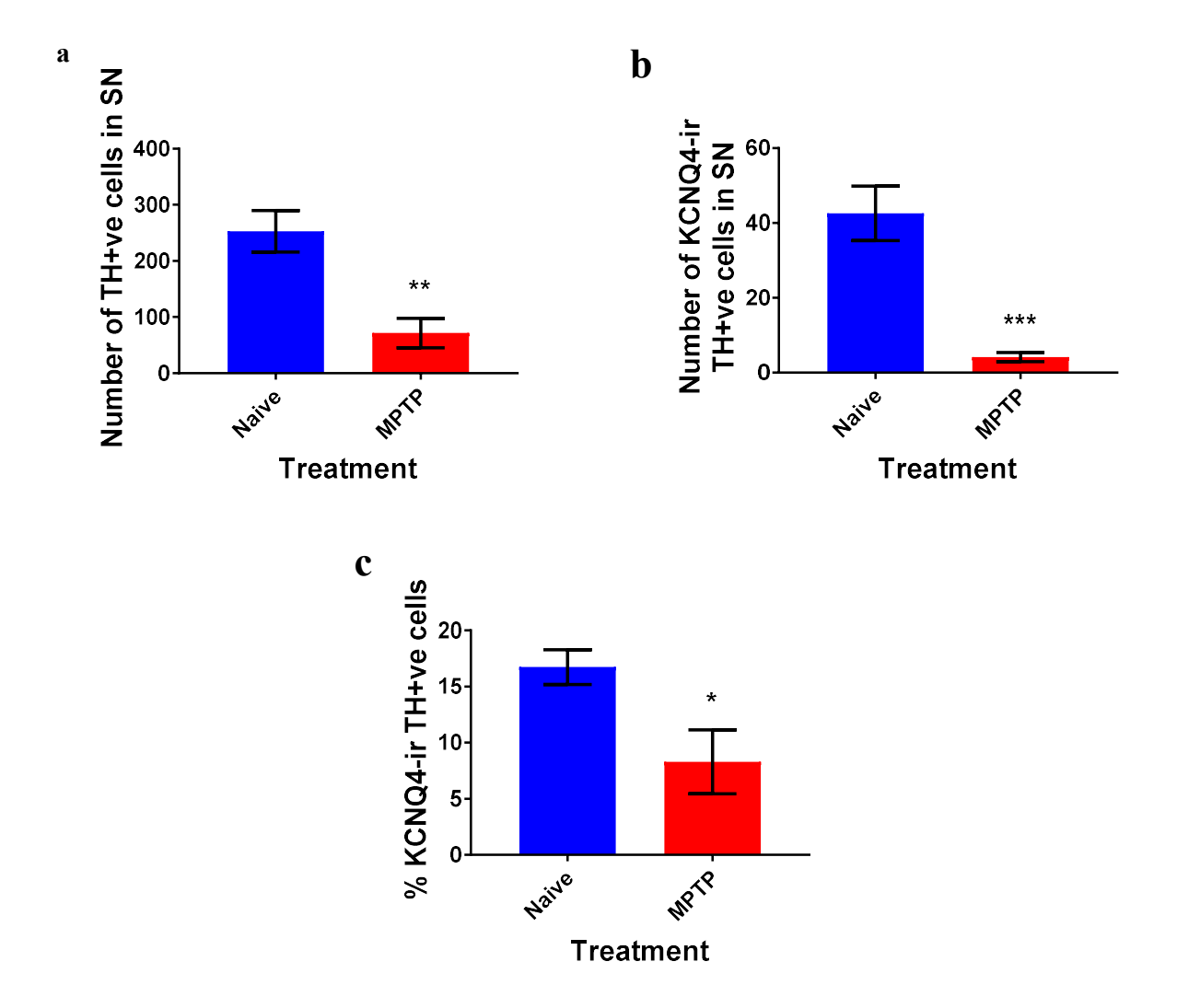


Figure 46 Quantitative analysis of KCNQ4 and TH in the SNpc of normal and MPTP common marmosets

Summary bar charts showing the reduction of TH+ve neurons in SNpc of MPTP treated marmosets (n=5) (a), a reduction in the number of co-localised KCNQ4-ir TH+ve cells in the SNpc (b) and the percentage of TH+ve, KCNQ4-ir cells in the SNpc of MPTP treated marmosets compared with naïve animals (c). Data are expressed as mean, SEM; *p < 0.05, **p < 0.01, ***p < 0.001; vs control tissue (n=5) per treatment) by Student's unpaired t-test.

6.3.2 The expression of KCNQ4 positive structures is reduced within the layers of the gastrointestinal wall of the MPTP primate model.

There were numerous KCNQ4-ir punctate structures in the longitudinal layers and elongated strands in the circular layer. In MPTP treated marmosets, there was a marked reduction in the number of KCNQ4-ir structures and staining intensity in the ileum (Figure 47 a & b). Immunoreactivity in the colon was not markedly affected by the treatment (Figure 47 c & d).

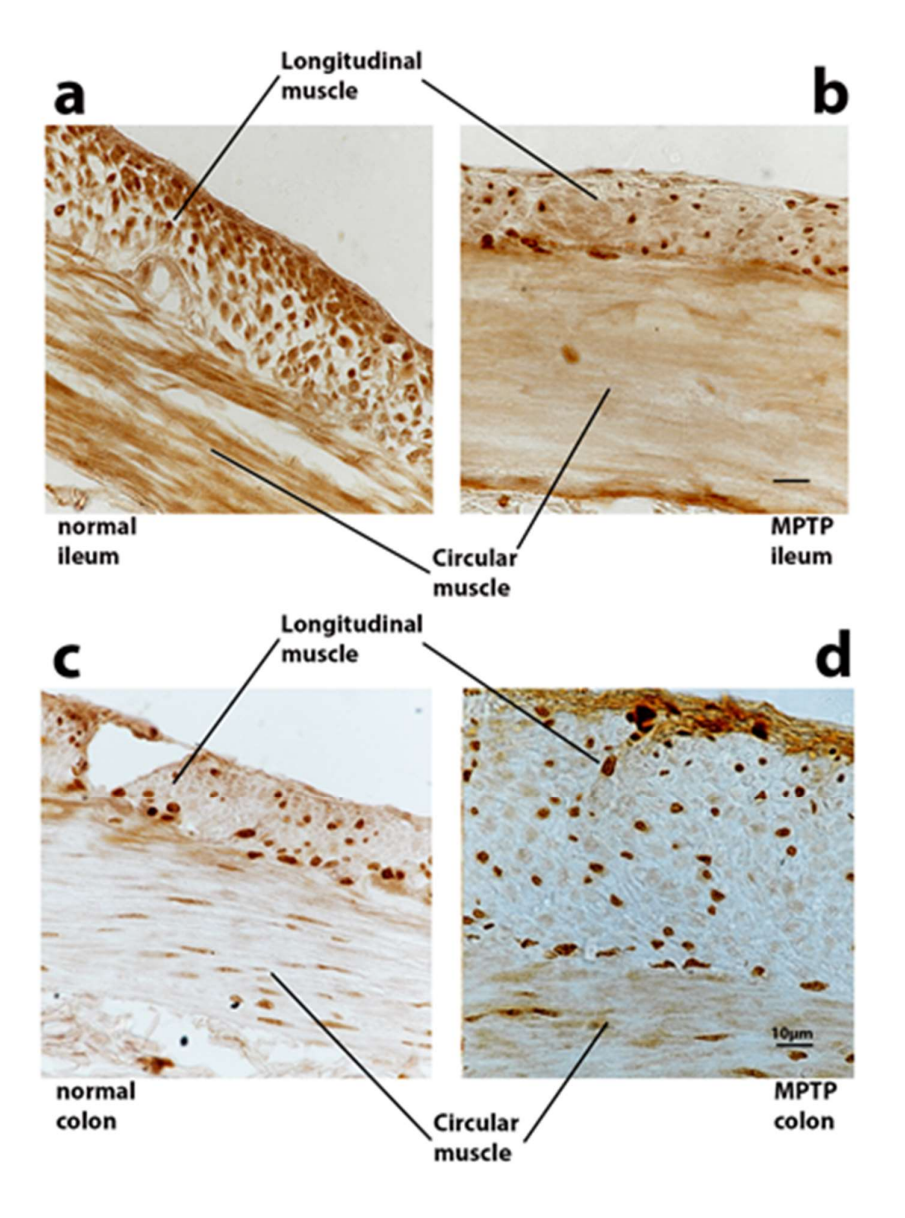


Figure 47 KCNQ4-immunoreactivity in the gastrointestinal tract of naïve and MPTP treated marmosets.

Brightfield microscopy images of KCNQ4 immunoreactivity in the normal (a, c) and MPTP (b, d) ileum (a, b) and colon (c, d).

Following MPTP-treatment, there was a statistically significant reduction in the intensity of KCNQ4-ir in the longitudinal and circular muscles layers and in the submucosa of the ileum but not in the colon (Figure 48a). The number of punctate KCNQ4-ir structures (Figure 48b) and the mean coverage of these structures (Figure 48c) were significantly reduced following MPTP treatment in the longitudinal muscle layer of the ileum but not in the colon. The size of the KCNQ-ir cells in the logitudinal muscle layer were not significantly different in sections from MPTP treated animals compared to naive control tissue (Figure 48d).

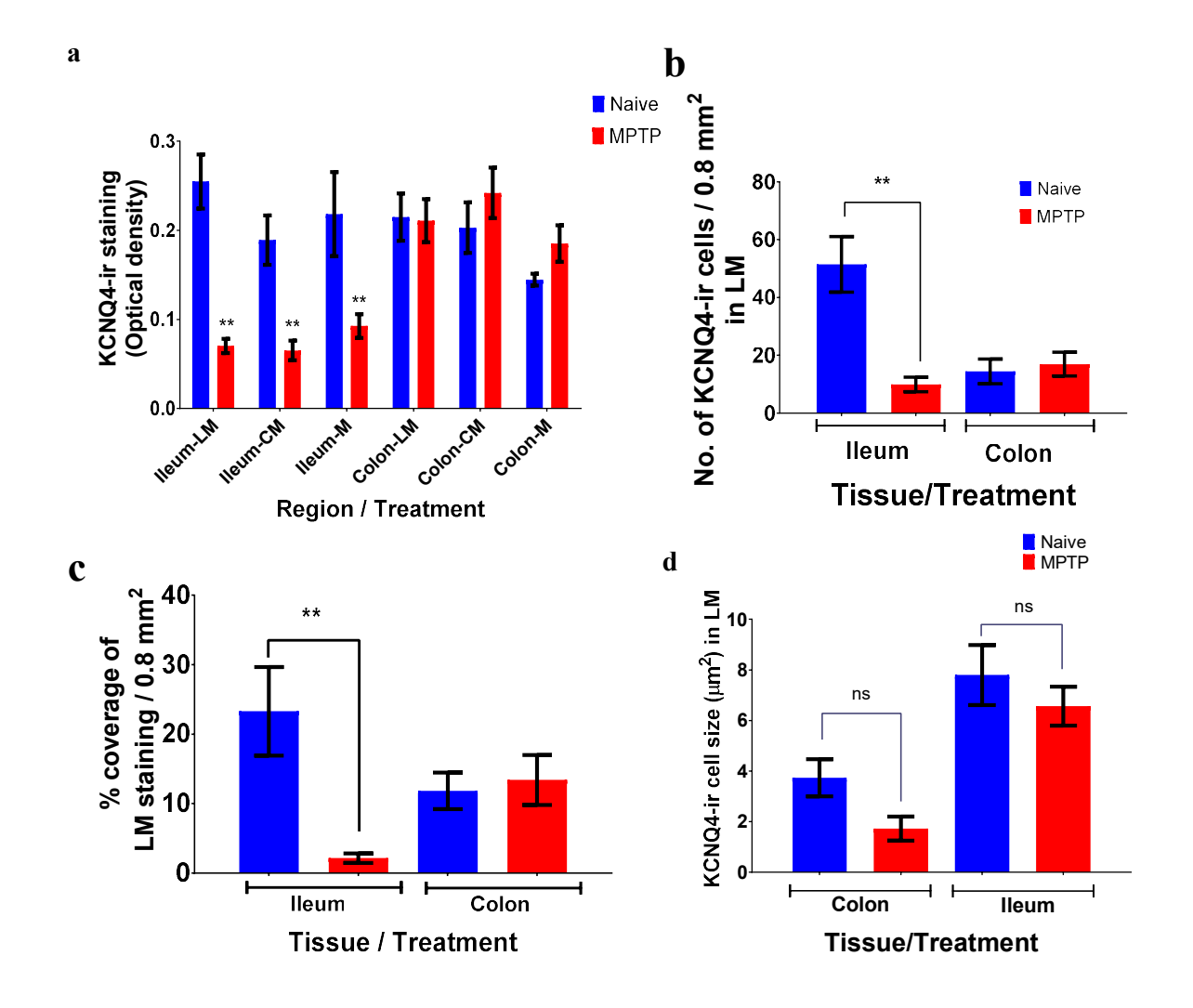


Figure 48 Quantitative analysis of KCNQ4-ir in the ileum and colon of normal and MPTP common marmosets.

Summary bar charts showing average optical density of KCNQ-ir (a), in various regions of the GIT. LM = longitudinal muscle, CM = circular muscle, M = mucosa. The number of KCNQ-ir cells in the LM (b), percentage coverage of staining of KCNQ4-ir in the LM (c) per $0.8mm^2$ region of interest and mean cell size in μm^2 (d). Data are expressed as mean, SEM; **p < 0.01; vs control tissue (n=5 per treatment) by one-way ANOVA followed by Sidak post hoc test.

6.3.3 KCNQ4 positive structures are present on smooth muscle cells of the gastrointestinal tract

In order to localise the KCNQ4-ir structures to the smooth muscle we performed double labelling studies with anti-Smooth muscle γ & α -actin antibody (SMA). The KCNQ4-ir structures colocalised with smooth muscle actin within the longitudinal and circular muscle layers (Figure 49).

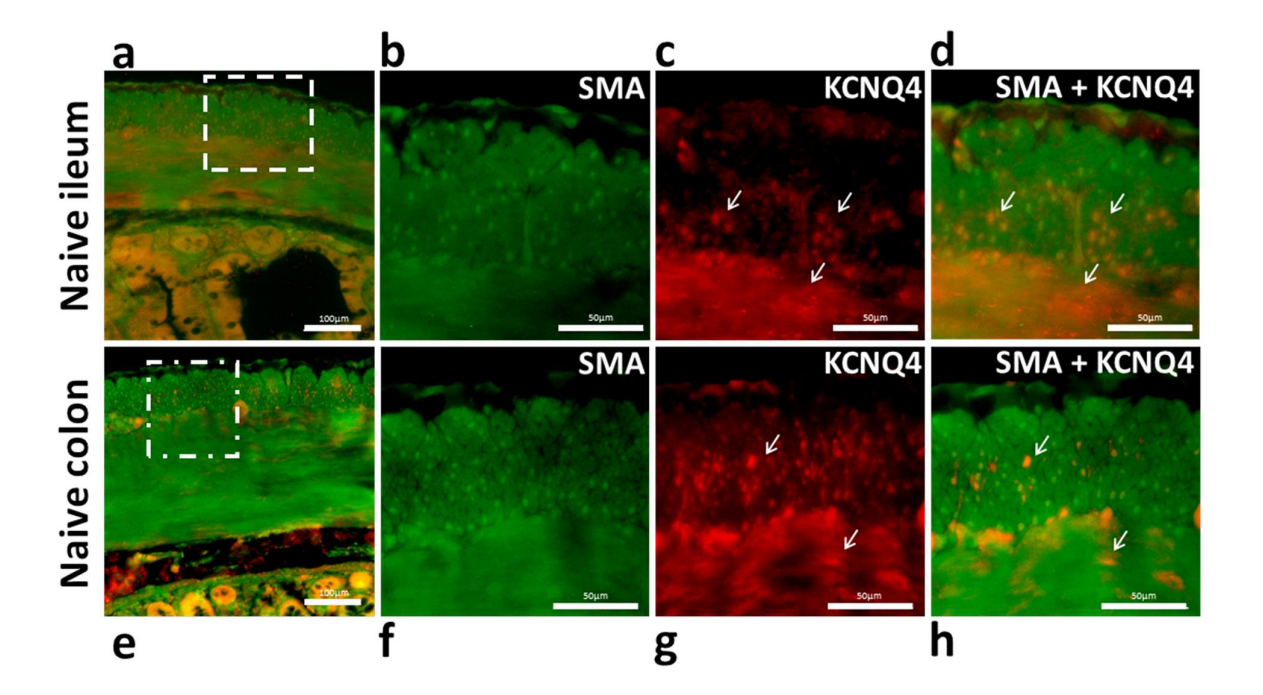


Figure 49 Immunofluorescent staining for KCNQ4 in smooth muscle layers of gastrointestinal tract in naive marmosets.

Immunofluorescent staining for KCNQ4 and SMA in the ileum (a-d) and colon (e-h) of naïve marmosets. Higher magnification images shown in b-d and f-g. Anti-SMA antibody (green) is used to detect smooth muscle (b&f), the anti-KCNQ4 for Kv7.4 channels (red, c & g) and merged images showing co-localisation (d & h). White arrows indicate cells with KCNQ4 expression.

6.3.4 The expression of KCNQ4 positive structures is increased in the muscular layer of the bladder in the MPTP primate model.

The number of KCNQ4-ir structures were significantly higher (Figure 50c) in the bladder of MPTP treated marmosets compared with naïve. Consequently, the optical density of the staining was also greater in the MPTP treated marmosets.

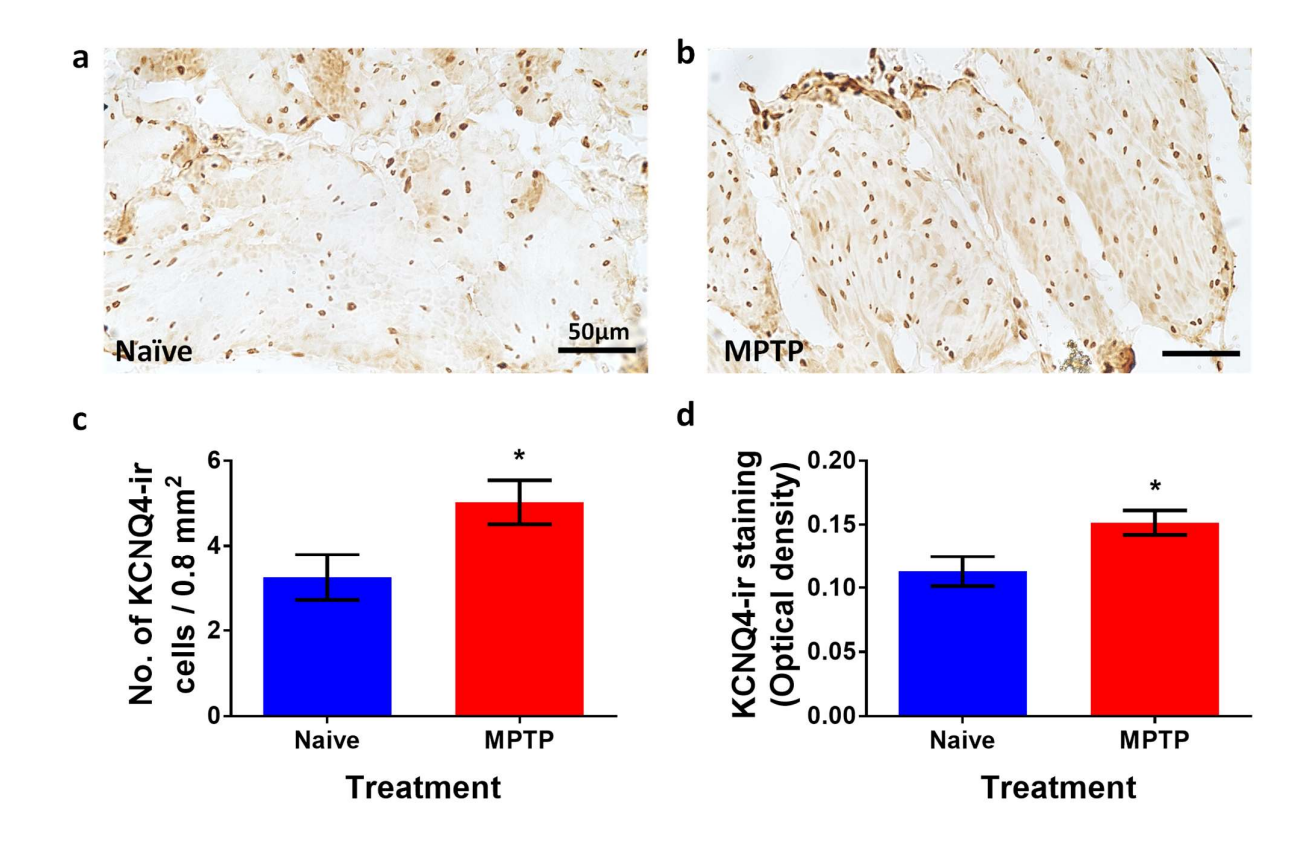


Figure 50 KCNQ4-immunoreactivity in the bladder muscle of naïve and MPTP treated marmosets.

Brightfield microscopy images of KCNQ4 immunoreactivity in the normal (a) and MPTP (b) bladder. Summary bar charts (n=5 per treatment) showing the number of KCNQ-ir cells (c) and average optical density of KCNQ-ir (d) per 0.8mm² region of interest in MPTP and naïve marmoset bladder tissue. Data are expressed as mean, SEM; *p < 0.05; vs naïve tissue by unpaired t-test.

6.3.5 A significant reduction in KCNQ4 mRNA expression in the ileum of MPTP treated marmosets.

To ascertain whether the difference in KCNQ4 between treatments, seen by immunohistochemical analysis, were due to alterations at mRNA level, qPCR was performed on tissue segments from naïve and MPTP treated animals. The expression of KCNQ4 mRNA in the ileum was significantly lower in MPTP treated animals (Figure 51 d), which corresponds with the lower Kv7.4 immunoreactivity in the ileum (Figure 48). There was no significant difference in mRNA expression in the in the colon or bladder (Figure 51 d).

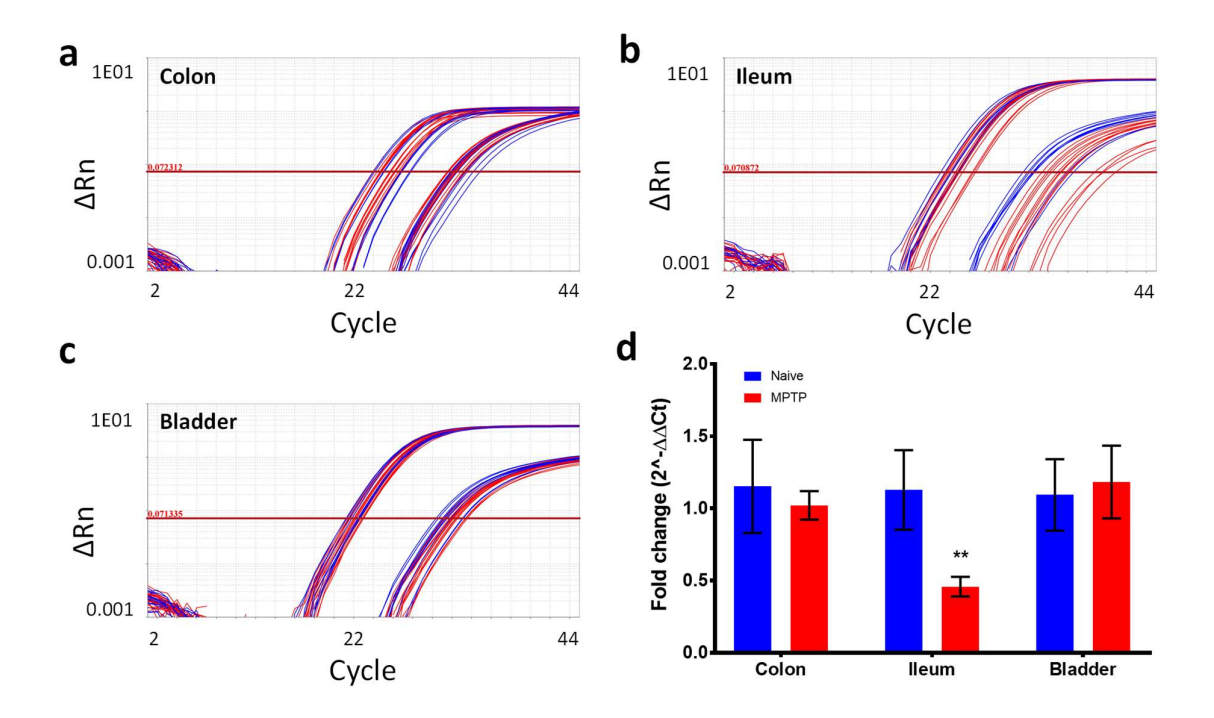


Figure 51 mRNA expression of KCNQ4 in different tissues from naive and MPTP treated marmosets.

Amplification plots of KCNQ4 mRNA from the tissues of naïve (blue) and MPTP treated (red) colon (a), ileum (b), and bladder (c). Summary bar charts of qPCR detection of KCNQ4 expression in various tissue segments with reference to the housekeeping gene (HPRT1 – threshold ~ cycle 22) (d). Data are expressed as mean, SEM; **p < 0.001; vs naïve tissue by unpaired t-test ($n \ge 4$).

6.4 Discussion

Using the MPTP treated common marmoset, a gold standard model of Parkinson PD, we have found a significant reduction of KCNQ4-ir, in the CNS and periphery. Firstly, we showed that

MPTP administration caused a significant decrease in dopaminergic (TH+ve) neurons of the SNpc. Compared to controls the MPTP treated marmosets exhibited on average approximately 70% loss of dopaminergic neurons (Figure 46a), confirming it as a pathologically valid model of PD. K_v 7.4 channels were found to be expressed on a small portion of dopaminergic neurons of the SNpc (Figure 45 a-d, Figure 46c). This is the first-time expression of KCNQ4 has been shown in the dopaminergic neurons of the marmoset substantia nigra although it has been shown previously in rat (Hansen et al., 2006) and mouse (Kharkovets et al., 2000) brain. Both rodent species show substantial colocalization between KCNQ4 expression and TH+ve neurons implying that the majority of dopaminergic neurons in the SNpc of the rodent express KCNQ4. In our study control marmoset immunoreactivity was quantified as only ~17% of TH+ve neurons that also express KCNQ4. This may represent a species difference and it would be interesting to assess expression in the human brain to understand the level of colocalization and to see which species correlates better in this aspect.

With dopaminergic neuron loss in the MPTP treated marmosets (Figure 46a) it would be expected that KCNQ4-ir TH+ve neurons would also decline (Figure 46b). Interestingly we found that the percentage of TH+ve neurons that express KCNQ4 was significantly lower in MPTP treated marmosets compared with control (Figure 46c). This implies that KCNQ4-ir, TH+ve cells are more vulnerable to cell death after MPTP administration. Alternatively, KCNQ4 may be downregulated in the SNpc upon MPTP administration. As with other KCNQ encoded channels K_v7.4 modulate excitability of neurons, dampening firing frequency upon their activation (Li et al., 2017). The Kv7 channel activator, Retigabine, has been shown *in vitro* and in *ex vivo* rat brain slice preparations to inhibit neuronal excitability and dopamine neurotransmission in mesencephalic dopaminergic neurons (Hansen et al., 2006). Interestingly, Hansen et al. (2006) reports that only a fraction of dopaminergic neurons in the SNpc showed increased excitability in the presence of the Kv7 blocker XE-991. The authors suggest that this is perhaps due to KCNQ being differentially expressed, in terms of density or subcellular composition, among DA neurons in the SNpc which is supported by the expression pattern that we have found in our study with the marmoset. A recent report has shown neuroprotective effects of XE-991, a blocker of K_v7 channels, in a rat model of Parkinson's

disease. Intracerebroventricular administration of XE-991 attenuated motor deficits, reduced the impact on striatal dopamine levels and dopaminergic neuron loss in the SNpc after 6-hydroxydopamine (6-OHDA) administration (Liu et al., 2018). With our results in SNpc counts in context of the neuroprotection observed by blockade of KCNQ channels in Liu et al., 2018, it seems more plausible that KCNQ4 expressing dopaminergic neurons are more vulnerable to MPTP mediated cell death.

The oxidative stress hypothesis of Parkinson's disease has received much attention and evidence in support of it as a contributing factor has been gained from MPTP animal models (Jackson-Lewis & Smeyne, 2005). A possible mechanism of increased susceptibility of KCNQ-ir neurons to neurodegeneration may be through alteration of the channel by oxidative modification. The KCNQ channels, including K_v 7.4, contain a triplet of cysteines in the linker between subunits 2 and 3, which is sensitive to oxidative modification causing a potent augmentation of the M-current (Gamper et al., 2006). Over-activation of KCNQ channels has been shown to lead to excessive K^+ efflux and increased cell death in hippocampal and cortical neurons (Zhou et al., 2011). This may be a mechanism through which we also see vulnerability of KCNQ-ir, TH+ve neurons to cell death in the marmoset MPTP model (Figure 46c).

Conversely another report points to augmentation of the KCNQ channels and silencing of neurons during a hypoxic event as protective and they suggest that it may be a cell rescue mechanism in their hippocampal slice experiments (Gamper et al., 2006). Activation of K_v7 channels in 6-OHDA treated rats has been shown to reduce the severity of L-DOPA induced dyskinesia (LID), although this is believed to be an action more specific to Kv7.2/3 and in the same study, administration of the non-specific K_v7 channel blocker XE-991 did not exacerbate LID readouts in the model (Sander et al., 2012, 2013). It is difficult to conclude whether activation or inhibition of Kv7 channels in the CNS would be protective in neurodegeneration, but it is something which requires further unravelling.

In this study we also showed for the first-time expression of KCNQ4-ir structures in the gastrointestinal tract (Figure 47) and the bladder (Figure 50) of the marmoset. In the gastrointestinal

tract KCNQ4-ir co-localised with smooth muscle actin expression (Figure 49), which has also been shown in the mouse gastrointestinal tract (Jepps et al., 2009) and human arteries (Ng et al., 2011). There was also KCNQ4-ir in regions that looked like neuronal cells of the myenteric plexus, but without IHC in stretch preparations to reveal the plexi and double labelling we cannot confirm that in this instance.

Using our automated quantification technique, described in the methods, we found a significant reduction in KCNQ4-ir in the ileum of MPTP treated marmosets but not in the colon, suggesting a downregulation of K_v7.4 channels (Figure 48) in the small intestine. Our findings were strengthened by observation of lower expression of KCNQ4 mRNA in the ileum (Figure 51). Functional studies performed by Coletto et al., (2019), using tissue segments of the ileum from MPTP treated marmosets in organ bath experiments show impaired EFS induced relaxation. They also showed a lack of potentiation of the EFS response when the ileum segments were incubated with L-NAME, compared to tissue from control animals. This was observed despite no evidence of reduction in nNOS-ir neurons in the myenteric plexus (Coletto et al., 2019). That would imply that although nitric oxide (NO) is generated in those strips, in response to EFS, it is not able to have an effect and attempting to block synthesis with L-NAME is futile as there is some other part of the mechanism of NO induced relaxation that is impaired. Reduced expression of the K_v7.4 channel has been shown in the corpus cavernosum of the spontaneously hypertensive, heart failure-prone (SHHF) rat model, which also has impairment of the mechanism of smooth muscle relaxation (Jepps et al., 2016). In the rat corpus cavernosum of the SHHF rat, relaxations due to the NO-donor sodium nitroprusside (SNP) were significantly reduced compared to normal rats. This was postulated to be due to the reduced KCNQ expression as SNP relaxation can be attenuated by blocking the KCNQ channels with Linopirdine. A significant reduction in Kv7.4 expression was also seen in another study with a spontaneously hypertensive rat in the aorta and renal artery, and again NO mediated relaxations of these tissues ex vivo was impaired. Using whole cell electrophysiology on Kv7.4 overexpressing human embryonic kidney cells Stott et al., (2015) saw K+ currents generated that were enhanced by cyclic GMP (cGMP) and blocked by Linopirdine (Stott et al., 2015). At least in rat vascular smooth muscle this all points to a pivotal role of KCNQ4 in vasorelaxation induced by

endogenous vasodilators acting via cGMP. If a similar role is played by the channel in the gastrointestinal tract, then the reduced expression that we see in the ileum from MPTP marmosets in our study may have a functional effect contributing to impaired relaxation, similar to the vessels of the SHHF rat model. We performed no functional work in these tissues as these were historical samples available to us, but the reduction of Kv7.4 channels in the ileum may contribute to the impaired relaxation and increased spontaneous activity that is seen in Coletto et al., (2019).

Small intestinal dysfunction has not been a focus of many investigations in GI dysfunction in PD and its models. When it is investigated the composition of the microbiome is focussed on due to the presentation SIBO in PD patients. A mouse model of MPTP showed no functional differences in transit time of the small intestine compared to control animals (Anderson et al., 2007), however three different studies objectively measuring small intestine transit time in PD patients showed significant delay in small intestine transit time compared to matched controls (Dutkiewicz et al., 2015b; Knudsen, Haase, et al., 2017; Su et al., 2017). The differences between the species may represent genuine species difference or may be reflective of the neurodegeneration observed with MPTP treated mice only displaying mean 57% dopaminergic neuron loss (Anderson et al., 2007). The symptom of slowed transit time does not necessarily conflict with the findings of hyperactivity, impaired relaxation, and a reduction of Kv7.4 (present study) in the marmoset model. Transit time is based on the peristaltic reflex, which is a co-ordination of relaxation and contraction mechanisms. Luminal contents are propelled by an ascending contraction and a distal response of relaxation which is sometimes followed by a contraction (Hasler, 2008). Dysfunction of this distal relaxation mechanism can impair transit of a bolus through gastrointestinal structures.

From the results of our studies it is likely that the Kv7.4 channel is not involved in the increased frequency of spontaneous contractions and dysregulation of epithelial ion transport seen in the MPTP treated marmoset colon in a previous study, as we saw no differences in expression of Kv7.4-ir or mRNA in the colon segments in our study.

The urinary dysfunction in human PD patients has been shown to correlate with disease severity and reduced nigrostriatal dopaminergic function via imaging studies (Sakakibara, Shinotoh, et al.,

2001). Local changes were observed in isolated segments from the MPTP treated marmosets, where spontaneous activity and EFS induced contractile activity was increased in bladder tissue from the MPTP treated marmosets. Although Pritchard et al., (2017) saw no indication of postsynaptic cholinergic or purinergic alteration in the MPTP marmoset tissue the contractile responses to EFS contained a reduced cholinergic component and an increased purinergic component compared to bladder segments from naïve tissue. In the human bladder, Kv7 channel modulation effects contractility similarly to its effect in the gastrointestinal tract by inducing relaxation upon activation and enhancing contractility when blocked (Bientinesi et al., 2017; Svalø et al., 2015). Of note, during its trials as an anti-epileptic, Retigabine (a Kv7 activator) had a notable side effect of urinary retention (Brickel et al., 2012) and Flupirtine, another Kv7 activator, was trialled as a therapy for overactive bladder (Michel et al., 2012). Our results also show a small but statistically significant increase in Kv7.4 positive cells and increased Kv7.4 staining in the bladder from MPTP treated marmosets. Increased expression would hypothetically lead to an increased relaxation effect, although we performed no functional assessments. If causative, this would be opposing the urinary dysfunction, hyperreflexia and increased contractile activity seen in humans with PD (Campeau et al., 2011; Fitzmaurice et al., 1985), and PD models in marmosets (Albanese et al., 1988; Pritchard et al., 2017) and rodents (Mitra et al., 2015; Soler et al., 2011). Bladder outflow obstruction (BOO) is one cause of overactive bladder syndrome (OAB) and displays symptoms of urgency and nocturia, symptoms also found in PD patients with urinary dysfunction. Kv7 channels were analysed in bladder samples from patients undergoing cystoscopy with and without BOO. Molecular analysis revealed upregulation of mRNA for the Kv7.1 channel, there were no differences of mRNA for Kv7.4, but they hypothesised that this upregulation was a local compensatory mechanism to attempt to maintain normal bladder function in BOO patients (Svalø et al., 2015). We also saw no increase in mRNA of KCNQ4, but we did see an increase in the immunoreactivity for protein indicating a potential post-translational modification of KCNQ4 in an attempt to compensate for overactivity in the bladder in the MPTP marmoset model.

As mentioned, the increase in Kv7 channel expression in a PD bladder may lead to increased relaxatory effects or lower basal tone. This may also lend itself to a cause of voiding symptoms

such as retardation of initiation, intermittency or prolongation, observed in patients with PD (Sakakibara, Hattori, et al., 2001).

It is not known whether alteration of $K_v7.4$ channels occur in PD, but the current observations in this primate model of PD suggest that the role of $K_v7.4$ needs to be further investigated in this and other models as well as in PD. Impaired local signal transduction and impaired muscular activity may have a direct bearing on the gastrointestinal and urinary dysfunction in PD and therefore further studies need to be conducted to elucidate the mechanism of this alteration and its functional consequences. Furthermore, modulation of central KCNQ channels may provide therapeutic benefit in the motor symptoms associated with Parkinson's disease and can be a novel target to halt the progression of the disease.

7 GENERAL DISCUSSION

Non-motor symptoms (NMS) of PD have historically been under-recognised, despite mentions of many NMS such as sleep disturbances, autonomic dysfunction, and pain in James Parkinson's original description of the disease over 200 years ago. NMS are treated currently with symptomatic therapies. Holistic treatments are not possible due to our lack of understanding of the link between pathophysiology of motor and non-motor symptoms. Therefore, each symptom is treated individually standalone, separate from the underlying cause.

Gastrointestinal and urinary symptoms greatly affect the quality of life of patients with PD and present important challenges to the management of the disease as it progresses. The most frequently reported issues with these systems are bladder dysfunction in the form of nocturia, increased frequency, increased urgency and gastrointestinal dysfunction presenting as constipation, excess salivation, dysphagia.

We chose to use different models of Parkinson's disease in different animals to see if we can find common changes in their pathology which may lead to GI and urinary dysfunction. The toxin induced models were used for our experiments as they have extensively researched pathology and good construct validity. The toxin models do present a limitation as they cause rapid degeneration of the SNpc, which is unlike the slow progression of the human disease. Therefore, we assessed GI and urinary dysfunction in models with differing extents of pathology, as NMSs are present at various stages of the disease. The models that we used also differ in their lesion location as 6-OHDA treatment results in a unilateral lesion model whereas MPTP administration results in a bilateral lesion. Using different models to assess similar readouts was performed intentionally to understand whether a common mechanistic theme could be uncovered rather than specific toxin induced changes, which would not be present in the human disease condition.

Our work focussed on evaluation of overt local adaptive changes that may occur because of central dopaminergic loss, using various ex vivo assays. It is important to understand the limitations of our work when putting our results into context of the physiological outcomes. Motor patterns of the GI tract and urinary bladder can be modulated by external factors via central nervous system modulation, but also nutrient compositions inside the organs themselves. Organs have different spatial profiles; the ileum and colon are split into distal and proximal, and the bladder dome is distinct in its molecular profile from the bladder base. In the organ bath setting and some of the molecular techniques used here, we have separated these tissues from their extrinsic modulation and we are not able to tease apart the differences in such spatial regions. Therefore we were only able to treat the organ as one homogenous tissue. Despite these limitations we sought to understand neuropathological and peripheral changes related to gastrointestinal and urinary dysfunction resulting from toxin induced dopaminergic neuron depletion. Research such as this aims to aid the development of interventions to improve quality of life but also potentially identify biomarkers and increase the understanding of "at risk" populations to enable earlier intervention.

Figure 52 and the discussion below summarise our findings from each chapter and their implications for future directions of study.

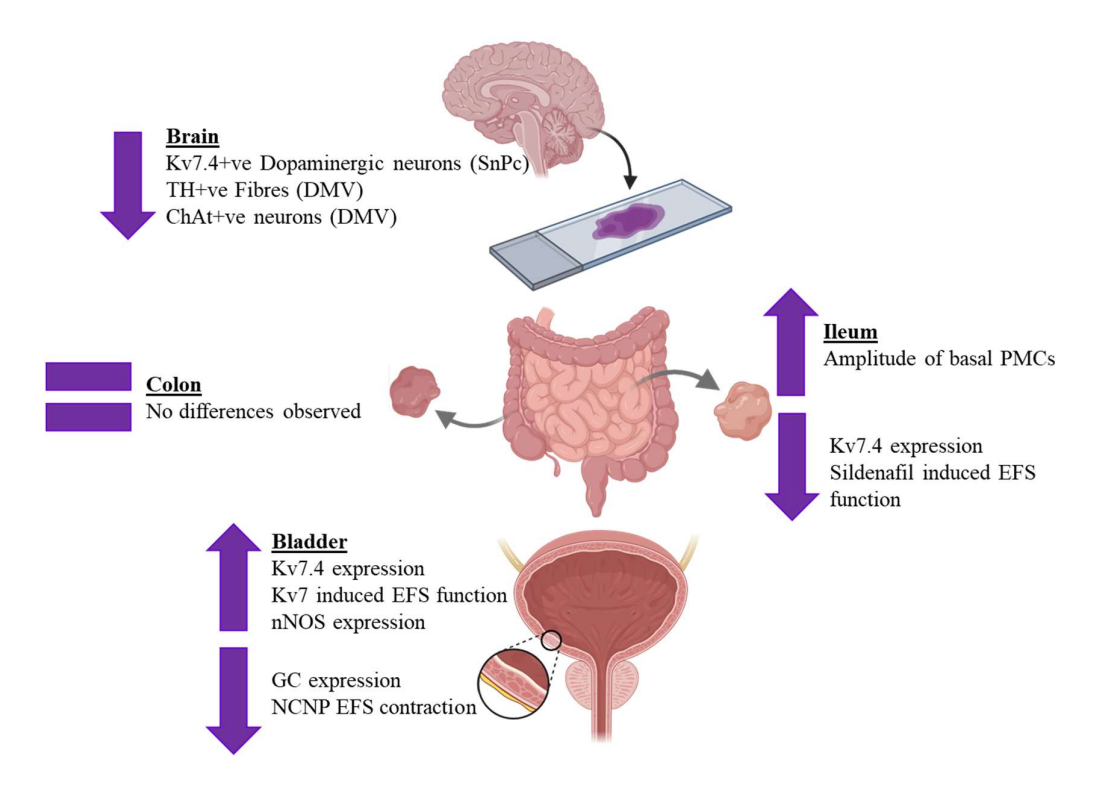


Figure 52 Summary of thesis findings

Changes observed in our studies in animal models of PD related to gastrointestinal and urinary dysfunction. Created with BioRender.com

In chapter 3 we built upon the work of others by showing a more physiologically relevant effect of modulation of the Kv7 channels in gastrointestinal smooth muscle structures. We further characterised the role and distribution of Kv7 channels in gastrointestinal tissues and motility. Our results show the first functional evidence that Kv7 channels play a key role in regulating intestinal motility, and that Kv7channel activity occurs within both myogenic and neurogenic circuitry within the gastrointestinal tract. We determined that pharmacological inhibition of Kv7 channels increased peristaltic like motor activity and Kv7 activation diminished it in the ileum and colon. Our results infer that the activation of Kv7 channels by Retigabine works to both effect the frequency of

CPMCs by suppressing action potentials and neurotransmitter release by neurons and effects the amplitude by causing relaxation in the muscle, via hyperpolarisation of smooth muscle cells. Immunohistochemical characterisation uncovered that the Kv7.4 channels are present on the smooth muscle layers and within the myenteric plexus. The functional effects on frequency and amplitude of Kv7 drugs in our system confirm this, with frequency primarily governed neuronally and amplitude driven myogenically. A lack of double labelling of Kv7.4 with a marker of ICCs means that we cannot confirm any expression on ICCs, this is a future piece of information needed, which if present may also contribute to the functional effects on frequency by Kv7 modulation.

In studies with human taenia coli strips a Kv7 channel blocker, XE-991, produced irreversible concentration dependent contractions. Retigabine, a Kv7 channel activator, produced concentration dependent relaxations of precontracted human taenia coli strips. This information combined with our results means that it is likely that Kv7 channels are important in peristaltic movement in the human GIT. Therefore, our assay may be used as a step in the translational path for Kv7 modulation as a therapeutic intervention for gastrointestinal disorders.

We were also able to show fundamental concepts of biological differences between the two gastrointestinal organs in our motility set up. Peristaltic motor complexes of the ileum and colon show different motility pattern profiles in our system. The IPMCs of the ileum consist of small, fast contractions building upon each other to produce waves of increases in IP followed by periods of quiescence. The colon, when distended, produces regular more pronounced increases in IP due to proximal contractions which propagate aborally. We attempted to characterise the differences further by looking at the inherent fluctuations of the tissue which can also be termed as contractility. This can be viewed when stretching out the traces to view an individual motor complex, with rest periods either side. Again, here the different organs differed in their contractility patterns. The differences in motor patterns between the two tissues are likely to be indicative of the differences in structure and functional roles between the colon and small intestine.

In chapter 4 we used the motility assay to compare ex vivo motility patterns of the ileum and colon from mice treated with MPTP and naïve controls, with a focus on Kv7 modulation. This is the first

time, to our knowledge, that tissues from a model with neurodegeneration in the nigra have been put through this type of organ bath system to measure motility. Here we show that in the ileum of MPTP treated animals, these basal complexes, although still regular in frequency, exhibit increased amplitude and magnitude compared to the ileum tissue from sham treated controls. There were no differences in the basal activity of the colon and the effects of Kv7 channel modulation were similar between MPTP and saline animals in both tissues.

Our dosing regimen led to the successful generation of animals with lesions in the substantia nigra with an average of \sim 36% loss of dopaminergic neurons in the SNpc. This led to dysfunction in the gastrointestinal system of MPTP treated animals in the form of hyperactivity of the ileum.

Effects on amplitude can be multifaceted and, in these experiments, we also assessed the contractility of the segments from MPTP treated mice. Contractility is where the most obvious effects can be seen in our study. Without further pharmacological manipulation, we were unable to determine the molecular basis for this contractility and for the differences observed. It is likely that this contractility is simply the basic electrical rhythm of the tissue, but it is difficult to determine as the small intestine movements are made up of several types, such as slow waves, longitudinal oscillations and peristaltic movements. Spatiotemporal maps are used frequently for such motility assessments. Although they include similar organ bath apparatus to ours, they use video recording equipment and frame by frame analysis of the movement of the segments. Video recording of the intestinal segments whilst in the organ bath would add sensitivity to the system and allow us to view the direction of peristaltic movements. Insertion of a small bead, into this preparation, would mimic the movement of a bolus through the segment. This would allow us to see whether the impairments of contractility, that we see, alter transit. Protein or RNA quantification of samples from these animals, may allow us to better understand the mechanisms behind these changes.

The lack of a difference between tissues from MPTP treated mice and sham treated mice to Kv7 modulators lead us to believe that the hyperactivity seen in the MPTP treated ileum segments was due to impairment of a different mechanism. This was despite previously observing reduced expression of Kv7.4 channels in the ileum of the marmoset MPTP model. Ultimately, studies on

human tissue from PD patients will inform on whether Kv7 channel plays a role in the gastrointestinal dysfunction in PD.

Chapter 5 focused on the comparison of ex vivo contractility patterns and protein expression in the bladder, ileum and colon from rats treated with 6-OHDA, sham and naïve controls, with a focus on Kv7 modulation. In this study we chose to induce nigral lesions via striatal injection to mimic an earlier stage of disease, with lesser dopaminergic loss to assess gastrointestinal and urinary dysfunction. This is the first such work investigating local autonomic dysfunction in a partial lesion model.

Firstly, we showed that simply increasing the 6-OHDA dose at one site in the striatum is not sufficient to induce increased neuropathology in the SNpc or the DMV, at least with the concentrations that we have used. We show for the first time that striatal neurotoxin administration can also lead to neurodegeneration in the DMV of ChAT+ve neurons and TH-ir fibres. This was previously shown only with SNpc administration of 6-OHDA and the fibres surrounding the ChAT neurons had not previously been assessed for neurotransmitter expression. Our work strengthens the idea of a nigrostriatal link to the DMV. The functional effects of this are likely to be mostly evident in assessment of gastric motility, as that is a process heavily reliant on DMV modulation. As gastroparesis is a NMS in a proportion of PD patients, this nigrostriatal-DMV link should be further investigated in patients.

In our peripheral assessments we did not see any difference in the responses of any of the tissues to increasing concentrations of carbachol nor increasing frequencies of EFS in either treatment group. Therefore, it is likely that in animal models at least, larger dopaminergic loss is needed to elicit overt differences in contractility of the colon, ileum, and bladder measurable via cholinergic and electric field stimuli.

The reduction in the EFS response in the presence of Retigabine was seen equally in the tissues dissected from 6-OHDA injected animals. We looked at Kv7.4 expression via immunohistochemistry in the different layers of these tissues but found no significant differences

between treated, sham, and naïve tissue indicating that Kv7 channels are not affected in the GIT in this model. We can therefore conclude that striatal 6-OHDA injection resulting in partial dopaminergic loss does not lead to effects on Kv7 function or Kv7.4 expression in the colon or ileum. Based on this and our results from the MPTP treated mouse with a partial lesion that also showed no GIT differences in Kv7 channel functionally, it is plausible that Kv7 alterations in the GIT are produced from larger dopaminergic loss in the SNpc.

Incubation of segments of gastrointestinal tissue with Sildenafil results in an expected decrease in magnitude of contraction to 10Hz EFS. However, the ileum tissue from 6-OHDA tissue did not show any reduction due to Sildenafil at any concentration and this response was significantly different to that of the ileum segments from sham and naïve animals. This highlights an impaired relaxation mechanism in the ileum of 6-OHDA treated animals. Investigations into the small intestine in animal models of PD are variable. Some groups observed increases in the number of dopaminergic neurons, nNOS positive neurons and a reduction in ChAT positive cells in the duodenum. Conversely, other studies show a reduction in nNOS positive cells with compensatory changes in the form of upregulation of VIP positive neurons. There is certainly a precedent for impaired relaxation mechanisms in the literature in animal models of PD and although the molecular origin in our experiments is novel, this is something which requires thorough investigation in PD patients.

Bladder tissues from this model is where we found most of our differences between treated and untreated animals. As with the MPTP marmoset tissues, we again saw an increased expression of Kv7.4 protein in the bladder of 6-OHDA lesioned animals. Our organ bath assessments with these tissues showed increased sensitivity to Retigabine induced reduction of EFS responses. Further experiments to uncover dose response relationships, using sham treated tissue and human PD tissue assessments will confirm the effect of Kv7 channels in PD. From our studies so far, in two different animal models, it seems that it may play a significant role.

The expression of nNOS was also increased in the bladder tissues from 6-OHDA animals which and presented functionally as increased effects of the NOS inhibitor LNAME. Interestingly the

levels of GC were significantly reduced in 6-OHDA bladder tissues. An EFS train of increasing frequency stimulation from 1-40Hz in the presence of atropine and purinergic desensitisation revealed a small but significant impairment of the non-cholinergic, non-purinergic contraction in tissues from 6-OHDA animals. Further work would be needed to confirm the mechanisms of the deficiencies of the non-cholinergic, non-purinergic responses to EFS observed in the bladders of this partial lesion model of PD. In a partial lesion, unilateral, model one would not expect the results to be so pronounced that they would affect overall motility, but this model has allowed us to tease apart some molecular changes which have functional pharmacological implications.

In chapter 6 we investigated the expression of Kv7 channels in the brain, GIT, and bladder of MPTP treated marmosets compared with naïve controls. We found that the percentage of TH+ve neurons in the SNpc that express KCNQ4 was significantly lower in MPTP treated marmosets compared with control. This implies that KCNQ4-ir, TH+ve cells are more vulnerable to cell death after MPTP administration. Literature reports have been conflicting as to whether activation or inhibition of Kv7 channels in the rodent CNS are protective in neurodegeneration, but it is something which requires further investigation should Kv7 channels become a target for central or peripheral modulation in PD patients. The presence of Kv7.4 channels in dopaminergic neurons of the SNpc of the marmoset is a novel finding of this work and shows a much lower expression profile to the previous assessments in rodents. This may represent a species difference and it would be interesting to assess expression in the human brain to understand the level of colocalization and to see if it can be a useful target.

In this study we also showed for the first-time expression of Kv7.4 immunoreactive structures in the gastrointestinal tract and the bladder of the marmoset. The channel was also affected in the peripheral tissues in this model with reduced expression in various cell types of the ileum and increased expression in the bladder detrusor muscle. We found no differences in Kv7.4 expression in the colon tissues between the two treatment groups.

Functional studies performed by others, using tissue segments of the ileum from MPTP treated marmosets in organ bath experiments, show impaired EFS induced relaxation. Additionally,

reduced expression of the Kv7.4 channel has been shown in the corpus cavernosum of the spontaneously hypertensive, heart failure-prone (SHHF) rat model, which also has impairment of the mechanism of smooth muscle relaxation. It remains to be seen in functional experiments with MPTP treated marmoset whether differences in small intestinal transit are apparent alongside these molecular changes. Three different studies objectively measuring small intestine transit time in PD patients showed significant delay in small intestine transit time compared to matched controls. The symptom of slowed transit time does not necessarily conflict with the findings of hyperactivity, impaired relaxation, and a reduction of Kv7.4 in the marmoset model. Transit time is based on the peristaltic reflex, which is a co-ordination of relaxation and contraction mechanisms. Luminal contents are propelled by an ascending contraction and a distal response of relaxation which is sometimes followed by a contraction. Dysfunction of this distal relaxation mechanism can impair transit of a bolus through gastrointestinal structures.

The increase in Kv7 channel expression in a PD bladder may lead to increased relaxatory effects or lower basal tone. This could be a compensatory mechanism to overactivity or be a cause of voiding symptoms such as retardation of initiation, intermittency, or prolongation, observed in patients with PD. Again, functional experiments with MPTP treated marmoset need to be performed to build upon this and assess whether bladder dysfunction is apparent alongside these molecular changes and can be modulated in vivo using pharmacological modulators of Kv7 channels.

It is not known whether alteration of Kv7.4 channels occur in PD, but the current observations in this primate model of PD suggest that the role of Kv7.4 needs to be further investigated in patient samples. Impaired local signal transduction and impaired muscular activity may have a direct bearing on the gastrointestinal and urinary dysfunction in PD and therefore further studies need to be conducted to elucidate the origin of this alteration and its functional consequences. Furthermore, modulation of central KCNQ channels may provide therapeutic benefit in the motor symptoms associated with Parkinson's disease and can be a novel target to halt the progression of the disease.

The results of this thesis suggest that central nigrostriatal dopaminergic denervation is associated with overactivity in the ileum and impaired relaxation in the bladder of these models. This can

result in dysregulated smooth muscle motor activity, leading to gastrointestinal and urinary dysfunction in PD. The mechanisms that we have uncovered here require further validation, to assess their role in the human condition, and to understand whether they can be targeted to alleviate some of the autonomic symptoms of PD. If Kv7 channels are found to be relevant to gastrointestinal and/or urinary dysfunction in human PD, this presents an opportunity for already known druggable target to be tested using translatable models, with the aim of alleviating some of these debilitating symptoms. This thesis and subsequent publications will hopefully enable future assessments to be performed in human samples based on our findings and lead to a translational path from pre-clinical to clinical therapeutic interventions.

8 APPENDICES

APPENDIX 1 - SCRIPTS USED IN AUTOMATED IMAGE ANALYSIS (IMAGEJ). 249

Appendix 2 – Scripts used for automated fluctuation analysis (Spike 2 software). 252

APPENDIX 1 - SCRIPTS USED IN AUTOMATED IMAGE ANALYSIS (IMAGEJ).

Automated image processing macro in preparation for cell counting: run("Auto Local Threshold", "method=Phansalkar radius=15 parameter 1=0 parameter 2=0 white"); run("Fill Holes"); run("Watershed"); setOption("BlackBackground", false); run("Convert to Mask"); Automated cell counting macro in after manual ROI setting: roiManager("Select", 0); run("Analyze Particles...", "size=2-Infinity show=Outlines summarize add"); close(); roiManager("Select", 1); run("Analyze Particles...", "size=2-Infinity show=Outlines summarize add"); close(); roiManager("Select", 2); run("Analyze Particles...", "size=2-Infinity show=Outlines summarize add"); close();

```
roiManager("Select", 3);
run("Analyze Particles...", "size=2-Infinity show=Outlines summarize add");
close();
roiManager("Select", 4);
run("Analyze Particles...", "size=2-Infinity show=Outlines summarize add");
close();
roiManager("Select", 5);
run("Analyze Particles...", "size=2-Infinity show=Outlines summarize add");
close();
roiManager("Select", 6);
run("Analyze Particles...", "size=2-Infinity show=Outlines summarize add");
close();
roiManager("Select", 7);
run("Analyze Particles...", "size=2-Infinity show=Outlines summarize add");
close();
roiManager("Select", 8);
run("Analyze Particles...", "size=2-Infinity show=Outlines summarize add");
close();
```

```
roiManager("Select", 9);
run("Analyze Particles...", "size=2-Infinity show=Outlines summarize add");
close();
```

APPENDIX 2 – SCRIPTS USED FOR AUTOMATED FLUCTUATION ANALYSIS (SPIKE 2 SOFTWARE).

```
var v21%; 'View created by FileOpen()
v21%:=View();
var ch1%; 'Memory channel created by MeasureToChan
CursorActive(0,4, 4, 0.1, "", "", "0.1", 0, 0); 'Peak find
CursorActive(1,0); 'Static
CursorActive(2,0); 'Static
CursorActive(3,0); 'Static
CursorActive(0,4, 4, 0.1, "", "", "0.1", 0, 0); 'Peak find
CursorActive(1,5, 4, "Cursor(0)", "Cursor(0)+1", "", "0.1", 0, 0); 'Trough find
CursorActive(2,0); 'Static
CursorActive(3,0); 'Static
view(loghandle());
window(0,0,50,100);
EditSelectAll();
EditClear();
view(loghandle()).WindowVisible(1);
view(v21%);
```

```
MeasureX(102, 1, "Cursor(0)", "0");
MeasureY(101, 4, "Cursor(0)", "Cursor(1)");
ch1% := MeasureToChan(0, "Channel 1", 7, 4, 4, 0.1, "0.1", 0, 1, "", 0);
repeat
  Interact("position cursors 2 and 3 around data to analyse",(255));
  if cursor(3)>cursor(2) then;
          Process(Cursor(2), Cursor(3), 0, 1, ch1%);
          VAR t:=cursor(2);
          VAR code% [4];
          var data [1];
          repeat
            t:=NextTime(ch1%,t,code%,data);
            If t \ge 0 then
               PrintLog("%8.3f\t%8.3f\n",t,data[0]);
               endif
          until t<0 or t>cursor(3);
          PrintLog("\n");
  endif
```

Gastrointestinal and urinary dysfunction in animal models of Parkinson's disease

until cursor(3)<cursor(2);

9 REFERENCES

- Abbott, G. W., Redford, K. E., Yoshimura, R. F., Manville, R. W., Moreira, L., Tran, K., Arena, G., Kookootsedes, A., Lasky, E., & Gunnison, E. (2021). KCNQ and KCNE isoform-dependent pharmacology rationalizes Native American dual use of specific plants as both analgesics and gastrointestinal therapeutics. *Frontiers in Physiology*, 1952.
- Abbott, Petrovitch, H., White, L. R., Masaki, K. H., Tanner, C. M., Curb, J. D., Grandinetti, A., Blanchette, P. L., Popper, J. S., & Ross, G. W. (2001). Frequency of bowel movements and the future risk of Parkinson's disease. *Neurology*, *57*(3), 456–462.
- Abdu, F., Hicks, G. A., Hennig, G., Allen, J. P., & Grundy, D. (2002). Somatostatin sst(2) receptors inhibit peristalsis in the rat and mouse jejunum. *Am J Physiol Gastrointest Liver Physiol*, 282(4), G624-33. https://doi.org/10.1152/ajpgi.00354.2001
- Abell, T. L., Bernstein, V. K., Cutts, T., Farrugia, G., Forster, J., Hasler, W. L., McCallum, R. W., Olden, K. W., Parkman, H. P., Parrish, C. R., Pasricha, P. J., Prather, C. M., Soffer, E. E., Twillman, R., & Vinik, A. I. (2006). Treatment of gastroparesis: A multidisciplinary clinical review. Neurogastroenterology & Motility, 18(4), 263–283. https://doi.org/10.1111/j.1365-2982.2006.00760.x

- Abrahamsen, H. N., Steiniche, T., Nexo, E., Hamilton-Dutoit, S. J., & Sorensen, B. S. (2003).

 Towards Quantitative mRNA Analysis in Paraffin-Embedded Tissues Using Real-Time

 Reverse Transcriptase-Polymerase Chain Reaction: A Methodological Study on Lymph

 Nodes from Melanoma Patients. *The Journal of Molecular Diagnostics : JMD*, 5(1), 34–41.
- Adduci, A., Martire, M., Taglialatela, M., Arena, V., Rizzo, G., Coco, C., & Currò, D. (2013). Expression and motor functional roles of voltage-dependent type 7 K+ channels in the human taenia coli. *European Journal of Pharmacology*, 721(1–3), 12–20.
- Ahlskog, J. E., & Muenter, M. D. (2001). Frequency of levodopa-related dyskinesias and motor fluctuations as estimated from the cumulative literature. *Movement Disorders: Official Journal of the Movement Disorder Society*, 16(3), 448–458.
- Aizawa, N., Wakamatsu, D., Kida, J., Otsuki, T., Saito, Y., Matsuya, H., Homma, Y., & Igawa, Y. (2017). Inhibitory effects of retigabine, a Kv7 channel activator, on mechanosensitive primary bladder afferent activities and nociceptive behaviors in rats. *Neurourology and Urodynamics*, 36(2), 280–285.
- Albanese, A., Jenner, P., Marsden, C. D., & Stephenson, J. D. (1988). Bladder hyperreflexia induced in marmosets by 1-methyl-4-phenyl-1,2,3,6-tetrahydropyridine. *Neuroscience Letters*, 87(1–2), 46–50.
- Alberico, S. L., Cassell, M. D., & Narayanan, N. S. (2015). The vulnerable ventral tegmental area in Parkinson's disease. *Basal Ganglia*, 5(2–3), 51–55.

- Albin, R. L., Young, A. B., & Penney, J. B. (1989). The functional anatomy of basal ganglia disorders. *Trends in Neurosciences*, *12*(10), 366–375.
- Albuquerque, J. C. S., Mendes, T. S., BrandÃo, M. G. S. A., Frota, A. F., Reis, T. D. de S. dos, Aguiar, L. M. V., & Graça, J. R. V. da. (2021). Structural bases of gastrointestinal motility changes in Parkinson's disease: Study in rats. *ABCD. Arquivos Brasileiros de Cirurgia Digestiva (São Paulo)*, 33.
- Alvarez-Fischer, D., Guerreiro, S., Hunot, S., Saurini, F., Marien, M., Sokoloff, P., Hirsch, E. C., Hartmann, A., & Michel, P. P. (2008). Modelling Parkinson-like neurodegeneration via osmotic minipump delivery of MPTP and probenecid. *Journal of Neurochemistry*, 107(3), 701–711. https://doi.org/10.1111/j.1471-4159.2008.05651.x
- Andersen, I. S., Buntzen, S., Rijkhoff, N. J. M., Dalmose, A. L., Djurhuus, J. C., & Laurberg, S. (2006). Ano-rectal motility responses to pelvic, hypogastric and pudendal nerve stimulation in the Göttingen minipig. *Neurogastroenterology & Motility*, 18(2), 153–161.
- Anderson, Carson, C., & McCloskey, K. D. (2009). KCNQ currents and their contribution to resting membrane potential and the excitability of interstitial cells of Cajal from the guinea pig bladder. *J Urol*, 182(1), 330–336. https://doi.org/10.1016/j.juro.2009.02.108
- Anderson, Noorian, A. R., Taylor, G., Anitha, M., Bernhard, D., Srinivasan, S., & Greene, J. G. (2007). Loss of enteric dopaminergic neurons and associated changes in colon motility in an MPTP mouse model of Parkinson's disease. *Experimental Neurology*, 207(1), 4–12. https://doi.org/10.1016/j.expneurol.2007.05.010

- Andersson, K.-E., & Arner, A. (2004). Urinary bladder contraction and relaxation: Physiology and pathophysiology. *Physiological Reviews*, 84(3), 935–986.
- Angela Pérez-Novo, C., Claeys, C., Speleman, F., Van Cauwenberge, P., Bachert, C., & Vandesompele, J. (2005). Impact of RNA quality on reference gene expression stability. *Biotechniques*, 39(1), 52–56.
- Annerino, D. M., Arshad, S., Taylor, G. M., Adler, C. H., Beach, T. G., & Greene, J. G. (2012).

 Parkinson's disease is not associated with gastrointestinal myenteric ganglion neuron loss.

 Acta Neuropathologica, 124(5), 665–680. https://doi.org/10.1007/s00401-012-1040-2
- Anselmi, L., Bove, C., Coleman, F. H., Le, K., Subramanian, M. P., Venkiteswaran, K., Subramanian, T., & Travagli, R. A. (2018). Ingestion of subthreshold doses of environmental toxins induces ascending Parkinsonism in the rat. *Npj Parkinson's Disease*, 4(1), 30.
- Anselmi, L., Toti, L., Bove, C., Hampton, J., & Travagli, R. A. (2017). A Nigro-Vagal pathway controls gastric motility and is affected in a rat model of parkinsonism. *Gastroenterology*, 153(6), 1581–1593.
- Antkiewicz-Michaluk, L., Wąsik, A., Możdżeń, E., Romańska, I., & Michaluk, J. (2014).

 Antidepressant-like effect of tetrahydroisoquinoline amines in the animal model of depressive disorder induced by repeated administration of a low dose of reserpine:

 Behavioral and neurochemical studies in the rat. *Neurotoxicity Research*, 26, 85–98.

- Apostolova, E., Zagorchev, P., Kokova, V., & Peychev, L. (2017). Retigabine diminishes the effects of acetylcholine, adrenaline and adrenergic agonists on the spontaneous activity of guinea pig smooth muscle strips in vitro. *Autonomic Neuroscience*, 203, 51–57.
- Aquino, C. C., & Fox, S. H. (2015). Clinical spectrum of levodopa-induced complications. *Movement Disorders*, 30(1), 80–89.
- Arai, N., Misugi, K., Goshima, Y., & Misu, Y. (1990). Evaluation of a 1-methyl-4-phenyl-1,2,3,6-tetrahydropyridine (MPTP)-treated C57 black mouse model for parkinsonism. *Brain Research*, 515(1–2), 57–63.
- Araki, I., & Kuno, S. (2000). Assessment of voiding dysfunction in Parkinson's disease by the international prostate symptom score. *Journal of Neurology, Neurosurgery & Psychiatry*, 68(4), 429–433.
- Arbouw, M. E. L., Movig, K. L. L., Koopmann, M., Poels, P. J. E., Guchelaar, H.-J., Egberts, T. C.
 G., Neef, C., & van Vugt, J. P. P. (2010). Glycopyrrolate for sialorrhea in Parkinson disease:
 A randomized, double-blind, crossover trial. *Neurology*, 74(15), 1203–1207.
 https://doi.org/10.1212/WNL.0b013e3181d8c1b7
- Arnhold, M., Dening, Y., Chopin, M., Arévalo, E., Schwarz, M., Reichmann, H., Gille, G., Funk, R.
 H., & Pan-Montojo, F. (2016). Changes in the sympathetic innervation of the gut in rotenone treated mice as possible early biomarker for Parkinson's disease. *Clinical Autonomic Research*, 26(3), 211–222.

- Ashraf, W., Pfeiffer, R. F., Park, F., Lof, J., & Quigley, E. M. M. (1997). Constipation in parkinson's disease: Objective assessment and response to psyllium. *Movement Disorders*, 12(6), 946–951. https://doi.org/10.1002/mds.870120617
- Astarloa, R., Mena, M. A., Sanchez, V., de la Vega, L., & de Yebenes, J. G. (1992). Clinical and pharmacokinetic effects of a diet rich in insoluble fiber on Parkinson disease. *Clinical Neuropharmacology*, 15(5), 375–380.
- Badri, A. V., Purohit, R. S., Skenazy, J., Weiss, J. P., & Blaivas, J. G. (2014). A review of lower urinary tract symptoms in patients with Parkinson's disease. *Current Urology Reports*, 15, 1–9.
- Bagheri, H., Damase-Michel, C., Lapeyre-Mestre, M., Cismondo, S., O'connell, D., Senard, J.-M., Rascol, O., & Montastruc, J.-L. (1999). A study of salivary secretion in Parkinson's disease.
 Clinical Neuropharmacology, 22(4), 213–215.
- Baijens, L. W. J., & Speyer, R. (2009). Effects of Therapy for Dysphagia in Parkinson's Disease: Systematic Review. *Dysphagia*, 24(1), 91–102. https://doi.org/10.1007/s00455-008-9180-1
- Barcia, C., Bahillo, A. S., Fernández-Villalba, E., Bautista, V., Poza Y Poza, M., Fernández-Barreiro, A., Hirsch, E. C., & Herrero, M.-T. (2004). Evidence of active microglia in substantia nigra pars compacta of parkinsonian monkeys 1 year after MPTP exposure. *Glia*, 46(4), 402–409. https://doi.org/10.1002/glia.20015

- Barhanin, J., Lesage, F., Guillemare, E., Fink, M., Lazdunski, M., & Romey, G. (1996). KvLQT1 and IsK (minK) proteins associate to form the IKs cardiac potassium current. *Nature*, 384(6604), 78.
- Barichella, M., Pacchetti, C., Bolliri, C., Cassani, E., Iorio, L., Pusani, C., Pinelli, G., Privitera, G., Cesari, I., Faierman, S. A., Caccialanza, R., Pezzoli, G., & Cereda, E. (2016). Probiotics and prebiotic fiber for constipation associated with Parkinson disease. *An RCT*, 87(12), 1274–1280. https://doi.org/10.1212/wnl.00000000000003127
- Barone, P., Antonini, A., Colosimo, C., Marconi, R., Morgante, L., Avarello, T. P., Bottacchi, E.,
 Cannas, A., Ceravolo, G., Ceravolo, R., Cicarelli, G., Gaglio, R. M., Giglia, R. M., Iemolo,
 F., Manfredi, M., Meco, G., Nicoletti, A., Pederzoli, M., Petrone, A., ... Dotto, P. D. (2009).
 The PRIAMO study: A multicenter assessment of nonmotor symptoms and their impact on
 quality of life in Parkinson's disease. *Movement Disorders*, 24(11), 1641–1649.
 https://doi.org/10.1002/mds.22643
- Barraud, Q., Lambrecq, V., Forni, C., McGuire, S., Hill, M., Bioulac, B., Balzamo, E., Bezard, E., Tison, F., & Ghorayeb, I. (2009). Sleep disorders in Parkinson's disease: The contribution of the MPTP non-human primate model. *Experimental Neurology*, 219(2), 574–582. https://doi.org/10.1016/j.expneurol.2009.07.019
- Barrenschee, M., Zorenkov, D., Böttner, M., Lange, C., Cossais, F., Scharf, A. B., Deuschl, G., Schneider, S. A., Ellrichmann, M., & Fritscher-Ravens, A. (2017). Distinct pattern of enteric

- phospho-alpha-synuclein aggregates and gene expression profiles in patients with Parkinson's disease. *Acta Neuropathologica Communications*, *5*(1), 1–14.
- Bayliss, W. M., & Starling, E. H. (1899). The movements and innervation of the small intestine.

 The Journal of Physiology, 24(2), 99.
- Beck, V. C., Isom, L. L., & Berg, A. T. (2021). Gastrointestinal symptoms and channelopathy-associated epilepsy. *The Journal of Pediatrics*, 237, 41-49. e1.
- Bergman, H., Feingold, A., Nini, A., Raz, A., Slovin, H., Abeles, M., & Vaadia, E. (1998).

 Physiological aspects of information processing in the basal ganglia of normal and parkinsonian primates. *Trends in Neurosciences*, 21(1), 32–38.
- Bergman, H., Raz, A., Feingold, A., Nini, A., Nelken, I., Hilla, B.-P., Hansel, D., & Reches, A. (1998). Physiology of MPTP tremor. *Movement Disorders*, 13(S3), 29–34.
- Berkowitz, D. M., & McCallum, R. W. (1980). Interaction of levodopa and metoclopramide on gastric emptying. *Clinical Pharmacology & Therapeutics*, 27(3), 414–420.
- Berthoud, H. R., Carlson, N. R., & Powley, T. L. (1991). Topography of efferent vagal innervation of the rat gastrointestinal tract. *American Journal of Physiology-Regulatory, Integrative and Comparative Physiology*, 260(1), R200–R207.
- Betts, M. J., O'Neill, M. J., & Duty, S. (2012). Allosteric modulation of the group III mGlu4 receptor provides functional neuroprotection in the 6-hydroxydopamine rat model of Parkinson's disease. *British Journal of Pharmacology*, 166(8), 2317–2330.

- Bientinesi, R., Mancuso, C., Martire, M., Bassi, P. F., Sacco, E., & Currò, D. (2017). KV7 channels in the human detrusor: Channel modulator effects and gene and protein expression. *Naunyn-Schmiedeberg's Archives of Pharmacology*, 390(2), 127–137.
- Biju, K. C., Evans, R. C., Shrestha, K., Carlisle, D. C., Gelfond, J., & Clark, R. A. (2018).
 Methylene blue ameliorates olfactory dysfunction and motor deficits in a chronic
 MPTP/probenecid mouse model of Parkinson's disease. *Neuroscience*, 380, 111–122.
- Bird, M. R., Woodward, M. C., Gibson, E. M., Phyland, D. J., & Fonda, D. (1994). Asymptomatic Swallowing Disorders in Elderly Patients with Parkinson's Disease: A Description of Findings on Clinical Examination and Videofluoroscopy in Sixteen Patients. *Age and Ageing*, 23(3), 251–254. https://doi.org/10.1093/ageing/23.3.251
- Blanchet, P. J., Konitsiotis, S., & Chase, T. N. (1998). Amantadine reduces levodopa-induced dyskinesias in parkinsonian monkeys. *Mov Disord*, *13*(5), 798–802. https://doi.org/10.1002/mds.870130507
- Blandini, F., & Armentero, M.-T. (2012). Animal models of Parkinson's disease. *The FEBS Journal*, 279(7), 1156–1166.
- Blandini, F., Balestra, B., Levandis, G., Cervio, M., Greco, R., Tassorelli, C., Colucci, M., Faniglione, M., Bazzini, E., & Nappi, G. (2009). Functional and neurochemical changes of the gastrointestinal tract in a rodent model of Parkinson's disease. *Neuroscience Letters*, 467(3), 203–207.

- Blandini, F., Levandis, G., Bazzini, E., Nappi, G., & Armentero, M.-T. (2007). Time-course of nigrostriatal damage, basal ganglia metabolic changes and behavioural alterations following intrastriatal injection of 6-hydroxydopamine in the rat: New clues from an old model. *European Journal of Neuroscience*, 25(2), 397–405.
- Bonito-Oliva, A., Masini, D., & Fisone, G. (2014). A mouse model of non-motor symptoms in Parkinson's disease: Focus on pharmacological interventions targeting affective dysfunctions. *Frontiers in Behavioral Neuroscience*, 8, 290.
- Bove, C., Anselmi, L., & Travagli, R. A. (2019). Altered gastric tone and motility response to brain-stem dopamine in a rat model of parkinsonism. *American Journal of Physiology-Gastrointestinal and Liver Physiology*, 317(1), G1–G7.
- Braak, H., de Vos, R. A. I., Bohl, J., & Del Tredici, K. (2006). Gastric α-synuclein immunoreactive inclusions in Meissner's and Auerbach's plexuses in cases staged for Parkinson's disease-related brain pathology. *Neuroscience Letters*, *396*(1), 67–72. https://doi.org/10.1016/j.neulet.2005.11.012
- Braak, H., Sastre, M., Bohl, J. R. E., de Vos, R. A. I., & Del Tredici, K. (2007). Parkinson's disease: Lesions in dorsal horn layer I, involvement of parasympathetic and sympathetic pre- and postganglionic neurons. *Acta Neuropathologica*, 113(4), 421–429. https://doi.org/10.1007/s00401-007-0193-x

- Braak, H., Tredici, K. D., Rüb, U., de Vos, R. A. I., Jansen Steur, E. N. H., & Braak, E. (2003).

 Staging of brain pathology related to sporadic Parkinson's disease. *Neurobiology of Aging*, 24(2), 197–211. https://doi.org/10.1016/S0197-4580(02)00065-9
- Brading, A. F., & Williams, J. H. (1990). Contractile responses of smooth muscle strips from rat and guinea-pig urinary bladder to transmural stimulation: Effects of atropine and alpha, beta-methylene ATP. *British Journal of Pharmacology*, 99(3), 493.
- Breger, L. S., & Fuzzati Armentero, M. T. (2019). Genetically engineered animal models of Parkinson's disease: From worm to rodent. *European Journal of Neuroscience*, 49(4), 533–560.
- Brickel, N., Gandhi, P., VanLandingham, K., Hammond, J., & DeRossett, S. (2012). The urinary safety profile and secondary renal effects of retigabine (ezogabine): A first-in-class antiepileptic drug that targets KCNQ (Kv7) potassium channels. *Epilepsia*, 53(4), 606–612.
- Brookes, S. J. H., Chen, B. N., Costa, M., & Humphreys, C. M. S. (1999). Initiation of peristalsis by circumferential stretch of flat sheets of guinea-pig ileum. *The Journal of Physiology*, *516*(2), 525–538.
- Brown, D. A., & Adams, P. R. (1980). Muscarinic suppression of a novel voltage-sensitive K+current in a vertebrate neurone. *Nature*, *283*, 673. https://doi.org/10.1038/283673a0
- Brown, D. A., & Passmore, G. M. (2009). Neural KCNQ (Kv7) channels. *British Journal of Pharmacology*, *156*(8), 1185–1195. https://doi.org/10.1111/j.1476-5381.2009.00111.x

- Browning, K. N., Renehan, W. E., & Travagli, R. A. (1999). Electrophysiological and morphological heterogeneity of rat dorsal vagal neurones which project to specific areas of the gastrointestinal tract. *The Journal of Physiology*, 517(2), 521–532.
- Brueggemann, L. I., Haick, J. M., Cribbs, L. L., & Byron, K. L. (2014). Differential activation of vascular smooth muscle Kv7.4, Kv7.5, and Kv7.4/7.5 channels by ML213 and ICA-069673.

 Mol Pharmacol, 86(3), 330–341. https://doi.org/10.1124/mol.114.093799
- Brusa, L., Petta, F., Farullo, G., Iacovelli, V., Ponzo, V., Iani, C., Stanzione, P., & Agró, E. F. (2017). Rotigotine effects on bladder function in patients with Parkinson's disease.

 Movement Disorders Clinical Practice, 4(4), 586–589.
- Brusa, L., Petta, F., Pisani, A., Moschella, V., Iani, C., Stanzione, P., Miano, R., & Finazzi-Agrò, E. (2007). Acute vs chronic effects of l-dopa on bladder function in patients with mild Parkinson disease. *Neurology*, 68(18), 1455–1459.
- Burré, J., Sharma, M., & Südhof, T. C. (2018). Cell biology and pathophysiology of α-synuclein.

 Cold Spring Harbor Perspectives in Medicine, 8(3).
- Bushmann, M., Dobmeyer, S. M., Leeker, L., & Perlmutter, J. S. (1989). Swallowing abnormalities and their response to treatment in Parkinson's disease. *Neurology*, *39*(10), 1309–1309.
- Bustin, S. A., Benes, V., Nolan, T., & Pfaffl, M. W. (2005). Quantitative real-time RT-PCR-a perspective. *Journal of Molecular Endocrinology*, *34*(3), 597–601.

- Calabresi, P., Di Filippo, M., Ghiglieri, V., Tambasco, N., & Picconi, B. (2010). Levodopa-induced dyskinesias in patients with Parkinson's disease: Filling the bench-to-bedside gap. *The Lancet Neurology*, *9*(11), 1106–1117.
- Camacho, M., Greenland, J. C., & Williams-Gray, C. H. (2021). The gastrointestinal dysfunction scale for Parkinson's disease. *Movement Disorders*, *36*(10), 2358–2366.
- Campeau, L., Soler, R., & Andersson, K.-E. (2011). Bladder dysfunction and parkinsonism: Current pathophysiological understanding and management strategies. *Current Urology Reports*, 12(6), 396–403.
- Campeau, L., Soler, R., Sittadjody, S., Pareta, R., Nomiya, M., Zarifpour, M., Opara, E. C., Yoo, J. J., & Andersson, K.-E. (2014). Effects of allogeneic bone marrow derived mesenchymal stromal cell therapy on voiding function in a rat model of Parkinson disease. *The Journal of Urology*, 191(3), 850–859.
- Carlsson, A., Lindqvist, M., & Magnusson, T. O. R. (1957). 3, 4-Dihydroxyphenylalanine and 5-hydroxytryptophan as reserpine antagonists. *Nature*, *180*(4596), 1200–1200.
- Carmona-Abellan, M., Martínez-Valbuena, I., DiCaudo, C., Marcilla, I., & Luquin, M. R. (2019).

 Cardiac sympathetic innervation in the MPTP non-human primate model of Parkinson disease. *Clinical Autonomic Research*, 29(4), 415–425.

- Carrick, D. M., Mehaffey, M. G., Sachs, M. C., Altekruse, S., Camalier, C., Chuaqui, R., Cozen, W., Das, B., Hernandez, B. Y., & Lih, C.-J. (2015). Robustness of next generation sequencing on older formalin-fixed paraffin-embedded tissue. *PloS One*, *10*(7), e0127353.
- Cersosimo, M. G., & Benarroch, E. E. (2012). Pathological correlates of gastrointestinal dysfunction in Parkinson's disease. *Neurobiology of Disease*, *46*(3), 559–564.
- Chai, X., Diwakarla, S., Pustovit, R. V., McQuade, R. M., Di Natale, M., Ermine, C. M., Parish, C. L., Finkelstein, D. I., & Furness, J. B. (2020). Investigation of nerve pathways mediating colorectal dysfunction in Parkinson's disease model produced by lesion of nigrostriatal dopaminergic neurons. *Neurogastroenterology & Motility*, 32(9), e13893.
- Chang, H. Y., Mashimo, H., & Goyal, R. K. (2003). IV. Current concepts of vagal efferent projections to the gut. *American Journal of Physiology-Gastrointestinal and Liver Physiology*, 284(3), G357–G366.
- Charcot, J. M. (1872). De la paralysie agitante. In Oeuvres Complètes (t 1) Leçons sur les maladies du système nerveux, pp. 155–188. A Delahaye, Paris. [In English: Charcot J-M. 1877. On Parkinson's Disease. In Lectures on Diseases of the Nervous System Delivered at the Salpêtrière (Transl. Sigerson G), Pp. 129–156. New Sydenham Society, London.], 1.
- Chaudhuri, K. R., Martinez-Martin, P., Schapira, A. H. V., Stocchi, F., Sethi, K., Odin, P., Brown,
 R. G., Koller, W., Barone, P., MacPhee, G., Kelly, L., Rabey, M., MacMahon, D., Thomas,
 S., Ondo, W., Rye, D., Forbes, A., Tluk, S., Dhawan, V., ... Olanow, C. W. (2006).
 International multicenter pilot study of the first comprehensive self-completed nonmotor

268

- symptoms questionnaire for Parkinson's disease: The NMSQuest study. *Movement Disorders*, 21(7), 916–923. https://doi.org/10.1002/mds.20844
- Chaumette, T., Lebouvier, T., Aubert, P., Lardeux, B., Qin, C., Li, Q., Accary, D., Bezard, E., Bruley des Varannes, S., & Derkinderen, P. (2009). Neurochemical plasticity in the enteric nervous system of a primate animal model of experimental Parkinsonism.

 Neurogastroenterology & Motility, 21(2), 215–222.
- Chen, H., Ordog, T., Chen, J., Young, D. L., Bardsley, M. R., Redelman, D., Ward, S. M., & Sanders, K. M. (2007). Differential gene expression in functional classes of interstitial cells of Cajal in murine small intestine. *Physiological Genomics*, 31(3), 492–509.
- Choi, Y., Kim, A., Kim, J., Lee, J., Lee, S. Y., & Kim, C. (2017). Optimization of RNA Extraction from Formalin-Fixed Paraffin-Embedded Blocks for Targeted Next-Generation Sequencing. *Journal of Breast Cancer*, 20(4), 393–399. https://doi.org/10.4048/jbc.2017.20.4.393
- Choudhury, G. R., & Daadi, M. M. (2018). Charting the onset of Parkinson-like motor and non-motor symptoms in nonhuman primate model of Parkinson's disease. *PLoS One*, *13*(8), e0202770.
- Chung, B. H., Choi, S. K., & Chang, K. C. (1996). Effects of nitric oxide on detrusor relaxation. The Journal of Urology, 155(6), 2090–2093.
- Church, F. C. (2021). Treatment options for motor and non-motor symptoms of Parkinson's disease. *Biomolecules*, 11(4), 612.

- Cicchetti, F., Brownell, A. L., Williams, K., Chen, Y. I., Livni, E., & Isacson, O. (2002).

 Neuroinflammation of the nigrostriatal pathway during progressive 6-OHDA dopamine degeneration in rats monitored by immunohistochemistry and PET imaging. *European Journal of Neuroscience*, 15(6), 991–998.
- Ciucci, M. R., Russell, J. A., Schaser, A. J., Doll, E. J., Vinney, L. M., & Connor, N. P. (2011).

 Tongue force and timing deficits in a rat model of Parkinson disease. *Behavioural Brain Research*, 222(2), 315–320. https://doi.org/10.1016/j.bbr.2011.03.057
- Clemente, C. M., Araújo, P. V., Palheta Jr, R. C., Ratts, Z. M., Fernandes, G. H., Rola, F. H., De Oliveira, R. B., Dos Santos, A. A., & Magalhães, P. J. (2008). Sildenafil inhibits duodenal contractility via activation of the NO–K+ channel pathway. *Fundamental & Clinical Pharmacology*, 22(1), 61–67.
- Coletto, E., Dolan, J. S., Pritchard, S., Gant, A., Hikima, A., Jackson, M. J., Benham, C. D., Chaudhuri, K. R., Rose, S., Jenner, P., & Iravani, M. M. (2019). Contractile dysfunction and nitrergic dysregulation in small intestine of a primate model of Parkinson's disease. *Npj Parkinson's Disease*, *5*(1), 1–12. https://doi.org/10.1038/s41531-019-0081-9
- Coletto, E., Tough, I. R., Pritchard, S., Hikima, A., Jackson, M. J., Jenner, P., Ray Chaudhuri, K., Cox, H. M., Iravani, M. M., & Rose, S. (2021). Dysregulation of epithelial ion transport and neurochemical changes in the colon of a parkinsonian primate. *Npj Parkinson's Disease*, 7(1), 1–11. https://doi.org/10.1038/s41531-020-00150-x

- Colucci, M., Cervio, M., Faniglione, M., De Angelis, S., Pajoro, M., Levandis, G., Tassorelli, C., Blandini, F., Feletti, F., De Giorgio, R., Dellabianca, A., Tonini, S., & Tonini, M. (2012).

 Intestinal dysmotility and enteric neurochemical changes in a Parkinson's disease rat model.

 Autonomic Neuroscience, 169(2), 77–86. https://doi.org/10.1016/j.autneu.2012.04.005
- Corbillé, A.-G., Coron, E., Neunlist, M., Derkinderen, P., & Lebouvier, T. (2014). Appraisal of the dopaminergic and noradrenergic innervation of the submucosal plexus in PD. *Journal of Parkinson's Disease*, 4(4), 571–576.
- Dadar, M., Gee, M., Shuaib, A., Duchesne, S., & Camicioli, R. (2020). Cognitive and motor correlates of grey and white matter pathology in Parkinson's disease. *NeuroImage: Clinical*, 27, 102353.
- de Moraes Thomasi, B. B., Valdetaro, L., Ricciardi, M. C. G., Hayashide, L., Fernandes, A. C. M. N., Mussauer, A., da Silva, M. L., da Cunha Faria-Melibeu, A., Ribeiro, M. G. L., & de Mattos Coelho-Aguiar, J. (2022). Enteric glial cell reactivity in colonic layers and mucosal modulation in a mouse model of Parkinson's disease induced by 6-hydroxydopamine. *Brain Research Bulletin*, 187, 111–121.
- Del Tredici, K., & Braak, H. (2012). Spinal cord lesions in sporadic Parkinson's disease. *Acta Neuropathologica*, *124*, 643–664.
- Del Tredici, K., Hawkes, C. H., Ghebremedhin, E., & Braak, H. (2010). Lewy pathology in the submandibular gland of individuals with incidental Lewy body disease and sporadic

- Parkinson's disease. *Acta Neuropathologica*, *119*(6), 703–713. https://doi.org/10.1007/s00401-010-0665-2
- DeLong, M. R., & Wichmann, T. (2015). Basal ganglia circuits as targets for neuromodulation in Parkinson disease. *JAMA Neurology*, 72(11), 1354–1360.
- Deumens, R., Blokland, A., & Prickaerts, J. (2002). Modeling Parkinson's disease in rats: An evaluation of 6-OHDA lesions of the nigrostriatal pathway. *Experimental Neurology*, 175(2), 303–317.
- Doi, H., Sakakibara, R., Sato, M., Masaka, T., Kishi, M., Tateno, A., Tateno, F., Tsuyusaki, Y., & Takahashi, O. (2012). Plasma levodopa peak delay and impaired gastric emptying in Parkinson's disease. *Journal of the Neurological Sciences*, 319(1), 86–88. https://doi.org/10.1016/j.jns.2012.05.010
- Domingos, J., Keus, S. H., Dean, J., de Vries, N. M., Ferreira, J. J., & Bloem, B. R. (2018). The European physiotherapy guideline for Parkinson's disease: Implications for neurologists. *Journal of Parkinson's Disease*, 8(4), 499–502.
- Drolet, R. E., Cannon, J. R., Montero, L., & Greenamyre, J. T. (2009). Chronic rotenone exposure reproduces Parkinson's disease gastrointestinal neuropathology. *Neurobiology of Disease*, 36(1), 96–102.

- Dutkiewicz, J., Szlufik, S., Nieciecki, M., Charzyńska, I., Królicki, L., Smektała, P., & Friedman, A. (2015a). Small intestine dysfunction in Parkinson's disease. *Journal of Neural Transmission*, 122(12), 1659–1661. https://doi.org/10.1007/s00702-015-1442-0
- Dutkiewicz, J., Szlufik, S., Nieciecki, M., Charzyńska, I., Królicki, L., Smektała, P., & Friedman, A. (2015b). Small intestine dysfunction in Parkinson's disease. *Journal of Neural Transmission*, 122(12), 1659–1661.
- Duty, S., & Jenner, P. (2011). Animal models of Parkinson's disease: A source of novel treatments and clues to the cause of the disease. *British Journal of Pharmacology*, *164*(4), 1357–1391. https://doi.org/10.1111/j.1476-5381.2011.01426.x
- Eaker, E. Y., Bixler, G. B., Dunn, A. J., Moreshead, W. V., & Mathias, J. R. (1987). Chronic alterations in jejunal myoelectric activity in rats due to MPTP. *American Journal of Physiology-Gastrointestinal and Liver Physiology*, 253(6), G809–G815.
- Eglen, R. M. (2001). Muscarinic receptors and gastrointestinal tract smooth muscle function. *Life Sciences*, 68(22–23), 2573–2578.
- El-Agnaf, O. M., Salem, S. A., Paleologou, K. E., Cooper, L. J., Fullwood, N. J., Gibson, M. J., Curran, M. D., Court, J. A., Mann, D. M., & Ikeda, S.-I. (2003). α-Synuclein implicated in Parkinson's disease is present in extracellular biological fluids, including human plasma.

 The FASEB Journal, 17(13), 1–16.

- Emmanouilidou, E., Melachroinou, K., Roumeliotis, T., Garbis, S. D., Ntzouni, M., Margaritis, L. H., Stefanis, L., & Vekrellis, K. (2010). Cell-produced α-synuclein is secreted in a calcium-dependent manner by exosomes and impacts neuronal survival. *Journal of Neuroscience*, 30(20), 6838–6851.
- Fasano, A., Bove, F., Gabrielli, M., Petracca, M., Zocco, M. A., Ragazzoni, E., Barbaro, F., Piano, C., Fortuna, S., Tortora, A., Di Giacopo, R., Campanale, M., Gigante, G., Lauritano, E. C., Navarra, P., Marconi, S., Gasbarrini, A., & Bentivoglio, A. R. (2013). The role of small intestinal bacterial overgrowth in Parkinson's disease. *Movement Disorders*, 28(9), 1241–1249. https://doi.org/10.1002/mds.25522
- Fasano, A., Visanji, N. P., Liu, L. W., Lang, A. E., & Pfeiffer, R. F. (2015). Gastrointestinal dysfunction in Parkinson's disease. *Lancet Neurol*, *14*(6), 625–639. https://doi.org/10.1016/S1474-4422(15)00007-1
- Fathian-Sabet, B., BLOCH, W., KLOTZ, T., NIGGEMANN, S., JACOBS, G., ADDICKS, K., & ENGELMANN, U. (2001). LOCALIZATION OF CONSTITUTIVE NITRIC OXIDE SYNTHASE ISOFORMS AND THE NITRIC OXIDE TARGET ENZYME SOLUBLE GUANYLYL CYCLASE IN THE HUMAN BLADDER. *The Journal of Urology*, *165*(5), 1724–1729. https://doi.org/10.1016/S0022-5347(05)66402-6
- Feng, X.-Y., Yan, J.-T., Zhang, X.-L., & Zhu, J.-X. (2019). Gastrointestinal non-motor dysfunction in Parkinson's disease model rats with 6-hydroxydopamine. *Physiological Research*, 68(2), 295–303.

- Ferraro, T. N., Golden, G. T., DeMattei, M., Hare, T. A., & Fariello, R. G. (1986). Effect of 1-methyl-4-phemyl-1,2,3,6-tetrahydropyridine (MPTP) on levels of glutathione in the extrapyramidal system of the mouse. *Neuropharmacology*, *25*(9), 1071–1074. https://doi.org/10.1016/0028-3908(86)90205-4
- Fitzmaurice, H., Fowler, C. J., Rickards, D., Kirby, R. S., Quinn, N. P., Marsden, C. D., Milroy, E. J. G., & Turner-Warwick, R. T. (1985). Micturition disturbance in Parkinson's disease.

 British Journal of Urology, 57(6), 652–656.
- Fleige, S., & Pfaffl, M. W. (2006). RNA integrity and the effect on the real-time qRT-PCR performance. *Molecular Aspects of Medicine*, 27(2–3), 126–139.
- Fornai, M., Pellegrini, C., Antonioli, L., Segnani, C., Ippolito, C., Barocelli, E., Ballabeni, V., Vegezzi, G., Al Harraq, Z., & Blandini, F. (2016). Enteric dysfunctions in experimental Parkinson's disease: Alterations of excitatory cholinergic neurotransmission regulating colonic motility in rats. *Journal of Pharmacology and Experimental Therapeutics*, 356(2), 434–444.
- Fornai, Schlüter, O. M., Lenzi, P., Gesi, M., Ruffoli, R., Ferrucci, M., Lazzeri, G., Busceti, C. L.,
 Pontarelli, F., Battaglia, G., Pellegrini, A., Nicoletti, F., Ruggieri, S., Paparelli, A., &
 Südhof, T. C. (2005). Parkinson-like syndrome induced by continuous MPTP infusion:
 Convergent roles of the ubiquitin-proteasome system and α-synuclein. *Proceedings of the National Academy of Sciences of the United States of America*, 102(9), 3413–3418.
 https://doi.org/10.1073/pnas.0409713102

- Forno, L. S., Langston, J. W., DeLanney, L. E., Irwin, I., & Ricaurte, G. A. (1986). Locus ceruleus lesions and eosinophilic inclusions in MPTP-treated monkeys. *Annals of Neurology: Official Journal of the American Neurological Association and the Child Neurology Society*, 20(4), 449–455.
- Fredriksson, A., Palomo, T., Chase, T., & Archer, T. (1999). Tolerance to a suprathreshold dose of L-Dopa in MPTP mice: Effects of glutamate antagonists. *Journal of Neural Transmission*, 106(3), 283–300. https://doi.org/10.1007/s007020050158
- Fry, C. H., Meng, E., & Young, J. S. (2010). The physiological function of lower urinary tract smooth muscle. *Autonomic Neuroscience*, *154*(1–2), 3–13.
- Fujiwara, H., Hasegawa, M., Dohmae, N., Kawashima, A., Masliah, E., Goldberg, M. S., Shen, J., Takio, K., & Iwatsubo, T. (2002). α-Synuclein is phosphorylated in synucleinopathy lesions. Nature Cell Biology, 4(2), 160–164.
- Furuya, T., Hayakawa, H., Yamada, M., Yoshimi, K., Hisahara, S., Miura, M., Mizuno, Y., & Mochizuki, H. (2004). Caspase-11 mediates inflammatory dopaminergic cell death in the 1-methyl-4-phenyl-1, 2, 3, 6-tetrahydropyridine mouse model of Parkinson's disease. *Journal of Neuroscience*, 24(8), 1865–1872.
- Gabrielli, M., Bonazzi, P., Scarpellini, E., Bendia, E., Lauritano, E. C., Fasano, A., Ceravolo, M.
 G., Capecci, M., Rita Bentivoglio, A., Provinciali, L., Tonali, P. A., & Gasbarrini, A.
 (2011). Prevalence of Small Intestinal Bacterial Overgrowth in Parkinson's Disease.
 Movement Disorders, 26(5), 889–892. https://doi.org/10.1002/mds.23566

- Gai, W. P., Blumbergs, P. C., Geffen, L. B., & Blessing, W. W. (1992). Age-related loss of dorsal vagal neurons in Parkinson's disease. *Neurology*, 42(11), 2106–2111.
- Galvan, A., & Wichmann, T. (2008). Pathophysiology of parkinsonism. *Clinical Neurophysiology*, 119(7), 1459–1474.
- Galvin, J. E., Schuck, T. M., Lee, V. M.-Y., & Trojanowski, J. Q. (2001). Differential expression and distribution of α-, β-, and γ-synuclein in the developing human substantia nigra. *Experimental Neurology*, *168*(2), 347–355.
- Gamper, N., Zaika, O., Li, Y., Martin, P., Hernandez, C. C., Perez, M. R., Wang, A. Y., Jaffe, D.
 B., & Shapiro, M. S. (2006). Oxidative modification of M-type K+ channels as a mechanism of cytoprotective neuronal silencing. *The EMBO Journal*, 25(20), 4996–5004.
 https://doi.org/10.1038/sj.emboj.7601374
- Giancola, F., Torresan, F., Repossi, R., Bianco, F., Latorre, R., Ioannou, A., Guarino, M., Volta, U.,
 Clavenzani, P., Mazzoni, M., Chiocchetti, R., Bazzoli, F., Travagli, R. A., Sternini, C., & De
 Giorgio, R. (2017). Downregulation of neuronal vasoactive intestinal polypeptide in
 Parkinson's disease and chronic constipation. *Neurogastroenterol Motil*, 29(5).
 https://doi.org/10.1111/nmo.12995
- Giannantoni, A., Conte, A., Proietti, S., Giovannozzi, S., Rossi, A., Fabbrini, G., Porena, M., & Berardelli, A. (2011). Botulinum toxin type A in patients with Parkinson's disease and refractory overactive bladder. *The Journal of Urology*, 186(3), 960–964.

- Glinka, Y. Y., & Youdim, M. B. H. (1995). Inhibition of mitochondrial complexes I and IV by 6-hydroxydopamine. *European Journal of Pharmacology: Environmental Toxicology and Pharmacology*, 292(3), 329–332. https://doi.org/10.1016/0926-6917(95)90040-3
- Goetz, C. G., Damier, P., Hicking, C., Laska, E., Müller, T., Olanow, C. W., Rascol, O., & Russ, H. (2007). Sarizotan as a treatment for dyskinesias in Parkinson's disease: A double-blind placebo-controlled trial. *Movement Disorders*, 22(2), 179–186.
 https://doi.org/10.1002/mds.21226
- Gómez-Benito, M., Granado, N., García-Sanz, P., Michel, A., Dumoulin, M., & Moratalla, R. (2020). Modeling Parkinson's disease with the alpha-synuclein protein. *Frontiers in Pharmacology*, 11, 356.
- Greenbaum, D., Colangelo, C., Williams, K., & Gerstein, M. (2003). Comparing protein abundance and mRNA expression levels on a genomic scale. *Genome Biology*, 4(9), 1–8.
- Greene, J. G. (2011). Animal models of gastrointestinal problems in Parkinson's disease. *J Parkinsons Dis*, 1(2), 137–149. https://doi.org/10.3233/JPD-2011-11033
- Greene, J. G., Noorian, A. R., & Srinivasan, S. (2009). Delayed gastric emptying and enteric nervous system dysfunction in the rotenone model of Parkinson's disease. *Experimental Neurology*, 218(1), 154–161.
- Greenwood, I. A., & Ohya, S. (2009). New tricks for old dogs: KCNQ expression and role in smooth muscle. *British Journal of Pharmacology*, *156*(8), 1196–1203.

- Gries, M., Christmann, A., Schulte, S., Weyland, M., Rommel, S., Martin, M., Baller, M., Röth, R., Schmitteckert, S., & Unger, M. (2021). Parkinson mice show functional and molecular changes in the gut long before motoric disease onset. *Molecular Neurodegeneration*, *16*(1), 1–23.
- Grinberg, L. T., Rueb, U., di Lorenzo Alho, A. T., & Heinsen, H. (2010). Brainstem pathology and non-motor symptoms in PD. *Journal of the Neurological Sciences*, 289(1), 81–88.
- Grosch, J., Winkler, J., & Kohl, Z. (2016). Early degeneration of both dopaminergic and serotonergic axons—a common mechanism in Parkinson's disease. *Frontiers in Cellular Neuroscience*, 10, 293.
- Grospe, G. M., Baker, P. M., & Ragozzino, M. E. (2018). Cognitive flexibility deficits following 6-OHDA lesions of the rat dorsomedial striatum. *Neuroscience*, 374, 80–90.
- Grötzsch, H., Sztajzel, R., & Burkhard, P. R. (2007). Levodopa-induced ocular dyskinesia in Parkinson's disease. *European Journal of Neurology*, *14*(10), 1124–1128.
- Han, N.-R., Kim, Y.-K., Ahn, S., Hwang, T.-Y., Lee, H., & Park, H.-J. (2021). A comprehensive phenotype of non-motor impairments and distribution of alpha-synuclein deposition in parkinsonism-induced mice by a combination injection of MPTP and probenecid. *Frontiers in Aging Neuroscience*, 12, 599045.
- Hanani, M. (1990). Rapid effects of MPTP in the mouse colon. *European Journal of Pharmacology*, 175(3), 273–277.

- Hansen, H. H., Ebbesen, C., Mathiesen, C., Weikop, P., Rønn, L. C., Waroux, O., Scuvee-Moreau, J., Seutin, V., & Mikkelsen, J. D. (2006). The KCNQ channel opener retigabine inhibits the activity of mesencephalic dopaminergic systems of the rat. *Journal of Pharmacology and Experimental Therapeutics*, 318(3), 1006–1019.
- Haskel, Y., & Hanani, M. (1994). Inhibition of gastrointestinal motility by MPTP via adrenergic and dopaminergic mechanisms. *Digestive Diseases and Sciences*, *39*(11), 2364–2367.
- Hasler, W. L. (2008). Motility of the small intestine and colon. *Textbook of Gastroenterology*, 231–263.
- Hasler, W. L. (2009). Motility of the small intestine and colon. *Textbook of Gastroenterology*, *1*, 231–263.
- Hassan, A.-A., Sleet, B., Cousins, Z., & Keating, C. D. (2020). TRPA1 channel activation inhibits motor activity in the mouse colon. *Frontiers in Neuroscience*, *14*, 471.
- Hauser, R. A., Salin, L., Juhel, N., & Konyago, V. L. (2007). Randomized trial of the triple monoamine reuptake inhibitor NS 2330 (tesofensine) in early Parkinson's disease. *Mov Disord*, 22(3), 359–365. https://doi.org/10.1002/mds.21258
- Hawkes, C. H., Del Tredici, K., & Braak, H. (2007). Parkinson's disease: A dual-hit hypothesis.

 Neuropathology and Applied Neurobiology, 33(6), 599–614.

- Hawkes, C. H., Del Tredici, K., & Braak, H. (2010). A timeline for Parkinson's disease.

 *Parkinsonism & Related Disorders, 16(2), 79–84.

 https://doi.org/10.1016/j.parkreldis.2009.08.007
- He, X., Yuan, W., Li, Z., Hou, Y., Liu, F., & Feng, J. (2018). 6-Hydroxydopamine induces autophagic flux dysfunction by impairing transcription factor EB activation and lysosomal function in dopaminergic neurons and SH-SY5Y cells. *Toxicology Letters*, 283, 58–68.
- Heetun, Z. S., & Quigley, E. M. M. (2012). Gastroparesis and Parkinson's disease: A systematic review. *Parkinsonism & Related Disorders*, *18*(5), 433–440. https://doi.org/10.1016/j.parkreldis.2011.12.004
- Hely, M. A., Reid, W. G. J., Adena, M. A., Halliday, G. M., & Morris, J. G. L. (2008). The Sydney multicenter study of Parkinson's disease: The inevitability of dementia at 20 years.
 Movement Disorders, 23(6), 837–844. https://doi.org/10.1002/mds.21956
- Hennig, G. W., Costa, M., Chen, B. N., & Brookes, S. J. H. (1999). Quantitative analysis of peristalsis in the guinea-pig small intestine using spatio-temporal maps. *The Journal of Physiology*, 517(2), 575–590.
- Holmqvist, S., Chutna, O., Bousset, L., Aldrin-Kirk, P., Li, W., Björklund, T., Wang, Z.-Y., Roybon, L., Melki, R., & Li, J.-Y. (2014). Direct evidence of Parkinson pathology spread from the gastrointestinal tract to the brain in rats. *Acta Neuropathologica*, *128*(6), 805–820.

- Huizinga, J. D., Stern, H. S., Chow, E., Diamant, N. E., & El-Sharkawy, T. Y. (1985).

 Electrophysiologic control of motility in the human colon. *Gastroenterology*, 88(2), 500–511.
- Hung, H. C., & Lee, E. H. (1996). The mesolimbic dopaminergic pathway is more resistant than the nigrostriatal dopaminergic pathway to MPTP and MPP+ toxicity: Role of BDNF gene expression. *Brain Res Mol Brain Res*, 41(1–2), 14–26.
- Hyson, H. C., Johnson, A. M., & Jog, M. S. (2002). Sublingual Atropine for sialorrhea secondary to parkinsonism: A pilot study. *Movement Disorders*, 17(6), 1318–1320. https://doi.org/10.1002/mds.10276
- Ikeda, Y., & Kanai, A. (2008). Urotheliogenic modulation of intrinsic activity in spinal cord-transected rat bladders: Role of mucosal muscarinic receptors. *American Journal of Physiology-Renal Physiology*, 295(2), F454–F461.
- Imbert, C., Bezard, E., Guitraud, S., Boraud, T., & Gross, C. E. (2000). Comparison of eight clinical rating scales used for the assessment of MPTP-induced parkinsonism in the Macaque monkey. *Journal of Neuroscience Methods*, *96*(1), 71–76.
- Inden, M., Kitamura, Y., Takeuchi, H., Yanagida, T., Takata, K., Kobayashi, Y., Taniguchi, T., Yoshimoto, K., Kaneko, M., Okuma, Y., Taira, T., Ariga, H., & Shimohama, S. (2007).
 Neurodegeneration of mouse nigrostriatal dopaminergic system induced by repeated oral administration of rotenone is prevented by 4-phenylbutyrate, a chemical chaperone. *Journal of Neurochemistry*, 101(6), 1491–1504. https://doi.org/10.1111/j.1471-4159.2006.04440.x

- Ipavec, V., Martire, M., Barrese, V., Taglialatela, M., & Currò, D. (2011). KV7 channels regulate muscle tone and nonadrenergic noncholinergic relaxation of the rat gastric fundus.

 *Pharmacological Research, 64(4), 397–409.
- Iravani, M. M., & Zar, M. A. (1994). Neuropeptide Y in rat detrusor and its effect on nervemediated and acetylcholine-evoked contractions. *British Journal of Pharmacology*, *113*(1), 95–102. PubMed. https://doi.org/10.1111/j.1476-5381.1994.tb16179.x
- Jackson, M. J., Smith, L. A., Al-Barghouthy, G., Rose, S., & Jenner, P. (2007). Decreased expression of l-dopa-induced dyskinesia by switching to ropinirole in MPTP-treated common marmosets. *Experimental Neurology*, 204(1), 162–170.
- Jackson-Lewis, V., & Przedborski, S. (2007). Protocol for the MPTP mouse model of Parkinson's disease. *Nature Protocols*, 2(1), 141–151.
- Jackson-Lewis, V., & Smeyne, R. J. (2005). MPTP and SNpc DA neuronal vulnerability: Role of dopamine, superoxide and nitric oxide in neurotoxicity. Minireview. *Neurotox Res*, 7(3), 193–201.
- Jenner, P. (1989). Clues to the mechanism underlying dopamine cell death in Parkinson's disease. *Journal of Neurology, Neurosurgery, and Psychiatry*, 52(Suppl), 22–28.
- Jepps, T. A., Bentzen, B. H., Stott, J. B., Povstyan, O. V., Sivaloganathan, K., Dalby-Brown, W., & Greenwood, I. A. (2014). Vasorelaxant effects of novel K(v)7.4 channel enhancers ML213

- and NS15370. *British Journal of Pharmacology*, *171*(19), 4413–4424. https://doi.org/10.1111/bph.12805
- Jepps, T. A., Greenwood, I. A., Moffatt, J. D., Sanders, K. M., & Ohya, S. (2009). Molecular and functional characterization of K(v)7 K(+) channel in murine gastrointestinal smooth muscles. *American Journal of Physiology Gastrointestinal and Liver Physiology*, 297(1), G107–G115. https://doi.org/10.1152/ajpgi.00057.2009
- Jepps, T. A., Olesen, S. P., & Greenwood, I. A. (2013). One man's side effect is another man's therapeutic opportunity: Targeting Kv7 channels in smooth muscle disorders. *British Journal of Pharmacology*, 168(1), 19–27. https://doi.org/10.1111/j.1476-5381.2012.02133.x
- Jepps, T. A., Olesen, S. P., Greenwood, I. A., & Dalsgaard, T. (2016). Molecular and functional characterization of Kv 7 channels in penile arteries and corpus cavernosum of healthy and metabolic syndrome rats. *British Journal of Pharmacology*, 173(9), 1478–1490. https://doi.org/10.1111/bph.13444
- Ji, G., Barsotti, R. J., Feldman, M. E., & Kotlikoff, M. I. (2002). Stretch-induced calcium release in smooth muscle. *The Journal of General Physiology*, 119(6), 533–543.
- Joshi, S., Balan, P., & Gurney, A. M. (2006). Pulmonary vasoconstrictor action of KCNQ potassium channel blockers. *Respiratory Research*, 7(1), 31–31. https://doi.org/10.1186/1465-9921-7-31

- Joshi, S., Sedivy, V., Hodyc, D., Herget, J., & Gurney, A. M. (2009). KCNQ Modulators Reveal a Key Role for KCNQ Potassium Channels in Regulating the Tone of Rat Pulmonary Artery Smooth Muscle. *Journal of Pharmacology and Experimental Therapeutics*, 329(1), 368.
- Jost, W. H. (2010). Gastrointestinal dysfunction in Parkinson's Disease. *Journal of the Neurological Sciences*, 289(1), 69–73. https://doi.org/10.1016/j.jns.2009.08.020
- Kadoguchi, N., Kimoto, H., Yano, R., Kato, H., & Araki, T. (2008). Failure of acute administration with proteasome inhibitor to provide a model of Parkinson's disease in mice. *Metabolic Brain Disease*, 23, 147–154.
- Kadoguchi, N., Umeda, M., Kato, H., & Araki, T. (2008). Proteasome inhibitor does not enhance MPTP neurotoxicity in mice. *Cellular and Molecular Neurobiology*, 28, 971–979.
- Kalf, J. G., Munneke, M., van den Engel-Hoek, L., de Swart, B. J., Borm, G. F., Bloem, B. R., & Zwarts, M. J. (2011). Pathophysiology of diurnal drooling in Parkinson's disease. *Movement Disorders*, 26(9), 1670–1676. https://doi.org/10.1002/mds.23720
- Kalf, J. G., Smit, A. M., Bloem, B. R., Zwarts, M. J., & Munneke, M. (2007). Impact of drooling in Parkinson's disease. *Journal of Neurology*, 254(9), 1227–1232.
- Kalia, L. V., & Lang, A. E. (2015). Parkinson's disease. *Lancet*, 386(9996), 896–912. https://doi.org/10.1016/S0140-6736(14)61393-3
- Kalia, L. V., Lang, A. E., Hazrati, L.-N., Fujioka, S., Wszolek, Z. K., Dickson, D. W., Ross, O. A., Van Deerlin, V. M., Trojanowski, J. Q., & Hurtig, H. I. (2015). Clinical correlations with

- Lewy body pathology in LRRK2-related Parkinson disease. *JAMA Neurology*, 72(1), 100–105.
- Kanaan, N. M., Kordower, J. H., & Collier, T. J. (2008). Age and region-specific responses of microglia, but not astrocytes, suggest a role in selective vulnerability of dopamine neurons after 1-methyl-4-phenyl-1, 2, 3, 6-tetrahydropyridine exposure in monkeys. *Glia*, 56(11), 1199–1214.
- Kapoor, S., Bourdoumis, A., Mambu, L., & Barua, J. (2013). Effective management of lower urinary tract dysfunction in idiopathic P arkinson's disease. *International Journal of Urology*, 20(1), 79–84.
- Karaosmanoglu, T., Aygun, B., Wade, P. R., & Gershon, M. D. (1996). Regional differences in the number of neurons in the myenteric plexus of the guinea pig small intestine and colon: An evaluation of markers used to count neurons. *The Anatomical Record: An Official Publication of the American Association of Anatomists*, 244(4), 470–480.
- Keating, C., Ewart, L., Grundy, L., Valentin, J. P., & Grundy, D. (2014). Translational potential of a mouse in vitro bioassay in predicting gastrointestinal adverse drug reactions in Phase I clinical trials. *Neurogastroenterology & Motility*, 26(7), 980–989. https://doi.org/10.1111/nmo.12349
- Kharkovets, T., Hardelin, J.-P., Safieddine, S., Schweizer, M., El-Amraoui, A., Petit, C., & Jentsch, T. J. (2000). KCNQ4, a K+ channel mutated in a form of dominant deafness, is expressed in

- the inner ear and the central auditory pathway. *Proceedings of the National Academy of Sciences*, 97(8), 4333–4338. https://doi.org/10.1073/pnas.97.8.4333
- Kitta, T., Chancellor, M. B., de Groat, W. C., Kuno, S., Nonomura, K., & Yoshimura, N. (2012).
 Suppression of bladder overactivity by adenosine A2A receptor antagonist in a rat model of Parkinson disease. *The Journal of Urology*, 187(5), 1890–1897.
- Kitta, T., Yabe, I., Kanno, Y., Higuchi, M., Ouchi, M., Togo, M., Moriya, K., Takahashi, I., Matsushima, M., & Sasaki, H. (2018). Long-term outcome of adenosine A2A receptor antagonist on lower urinary tract symptoms in male Parkinson disease patients. *Clinical Neuropharmacology*, 41(3), 98.
- Knudsen, K., Fedorova, T. D., Bekker, A. C., Iversen, P., Ostergaard, K., Krogh, K., &
 Borghammer, P. (2017). Objective Colonic Dysfunction is Far more Prevalent than
 Subjective Constipation in Parkinson's Disease: A Colon Transit and Volume Study. J
 Parkinsons Dis, 7(2), 359–367. https://doi.org/10.3233/jpd-161050
- Knudsen, K., Haase, A. M., Fedorova, T. D., Bekker, A. C., Ostergaard, K., Krogh, K., &
 Borghammer, P. (2017). Gastrointestinal Transit Time in Parkinson's Disease Using a
 Magnetic Tracking System. *J Parkinsons Dis*, 7(3), 471–479. https://doi.org/10.3233/jpd-171131
- Kordower, J. H., Chu, Y., Hauser, R. A., Freeman, T. B., & Olanow, C. W. (2008). Lewy body–like pathology in long-term embryonic nigral transplants in Parkinson's disease. *Nature Medicine*, 14(5), 504–506.

- Kubisch, C., Schroeder, B. C., Friedrich, T., Lütjohann, B., El-Amraoui, A., Marlin, S., Petit, C., & Jentsch, T. J. (1999). KCNQ4, a novel potassium channel expressed in sensory outer hair cells, is mutated in dominant deafness. *Cell*, *96*(3), 437–446.
- Kuersten, M., Tacke, M., Gerstl, L., Hoelz, H., Stülpnagel, C. V., & Borggraefe, I. (2020).
 Antiepileptic therapy approaches in KCNQ2 related epilepsy: A systematic review.
 European Journal of Medical Genetics, 63(1), 103628.
- Kunikowska, G., & Jenner, P. (2001). 6-Hydroxydopamine-lesioning of the nigrostriatal pathway in rats alters basal ganglia mRNA for copper, zinc- and manganese-superoxide dismutase, but not glutathione peroxidase. *Brain Research*, 922(1), 51–64. https://doi.org/10.1016/S0006-8993(01)03149-3
- Kupsch, A., Schmidt, W., Gizatullina, Z., Debska-Vielhaber, G., Voges, J., Striggow, F., Panther,
 P., Schwegler, H., Heinze, H.-J., & Vielhaber, S. (2014). 6-Hydroxydopamine impairs
 mitochondrial function in the rat model of Parkinson's disease: Respirometric, histological,
 and behavioral analyses. *Journal of Neural Transmission*, 121, 1245–1257.
- Kurkowska-Jastrzębska, I., Bałkowiec-Iskra, E., Ciesielska, A., Joniec, I., Cudna, A., Zaremba, M. M., Członkowski, A., & Członkowska, A. (2009). Decreased inflammation and augmented expression of trophic factors correlate with MOG-induced neuroprotection of the injured nigrostriatal system in the murine MPTP model of Parkinson's disease. *International Immunopharmacology*, 9(6), 781–791.

- Kurkowska-Jastrzębska, I., Wrońska, A., Kohutnicka, M., Członkowski, A., & Członkowska, A. (1999). The inflammatory reaction following 1-methyl-4-phenyl-1, 2, 3, 6-tetrahydropyridine intoxication in mouse. *Experimental Neurology*, 156(1), 50–61.
- Lai, F., Jiang, R., Xie, W., Liu, X., Tang, Y., Xiao, H., Gao, J., Jia, Y., & Bai, Q. (2018). Intestinal pathology and gut microbiota alterations in a methyl-4-phenyl-1, 2, 3, 6-tetrahydropyridine (MPTP) mouse model of Parkinson's disease. *Neurochemical Research*, 43(10), 1986–1999.
- Lama, J., Buhidma, Y., Fletcher, E. J., & Duty, S. (2021). Animal models of Parkinson's disease: A guide to selecting the optimal model for your research. *Neuronal Signaling*, 5(4), NS20210026.
- Langston, J. W., Ballard, P., Tetrud, J. W., & Irwin, I. (1983). Chronic Parkinsonism in humans due to a product of meperidine-analog synthesis. *Science (New York, N.Y.)*, 219(4587), 979–980.
- Langston, J. W., Quik, M., Petzinger, G., Jakowec, M., & Di Monte, D. A. (2000). Investigating levodopa-induced dyskinesias in the parkinsonian primate. *Annals of Neurology*, 47(4 Suppl 1), S79-89.
- Lebouvier, T., Chaumette, T., Damier, P., Coron, E., Touchefeu, Y., Vrignaud, S., Naveilhan, P., Galmiche, J. P., Bruley des Varannes, S., Derkinderen, P., & Neunlist, M. (2008).

 Pathological lesions in colonic biopsies during Parkinson's disease. *Gut*, *57*(12), 1741.
- Lebouvier, T., Neunlist, M., Bruley des Varannes, S., Coron, E., Drouard, A., N'Guyen, J. M., Chaumette, T., Tasselli, M., Paillusson, S., Flamand, M., Galmiche, J. P., Damier, P., &

- Derkinderen, P. (2010). Colonic biopsies to assess the neuropathology of Parkinson's disease and its relationship with symptoms. *PLOS ONE*, *5*(9), e12728. https://doi.org/10.1371/journal.pone.0012728
- Lee, K.-J., Vos, R., Janssens, J., & Tack, J. (2003). Effects of sildenafil on duodenal motor response to acid, duodenal sensitivity to acid and the perception of duodenal distension in healthy subjects. *Gastroenterology*, 4(124), A163.
- Lee, & Lu, K. T. (1995). Neurotoxicity of MPTP and Uptake of MPPT into Dopamine and Norepinephrine Neurons in Mice. In L. C. Tang & S. J. Tang (Eds.), *Neurochemistry in Clinical Application* (pp. 29–46). Springer US.
- Leibner, J., Ramjit, A., Sedig, L., Dai, Y., Wu, S. S., Jacobson, C., Okun, M. S., Rodriguez, R. L., Malaty, I. A., & Fernandez, H. H. (2010). The impact of and the factors associated with drooling in Parkinson's disease. *Parkinsonism & Related Disorders*, 16(7), 475–477.
- Levandis, G., Balestra, B., Siani, F., Rizzo, V., Ghezzi, C., Ambrosi, G., Cerri, S., Bonizzi, A., Vicini, R., & Vairetti, M. (2015). Response of colonic motility to dopaminergic stimulation is subverted in rats with nigrostriatal lesion: Relevance to gastrointestinal dysfunctions in Parkinson's disease. *Neurogastroenterology & Motility*, 27(12), 1783–1795.
- Li, J.-Y., Englund, E., Holton, J. L., Soulet, D., Hagell, P., Lees, A. J., Lashley, T., Quinn, N. P., Rehncrona, S., & Björklund, A. (2008). Lewy bodies in grafted neurons in subjects with Parkinson's disease suggest host-to-graft disease propagation. *Nature Medicine*, *14*(5), 501–503.

- Li, M., Johnson, C. P., Adams, M. B., & Sarna, S. K. (2002). Cholinergic and nitrergic regulation of in vivo giant migrating contractions in rat colon. *American Journal of Physiology-Gastrointestinal and Liver Physiology*, 283(3), G544–G552.
- Lim. (2010). Non-mammalian animal models of Parkinson's disease for drug discovery. *Expert Opinion on Drug Discovery*, *5*(2), 165–176.
- Lim, S.-Y., Fox, S. H., & Lang, A. E. (2009). Overview of the extranigral aspects of Parkinson disease. *Archives of Neurology*, 66(2), 167–172.
- Lin, C.-H., Lin, J.-W., Liu, Y.-C., Chang, C.-H., & Wu, R.-M. (2014). Risk of Parkinson's disease following severe constipation: A nationwide population-based cohort study. *Parkinsonism & Related Disorders*, 20(12), 1371–1375. https://doi.org/10.1016/j.parkreldis.2014.09.026
- Liu, H., Jia, L., Chen, X., Shi, L., & Xie, J. (2018). The Kv7/KCNQ channel blocker XE991 protects nigral dopaminergic neurons in the 6-hydroxydopamine rat model of Parkinson's disease. *Brain Res Bull*, 137, 132–139. https://doi.org/10.1016/j.brainresbull.2017.11.011
- Liu, Sakakibara, R., Odaka, T., Uchiyama, T., Uchiyama, T., Yamamoto, T., Ito, T., Asahina, M., Yamaguchi, K., Yamaguchi, T., & Hattori, T. (2005). Mosapride citrate, a novel 5-HT4 agonist and partial 5-HT3 antagonist, ameliorates constipation in parkinsonian patients. *Mov Disord*, 20(6), 680–686. https://doi.org/10.1002/mds.20387
- Liu, Wei, B., Bi, Q., Sun, Q., Li, L., He, J., Weng, Y., Zhang, S., Mao, G., & Bao, Y. (2020).

 MPTP-induced impairment of cardiovascular function. *Neurotoxicity Research*, 38, 27–37.

- Luheshi, G., & Zar, A. (1990). Purinoceptor desensitization impairs but does not abolish the non-cholinergic motor transmission in rat isolated urinary bladder. *European Journal of Pharmacology*, 185(2–3), 203–208.
- Luk, K. C., Song, C., O'Brien, P., Stieber, A., Branch, J. R., Brunden, K. R., Trojanowski, J. Q., & Lee, V. M.-Y. (2009). Exogenous α-synuclein fibrils seed the formation of Lewy body-like intracellular inclusions in cultured cells. *Proceedings of the National Academy of Sciences*, 106(47), 20051–20056.
- Lundberg, J. O., & Weitzberg, E. (2013). Biology of nitrogen oxides in the gastrointestinal tract. *Gut*, 62(4), 616.
- Macleod, A. D., Taylor, K. S., & Counsell, C. E. (2014). Mortality in Parkinson's disease: A systematic review and meta-analysis. *Mov Disord*, 29(13), 1615–1622. https://doi.org/10.1002/mds.25898
- Malysz, J., & Petkov, G. V. (2020). Detrusor Smooth Muscle KV7 Channels: Emerging New Regulators of Urinary Bladder Function. *Frontiers in Physiology*, 11, 1004.
- Mani, B. K., Robakowski, C., Brueggemann, L. I., Cribbs, L. L., Tripathi, A., Majetschak, M., & Byron, K. L. (2016). Kv7. 5 potassium channel subunits are the primary targets for PKA-dependent enhancement of vascular smooth muscle Kv7 currents. *Molecular Pharmacology*, 89(3), 323–334.

- Marks, L., Turner, K., O'Sullivan, J., Deighton, B., & Lees, A. (2001). DROOLING IN

 PARKINSON'S DISEASE: A NOVEL SPEECH AND LANGUAGE THERAPY

 INTERVENTION. International Journal of Language & Communication Disorders,

 36(S1), 282–287. https://doi.org/10.3109/13682820109177898
- Martinez-Martin, P., Chaudhuri, K. R., Rojo-Abuin, J. M., Rodriguez-Blazquez, C., Alvarez-Sanchez, M., Arakaki, T., Bergareche-Yarza, A., Chade, A., Garretto, N., & Gershanik, O. (2015). Assessing the non-motor symptoms of Parkinson's disease: MDS-UPDRS and NMS Scale. *European Journal of Neurology*, 22(1), 37–43.
- Martire, M., Castaldo, P., D'Amico, M., Preziosi, P., Annunziato, L., & Taglialatela, M. (2004). M channels containing KCNQ2 subunits modulate norepinephrine, aspartate, and GABA release from hippocampal nerve terminals. *Journal of Neuroscience*, 24(3), 592–597.
- Matsuda, Y., Fujii, T., Suzuki, T., Yamahatsu, K., Kawahara, K., Teduka, K., Kawamoto, Y., Yamamoto, T., Ishiwata, T., & Naito, Z. (2011). Comparison of fixation methods for preservation of morphology, RNAs, and proteins from paraffin-embedded human cancer cell-implanted mouse models. *Journal of Histochemistry & Cytochemistry*, 59(1), 68–75.
- Mazzio, E. A., Reams, R. R., & Soliman, K. F. A. (2004). The role of oxidative stress, impaired glycolysis and mitochondrial respiratory redox failure in the cytotoxic effects of 6-hydroxydopamine in vitro. *Brain Research*, 1004(1), 29–44. https://doi.org/10.1016/j.brainres.2003.12.034

- McCoy, E. J., & Baker, R. D. (1968). Effect of feeding on electrical activity of dog's small intestine. *American Journal of Physiology-Legacy Content*, 214(6), 1291–1295.
- McDowell, K. A., Hadjimarkou, M. M., Viechweg, S., Rose, A. E., Clark, S. M., Yarowsky, P. J., & Mong, J. A. (2010). Sleep alterations in an environmental neurotoxin-induced model of parkinsonism. *Experimental Neurology*, 226(1), 84–89.
- McQuade, R. M., Singleton, L. M., Wu, H., Lee, S., Constable, R., Di Natale, M., Ringuet, M. T., Berger, J. P., Kauhausen, J., & Parish, C. L. (2021). The association of enteric neuropathy with gut phenotypes in acute and progressive models of Parkinson's disease. *Scientific Reports*, 11(1), 7934.
- McRorie, J., Meerveld, B. G.-V., & Rudolph, C. (1998). Characterization of propagating contractions in proximal colon of ambulatory mini pigs. *Digestive Diseases and Sciences*, 43, 957–963.
- Meacham, C. E., & Morrison, S. J. (2013). Tumour heterogeneity and cancer cell plasticity. *Nature*, 501(7467), 328–337.
- Melo, A., & Monteiro, L. (2013). Swallowing improvement after levodopa treatment in idiopathic Parkinson's disease: Lack of evidence. *Parkinsonism & Related Disorders*, 19(3), 279–281. https://doi.org/10.1016/j.parkreldis.2012.11.017
- Mendez, I., Viñuela, A., Astradsson, A., Mukhida, K., Hallett, P., Robertson, H., Tierney, T., Holness, R., Dagher, A., & Trojanowski, J. Q. (2008). Dopamine neurons implanted into

- people with Parkinson's disease survive without pathology for 14 years. *Nature Medicine*, 14(5), 507–509.
- Meredith, G. E., Totterdell, S., Petroske, E., Santa Cruz, K., Callison, R. C., & Lau, Y. S. (2002). Lysosomal malfunction accompanies alpha-synuclein aggregation in a progressive mouse model of Parkinson's disease. *Brain Research*, *956*(1), 156–165. https://doi.org/10.1016/S0006-8993(02)03514-X
- Michel, M. C., Radziszewski, P., Falconer, C., Marschall-Kehrel, D., & Blot, K. (2012).

 Unexpected frequent hepatotoxicity of a prescription drug, flupirtine, marketed for about 30 years. *British Journal of Clinical Pharmacology*, 73(5), 821–825.
- Michel, M. C., & Vrydag, W. (2006). A1-, α2-and β-adrenoceptors in the urinary bladder, urethra and prostate. *British Journal of Pharmacology*, 147(S2), S88–S119.
- Milber, J. M., Noorigian, J. V., Morley, J. F., Petrovitch, H., White, L., Ross, G. W., & Duda, J. E. (2012). Lewy pathology is not the first sign of degeneration in vulnerable neurons in Parkinson disease. *Neurology*, 79(24), 2307–2314.
- Mitchell, I. J., Cross, A. J., Sambrook, M. A., & Crossman, A. R. (1985). Sites of the neurotoxic action of 1-methyl-4-phenyl-1, 2, 3, 6-tetrahydropyridine in the macaque monkey include the ventral tegmental area and the locus coeruleus. *Neuroscience Letters*, 61(1–2), 195–200.
- Mitra, R., Aronsson, P., Winder, M., Tobin, G., Bergquist, F., & Carlsson, T. (2015). Local Change in Urinary Bladder Contractility Following CNS Dopamine Denervation in the 6-OHDA Rat

- Model of Parkinson's Disease. *Journal of Parkinson's Disease*, *5*(2), 301–311. https://doi.org/10.3233/JPD-140509
- Mogi, M., Togari, A., Tanaka, K., Ogawa, N., Ichinose, H., & Nagatsu, T. (2000). Increase in level of tumor necrosis factor-α in 6-hydroxydopamine-lesioned striatum in rats is suppressed by immunosuppressant FK506. *Neuroscience Letters*, 289(3), 165–168.
- Montgomery, B. S., & Fry, C. H. (1992). The action potential and net membrane currents in isolated human detrusor smooth muscle cells. *The Journal of Urology*, *147*(1), 176–184.
- Morita, T., Tsujii, T., & Dokita, S. (1992). Regional difference in functional roles of cAMP and cGMP in lower urinary tract smooth muscle contractility. *Urologia Internationalis*, 49(4), 191–195.
- Muller, T., Erdmann, C., Bremen, D., Schmidt, W. E., Muhlack, S., Woitalla, D., & Goetze, O. (2006). Impact of gastric emptying on levodopa pharmacokinetics in Parkinson disease patients. *Clinical Neuropharmacology*, 29(2), 61–67.
- Nagayama, T., Zhang, M., Hsu, S., Takimoto, E., & Kass, D. A. (2008). Sustained soluble guanylate cyclase stimulation offsets nitric-oxide synthase inhibition to restore acute cardiac modulation by sildenafil. *Journal of Pharmacology and Experimental Therapeutics*, 326(2), 380–387.

- Nakahira, Y., HASHITANI, H., FUKUTA, H., SASAKI, S., KOHRI, K., & SUZUKI, H. (2001). Effects of isoproterenol on spontaneous excitations in detrusor smooth muscle cells of the guinea pig. *The Journal of Urology*, *166*(1), 335–340.
- Natale, G., Kastsiushenka, O., Fulceri, F., Ruggieri, S., Paparelli, A., & Fornai, F. (2010). MPTP-induced parkinsonism extends to a subclass of TH-positive neurons in the gut. *Brain Research*, *1355*, 195–206. https://doi.org/10.1016/j.brainres.2010.07.076
- Ng, F. L., Davis, A. J., Jepps, T. A., Harhun, M. I., Yeung, S. Y., Wan, A., Reddy, M., Melville, D., Nardi, A., Khong, T. K., & Greenwood, I. A. (2011). Expression and function of the K+ channel KCNQ genes in human arteries. *British Journal of Pharmacology*, *162*(1), 42–53. https://doi.org/10.1111/j.1476-5381.2010.01027.x
- Nickolson, V. J., William Tam, S., Myers, M. J., & Cook, L. (1990). DuP 996 (3, 3-bis (4-pyrindinylmethyl)-1-phenylindolin-2-one) enhances the stimulus-induced release of acetylcholine from rat brain in vitro and in vivo. *Drug Development Research*, 19(3), 285–300.
- Nishikawa, N., Nagai, M., Tsujii, T., Iwaki, H., Yabe, H., & Nomoto, M. (2012). Coadministration of Domperidone Increases Plasma Levodopa Concentration in Patients With Parkinson Disease. *Clinical Neuropharmacology*, *35*(4), 182–184. https://doi.org/10.1097/WNF.0b013e3182575cdb

- Noorian, A. R., Taylor, G. M., Annerino, D. M., & Greene, J. G. (2011). Neurochemical phenotypes of myenteric neurons in the rhesus monkey. *Journal of Comparative Neurology*, 519(17), 3387–3401. https://doi.org/10.1002/cne.22679
- O'Donnell, A.-M., Coyle, D., & Puri, P. (2017). Decreased expression of Kv7 channels in Hirchsprung's disease. *Journal of Pediatric Surgery*, 52(7), 1177–1181.
- Oestreicher, E., Sengstock, G. J., Riederer, P., Olanow, C. W., Dunn, A. J., & Arendash, G. W. (1994). Degeneration of nigrostriatal dopaminergic neurons increases iron within the substantia nigra: A histochemical and neurochemical study. *Brain Research*, 660(1), 8–18. https://doi.org/10.1016/0006-8993(94)90833-8
- O'Gorman Tuura, R. L., Baumann, C. R., & Baumann-Vogel, H. (2018). Beyond dopamine:

 GABA, glutamate, and the axial symptoms of Parkinson disease. *Frontiers in Neurology*, 9, 806.
- Ohya, S., Asakura, K., Muraki, K., Watanabe, M., & Imaizumi, Y. (2002). Molecular and functional characterization of ERG, KCNQ, and KCNE subtypes in rat stomach smooth muscle. *American Journal of Physiology-Gastrointestinal and Liver Physiology*, 282(2), G277–G287.
- Orimo, S., Amino, T., Itoh, Y., Takahashi, A., Kojo, T., Uchihara, T., Tsuchiya, K., Mori, F., Wakabayashi, K., & Takahashi, H. (2005). Cardiac sympathetic denervation precedes neuronal loss in the sympathetic ganglia in Lewy body disease. *Acta Neuropathologica*, 109(6), 583–588. https://doi.org/10.1007/s00401-005-0995-7

- Oshikawa, T., Kuroiwa, H., Yano, R., Yokoyama, H., Kadoguchi, N., Kato, H., & Araki, T. (2009).

 Systemic administration of proteasome inhibitor protects against MPTP neurotoxicity in mice. *Cellular and Molecular Neurobiology*, 29, 769–777.
- O'Sullivan, S. S., Massey, L. A., Williams, D. R., Revesz, T., Lees, A., & Holton, J. (2009).

 Parkinson's disease with Onuf's nucleus involvement mimicking multiple system atrophy.

 Case Reports, 2009, bcr0820080774.
- Pan-Montojo, F., Anichtchik, O., Dening, Y., Knels, L., Pursche, S., Jung, R., Jackson, S., Gille, G.,
 Spillantini, M. G., Reichmann, H., & Funk, R. H. W. (2010). Progression of Parkinson's
 Disease Pathology Is Reproduced by Intragastric Administration of Rotenone in Mice.
 PLOS ONE, 5(1), e8762. https://doi.org/10.1371/journal.pone.0008762
- Paredes-Rodriguez, E., Vegas-Suarez, S., Morera-Herreras, T., De Deurwaerdere, P., & Miguelez, C. (2020). The noradrenergic system in Parkinson's disease. *Frontiers in Pharmacology*, 11, 435.
- Parkinson, J. (1817). An Essay on the Shaking Palsy. Whittingham and Rowland.
- Parkkinen, L., Pirttilä, T., & Alafuzoff, I. (2008). Applicability of current staging/categorization of α-synuclein pathology and their clinical relevance. *Acta Neuropathologica*, 115, 399–407.
- Paxinos, G., & Watson, C. (2009). The rat brain in stereotaxic coordinates. Elsevier.

- Peiris, M., Hockley, J. R., Reed, D. E., Smith, E. S. J., Bulmer, D. C., & Blackshaw, L. A. (2017).
 Peripheral KV7 channels regulate visceral sensory function in mouse and human colon.
 Molecular Pain, 13, 1744806917709371.
- Pellegrini, C., Fornai, M., Colucci, R., Tirotta, E., Blandini, F., Levandis, G., Cerri, S., Segnani, C., Ippolito, C., & Bernardini, N. (2016). Alteration of colonic excitatory tachykininergic motility and enteric inflammation following dopaminergic nigrostriatal neurodegeneration.
 Journal of Neuroinflammation, 13(1), 146.
- Penttinen, A.-M., Suleymanova, I., Albert, K., Anttila, J., Voutilainen, M. H., & Airavaara, M. (2016). Characterization of a new low-dose 6-hydroxydopamine model of Parkinson's disease in rat. *Journal of Neuroscience Research*, 94(4), 318–328.
- Perlberg, S., & Caine, M. (1982). Adrenergic response of bladder muscle in prostatic obstruction: Its relation to detrusor instability. *Urology*, 20(5), 524–527.
- Persson, K., Alm, P., Johansson, K., Larsson, B., & Andersson, K.-E. (1993). Nitric oxide synthase in pig lower urinary tract: Immunohistochemistry, NADPH diaphorase histochemistry and functional effects. *British Journal of Pharmacology*, 110(2), 521–530.
- Persson, K., & Andersson, K.-E. (1992). Nitric oxide and relaxation of pig lower urinary tract.

 British Journal of Pharmacology, 106(2), 416–422.
- Pessiglione, M., Guehl, D., Jan, C., François, C., Hirsch, E. C., Féger, J., & Tremblay, L. (2004).

 Disruption of self-organized actions in monkeys with progressive MPTP-induced

- parkinsonism: II. Effects of reward preference. *European Journal of Neuroscience*, 19(2), 437–446.
- Pfaffl, M. W. (2001). A new mathematical model for relative quantification in real-time RT–PCR.

 Nucleic Acids Research, 29(9), e45–e45.
- Pfeiffer, R. F., Wszolek, Z. K., & Ebadi, M. (2004). Parkinson's Disease. CRC Press.
- Phillips, K. A., Ross, C. N., Spross, J., Cheng, C. J., Izquierdo, A., Biju, K. C., Chen, C., Li, S., & Tardif, S. D. (2017). Behavioral phenotypes associated with MPTP induction of partial lesions in common marmosets (Callithrix jacchus). *Behavioural Brain Research*, 325, 51–62.
- Phillips, & Powley. (2007). Innervation of the gastrointestinal tract: Patterns of aging. *Autonomic Neuroscience*, 136(1–2), 1–19. https://doi.org/10.1016/j.autneu.2007.04.005
- Pifl, C., Reither, H., Del Rey, N. L.-G., Cavada, C., Obeso, J. A., & Blesa, J. (2017). Early paradoxical increase of dopamine: A neurochemical study of olfactory bulb in asymptomatic and symptomatic MPTP treated monkeys. *Frontiers in Neuroanatomy*, 11, 46.
- Pifl, C., Schingnitz, G., & Hornykiewicz, O. (1991). Effect of 1-methyl-4-phenyl-1, 2, 3, 6-tetrahydropyridine on the regional distribution of brain monoamines in the rhesus monkey.

 Neuroscience, 44(3), 591–605.
- Pontone, G. M., & Mills, K. A. (2021). Optimal treatment of depression and anxiety in Parkinson's disease. *The American Journal of Geriatric Psychiatry*, 29(6), 530–540.

- Postuma, R. B., Berg, D., Stern, M., Poewe, W., Olanow, C. W., Oertel, W., Obeso, J., Marek, K.,
 Litvan, I., Lang, A. E., Halliday, G., Goetz, C. G., Gasser, T., Dubois, B., Chan, P., Bloem,
 B. R., Adler, C. H., & Deuschl, G. (2015). MDS clinical diagnostic criteria for Parkinson's disease. *Mov Disord*, 30(12), 1591–1601. https://doi.org/10.1002/mds.26424
- Praveen Rajneesh, C., Liou, J.-C., Hsieh, T.-H., Lin, J.-H., & Peng, C.-W. (2020). The voiding efficiency in rat models with dopaminergic brain lesions induced through unilateral and bilateral intrastriatal injections. *Plos One*, *15*(12), e0243452.
- Pritchard, S., Jackson, M. J., Hikima, A., Lione, L., Benham, C. D., Chaudhuri, K. R., Rose, S., Jenner, P., & Iravani, M. M. (2017). Altered detrusor contractility in MPTP-treated common marmosets with bladder hyperreflexia. *PLOS ONE*, 12(5), e0175797. https://doi.org/10.1371/journal.pone.0175797
- Provence, A., Angoli, D., & Petkov, G. V. (2018). Kv7 channel pharmacological activation by the novel activator ML213: Role for heteromeric Kv7. 4/Kv7. 5 channels in guinea pig detrusor smooth muscle function. *Journal of Pharmacology and Experimental Therapeutics*, 364(1), 131–144.
- Provence, A., Malysz, J., & Petkov, G. V. (2015). The novel KV7. 2/KV7. 3 channel opener ICA-069673 reveals subtype-specific functional roles in guinea pig detrusor smooth muscle excitability and contractility. *Journal of Pharmacology and Experimental Therapeutics*, 354(3), 290–301.

- Przedborski, S., Jackson-Lewis, V., Naini, A. B., Jakowec, M., Petzinger, G., Miller, R., & Akram, M. (2001). The parkinsonian toxin 1-methyl-4-phenyl-1,2,3,6-tetrahydropyridine (MPTP):

 A technical review of its utility and safety. *Journal of Neurochemistry*, 76(5), 1265–1274.

 https://doi.org/10.1046/j.1471-4159.2001.00183.x
- Rajneesh, C. P., Hsieh, T.-H., Chen, H.-C., Liou, J.-C., Lin, B.-S., Wu, C.-W. G., Lai, C.-H., & Peng, C.-W. (2023). A time-course study of urodynamic analyses in rat models with dopaminergic depletion induced through unilateral and bilateral 6-hydroxydopamine injections. *Journal of the Formosan Medical Association*, 122(3), 239–248.
- Robertson, B. E., Schubert, R., Hescheler, J., & Nelson, M. T. (1993). cGMP-dependent protein kinase activates Ca-activated K channels in cerebral artery smooth muscle cells. *American Journal of Physiology-Cell Physiology*, 265(1), C299–C303.
- Robertson, Renwick, A. G., Macklin, B., Jones, S., Waller, D. G., George, C. F., & Fleming, J. S. (1992). The influence of levodopa on gastric emptying in healthy elderly volunteers. *Eur J Clin Pharmacol*, 42(4), 409–412.
- Rode, F., Svalø, J., Sheykhzade, M., & Rønn, L. C. B. (2010). Functional effects of the KCNQ modulators retigabine and XE991 in the rat urinary bladder. *European Journal of Pharmacology*, 638(1–3), 121–127.
- Rojo, A. I., Cavada, C., de Sagarra, M. R., & Cuadrado, A. (2007). Chronic inhalation of rotenone or paraquat does not induce Parkinson's disease symptoms in mice or rats. *Experimental Neurology*, 208(1), 120–126. https://doi.org/10.1016/j.expneurol.2007.07.022

- Rota, L., Pellegrini, C., Benvenuti, L., Antonioli, L., Fornai, M., Blandizzi, C., Cattaneo, A., & Colla, E. (2019). Constipation, deficit in colon contractions and alpha-synuclein inclusions within the colon precede motor abnormalities and neurodegeneration in the central nervous system in a mouse model of alpha-synucleinopathy. *Translational Neurodegeneration*, 8(1), 1–15.
- Ruetten, H., Zabel, U., Linz, W., & Schmidt, H. H. (1999). Downregulation of soluble guanylyl cyclase in young and aging spontaneously hypertensive rats. *Circulation Research*, 85(6), 534–541.
- Sakakibara, R., Hattori, T., Uchiyama, T., & Yamanishi, T. (2001). Videourodynamic and sphincter motor unit potential analyses in Parkinson's disease and multiple system atrophy. *Journal of Neurology, Neurosurgery, and Psychiatry*, 71(5), 600.
- Sakakibara, R., Shinotoh, H., Uchiyama, T., Yoshiyama, M., Hattori, T., & Yamanishi, T. (2001).

 SPECT imaging of the dopamine transporter with [123I]-β-CIT reveals marked decline of nigrostriatal dopaminergic function in Parkinson's disease with urinary dysfunction. *Journal of the Neurological Sciences*, 187(1–2), 55–59.
- Sakakibara, R., Tateno, F., Yamamoto, T., Uchiyama, T., & Yamanishi, T. (2018). Urological dysfunction in synucleinopathies: Epidemiology, pathophysiology and management. Clinical Autonomic Research, 28, 83–101.
- Sakakibara, R., Uchiyama, T., Yamanishi, T., Shirai, K., & Hattori, T. (2008). Bladder and bowel dysfunction in Parkinson's disease. *Journal of Neural Transmission*, 115, 443–460.

- Sammour, Z. M., Gomes, C. M., Barbosa, E. R., Lopes, R. I., Sallem, F. S., Trigo-Rocha, F. E., Bruschini, H., & Srougi, M. (2009). Voiding dysfunction in patients with Parkinson's disease: Impact of neurological impairment and clinical parameters. *Neurourology and Urodynamics: Official Journal of the International Continence Society*, 28(6), 510–515.
- Sampath, C., Kalpana, R., Ansah, T., Charlton, C., Hale, A., Channon, K. M., Srinivasan, S., & Gangula, P. R. (2019). Impairment of Nrf2-and nitrergic-mediated gastrointestinal motility in an MPTP mouse model of Parkinson's disease. *Digestive Diseases and Sciences*, 64(12), 3502–3517.
- Sander, S. E., Lambrecht, C., & Richter, A. (2013). The K(V)7.2/3 preferring channel opener ICA 27243 attenuates L-DOPA-induced dyskinesia in hemiparkinsonian rats. *Neuroscience Letters*, *545*, 59–63. https://doi.org/10.1016/j.neulet.2013.04.017
- Sander, S. E., Lemm, C., Lange, N., Hamann, M., & Richter, A. (2012). Retigabine, a K(V)7 (KCNQ) potassium channel opener, attenuates L-DOPA-induced dyskinesias in 6-OHDA-lesioned rats. *Neuropharmacology*, 62(2), 1052–1061. https://doi.org/10.1016/j.neuropharm.2011.10.016
- Sanders, K. M. (2008). Regulation of smooth muscle excitation and contraction.

 Neurogastroenterology & Motility, 20, 39–53.
- Sanders, K. M., Koh, S. D., Ro, S., & Ward, S. M. (2012). Regulation of gastrointestinal motility—
 Insights from smooth muscle biology. *Nature Reviews Gastroenterology & Hepatology*,
 9(11), 633–645.

- Sanguinetti, M. C., Curran, M. E., Zou, A., Shen, J., Specter, P. S., Atkinson, D. L., & Keating, M. T. (1996). Coassembly of KVLQT1 and minK (IsK) proteins to form cardiac IKS potassium channel. *Nature*, 384, 80. https://doi.org/10.1038/384080a0
- Santiago, R. M., Barbieiro, J., Lima, M. M., Dombrowski, P. A., Andreatini, R., & Vital, M. A. (2010). Depressive-like behaviors alterations induced by intranigral MPTP, 6-OHDA, LPS and rotenone models of Parkinson's disease are predominantly associated with serotonin and dopamine. *Progress in Neuro-Psychopharmacology and Biological Psychiatry*, 34(6), 1104–1114.
- Santos, J. R., Cunha, J. A., Dierschnabel, A. L., Campêlo, C. L., Leão, A. H., Silva, A. F., Engelberth, R. C., Izídio, G. S., Cavalcante, J. S., & Abílio, V. C. (2013). Cognitive, motor and tyrosine hydroxylase temporal impairment in a model of parkinsonism induced by reserpine. *Behavioural Brain Research*, 253, 68–77.
- Santoso, A. G. H., Lo, W. N., & Liang, W. (2011). Urothelium-dependent and urothelium-independent detrusor contractility mediated by nitric oxide synthase and cyclooxygenase inhibition. *Neurourology and Urodynamics*, 30(4), 619–625.
- Sauer, H., & Oertel, W. H. (1994). Progressive degeneration of nigrostriatal dopamine neurons following intrastriatal terminal lesions with 6-hydroxydopamine: A combined retrograde tracing and immunocytochemical study in the rat. *Neuroscience*, *59*(2), 401–415.
- Schapira, A. H. V., Chaudhuri, K. R., & Jenner, P. (2017). Non-motor features of Parkinson disease. *Nature Reviews Neuroscience*, 18, 435. https://doi.org/10.1038/nrn.2017.62

- Schindelin, J., Arganda-Carreras, I., Frise, E., Kaynig, V., Longair, M., Pietzsch, T., Preibisch, S.,
 Rueden, C., Saalfeld, S., Schmid, B., Tinevez, J.-Y., White, D. J., Hartenstein, V., Eliceiri,
 K., Tomancak, P., & Cardona, A. (2012). Fiji: An open-source platform for biological-image analysis. *Nature Methods*, 9, 676. https://doi.org/10.1038/nmeth.2019
- Schintu, N., Frau, L., Ibba, M., Garau, A., Carboni, E., & Carta, A. R. (2009). Progressive dopaminergic degeneration in the chronic MPTPp mouse model of Parkinson's disease.

 Neurotoxicity Research, 16, 127–139.
- Schneider, C. A., Rasband, W. S., & Eliceiri, K. W. (2012). NIH Image to ImageJ: 25 years of image analysis. *Nature Methods*, *9*, 671. https://doi.org/10.1038/nmeth.2089
- Schreiber, D., Jost, V., Bischof, M., Seebach, K., Lammers, W. J., Douglas, R., & Schäfer, K.-H. (2014). Motility patterns of ex vivo intestine segments depend on perfusion mode. *World Journal of Gastroenterology: WJG*, 20(48), 18216.
- Schroeder, A., Mueller, O., Stocker, S., Salowsky, R., Leiber, M., Gassmann, M., Lightfoot, S., Menzel, W., Granzow, M., & Ragg, T. (2006). The RIN: an RNA integrity number for assigning integrity values to RNA measurements. *BMC Molecular Biology*, 7(1), 1–14.
- Sedelis, M., Hofele, K., Auburger, G. W., Morgan, S., Huston, J. P., & Schwarting, R. K. W. (2000). MPTP Susceptibility in the Mouse: Behavioral, Neurochemical, and Histological Analysis of Gender and Strain Differences. *Behavior Genetics*, *30*(3), 171–182. https://doi.org/10.1023/A:1001958023096

- Seerden, T. C., Lammers, W., De Winter, B. Y., De Man, J. G., & Pelckmans, P. A. (2005).
 Spatiotemporal electrical and motility mapping of distension-induced propagating oscillations in the murine small intestine. *American Journal of Physiology-Gastrointestinal and Liver Physiology*, 289(6), G1043–G1051.
- Selyanko, A. A., Hadley, J. K., Wood, I. C., Abogadie, F. C., Delmas, P., Buckley, N. J., London, B., & Brown, D. A. (1999). Two Types of K+ Channel Subunit, Erg1 and KCNQ2/3, Contribute to the M-Like Current in a Mammalian Neuronal Cell. *Journal of Neuroscience*, 19(18), 7742–7756. https://doi.org/10.1523/JNEUROSCI.19-18-07742.1999
- Seppi, K., Weintraub, D., Coelho, M., Perez-Lloret, S., Fox, S. H., Katzenschlager, R., Hametner, E.-M., Poewe, W., Rascol, O., Goetz, C. G., & Sampaio, C. (2011). The Movement Disorder Society Evidence-Based Medicine Review Update: Treatments for the non-motor symptoms of Parkinson's disease. *Movement Disorders*, 26(S3), S42–S80. https://doi.org/10.1002/mds.23884
- Sharman, S. K., Islam, B. N., Hou, Y., Usry, M., Bridges, A., Singh, N., Sridhar, S., Rao, S., & Browning, D. D. (2017). Sildenafil normalizes bowel transit in preclinical models of constipation. *PLoS One*, *12*(4), e0176673.
- Shimamoto, Y., Kitamura, H., Niimi, K., Yoshikawa, Y., Hoshi, F., Ishizuka, M., & Takahashi, E. (2013). Selection of suitable reference genes for mRNA quantification studies using common marmoset tissues. *Molecular Biology Reports*, 40(12), 6747–6755. https://doi.org/10.1007/s11033-013-2791-0

- Shimoji, M., Zhang, L., Mandir, A. S., Dawson, V. L., & Dawson, T. M. (2005). Absence of inclusion body formation in the MPTP mouse model of Parkinson's disease. *Molecular Brain Research*, 134(1), 103–108. https://doi.org/10.1016/j.molbrainres.2005.01.012
- Siderowf, A., Concha-Marambio, L., Lafontant, D.-E., Farris, C. M., Ma, Y., Urenia, P. A., Nguyen, H., Alcalay, R. N., Chahine, L. M., & Foroud, T. (2023). Assessment of heterogeneity among participants in the Parkinson's Progression Markers Initiative cohort using α-synuclein seed amplification: A cross-sectional study. *The Lancet Neurology*, 22(5), 407–417.
- Silva-Martins, S., Beserra-Filho, J. I. A., Maria-Macêdo, A., Custódio-Silva, A. C., Soares-Silva, B., Silva, S. P., Lambertucci, R. H., Silva, R. H., Dos Santos, J. R., & Gandhi, S. R. (2021). Myrtenol complexed with β-cyclodextrin ameliorates behavioural deficits and reduces oxidative stress in the reserpine-induced animal model of Parkinsonism. *Clinical and Experimental Pharmacology and Physiology*, 48(11), 1488–1499.
- Sinen, O., Özkan, A., Ağar, A., & Bülbül, M. (2021). Neuropeptide-S prevents 6-OHDA-induced gastric dysmotility in rats. *Brain Research*, 1762, 147442.
- Singaram, C., Gaumnitz, E. A., Torbey, C., Ashraf, W., Quigley, E. M. M., Sengupta, A., & Pfeiffer, R. (1995). Dopaminergic defect of enteric nervous system in Parkinson's disease patients with chronic constipation. *The Lancet*, *346*(8979), 861–864.

- Singh, N. A., Charlier, C., Stauffer, D., DuPont, B. R., Leach, R. J., Melis, R., Ronen, G. M., Bjerre, I., Quattlebaum, T., & Murphy, J. V. (1998). A novel potassium channel gene, KCNQ2, is mutated in an inherited epilepsy of newborns. *Nature Genetics*, *18*(1), 25–29.
- Slanzi, A., Iannoto, G., Rossi, B., Zenaro, E., & Constantin, G. (2020). In vitro models of neurodegenerative diseases. *Frontiers in Cell and Developmental Biology*, 8, 328.
- Slovin, H., Abeles, M., Vaadia, E., Haalman, I., Prut, Y., & Bergman, H. (1999). Frontal cognitive impairments and saccadic deficits in low-dose MPTP-treated monkeys. *Journal of Neurophysiology*, 81(2), 858–874.
- Smith, L., De Salvia, M., Jenner, P., & Marsden, C. D. (1996). An appraisal of the antiparkinsonian activity of piribedil in 1-methyl-4-phenyl-1, 2, 3, 6-tetrahydropyridine-treated common marmosets. *Movement Disorders*, 11(2), 125–135.
- Soler, R., Füllhase, C., Hanson, A., Campeau, L., Santos, C., & Andersson, K.-E. (2012). Stem cell therapy ameliorates bladder dysfunction in an animal model of Parkinson disease. *The Journal of Urology*, *187*(4), 1491–1497.
- Soler, R., Füllhase, C., Santos, C., & Andersson, K.-E. (2011). Development of bladder dysfunction in a rat model of dopaminergic brain lesion. *Neurourology and Urodynamics*, 30(1), 188– 193.

- Sopory, S., Kaur, T., & Visweswariah, S. S. (2004). The cGMP-binding, cGMP-specific phosphodiesterase (PDE5): Intestinal cell expression, regulation and role in fluid secretion. *Cellular Signalling*, 16(6), 681–692.
- Spencer, N. J., Smith, C. B., & Smith, T. K. (2001). Role of muscle tone in peristalsis in guinea-pig small intestine. *The Journal of Physiology*, *530*(2), 295–306.
- Spillantini, M. G., Schmidt, M. L., Lee, V. M. Y., Trojanowski, J. Q., Jakes, R., & Goedert, M. (1997). [Alpha]-Synuclein in Lewy bodies. *Nature*, 388(6645), 839–840.
- Srivanitchapoom, P., Pandey, S., & Hallett, M. (2014). Drooling in Parkinson's disease: A review.

 *Parkinsonism & Related Disorders, 20(11), 1109–1118.
- Stockwell, K. A., Scheller, D., Rose, S., Jackson, M. J., Tayarani-Binazir, K., Iravani, M. M., Smith, L. A., Olanow, C. W., & Jenner, P. (2009). Continuous administration of rotigotine to MPTP-treated common marmosets enhances anti-parkinsonian activity and reduces dyskinesia induction. *Experimental Neurology*, 219(2), 533–542. https://doi.org/10.1016/j.expneurol.2009.07.011
- Storch, A., Schneider, C. B., Klingelhöfer, L., Odin, P., Fuchs, G., Jost, W. H., Martinez-Martin, P., Koch, R., Reichmann, H., & Chaudhuri, K. R. (2015). Quantitative assessment of non-motor fluctuations in Parkinson's disease using the Non-Motor Symptoms Scale (NMSS). *Journal of Neural Transmission*, 122, 1673–1684.

- Stott, & Barker, R. A. (2014). Time course of dopamine neuron loss and glial response in the 6-OHDA striatal mouse model of P arkinson's disease. *European Journal of Neuroscience*, 39(6), 1042–1056.
- Stott, J. B., Barrese, V., & Greenwood, I. A. (2016). Kv7 channel activation underpins EPAC-dependent relaxations of rat arteries. *Arteriosclerosis, Thrombosis, and Vascular Biology*, 36(12), 2404–2411.
- Stott, J. B., Barrese, V., Jepps, T. A., Leighton, E. V., & Greenwood, I. A. (2015). Contribution of Kv7 channels to natriuretic peptide mediated vasodilation in normal and hypertensive rats. *Hypertension*, 65(3), 676–682.
- Stott, J. B., & Greenwood, I. A. (2015). Complex role of Kv7 channels in cGMP and cAMP-mediated relaxations. *Channels*, 9(3), 117–118.
- Streng, T., Christoph, T., & Andersson, K.-E. (2004). Urodynamic effects of the K+ channel (KCNQ) opener retigabine in freely moving, conscious rats. *The Journal of Urology*, 172(5), 2054–2058.
- Su, A., Gandhy, R., Barlow, C., & Triadafilopoulos, G. (2017). Utility of the wireless motility capsule and lactulose breath testing in the evaluation of patients with Parkinson's disease who present with functional gastrointestinal symptoms. *BMJ Open Gastroenterology*, 4(1), e000132.

- Suh, B.-C., Inoue, T., Meyer, T., & Hille, B. (2006). Rapid Chemically Induced Changes of PtdIns(4,5)P(2) Gate KCNQ Ion Channels. *Science (New York, N.Y.)*, 314(5804), 1454–1457. https://doi.org/10.1126/science.1131163
- Sui, G. P., Rothery, S., Dupont, E., Fry, C. H., & Severs, N. J. (2002). Gap junctions and connexin expression in human suburothelial interstitial cells. *BJU International*, *90*(1), 118–129.
- Sullivan, K. L., Staffetti, J. F., Hauser, R. A., Dunne, P. B., & Zesiewicz, T. A. (2006). Tegaserod (Zelnorm) for the treatment of constipation in Parkinson's disease. *Mov Disord*, 21(1), 115–116. https://doi.org/10.1002/mds.20666
- Sung, H. Y., Kim, J.-S., Lee, K.-S., Kim, Y.-I., Song, I.-U., Chung, S.-W., Yang, D.-W., Cho, Y.
 K., Park, J. M., & Lee, I. S. (2010). The prevalence and patterns of pharyngoesophageal dysmotility in patients with early stage Parkinson's disease. *Movement Disorders*, 25(14), 2361–2368.
- Sutton, J. P. (2013). Dysphagia in Parkinson's disease is responsive to levodopa. *Parkinsonism & Related Disorders*, 19(3), 282–284. https://doi.org/10.1016/j.parkreldis.2012.11.007
- Suttrup, I., Suttrup, J., Suntrup-Krueger, S., Siemer, M. L., Bauer, J., Hamacher, C., Oelenberg, S., Domagk, D., Dziewas, R., & Warnecke, T. (2017). Esophageal dysfunction in different stages of Parkinson's disease. *Neurogastroenterology & Motility*, 29(1), e12915-n/a. https://doi.org/10.1111/nmo.12915

- Suzuki, M., Asada, Y., Ito, J., Hayashi, K., Inoue, H., & Kitano, H. (2003). Activation of cerebellum and basal ganglia on volitional swallowing detected by functional magnetic resonance imaging. *Dysphagia*, 18(2), 71–77.
- Svalø, J., Sheykhzade, M., Nordling, J., Matras, C., & Bouchelouche, P. (2015). Functional and molecular evidence for K v 7 channel subtypes in human detrusor from patients with and without bladder outflow obstruction. *PloS One*, *10*(2), e0117350.
- Svensson, E., Horváth-Puhó, E., Thomsen, R. W., Djurhuus, J. C., Pedersen, L., Borghammer, P., & Sørensen, H. T. (2015). Vagotomy and subsequent risk of Parkinson's disease. *Annals of Neurology*, 78(4), 522–529. https://doi.org/10.1002/ana.24448
- Szurszewski, J. H. (1969). A migrating electric complex of canine small intestine. *American Journal of Physiology-Legacy Content*, 217(6), 1757–1763.
- Tai, C., Wang, J., Jin, T., Wang, P., Kim, S.-G., Roppolo, J. R., & de Groat, W. C. (2009). Brain switch for reflex micturition control detected by FMRI in rats. *Journal of Neurophysiology*, 102(5), 2719–2730.
- Takahashi, H., & Wakabayashi, K. (2001). The cellular pathology of Parkinson's disease. *Neuropathology*, 21(4), 315–322.
- Tan, A. H., Mahadeva, S., Thalha, A. M., Gibson, P. R., Kiew, C. K., Yeat, C. M., Ng, S. W., Ang,S. P., Chow, S. K., Tan, C. T., Yong, H. S., Marras, C., Fox, S. H., & Lim, S.-Y. (2014).

- Small intestinal bacterial overgrowth in Parkinson's disease. *Parkinsonism & Related Disorders*, 20(5), 535–540. https://doi.org/10.1016/j.parkreldis.2014.02.019
- Tanabe, Y., Hotokezaka, M., Mibu, R., & Tanaka, M. (2002). Effects of extrinsic autonomic denervation and myenteric plexus transection on colonic motility in conscious dogs. *Surgery*, 132(3), 471–479.
- Tanahashi, Y., Komori, S., Matsuyama, H., Kitazawa, T., & Unno, T. (2021). Functions of muscarinic receptor subtypes in gastrointestinal smooth muscle: A review of studies with receptor-knockout mice. *International Journal of Molecular Sciences*, 22(2), 926.
- Tanaka, Y., Kato, T., Nishida, H., Yamada, M., Koumura, A., Sakurai, T., Hayashi, Y., Kimura, A., Hozumi, I., Araki, H., Murase, M., Nagaki, M., Moriwaki, H., & Inuzuka, T. (2011). Is there a delayed gastric emptying of patients with early-stage, untreated Parkinson's disease? An analysis using the 13C-acetate breath test. *Journal of Neurology*, 258(3), 421–426. https://doi.org/10.1007/s00415-010-5769-z
- Tatton, N. A., & Kish, S. J. (1997). In situ detection of apoptotic nuclei in the substantia nigra compacta of 1-methyl-4-phenyl-1, 2, 3, 6-tetrahydropyridine-treated mice using terminal deoxynucleotidyl transferase labelling and acridine orange staining. *Neuroscience*, 77(4), 1037–1048.
- Thomas, J., Wang, J., Takubo, H., Sheng, J., de Jesus, S., & Bankiewicz, K. S. (1994). A 6-Hydroxydopamine-Induced Selective Parkinsonian Rat Model: Further Biochemical and

- Behavioral Characterization. *Experimental Neurology*, *126*(2), 159–167. https://doi.org/10.1006/exnr.1994.1054
- Thomson, H. J., Busuttil, A., Eastwood, M. A., Smith, A. N., & Elton, R. A. (1986). The submucosa of the human colon. *Journal of Ultrastructure and Molecular Structure Research*, 96(1–3), 22–30.
- Tian, Y. M., Chen, X., Luo, D. Z., Zhang, X. H., Xue, H., Zheng, L. F., Yang, N., Wang, X. M., & Zhu, J. X. (2008). Alteration of dopaminergic markers in gastrointestinal tract of different rodent models of Parkinson's disease. *Neuroscience*, 153(3), 634–644. https://doi.org/10.1016/j.neuroscience.2008.02.033
- Titova, N., Schapira, A. H., Chaudhuri, K. R., Qamar, M. A., Katunina, E., & Jenner, P. (2017).
 Nonmotor symptoms in experimental models of Parkinson's disease. *International Review of Neurobiology*, 133, 63–89.
- Tomac, A., Lindqvist, E., Lin, L. F. H., Ögren, S. O., Young, D., Hoffer, B. J., & Olson, L. (1995).

 Protection and repair of the nigrostriatal dopaminergic system by GDNF in vivo. *Nature*,

 373, 335. https://doi.org/10.1038/373335a0
- Toti, L., & Travagli, R. A. (2014). Gastric dysregulation induced by microinjection of 6-OHDA in the substantia nigra pars compacta of rats is determined by alterations in the brain-gut axis.

 *American Journal of Physiology Gastrointestinal and Liver Physiology, 307(10), G1013—G1023. https://doi.org/10.1152/ajpgi.00258.2014

- Troche, M. S., Brandimore, A. E., Foote, K. D., & Okun, M. S. (2013). Swallowing and deep brain stimulation in Parkinson's disease: A systematic review. *Parkinsonism & Related Disorders*, 19(9), 783–788.
- Unger, M. M., Möller, J. C., Mankel, K., Schmittinger, K., Eggert, K. M., Stamelou, M., Stiasny-Kolster, K., Bohne, K., Bodden, M., Mayer, G., Oertel, W. H., & Tebbe, J. J. (2011).
 Patients with idiopathic rapid-eye-movement sleep behavior disorder show normal gastric motility assessed by the 13C-octanoate breath test. *Movement Disorders*, 26(14), 2559–2563. https://doi.org/10.1002/mds.23933
- Ungerstedt, U. (1971a). Adipsia and aphagia after 6-hydroxydopamine induced degeneration of the nigro-striatal dopamine system. *Acta Physiologica Scandinavica*, 82(S367), 95–122.
- Ungerstedt, U. (1971b). Postsynaptic supersensitivity after 6-hydroxy-dopamine induced degeneration of the nigro-striatal dopamine system. *Acta Physiologica Scandinavica*, 82(S367), 69–93.
- Ungerstedt, U. (1971c). Striatal dopamine release after amphetamine or nerve degeneration revealed by rotational behaviour. *Acta Physiologica Scandinavica*, 82(S367), 49–68.
- Uvelius, B. (1976). Isometric and isotonic length-tension relations and variations in cell length in longitudinal smooth muscle from rabbit urinary bladder. *Acta Physiologica Scandinavica*, 97(1), 1–12.

- VanderHorst, V. G., Samardzic, T., Saper, C. B., Anderson, M. P., Nag, S., Schneider, J. A., Bennett, D. A., & Buchman, A. S. (2015). A-synuclein pathology accumulates in sacral spinal visceral sensory pathways. *Annals of Neurology*, 78(1), 142–149.
- Verhave, P. S., Jongsma, M. J., Van den Berg, R. M., Vis, J. C., Vanwersch, R. A., Smit, A. B., Van Someren, E. J., & Philippens, I. H. (2011). REM sleep behavior disorder in the marmoset MPTP model of early Parkinson disease. *Sleep*, 34(8), 1119–1125.
- Vieira, J. C. F., Bassani, T. B., Santiago, R. M., Guaita, G. de O., Zanoveli, J. M., da Cunha, C., & Vital, M. A. (2019). Anxiety-like behavior induced by 6-OHDA animal model of Parkinson's disease may be related to a dysregulation of neurotransmitter systems in brain areas related to anxiety. *Behavioural Brain Research*, *371*, 111981.
- Visanji, N. P., Gomez-Ramirez, J., Johnston, T. H., Pires, D., Voon, V., Brotchie, J. M., & Fox, S. H. (2006). Pharmacological characterization of psychosis-like behavior in the MPTP-lesioned nonhuman primate model of Parkinson's disease. *Movement Disorders*, 21(11), 1879–1891. https://doi.org/10.1002/mds.21073
- Visanji, N. P., Marras, C., Hazrati, L.-N., Liu, L. W. C., & Lang, A. E. (2014). Alimentary, my dear Watson? The challenges of enteric α-synuclein as a Parkinson's disease biomarker.

 Movement Disorders, 29(4), 444–450. https://doi.org/10.1002/mds.25789
- Vo, Q., Gilmour, T. P., Venkiteswaran, K., Fang, J., & Subramanian, T. (2014). Polysomnographic features of sleep disturbances and REM sleep behavior disorder in the unilateral 6-OHDA lesioned hemiparkinsonian rat. *Parkinson's Disease*, 2014.

- Wakabayashi, K., Tanji, K., Odagiri, S., Miki, Y., Mori, F., & Takahashi, H. (2013). The Lewy body in Parkinson's disease and related neurodegenerative disorders. *Molecular Neurobiology*, 47, 495–508.
- Wang, Curran, M. E., Splawski, I., Burn, T. C., Millholland, J. M., VanRaay, T. J., Shen, J.,
 Timothy, K. W., Vincent, G. M., de Jager, T., Schwartz, P. J., Towbin, J. A., Moss, A. J.,
 Atkinson, D. L., Landes, G. M., Connors, T. D., & Keating, M. T. (1996). Positional cloning of a novel potassium channel gene: KVLQT1 mutations cause cardiac arrhythmias. *Nature Genetics*, 12, 17. https://doi.org/10.1038/ng0196-17
- Wang, Lian, H., Cai, Q.-Q., Song, H.-Y., Zhang, X.-L., Zhou, L., Zhang, Y.-M., Zheng, L.-F., & Zhu, J.-X. (2014). No direct projection is observed from the substantia nigra to the dorsal vagus complex in the rat. *Journal of Parkinson's Disease*, 4(3), 375–383.
- Wang, Y., Tar, M. T., Fu, S., Melman, A., & Davies, K. P. (2014). Diabetes attenuates urothelial modulation of detrusor contractility and spontaneous activity. *International Journal of Urology*, 21(10), 1059–1064.
- Ward, S. M., Harney, S. C., Bayguinov, J. R., McLaren, G. J., & Sanders, K. M. (1997).

 Development of electrical rhythmicity in the murine gastrointestinal tract is specifically encoded in the tunica muscularis. *The Journal of Physiology*, 505(1), 241–258.
- Warnecke, T., Hamacher, C., Oelenberg, S., & Dziewas, R. (2014). Off and on state assessment of swallowing function in Parkinson's disease. *Parkinsonism & Related Disorders*, 20(9), 1033–1034. https://doi.org/10.1016/j.parkreldis.2014.06.016

- Warnecke, T., Schäfer, K. H., Claus, I., Del Tredici, K., & Jost, W. H. (2022). Gastrointestinal involvement in Parkinson's disease: Pathophysiology, diagnosis, and management. *Npj Parkinson's Disease*, 8(1), 31.
- Wattchow, D., Brookes, S., Murphy, E., Carbone, S., De Fontgalland, D., & Costa, M. (2008).

 Regional variation in the neurochemical coding of the myenteric plexus of the human colon and changes in patients with slow transit constipation. *Neurogastroenterology & Motility*, 20(12), 1298–1305.
- Weisbrodt, N. W., Copeland, E. M., Moore, E. P., Kearley, R. W., & Johnson, L. R. (1975). Effect of vagotomy on electrical activity of the small intestine of the dog. *American Journal of Physiology-Legacy Content*, 228(2), 650–654.
- Winge, K., & Fowler, C. J. (2006). Bladder dysfunction in Parkinsonism: Mechanisms, prevalence, symptoms, and management. *Movement Disorders*, 21(6), 737–745.
- Winge, K., Friberg, L., Werdelin, L., Nielsen, K. K., & Stimpel, H. (2005). Relationship between nigrostriatal dopaminergic degeneration, urinary symptoms, and bladder control in Parkinson's disease. *European Journal of Neurology*, *12*(11), 842–850.
- Winks, J. S., Hughes, S., Filippov, A. K., Tatulian, L., Abogadie, F. C., Brown, D. A., & Marsh, S. J. (2005). Relationship between membrane phosphatidylinositol-4,5-bisphosphate and receptor-mediated inhibition of native neuronal M channels. *J Neurosci*, 25(13), 3400–3413. https://doi.org/10.1523/jneurosci.3231-04.2005

- Wirdefeldt, K., Odin, P., & Nyholm, D. (2016). Levodopa–carbidopa intestinal gel in patients with Parkinson's disease: A systematic review. *CNS Drugs*, *30*, 381–404.
- Wladyka, C. L., & Kunze, D. L. (2006). KCNQ/M-currents contribute to the resting membrane potential in rat visceral sensory neurons. *The Journal of Physiology*, *575*(1), 175–189.
- Wolff, C., Schott, C., Porschewski, P., Reischauer, B., & Becker, K.-F. (2011). Successful protein extraction from over-fixed and long-term stored formalin-fixed tissues. *PLoS One*, *6*(1), e16353.
- Wright, G. W., Parsons, S. P., Loera-Valencia, R., Wang, X.-Y., Barajas-López, C., & Huizinga, J.
 D. (2014). Cholinergic signalling-regulated KV7. 5 currents are expressed in colonic ICCIM but not ICC-MP. *Pflügers Archiv-European Journal of Physiology*, 466(9), 1805–1818.
- Yang, Y.-L., Ran, X.-R., Li, Y., Zhou, L., Zheng, L.-F., Han, Y., Cai, Q.-Q., Wang, Z.-Y., & Zhu, J.-X. (2019). Expression of dopamine receptors in the lateral hypothalamic nucleus and their potential regulation of gastric motility in rats with lesions of bilateral substantia nigra.
 Frontiers in Neuroscience, 13, 195.
- Yeung, S. Y. M., & Greenwood, I. A. (2005). Electrophysiological and functional effects of the KCNQ channel blocker XE991 on murine portal vein smooth muscle cells. *British Journal of Pharmacology*, 146(4), 585–595.
- Yoshimura, N., Kuno, S., Chancellor, M. B., De Groat, W. C., & Seki, S. (2003). Dopaminergic mechanisms underlying bladder hyperactivity in rats with a unilateral 6-hydroxydopamine

- (6-OHDA) lesion of the nigrostriatal pathway. *British Journal of Pharmacology*, 139(8), 1425–1432.
- Yoshimura, N., Mizuta, E., Kuno, S., Sasa, M., & Yoshida, O. (1993). The dopamine D1 receptor agonist SKF 38393 suppresses detrusor hyperreflexia in the monkey with parkinsonism induced by 1-methyl-4-phenyl-1, 2, 3, 6-tetrahydropyridine (MPTP). *Neuropharmacology*, 32(4), 315–321.
- Yoshimura, N., Mizuta, E., Yoshida, O., & Kuno, S. (1998). Therapeutic effects of dopamine d1/d2receptor agonists on detrusor hyperreflexia in 1-methyl-4-phenyl-1, 2, 3, 6-tetrahydropyridine-lesioned parkinsonian cynomolgus monkeys. *Journal of Pharmacology and Experimental Therapeutics*, 286(1), 228–233.
- Yu, H., Wu, M., Hopkins, C., Engers, J., Townsend, S., Lindsley, C., McManus, O. B., & Li, M.
 (2010). A small molecule activator of KCNQ2 and KCNQ4 channels. In *Probe Reports* from the NIH Molecular Libraries Program. National Center for Biotechnology Information (US).
- Yuyama, N., Mizuno, J., Tsuzuki, H., Wada-Takahashi, S., Takahashi, O., & Tamura, K. (2002).

 Effects of extrinsic autonomic inputs on expression of c-Fos immunoreactivity in myenteric neurons of the guinea pig distal colon. *Brain Research*, 948(1–2), 8–16.
- Zangaglia, R., Martignoni, E., Glorioso, M., Ossola, M., Riboldazzi, G., Calandrella, D., Brunetti,
 G., & Pacchetti, C. (2007). Macrogol for the treatment of constipation in Parkinson's
 disease. A randomized placebo-controlled study. *Movement Disorders*, 22(9), 1239–1244.

- Zheng, L.-F., Song, J., Fan, R.-F., Chen, C.-L., Ren, Q.-Z., Zhang, X.-L., Feng, X.-Y., Zhang, Y., Li, L.-S., & Zhu, J.-X. (2014). The role of the vagal pathway and gastric dopamine in the gastroparesis of rats after a 6-hydroxydopamine microinjection in the substantia nigra. *Acta Physiologica*, 211(2), 434–446.
- Zhong, Y., Liu, H., Liu, G., Zhao, L., Dai, C., Liang, Y., Du, J., Zhou, X., Mo, L., & Tan, C. (2022). A review on pathology, mechanism, and therapy for cerebellum and tremor in Parkinson's disease. *Npj Parkinson's Disease*, 8(1), 82.
- Zhou, X., Wei, J., Song, M., Francis, K., & Yu, S. P. (2011). Novel role of KCNQ2/3 channels in regulating neuronal cell viability. *Cell Death Differ*, 18(3), 493–505.
 https://doi.org/10.1038/cdd.2010.120
- Zhu, H. C., Zhao, J., Luo, C. Y., & Li, Q. Q. (2012). Gastrointestinal dysfunction in a Parkinson's disease rat model and the changes of dopaminergic, nitric oxidergic, and cholinergic neurotransmitters in myenteric plexus. *Journal of Molecular Neuroscience*, 47(1), 15–25.